Evaluation of the aerodynamics of new drag reduction technologies for light-duty vehicles: summary report (public version)

de Souza, Fenella; Larose, Guy L.; McTavish, Sean; Leuschen, Jason

Laboratory Technical Report (National Research Council of Canada. Aerospace. Aerodynamics Laboratory); no. LTR-AL-2017-0001, 2017-09-12

NRC·CNRC

AERODYNAMICS LABORATORY

Evaluation of the aerodynamics of new drag reduction technologies for light-duty vehicles: Summary Report (public version)

Unclassified Unlimited

LTR-AL-2017-0001

Tuesday 12th September, 2017

Fenella de Souza, Guy L. Larose, Sean McTavish and Jason Leuschen

National Research Council Canada | Conseil national de recherches Canada

Canada

AERODYNAMICS LABORATORY

Evaluation of the aerodynamics of new drag reduction technologies for light-duty vehicles: Summary Report (public version)

Report No.: LTR-AL-2017-0001

Date: Tuesday 12th September, 2017

Authors: Fenella de Souza, Guy L. Larose, Sean McTavish and Jason Leuschen

Classification:	Unclassified	**Distribution:**	Unlimited
For:	ecoTECHNOLOGY for Vehicles Stewardship and Sustainable Transportation Programs Transport Canada		
Project #:	A1-005483		
Submitted by:	Dr. Mike Benner, **Director of Research and Development, Aerodynamics**		
Approved by:	Jerzy Komorowski, **General Manager, NRC Aerospace**		

Pages:	169	**Copy No:**	
Figures:	129	**Tables:**	6

Disclaimer

This report reflects the views of the authors only and does not reflect the views or policies of Transport Canada.

Neither Transport Canada, nor its employees, makes any warranty, express or implied, or assumes any legal liability or responsibility for the accuracy or completeness of any information contained in this report, or process described herein, and assumes no responsibility for anyone's use of the information. Transport Canada is not responsible for errors or omissions in this report and makes no representations as to the accuracy or completeness of the information.

Transport Canada does not endorse products or companies. Reference in this report to any specific commercial products, process, or service by trade name, trademark, manufacturer, or otherwise, does not constitute or imply its endorsement, recommendation, or favoring by Transport Canada and shall not be used for advertising or service endorsement purposes. Trade or company names appear in this report only because they are essential to the objectives of the report.

References and hyperlinks to external web sites do not constitute endorsement by Transport Canada of the linked web sites, or the information, products or services contained therein. Transport Canada does not exercise any editorial control over the information you may find at these locations.

Executive Summary

Transport Canada, through its ecoTECHNOLOGY for Vehicles program, and Environment & Climate Change Canada's Transportation Division, have commissioned a multi-phase project to investigate the aerodynamics of recently introduced drag reduction technologies for light-duty vehicles (LDVs). The intent was to evaluate the level of drag reduction associated with each technology as a function of vehicle size class and to provide guidance to policy makers for the implementation of emerging technologies in Canada and the U.S. This body of work has led to the establishment of a reliable and comprehensive database on the influence of drag reduction technologies for LDVs based on 25 vehicles covering most classes of available production vehicles in North America.

The technologies were evaluated through direct measurements of aerodynamic forces on full-scale vehicles equipped with the devices in the 9 m Wind Tunnel of the National Research Council Canada. This tunnel is equipped with wheel rollers, a moving ground plane between the wheels, boundary layer suction and a system to simulate road-representative turbulent winds. Four vehicle chassis struts are connected to an external six-component balance and permit independent front and rear ride height control. The vehicles were mounted on a turntable and measurements were acquired over a range of wind angles of up to 10 degrees.

Two categories of drag reduction technologies were evaluated, i) those currently offered by the original equipment manufacturers (i.e., active grille shutters, partial underbody covers, bumper and wheel air dams); and, ii) emerging technologies recently introduced or that have market introduction potential, i.e., active ride height control, actively deployable bumper air dams and full underbody covers. The wind tunnel tests were grouped into distinct sub-studies in order to investigate specific technologies alone or in combination.

Many results in this report are presented in terms of wind-averaged drag area, which is a weighted average of the drag coefficient, based on typical wind speeds and angles encountered on North American highways, multiplied by the vehicle frontal area. The concept of wind-averaged drag provides an improved characterization of the aerodynamics of drag reduction technologies for light-duty vehicles that includes cross-wind conditions, revealing information that would be missed by only taking into account the drag at 0 degree wind angle. This can lead to a better evaluation and optimization of drag reduction technologies for vehicles on the road. Drag area is more appropriate for vehicle-to-vehicle comparisons than the drag coefficient.

In general, the technologies investigated were effective. Of those currently available on the market, active grille shutters, covering most or all of the front surface of the radiator, were the most effective. Among emerging technologies that are expected to become more commonly available within a few years, active ride height systems were shown to be capable of signif-

icantly reducing drag for all vehicles tested in this study. Full underbody covers were also shown to be a promising emerging technology. The greatest potential for drag reduction identified in this study was for a scenario in which active ride height is combined with extending the bumper air dam.

The principal sub-studies, from which the main conclusions of this report were drawn, are described below:

- Active grille shutter and cooling study: Drag area was measured with the AGS fully closed or fully open, and at intermediate closure positions for some vehicles. An actuator was used to control the shutters remotely. For vehicles not equipped with AGS, a third-party or mock-up AGS system was installed. The maximum attainable benefit was investigated by sealing the external grille, representing the idealized scenario of the shutters located on the outer surface of the grille. Reduced drag-reduction performance due to leakage was assessed by testing vehicles with the grille shutters closed and sealed with tape. Closing the AGS produced a 1% to 5% reduction in wind-averaged drag area with respect to the open shutter configuration. Sealing the external grille further reduced the wind-averaged drag area by 1.5% to just over 5.5%, with respect to the closed shutter case, for all but 2 of the vehicles for which this was assessed. Sealing the AGS flaps was found to reduce drag area at 0 degree yaw by up to 1.4% with respect to the closed shutter case.

- OEM air dam study: Several vehicles were tested with and without the OEM bumper air dam and/or wheel dams to assess the effects of these components on vehicle drag. Maximum reductions in wind-averaged drag area of up to 2.3% for bumper air dams and up to 3% for wheel dams were measured.

- OEM underbody panel study: OEM underbody panels were removed systematically, from the rear to the front of the vehicle, so that the effect of each could be evaluated. The full OEM underbody panel system was found to provide a 0.5% to 1.5% reduction in wind-averaged drag area. In some cases, removing the rear panels only resulted in lower drag than with the full underbody panel set.

- Custom underbody panel study: Several vehicles were equipped with idealized, smooth underbody panelling. Similarly to the OEM underbody panel study, the panels were removed section by section from the rear to the front of the vehicle. Full underbody covers reduced the wind-averaged drag area of all 10 vehicles tested in this sub-study by 1.5% to close to 7%. For 7 of these vehicles, the wind-averaged drag area was reduced by more than 3%. For 3 of the 10 vehicles, the most favorable drag reduction configuration was with the rear-most custom panel removed.

- Variable ride height study: Using the chassis struts, the vehicle ride height was reduced systematically and its influence on vehicle drag was monitored. The ride height configurations tested were nominally -20 mm at the front only, -20 mm at the front and rear, -40 mm at the front combined with -20 mm at the rear, and -40 mm at the front and rear. Significant reductions in wind-averaged drag area, from 2% to over 6%, were observed for all vehicles as the ride height was reduced. More than half of the vehicles tested experienced maximum reductions in wind-averaged drag area of 5% or more.

- Custom/OEM extended air dam combined with ride height study: OEM or custom-built bumper air dams were extended by up to 60% of their original depth in combination with lowering the front and rear ride height by either 20 mm or 40 mm, in order to determine the maximum drag reduction that can be achieved by optimizing these parameters. Wind-averaged drag area reductions of at least 4% to over 9% were measured for certain combinations of air dam extension and ride height reduction. Reductions exceeding 10% in drag area at 0 degree yaw were measured for two of the vehicles tested in this sub-study.
- Study of drag technology combinations: In addition to the extended air dam/ride height study, this sub-study included tests to quantify the influence of fully-smooth underbody covers, rear wheel dams and closing the AGS with and without the OEM bumper air dam installed. The experiments revealed that both the full underbody cover and AGS drag reduction technologies were more effective when the OEM bumper air dam was installed.
- Study of the influence of turbulent flow: Four vehicles, each representing a different vehicle class, were tested in turbulent flow as well as in smooth flow. It was shown that road-representative turbulent winds can have a significant effect on the performance of drag reduction technologies, and that this effect can vary with the type of vehicle and technology. In some cases, technologies were effective in smooth flow but ineffective in turbulent flow, or vice-versa. Turbulence sometimes had opposite effects on the performance of different technologies: lowering the ride height reduced the wind-average drag area by 1% to 2.5% more in turbulent flow than in smooth flow for all 3 vehicles for which this was verified, whereas the ride height reduction/extended air dam technology was generally less effective in turbulent flow than in smooth flow for all 3 vehicles for which this comparison was made, and by up to 5% in drag area reduction at 0 degrees for 2 of the vehicles. Turbulence sometimes had opposite effects on different vehicles: the baseline wind-averaged drag was higher in turbulent flow than in smooth flow for some vehicles, by up to 1.9%, but lower for others, by up to 1.5%.

Throughout all sub-studies, it was observed that drag reduction technologies that worked well for one vehicle were not necessarily as effective, or even beneficial, for another one. In addition, interactions between different technologies might compound or reduce their influence, depending on the vehicle. This highlights the need for vehicle manufacturers to continue to perform validation checks of technologies for each new design and for the regulatory bodies to receive accurate data to apply credits where appropriate.

Table of Contents

List of Figures

List of Tables

Nomenclature

Symbols:

A	area [m^2]
C_D	drag-force coefficient $\left(= \frac{F_D}{1/2\rho U_{ref}^2 A}\right)$ [ ]
$C_D A$	drag area $\left(= \frac{F_D}{1/2\rho U_{ref}^2}\right)$ [m^2]
C_L	lift-force coefficient $\left(= \frac{F_L}{1/2\rho U_{ref}^2 A}\right)$ [ ]
WAC_D	wind-averaged drag coefficient [ ]
$WAC_D A$	wind-averaged drag area [m^2]
F_D	drag force [N]
F_L	lift force [N]
U	wind speed [m/s]
ρ	air density [kg/m^3]

Acronyms:

AGS	Active Grille Shutters
CV	Constant Velocity
DC	Direct Current
ECCC	Environment and Climate Change Canada
EPA	Environmental Protection Agency
EV	Electric Vehicle

eTV	ecoTECHNOLOGY for Vehicles
GESS	Ground Effects Simulation System
GHG	Greenhouse Gas
LDV	Light Duty Vehicle
NRC	National Research Council Canada
OEM	Original Equipment Manufacturer
RTS	Road Turbulence System
SAE	Society of Automotive Engineers
SUV	Sport Utility Vehicle
TC	Transport Canada

1. Introduction

1.1 Background

Transport Canada's ecoTECHNOLOGY for Vehicles Program (eTV) conducts in-depth safety, environmental, and performance testing on a range of new and emerging advanced vehicle technologies for light and heavy-duty vehicles. Results from these tests are helping to inform the development of environmental and safety regulations to ensure that new technologies are effective and can be introduced in Canada in a safe and timely manner.

At highway speeds (i.e., 80 km/h and above), aerodynamic drag is the most significant force of resistance that a vehicle must overcome. Therefore, improvements in a vehicle aerodynamic design can significantly improve fuel efficiency and contribute to the reduction of greenhouse gas (GHG) emissions. Most vehicle manufacturers have placed a renewed emphasis on aerodynamic design for passenger cars and trucks in recent years to meet increasingly stringent GHG emissions regulations in North America (EPA, 2010). Many of the latest aerodynamic technologies are known as "active aerodynamics", which activate under predetermined conditions to improve aerodynamic efficiency or overall performance such as heat/cooling management, aerodynamic stability and handling.

However, the aerodynamics of vehicles is physically complex. Adding a new active aerodynamic feature, such as an air dam or grille shutter, to a vehicle optimized aerodynamically in their absence, may not necessarily improve performance. Rather, a manufacturer may need to design a new vehicle as an "integrated system", particularly when it is seeking to maximize the benefits from newer active aerodynamic features. Currently, due to the proprietary nature of automotive design and development, limited public information exists about the optimal design of passenger vehicle aerodynamics, including how beneficial some of the newer active aerodynamic features may be in actual on-road conditions. Furthermore, current U.S. and Canadian test procedures used to demonstrate compliance with regulated GHG standards may not fully reflect the GHG benefits of these active features. Instead, the U.S. and Canadian regulations provide "allowances" or "credits" that aim to encourage and recognize innovative technologies such as active aerodynamics. This experimental study provides data to help assess the appropriateness of these allowances or credits for a variety of vehicle U.S. EPA size classes.

The work reported in this document also supports the commitment of Environment and Climate Change Canada (ECCC), Transportation Division, to work with the U.S. Environmental Protection Agency (EPA) to develop common standards for GHG emissions from light-duty vehicles (LDV). Maintaining a common Canada-U.S. approach to regulating GHG emissions from vehicles, 2017 and beyond, benefits not only the environment, but also consumers and the competitiveness of the North American car manufacturing industry. Continuing to maintain regulatory alignment with the U.S. minimizes the administrative burden on Canadian companies. Common Canada-U.S. standards are important to preserve the competitiveness of the Canadian automobile sector due to the high level of integration within the industry.

The main objectives of this experimental study were i) to quantify the aerodynamic drag changes due to new original equipment manufacturer (OEM) aerodynamic treatments (defined as add-on parts which primarily serve an aerodynamic function as opposed to aerodynamic features designed into the shape of the body); and ii) to explore the potential for improvement that could be realized by expanding the application of the current state of the art (defined as emerging drag reduction technologies that could be seen on production cars within two to four years).

Twenty-five LDVs were chosen to represent the range of "advanced" aerodynamics models equipped with active grille shutters, aerodynamic underbody panels, and air dams. Some vehicles have an OEM specific designation (e.g.*ECO*) suggesting that the vehicle is marketed having components or parts installed to improve fuel efficiency and reduce environmental impacts. Attention was given to choose vehicles from different utility and price segments. With reference to the U.S. EPA vehicle size class, vehicles in the following classes were selected: i) subcompact and compact cars; ii) midsize cars; iii) large cars; iv) sport utility vehicles (small and standard); v) minivans; and, vi) standard pick-up trucks.

The vehicles were selected by a steering committee that was established to guide this project. The committee was composed of representatives of Transport Canada's ecoTECHNOLOGY for Vehicles Program, Environment and Climate Change Canada's Transportation Division, U.S. Environmental Protection Agency, National Research Council Canada, Röchling Automotive of Germany, and Magna International, Exteriors of Canada.

Experiments were carried out in the 9 m Wind Tunnel in four phases, spanning a period from January 2014 to February 2016. The following is a complete list of the vehicles for which drag reduction technologies were evaluated:

- 2013 BMW 528i 2.0L, 4-cyl. Turbo;
- 2014 Chevrolet Cruze Eco 1.4 L DOHC I-4 turbo VVT;
- 2013 Chevrolet Malibu Eco 2.4L DOHC I-4 VVT DI with eAssist technology;
- 2013 Dodge Dart SXT 2.0L;
- 2013 Dodge Ram 1500 HFE Regular Cab;
- 2014 Ford Escape SE 1.6L EcoBoost, Ti-VCT, GTDI I-4;
- 2013 Ford F-150 XL 3.5L EcoBoost;
- 2013 Ford Focus SE 2.0L Ti-VCT GDI I-4;
- 2013 Ford Fusion Hybrid SE 2.0 L Atkinson-Cycle, DOHC 16-valve, I-4;
- 2014 Mazda 3 i-eloop S Grand Touring;
- 2014 Mazda 6 i-eloop Grand Touring;
- 2014 BMW X5 Xdrive 35i (TC);
- 2014 Subaru Crosstrek XV Hybrid 2.0i (TC);

- 2014 Ford Edge SE EcoBoost, 2.0L I4, Turbo, GDI, Ecoboost (TC);
- 2014 Ford Taurus SEL, 3.5L 24 Valve DOHC Ti-VCT V6 (TC);
- 2014 Honda Odyssey Touring, 3.5L, 24-valve, SOHC, i-VTEC, V6 (EEEC);
- 2014 Chevrolet Spark BEV 1LT (TC);
- 2015 Chevrolet Tahoe LS, 5.3L, EcoTec3 V8 VVT, GDI (TC);
- 2014 Chevrolet Impala, mild hybrid (EEEC);
- 2015 Nissan Pathfinder (EEEC);
- 2014 Jeep Cherokee Sport (4x2) (TC);
- 2014 Nissan Versa Note Plus (U.S. model, provided by the EPA);
- 2015 Nissan Murano AWD (TC);
- 2015 Toyota Sienna (TC); and
- 2016 Ford F-150 XL Ecoboost RWD (TC).

Vehicles were provided by Transport Canada (TC), Environment and Climate Change Canada (ECCC) and the U.S. Environmental Protection Agency (EPA). All vehicles were tested in smooth flow in the 9 m Wind Tunnel. Four vehicles representing different size classes were also tested in turbulent flow using the Road Turbulence System (RTS) of the 9 m Wind Tunnel: a small car, a large car, a standard SUV and a pick-up truck.

Full-scale wind-tunnel testing is the ideal choice for this work as it allows production vehicles to be evaluated without the expense of modeling (digitally or physically) and therefore provides a reliable evaluation of the aerodynamic drag most efficiently. To ensure appropriate boundary layer conditions, critical to the performance of underbody systems, the vehicles were tested with the Ground Effect Simulation System (GESS) in the 9 m Wind Tunnel.

In the following sections of this report, details on the test objectives and procedures, a description of the test programme and a summary of the results obtained during the four phases of this study are presented. The test logs for each phase can be found in Appendix A and identify the wind tunnel runs performed for each vehicle. These logs provide details of the test conditions and values of the zero-yaw and wind-averaged drag area, which is the drag coefficient multiplied by the vehicle frontal area, for selected runs. Photographs of the vehicles are presented in Appendix B. Appendix C presents the results in graphical form for each vehicle.

1.2 Objectives

As specified in the previous section, the main objectives of the present study were i) to quantify the aerodynamic drag changes due to new drag reduction technologies installed on production light-duty vehicles and ii) to explore the potential for improvement that could be realized by expanding application of the current state of the art. The new drag reduction technologies

addressed by the first objective above are: active grille shutters, partial underbody panels, and bumper and wheel air dams. The emerging technologies addressed by the second objective simulated the effects of deployable bumper air dams, active ride height where the clearance between the underbody and the road can be systematically reduced as a function of the road conditions, and full underbody covers. The importance of evaluating the performance of these technologies in turbulent flow, which is more representative of on-road conditions, and of comparing with the results obtained in smooth flow, was recognized. Therefore, some vehicles were tested in turbulent flow along with the standard smooth flow measurements.

To provide the elements of information to answer the specific questions that the steering committee wanted to address, the wind-tunnel tests were grouped into 12 categories or sub-studies:

- Test A1: Active grille shutter study;
- Test A2: Cooling study (external grille sealing);
- Test B: Variable ride height study;
- Test C: Custom underbody panel study;
- Test D1: OEM underbody panel study;
- Test D2: OEM air dam study;
- Test E: Wheel study;
- Test F: HVAC study;
- Test G: Custom air dam combined with ride height study;
- Test H: OEM extended air dam study;
- Test I: Turbulent flow study; and
- Test J: Drag technology combinations.

Test category J was added in order to determine if the drag reduction associated with two different technologies tested separately was additive.

Not all tests were conducted on all vehicles. The test matrix was established based on the installed drag reduction technologies for a particular vehicle and the data already acquired per category of vehicles. The test matrix is presented in Section 3.1. In the test matrix and in much of the rest of this report, vehicle names have been replaced by generic labels based on vehicle size class.

2. Test setup and procedures

2.1 NRC 9 m Wind Tunnel

The test program was undertaken in the 9 m Wind Tunnel located in Ottawa, Ontario, Canada. The wind tunnel is a horizontal closed circuit atmospheric facility with a large test section (9.1 m wide $\times$ 9.1 m high $\times$ 22.9 m long) that is suitable for testing up to the largest LDV and even tractor-trailer combinations up to full scale. It is powered by an air-cooled 6.7 MW DC motor that provides a maximum wind speed of approximately 55 m/s (200 km/h) in an empty test section. An external mechanical, pyramidal balance senses the six-components of aerodynamic forces and moments. One of the vehicles of this study is shown in Figures 2.1 and 2.2 installed in the test section of the wind tunnel. A turntable (blue circular section of the test section floor) allows rotation of the model about a vertical axis to simulate the effect of cross winds.

The test section is equipped with a ground effect simulation system (GESS) composed of a centre belt with an exposed 1 m x 5.7 m area, four wheel rollers and four chassis struts for ride height control. Upstream of the turntable are two plenae for a distributed suction system, calibrated to reduce the displacement thickness of the floor boundary layer to 4 mm at the leading edge of the model, without inducing flow angularity at the model (Larose *et al.*, 2001). Breathers on the floor and walls at the test section exit are vented to the tunnel surroundings to equalize the otherwise negative pressure in the test section with atmospheric pressure.

2.2 Vehicle preparation and installation

The models were approximately centred along the length of the GESS belt, so that the front bumper of a typical passenger car is approximately 500 mm downstream of the leading edge of the belt. The belt runs under the vehicle, inboard of the wheels, as shown in Figures 2.1 and 2.2.

The GESS wheel rollers do not support the weight of the vehicle, so pre-test preparations included measuring the baseline ride height and removing the suspension springs. The vehicles were mounted in the test section on four struts clamped to the rocker panels. The rear-strut clamps allow small longitudinal displacement of the vehicle, as shown in Figure 2.3, so that the ride height can be adjusted independently at the front and rear support points.

Exceptionally, the wheelbase of some pick-up models was too long for the rear wheels to be on the GESS rollers. As a result, only the front wheels were on the rollers. The rear wheels were suspended 13 mm above the tunnel floor and did not rotate, as shown in Figure 2.4. The rear suspension was left intact and turnbuckles were used to slightly compress the rear springs.

Since the engines were not operated during testing, the vehicle driveshafts were removed to prevent transmission damage from wheel rotation without oil pressure. In most cases, this

Figure 2.1: View from downstream of a sports utility vehicle on the GESS in the 9 m Wind Tunnel.

Figure 2.2: View from upstream of a sports utility vehicle on the GESS in the 9 m Wind Tunnel. The numbers on the floor upstream of the blue circle relate to the yaw angle setting of the turntable, from 0° to 10° in this study.

Figure 2.3: Close-up view of a rear GESS strut and rear GESS clamp attached to the rocker panel of a SUV.

Figure 2.4: View of a pick-up truck installed on the GESS with the rear wheels suspended above the tunnel floor.

was accomplished by disassembling the CV joints, removing the axle, and reinstalling the CV joints to seal the differentials/transmissions and hold the wheel bearings in place.

Once the suspension springs were removed and the axles disengaged, no other modifications to the wheels and tires were necessary. The tire pressures were adjusted to the manufacturer specifications when the vehicles were received at NRC and the baseline ride height was measured before removal of the springs. The wheels rolled freely on the GESS rollers (wheels could be easily spun by hand) and the GESS system ensured that the wheel rotation matched the speed of the flow within a narrow tolerance. Figure 2.5 shows a close up of a wheel on the wheel roller.

Note that custom-made spacers had to be installed in lieu of the suspension spring to allow the vehicle to be set at the nominal ride height (distance between the crown of the wheel well and the ground with a 68 kg driver and passenger) and to allow a reduction of the ride height of up to 40 mm for the ride height study.

2.3 Baseline conditions

The baseline condition describes the vehicle as received with all doors and windows closed and external mirrors adjusted to driving positions, with the exception of the vehicle designated as midsize car 7, for which a smooth prototype underbody was installed. Before removing the

Figure 2.5: Close-up view of a light-duty vehicle wheel and GESS wheel roller in the 9 m Wind Tunnel.

springs from the vehicle suspension, the tire pressures were adjusted to manufacturer specifications and the ride heights were recorded with 68 kg (150 lb) of ballast on both front seats to represent the nominal ride heights. These nominal (baseline) ride heights were replicated in the wind tunnel with two exceptions: the vehicles designated as small car 1 and midsize car 6 were not ballasted during the ride height measurements. Fuel loads were recorded during nominal ride height measurements and were consistently small. For all vehicles equipped with grille shutters, the baseline condition corresponded to the case with the grille shutters 100% closed.

2.4 Active grille shutters

Active grille shutters (AGS) have been employed to aid cold-weather operation of heavy duty diesel engines for decades; however, their application to gasoline LDVs is more recent. Engines are primarily sized for acceleration demands; outside of towing and mountainous driving, high engine loads are seldom sustained for more than 30 seconds. In most ambient conditions there is generally a surplus of cooling capacity and the AGS can be safely closed, which may reduce drag, and therefore fuel consumption, by reducing the mass flow of air being forced through the radiator. AGS can also reduce engine/transmission warm up times and help retain heat during short shutdowns. The AGS must be very reliable, however, as failure in the closed position could result in engine damage due to overheating. This, along with cost, is why the OEM-installed AGS of most of the vehicles tested in this study only partially covered the radiator. Further, it is generally the lower radiator section that is covered, as can be seen for example in Figures 2.6 and 2.7. This may be due to the fact that the stagnation point of the incoming air is typically closer to the lower intake, and thus the differential pressure and consequently the drag reduction potential is higher for the lower intake compared to the upper intake.

Ideally, the AGS would be mounted at the exterior surface of the grille in order to achieve the greatest reduction in drag. As a styling compromise, they are typically mounted in the duct between the cooling air intake and the radiator, behind the grille and fascia, where they are not visible from the outside. Although aesthetically neutral and relatively lightweight, an AGS system adds cost and complexity to the vehicle as it requires additional programming, moving parts and an actuator.

All vehicles except pick-up truck 2 were equipped with production or mock-up grille shutters that could be 100% closed and 100% opened. For vehicles not equipped with an OEM-installed active grille shutter (AGS) system consisting of a frame, flaps and an actuator, Röchling Automotive installed a system made for the vehicle.

For vehicles for which no production AGS system existed, Röchling Automotive built mock-ups of grille shutters that completely covered the radiator with a solid panel and a mock-up frame. The solid panel could be removed to leave only the mock-up frame. Finally, the mock-up frame could be removed to mimic the 100% open condition. Such was the case for one of the minivans and two of the sports utility vehicles tested in this study. Figures 2.8 and 2.9 show an example of a mock-up AGS, the solid panel and the mock-up frame for a vehicle. For the

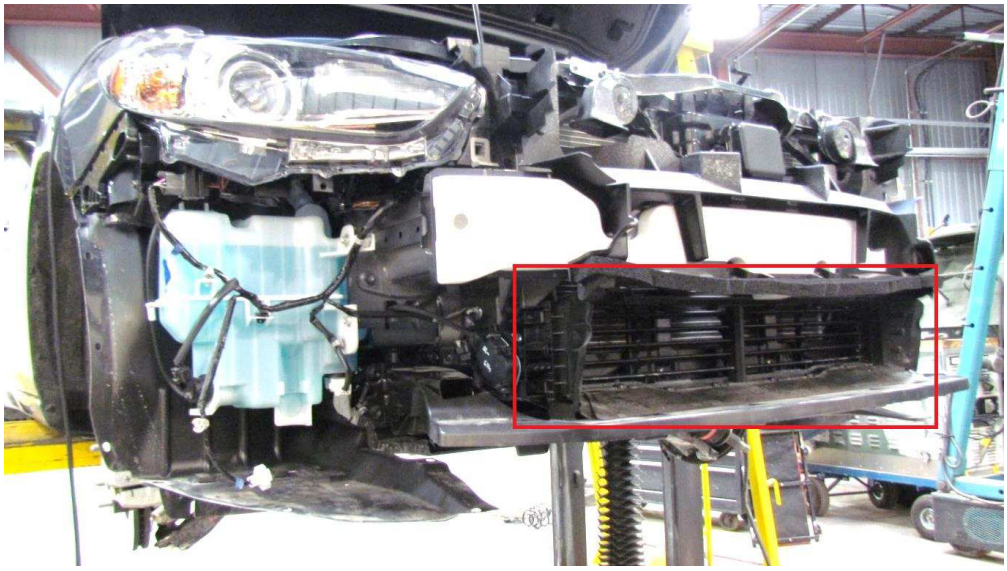

Figure 2.6: View of the front end of a vehicle with the front bumper removed, revealing the AGS (outlined in red) on the lower radiator.

Figure 2.7: View of the front end of a vehicle with the front fascia removed. The lower radiator is equipped with AGS, seen in the fully opened position in the picture.

other minivan, the grille shutter mock-up covered the lower and upper parts of the radiator independently and could be removed easily. This allowed to compare between three different grille shutter configurations: completely closed, lower shutter only closed and entirely open.

For the vehicles equipped with an OEM AGS, Röchling Automotive and/or Magna International removed the OEM actuator and replaced it with an actuator that could be controlled remotely from the passenger seat. In this way, tests to measure the level of drag reduction as a percentage of closure of the grille shutters could be conducted, as well as tests at 100% closed, 50% closed and 100% open.

Dynamic pressure on the AGS flaps increases as vehicle speed increases; this may cause deflection of the flaps that allows leakage of air through the AGS. To evaluate the effectiveness of the OEM-installed AGS in reducing the volume of flow through the radiator for selected vehicles, the area covered by the AGS was completely sealed with tape, as shown in Figure 2.10. The aerodynamic drag was measured with the AGS 100% closed and sealed with tape, followed by tests with the AGS 100% closed but unsealed. The difference between the two measurements indicated the influence of potential AGS leakage on the aerodynamic drag of the vehicle.

For certain vehicles, the external grille was completely sealed with tape in order to quantify how closely the AGS approach the maximum potential benefit of sealing the cooling system. An example of this is shown in Figure 2.11. The resulting drag reduction would likely be smaller than what could be achieved by redesigning the front fascia shape to take maximum advantage of this effect.

2.5 Active ride height concept

Several production vehicles have been equipped with ride height control systems of varying degrees of sophistication. Some are simple air spring systems with manual height control, others are designed to level the suspension to compensate for uneven loading and some serve the function of lowering ride height to improve cornering capability. In the context of this report, active ride height is typified by the recently introduced Mercedes S-Class which lowers itself 20-mm at highway speed to reduce drag. At lower speeds, where bump clearance and ramp approaches are critical, the vehicle rises to the original ride height. Reducing ride height is thought to lower drag by reducing the exposed tire frontal area (because the tires are deeper into the wheel wells) and/or by reducing flow volume under the vehicle, which tends to impinge on bluff underbody shapes. Active ride height, while costly and complex, has little or no effect on styling and may improve high-speed dynamics.

Because the vehicles in this study were supported by chassis struts and the suspension springs were removed, a ride height matrix could be run without further preparation. Since Mercedes uses a 20-mm reduction on production cars, this height was tested for each vehicle. A greater reduction of up to 40-mm was also considered to see if further drag reductions were possible. To determine if the savings could be attained by only having ride height control on one axle, thus saving cost and weight, the test matrix included pitch and heave motions. Finally it was speculated that lower ride heights may benefit less from underbody panelling, the deletion

Figure 2.8: View of the solid panel covering the radiator and part of the custom AGS built at NRC by Röchling Automotive, front bumper removed.

Figure 2.9: View of the mock-up AGS frame built at NRC by Röchling Automotive, front bumper removed.

Figure 2.10: AGS unit taped shut, revealed by bumper removal.

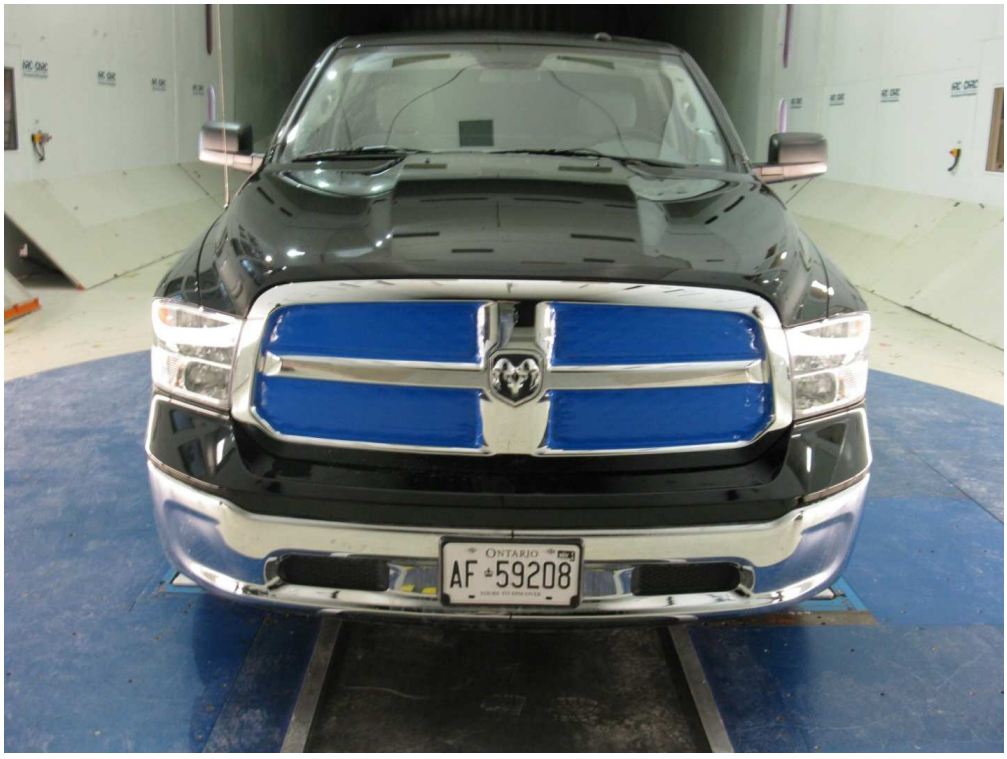

Figure 2.11: Front view of a light-duty vehicle with external cooling grille sealed with blue tape.

of which would partially compensate for the weight of the active suspension. To this end some vehicles were run through the ride height matrix with and without the OEM underbody panels. Due to time and geometry constraints it was not possible to run the complete ride height matrix for each vehicle.

2.6 Bumper and wheel air dams

Air dams are a relatively mature drag reduction technology. A bumper air dam is a strip of material extending from the front bumper, either with an approximately constant depth across the entire width of the vehicle or with varying depth, the largest depth being ahead of the front wheels and the lowest depth at the centre of the vehicle. Bumper air dams experience high drag forces but can reduce net drag by shielding the rest of the underbody from high speed flow. Wheel dams, similar in concept, are strips of material, in some cases flexible, that are typically anchored to the underbody of the vehicle at a strategic position ahead of the front and/or rear wheels to redirect the underbody flow around the wheels. Wheel dams are simple, inexpensive and lightweight but are moderately visible and susceptible to damage in winter conditions. Several vehicles were tested with and without OEM bumper air and/or wheel dams to assess the drag reduction performance of these technologies. Examples of bumper air dams and wheel dams can be seen in Figures 2.12 and 2.13.

2.7 Conceptual active bumper air dams

The potential savings of larger active air dams, that may violate current design specifications for bump and ramp clearance when deployed, was examined with an abbreviated design study for a few vehicles. It was speculated that the results from a larger air dam with the underbody panels removed may compare favourably with the baseline, in which case the cost/weight of the active air dam may be offset by elimination of the underbody panels. The geometry was determined by simple scaling of the vertical dimensions of the OEM air dams, where equipped. Based on favorable results in early tests, the investigation of air dam extension was pursued both separately and in combination with the study of conceptual active ride height, another promising technology, in subsequent tests. Examples of extended OEM and custom-built air dams can be found in Figures B.29(b), B.36 and B.37 in Appendix B.

2.8 Underbody smoothing panels (both OEM and idealized prototypes)

Underbody panels shield bluff underbody components (suspension, transmission, exhaust) from high-energy air. Their use on domestic vehicles has been increasing over the last few model cycles as fuel consumption targets become stricter. Many of the vehicles in this study were equipped with multiple OEM underbody panels, as shown in Figure 2.14(a). The pan-

Figure 2.12: Close-up views of OEM bumper air dams.

(a) Front wheel air dam (b) Rear wheel air dam

Figure 2.13: Close-up views of front and rear wheel air dams.

els were removed systematically so that the effect of each could be evaluated. Panels were removed starting with the rearmost to the foremost, as the upstream panels can have a significant influence on those downstream.

To quantify the maximum potential benefits of a full underbody panel package, without considering weight or cooling trade-offs, several of the vehicles were equipped with idealized, smooth underbodies as shown in Figure 2.14(b). These prototypes allowed for full suspension motion but often covered the exhaust system. Since there was no opportunity to optimize these designs, they may not be completely practical and are not likely to represent a true ideal.

2.9 Other tests

A number of additional tests were conducted for some vehicles to investigate the influence of various options or features on vehicle drag. These include:

- larger-than-baseline wheel/tire packages;
- solid wheel covers;
- front licence plates;
- decorative grille features;
- tailgate configuration (open, closed or removed);
- tonneau covers; and
- side steps.

2.10 Data acquisition, test procedures and analysis

Following standard wind-tunnel procedures at the 9 m Wind Tunnel, the data acquisition system was configured for a sampling time of 40 s per test condition. The recorded time series data were averaged over this sampling period to ensure reliable and repeatable aerodynamic force, dynamic pressure, and wind speed measurements. A repeatability study indicated that the uncertainty margin on the drag area measurements was on the order of 0.25% difference between measurements. Therefore, all variations of drag area in excess of 0.3% or more are considered as statistically significant in this study.

For yaw angle sweeps, after a 5-point yaw angle tare of the wind-off values, the wind speed was increased to the target reference speed of 110 km/h (except for some early tests where a target reference speed of 105 km/h was used) and data were acquired from 0 degree yaw to +10 degree yaw (positive clockwise when facing the flow) in increments of 2 degrees. For some tests, measurements and tares were performed at negative yaw angles as well. For speed sweeps, after a 1-point tare of the wind-off values at 0 degrees, the speed was increased from 60 km/h to 140 km/h in increments of 20 km/h, and aerodynamic force data were measured

(a) OEM underbody panels

(b) Prototype, smooth underbody panels

Figure 2.14: OEM and custom underbody panels on a vehicle. (a) OEM underbody panels (in black) on either side of the engine, cabin floor and immediately ahead of the rear suspension. (b) Prototype, smooth underbody panels.

at each speed step for 40 s. Note that in all cases, the wheel rollers and centre belt speeds were synchronized with the blockage-corrected flow speed in real time.

Wind-tunnel testing occurs in a current of air with finite boundaries (walls and ceiling) that influence the flow around the model as it blocks part of this current. This contrasts real driving conditions where the air is free to expand around the model blockage, without interference from the nearby walls or ceiling. Though the vehicles in the current investigation were relatively small compared to the test section area, corrections for boundary interference effects using the Maskell III blockage correction technique were carried out for all test runs (Hackett and Cooper, 2001). The maximum adjustment to speed and drag area was 5% and 10%, respectively, for the vehicle producing the highest blockage at a yaw angle of 10 degrees, which represents the worst blockage case. All force, speed and yaw data contained in this report have been corrected for blockage effects.

Since precise frontal area data were not available, absolute drag coefficients as typically reported in automotive publications are not presented in this report. Instead, the results are presented in terms of C_DA (drag area in m^2) or percentage changes of drag area with respect to the C_DA of the baseline configuration. C_DA offers a more complete understanding of aerodynamic resistance as it captures the effect of frontal area, which is equally as important as C_D, which captures the efficiency of the vehicle shape. While manufacturers have generally been lowering C_D from model to model, they have often simultaneously increased vehicle size, offsetting the efficiency gains to some degree. Any discussion of vehicle design with the aim of reducing aerodynamic drag must consider frontal area. Vehicle frontal area directly impacts, and can be the most easily changed parameter affecting, drag force and hence fuel consumption due to aerodynamic causes.

In order to take into account that vehicles are generally travelling in a windy environment from potentially all wind azimuth angles, the wind-averaged drag area WAC_DA was calculated for all cases where a yaw sweep from 0 to 10 degrees was carried out. The calculations were based on the procedure suggested by the SAE (2012) for a vehicle speed of 100 km/h. Although this procedure was devised for heavy-duty vehicles, this study has demonstrated its applicability and usefulness for LDVs as well. The SAE procedure assumes:

1. an annual mean wind speed of 11 km/h near the ground in North America;
2. the probability of exceeding a certain wind speed follows a Weibull distribution; and
3. the wind speed has an equal probability of coming from any direction.

Combined with measurement of drag area for a wide range of yaw angles up to 10 degrees, this calculation procedure is an efficient tool to correlate aerodynamic drag reduction with long term fuel efficiency (SAE, 2012).

2.11 Tests in turbulent flow

The influence of flow turbulence on drag reduction technologies for light-duty vehicles was studied. The Road Turbulence System (RTS), developed in a companion study commissioned

by Transport Canada's ecoTECHNOLOGY for Vehicles Program (McAuliffe and D'Auteuil, 2016) and shown to be relevant for the study of the aerodynamics of LDVs by McAuliffe *et al.* (2016), was used for the experiments.

3. Experimental results and discussions

3.1 Test program

Table 3.1 presents a summary of the test program for all the vehicles of this study. An X in the matrix indicates that the particular test category defined earlier was carried out. The active grille shutter/cooling study was performed for all vehicles, while the ride height and OEM air dam studies were done for almost all vehicles. Four vehicles were tested in both smooth and turbulent flow. A description of the runs carried out for each vehicle is found in the test logs for each phase of the study, which are included in Appendix A.

The order of appearance of the vehicles in Table 3.1 follows the order in which the tests were conducted with the exception of small car 2, which was tested in turbulent flow at a later time, immediately prior to pick-up truck 3. A total of 649 runs were conducted over a cumulative period of 47 days in the 9 m Wind Tunnel.

3.2 Baseline tests

The variations of the drag area as a function of yaw angle for the vehicles tested in this study are presented in Figure 3.1 for baseline conditions in smooth flow. The results for cars are shown in the upper graph, whereas those for SUVs, minivans and pick-up trucks are included in the lower graph. Some tests were conducted at a mean wind speed of 110 km/h, while others were performed at 103 km/h. As defined in Section 2.3, the ride height was set to the nominal height measured with occupants of 68 kg in the two front seats for all vehicles except small car 1 and midsize car 6. The grille shutters were closed for all vehicles except pick-up truck 2, which was not equipped with either production or mock-up AGS. The vehicles were on the GESS with the wheels spinning and the belt moving at the blockage-corrected speed of the flow. Exceptionally, midsize car 7 had smooth prototype underbody panels installed for the baseline tests.

The shape of the drag area curves with a minimum at a yaw angle of 0° is typical for light-duty vehicles. As expected, the trucks, minivans and SUVs have higher drag areas than the cars. Not surprisingly, the three pick-up trucks have the highest wind-averaged drag areas of all the vehicles tested. The wind-averaged drag areas of the pick-ups are double those of the lowest-drag vehicles. The drag curve of pick-up truck 2 is significantly higher than that of pick-up trucks 1 and 3. Also notable is large car 1, a large sedan with a wind-averaged drag area that is significantly higher than that of the other cars, and that approaches the small, lowest-drag SUVs, namely small SUV 5 and small SUV 2, in terms of drag performance. Both minivans have drag areas that are comparable to those of the small and mid-size SUVs, with minivan 1 performing better than minivan 2, while standard SUV 2 has the highest drag area out of all the SUVs and minivans. The wind-averaged drag areas of small cars 1 and 3 equal or exceed those of all the midsize cars and approach that of large car 2.

	Test Category										
Vehicle	A1: AGS	A2: cooling	B: ride height	C: custom underbody	D1: OEM underbody	D2: OEM air/ wheel dam	G: air dam/ ride height	H: extended air dam	I: turbulent flow	J: technology combinations	Other
small car 1	X				X	X					wheel covers
midsize car 6	X	X	X		X						
midsize car 7	X		X	X	X	X					wheel covers, licence plate
midsize car 2	X		X	X	X	X		X			
small SUV 1	X	X	X	X	X						wheel covers, licence plate
midsize car 3	X	X		X	X	X					grille smoothed
midsize car 5	X	X	X	X	X						wheel covers, licence plate
midsize car 1	X	X	X		X	X					front end ducts
midsize car 4	X	X	X		X	X					wheel covers
pick-up truck 1	X	X	X	X		X		X			tonneau cover, aftermarket wheels
pick-up truck 2		X			X	X					running boards, aftermarket wheels, tailgate
standard SUV 1	X		X		X	X					
small SUV 2	X	X	X		X	X					
small SUV 3	X	X	X	X							
minivan 1	X		X	X							
small car 2	X		X		X	X	X	X	X		HVAC
large car 1	X	X	X	X	X	X	X	X	X		
standard SUV 2	X	X	X	X		X	X	X	X		
large car 2	X	X	X		X	X					
small SUV 4	X		X	X		X					
small car 3	X		X	X		X	X	X		X	
minivan 2	X		X	X		X				X	
small SUV 5	X	X	X	X							
small SUV 6	X		X	X		X	X	X		X	
pick-up truck 3	X			X		X	X	X	X	X	licence plate, tailgate, windows

Table 3.1: Test Matrix.

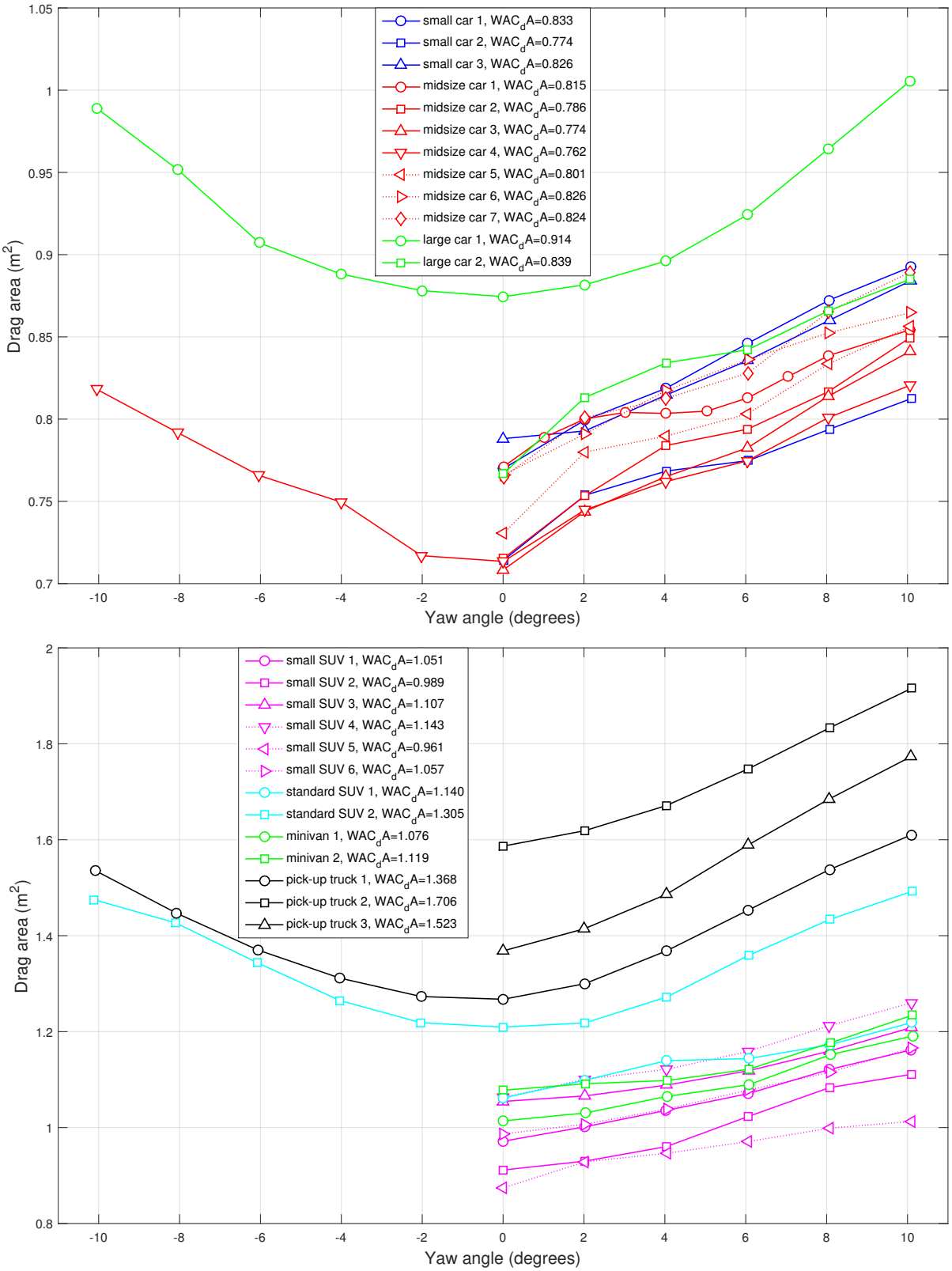

Figure 3.1: Variations of the drag area $C_D A$ in m^2 as a function of yaw angle for all cars (top) and all SUVs, minivans and pick-ups (bottom) tested in smooth flow.

The increase in the drag area with yaw angle is more pronounced for large vehicles with large side areas, such as the pick-up trucks and standard SUV 2, than for smaller vehicles with smaller side areas. It is interesting to note more complex interactions between yaw angle and drag area, especially for midsize car 1, midsize car 5, midsize car 7 and large car 2. This may indicate changing interactions between devices such as bumper or wheel dams or wheel well ventilation.

It is worth underlining that small SUV 3, standard SUV 1 and small SUV 4 have identical drag areas at 0 degree yaw, but the variation of their respective drag areas with yaw angle is different, as are their wind-averaged drag areas. This reinforces the concept of wind-averaged drag area as a more refined approach to characterize the aerodynamic drag associated with a vehicle as opposed to just the drag area at 0 degrees.

Figure 3.2 shows the drag area curves for the four vehicles that were tested in both smooth and turbulent flow. For the pick-up truck and large car, the wind-averaged drag area was lower in turbulent flow than in smooth flow. The opposite was true for the small car and standard SUV. Shape is likely important, and it can be noted that the small car and standard SUV have large side areas, particularly towards the rear of the vehicle.

The influence of the flow turbulence varies with yaw angle to a degree that seems to depend on the type of vehicle. For the large, boxy vehicles (ie. the pick-up truck and standard SUV), there is a greater variation of the effect of turbulence on drag area with yaw angle than for the more streamlined vehicles (ie. the large car and the small car). The drag area in turbulent flow is higher than in smooth flow at 0 degrees and reverses to lower than in smooth flow at

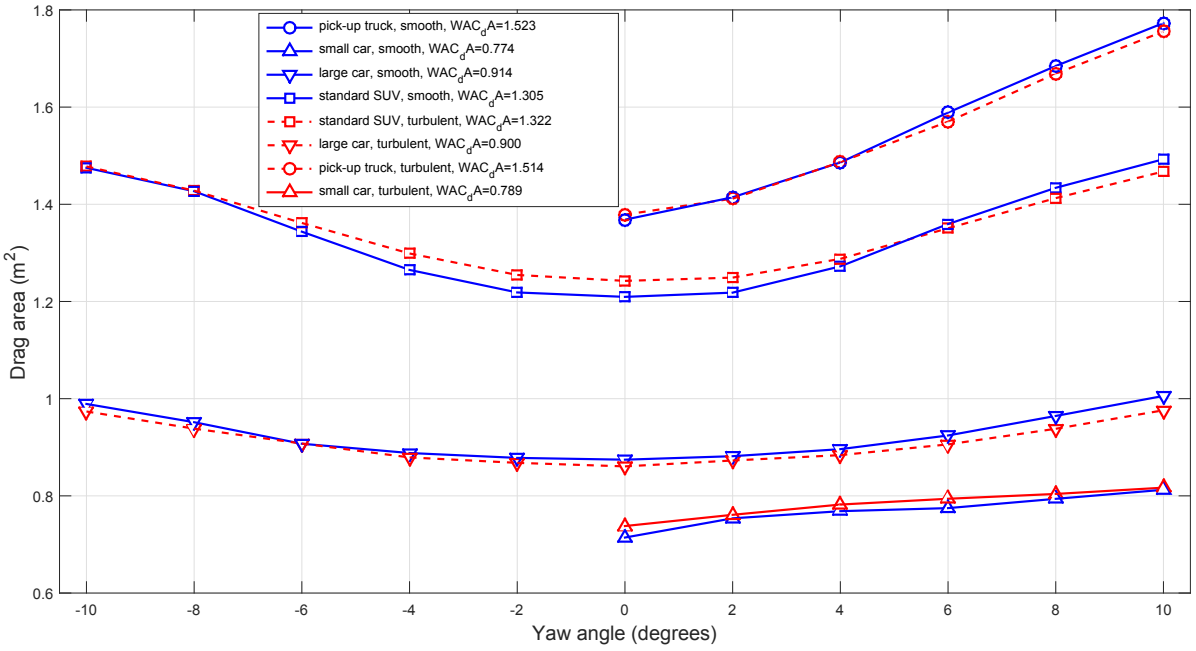

Figure 3.2: Variations of drag area as a function of yaw angle for the vehicles tested in smooth and turbulent flow.

6 to 10 degrees for the boxy vehicles. By comparison, the drag area is consistently lower or higher, respectively, in turbulent flow than in smooth flow for the more streamlined vehicles. Sharper edges might trigger more changes in the flow around the boxy vehicles with changes in wind direction. However, for all four vehicles, incoming turbulent flow tended to flatten the baseline drag area versus yaw angle curve with respect to the smooth flow case, making the drag of the vehicle slightly less sensitive to changes in wind angle.

Turbulent wind tunnel flow had a slightly larger effect on the overall drag of the more streamlined vehicles than on that of the more boxy vehicles. The changes in wind-averaged drag due to incoming turbulent flow was +1.9% and -1.5% for the small and large cars, respectively, and +1.3% and only -0.6% for the standard SUV and pick-up truck, respectively.

Figure 3.3 presents the variation of drag area at 0 degrees with speed for all vehicles at baseline, smooth flow conditions. The data for cars are shown in the upper graph while that of SUVs, minivans and pick-up trucks are plotted in the lower graph. The speed was varied from approximately 60 km/h to 140 km/h, in increments of roughly 20 km/h.

For a number of vehicles, Figure 3.3 shows that the drag area drops with increasing speed and reaches a plateau in the 100 to 120 km/h range, above which it remains constant. This is consistent with the common assumption that the drag coefficient of light-duty vehicles is insensitive to speed, and consequently to Reynolds number, at typical highway speeds and beyond. Since the Reynolds number represents the ratio of inertial forces to viscous forces, this implies that viscous or surface effects become negligible compared to inertial or pressure drag at these speeds. However, the drag area of certain vehicles clearly continues to decrease with speed even up to 140 km/h. This is particularly noticeable for minivan 1, small car 2, standard SUV 1 and small SUVs 2, 3 and 4. In contrast, the drag area of large car 1 and small SUV 5 increases slightly with speed in this range. These results indicate that the speed at which the drag coefficient becomes insensitive to Reynolds number is a function of vehicle shape and cannot be assumed to be the same for all vehicles. This may have implications for the analysis of coast-down tests as well as for consistency in the drag coefficient values claimed by different OEMs.

3.3 Active grille shutter and cooling study (test categories A1 & A2)

3.3.1 Closing the AGS

The wind-averaged drag area measured with the active grille shutters (AGS) opened and closed is shown in the bar graphs of Figure 3.4 for all vehicles in smooth flow conditions. Cars are shown in the upper graph, while the larger vehicles are shown in the lower graph. The light blue shaded area represents the wind-averaged drag area for the baseline case of Figure 3.1 with the grille shutters 100% closed. The magenta shaded area on top of the light blue represents the additional wind-averaged drag area associated with completely opening the grille shutters. The reduction in wind-averaged drag area that can be achieved by closing the grille shutters is represented in Figure 3.5.

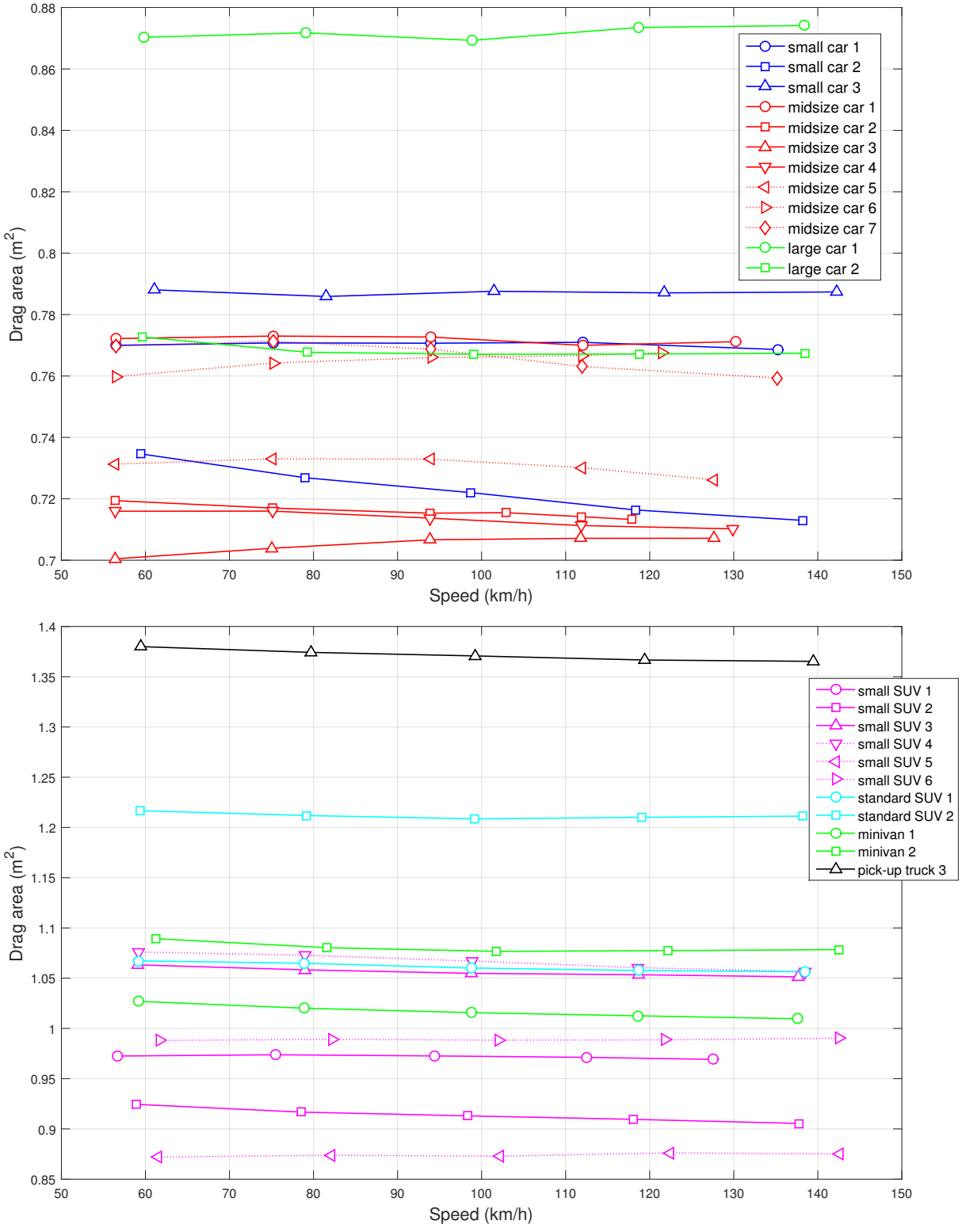

Figure 3.3: Variations of the drag area $C_D A$ in m^2 as a function of speed at 0 degree yaw for all cars (top) and all SUVs, minivans and pick-ups (bottom) tested in smooth flow.

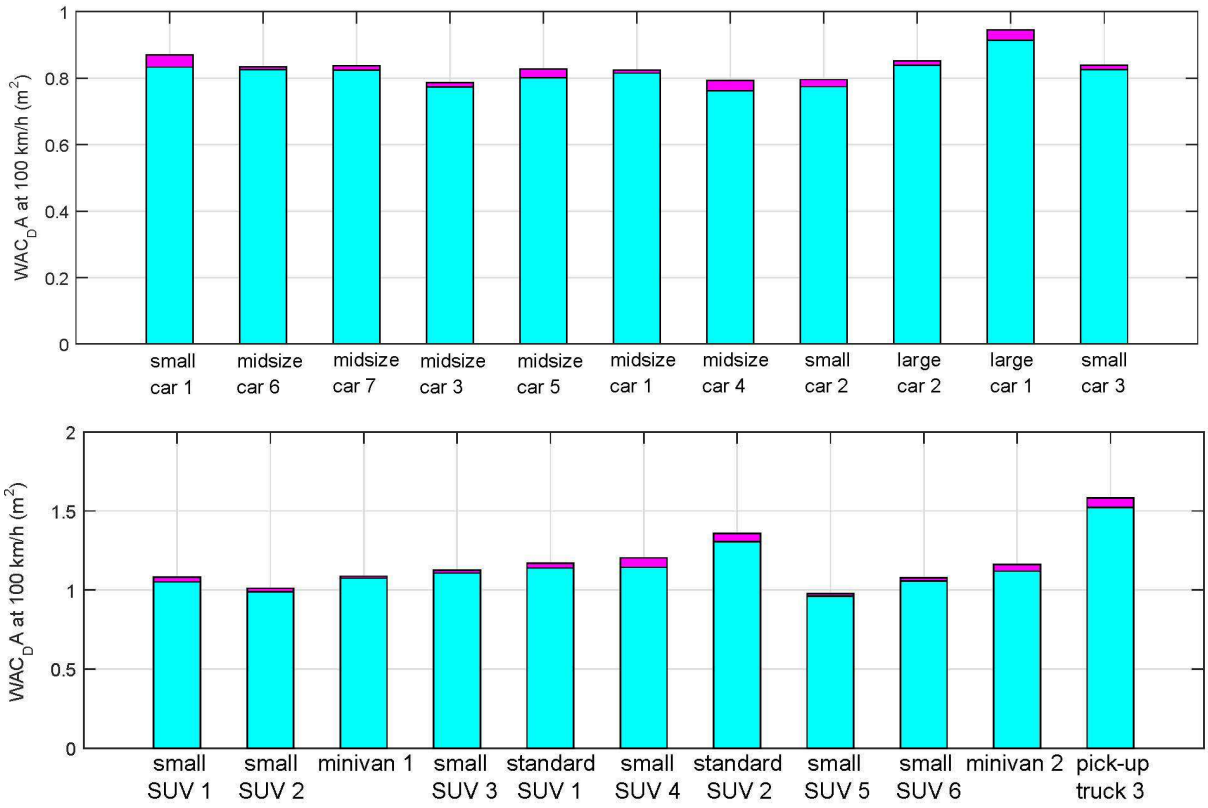

Figure 3.4: Wind-averaged drag area for cars (top) and larger vehicles (bottom) in smooth flow with the grille shutters opened and closed. Shutters closed (light blue); additional wind-averaged drag area associated with fully opening the shutters (magenta).

The results indicate that the grille shutters were effective at reducing drag for all vehicles in smooth flow. Closing the shutters reduced the wind-averaged drag area by 1 to 5% depending on the vehicle. Open shutter yaw angle sweeps were not done for midsize car 2 and pick-up truck 1, but closing the AGS reduced the drag area at 0 degree yaw by close to 3% for both vehicles.

AGS performance is thought to be a function of vehicle design rather than vehicle class or size. The extent to which the frontal area of the radiator is shielded by the shutters likely affects the drag reduction capability of the AGS. It is thought that the more the flow is blocked from entering the engine compartment and reaching the radiator, the lower the drag area. Vehicles with AGS that completely or nearly completely cover the radiator (such as pick-up trucks 1 and 3, small car 1, small SUVs 1 and 4, both standard SUVs and both minivans) are thus expected to experience a larger percentage drop in drag area than vehicles for which the AGS only partially cover the radiator (such as small cars 2 and 3, large car 1 and small SUVs 5 and 6). Figures 3.4 and 3.5 support this assertion with some exceptions. Similarly, in a vehicle where upper and lower sections of the AGS can be closed independently, such as pick-up truck 3, the amount of drag reduction achieved by closing one section of the shutters appeared to be related to the amount of radiator area covered by that section.

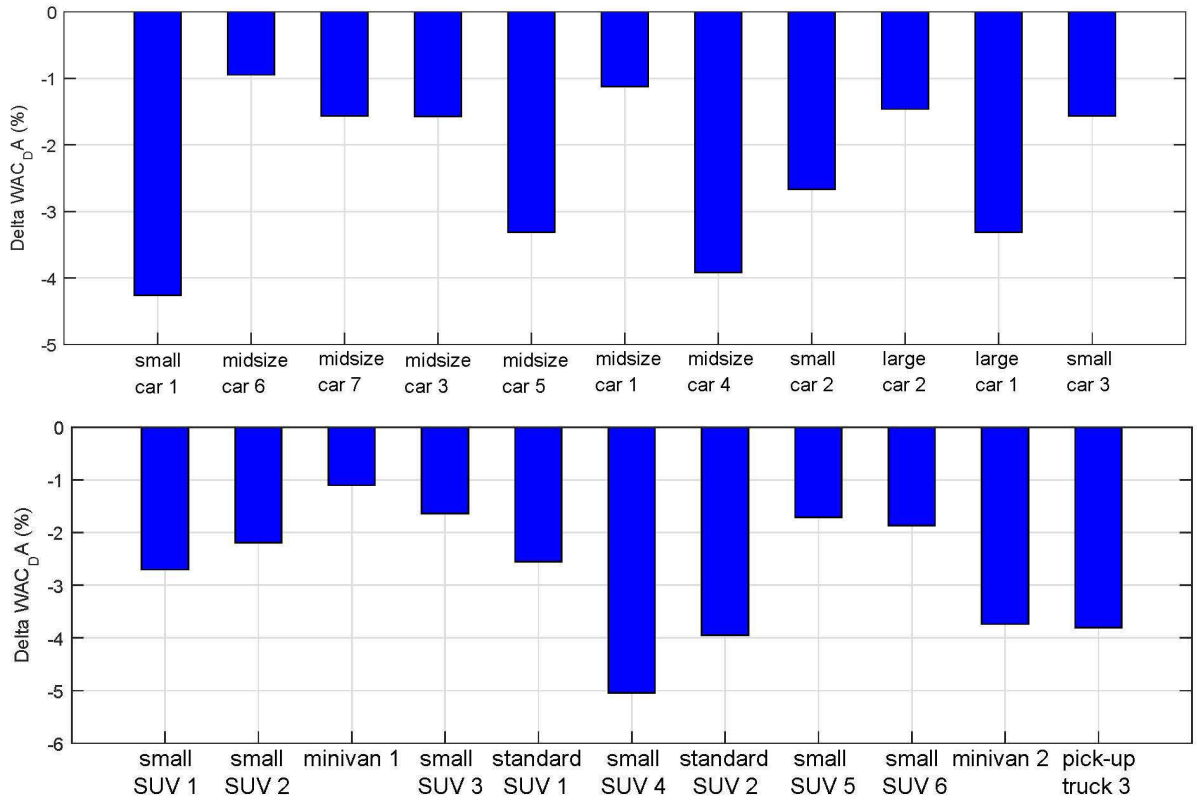

Figure 3.5: Percentage of reduction in wind-averaged drag area due to closing the grille shutters of cars (top) and larger vehicles (bottom) in smooth flow.

The exceptions to the above-mentioned assertion include minivan 1, for which closing the AGS, which cover the entire radiator, only reduced the wind-averaged drag by approximately 1%. It was observed that flow through the front end and in the engine compartment of minivan 1 is relatively more obstructed than for small SUV 4 and both standard SUVs. Also, large car 1 and small car 2, whose AGS cover only the lower part of the radiator, produced a greater reduction in drag than the full-coverage AGS of standard SUV 1. It appears that the effectiveness of the AGS in reducing the drag area is dependant not only on the proportion of AGS coverage but also on the flow pattern at the entrance and in the engine compartment. If the volume around the engine is restrained by several ancillary devices (often seen in hybrid vehicles), the flow in the engine compartment is already somewhat restricted, and the drag area appears to be less dependant on whether or not the flow through the radiator is reduced with the AGS.

AGS performance was found to also depend on speed for some vehicles. However, the variation with speed of drag area reduction at 0 degrees due to AGS closure was of the order of 1% or less.

3.3.2 Sealing the AGS/radiator inlet or external grille

Potential drag reduction missed through imperfect execution of the AGS system can be evaluated by sealing the AGS by solidly taping the flaps shut or alternatively, by sealing the radiator inlet. Leakage may be due to flex of the AGS flaps, tolerances required for manufacturing and thermal expansion or hysteresis in the actuation mechanisms. Figure 3.6 shows the change in drag area at 0 degree yaw caused by sealing either the closed AGS or the radiator inlet with tape. The tests were conducted in smooth flow and with a prototype smooth underbody installed on all vehicles except small car 1, midsize cars 1 and 6 and small SUV 2. A potential drag reduction of more than 0.5% was identified for seven of the vehicles. For five of these vehicles, the potential reduction was approximately 1 to 1.4%. Considering the total drag reduction possible with perfectly sealed grille shutters could be on the order of between 3 and 5% for these vehicles, losing 0.5 to 1.5% of the potential improvement is significant.

For certain vehicles, the external grille was completely sealed with tape in order to quantify how closely the AGS realize the maximum potential benefit of sealing the cooling system. The percentage reduction in drag area at 0 degree yaw, as compared to the closed shutter case, is shown in Figure 3.7 for some vehicles. For these vehicles, sealing the external grille resulted in significantly greater drag area reductions than sealing the AGS system. Potential drag area reductions at 0 degree yaw of over 6% for pick-up truck 2 and midsize car 1, and of more than 11% for midsize car 6 were identified. Interestingly, Figure 3.5 shows that midsize car 6's AGS system was one of the least effective at reducing drag among all the cars. Figure 3.6 shows that this was not due to leakage. Rather, the large reduction in drag area shown in Figure 3.7 suggests that the external grille design, which determines how the air gets to the AGS system, has a greater impact on the drag area than the AGS flap design for this vehicle. The same can be concluded for all vehicles shown in both Figure 3.6 and Figure 3.7.

The effect of sealing the external grille on the wind-averaged drag area is shown in Figure 3.8 for a number of vehicles. Reductions of between 3 and 6% compared to the closed shutter case were measured for midsize cars 1 and 5, pick-up truck 1 and large car 2. The tests on pick-up truck 1, standard SUV 2 and small SUV 4 were conducted with a prototype smooth underbody installed; all other vehicles were referenced to baseline conditions.

Since the results shown in Figures 3.7 and 3.8 are compared to the AGS closed condition, it could be assumed that the effect would be additive. For example, a properly designed external AGS system should be able to realize a reduction in wind-averaged drag of almost 7% for midsize car 1 (1.1% from AGS closure + 5.6% from external sealing). The potential reductions in drag are very large, but likely smaller than what could be achieved by redesigning the front fascia shape to take maximum advantage of this effect. Finally, for 3 of the 4 vehicles for which results were plotted in both Figures 3.7 and 3.8, the percentage reduction of wind-averaged drag area was less than that of drag area at 0 degree yaw, underlining the importance of considering wind-averaged drag to evaluate drag reduction performance.

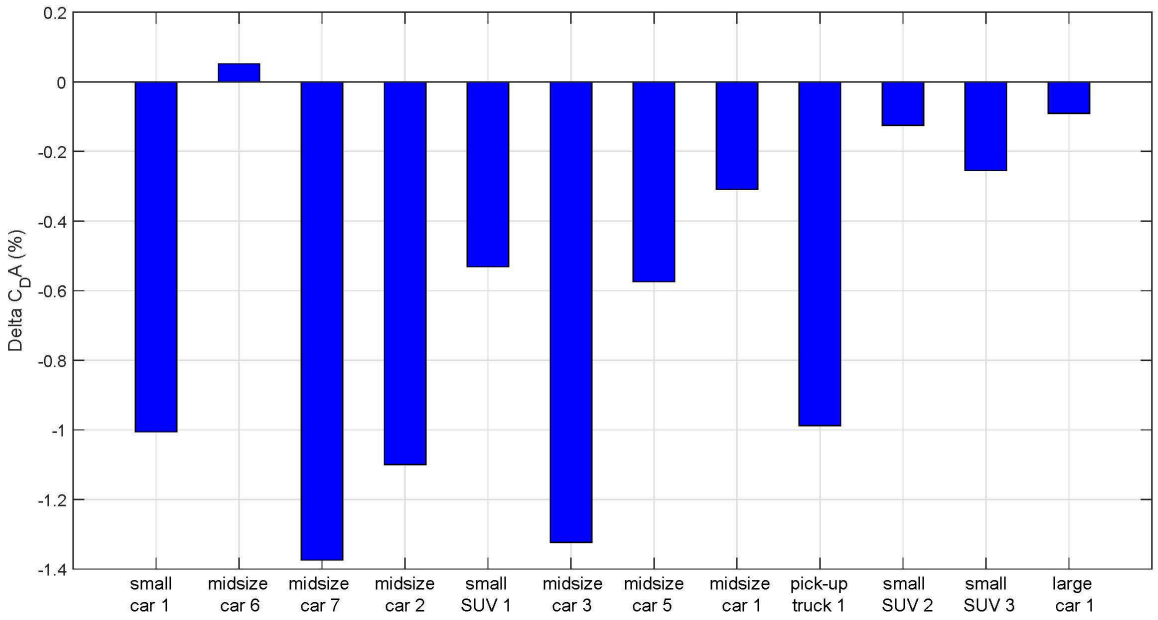

Figure 3.6: Change in drag area at 0 degree yaw due to sealing the AGS flaps or radiator inlet with tape. Tests were conducted in smooth flow at the respective reference wind speed for each vehicle, with a prototype smooth underbody installed on all vehicles except small car 1, midsize cars 1 and 6 and small SUV 2.

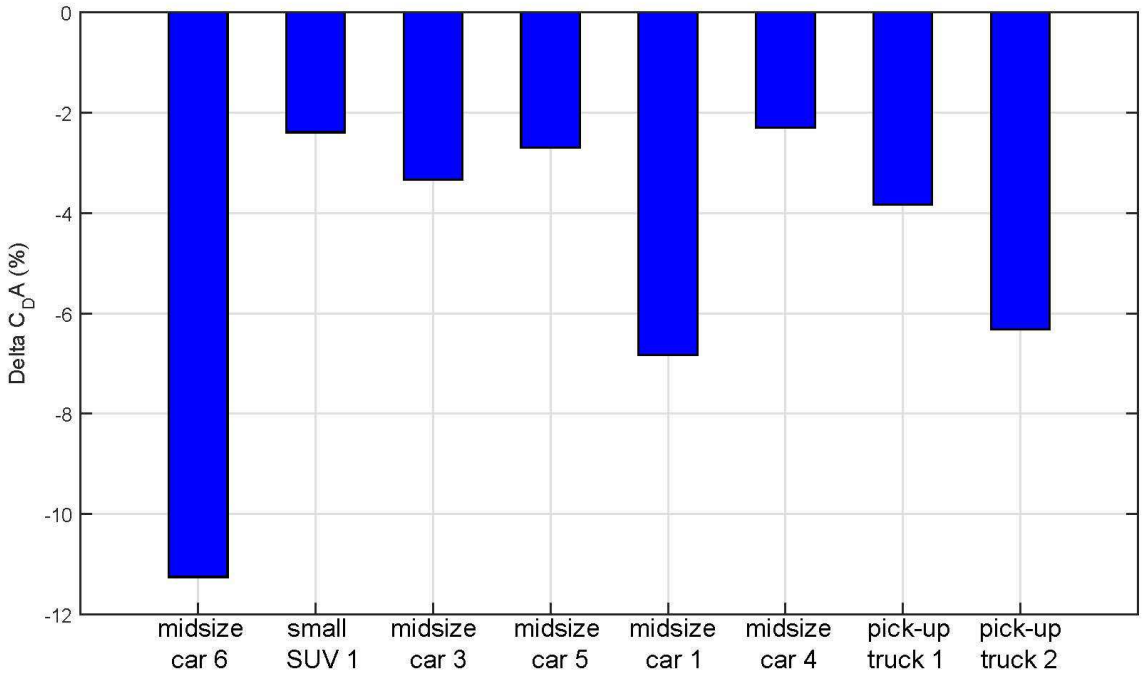

Figure 3.7: Change in drag area at 0 degree yaw due to sealing the external grille with tape with respect to the closed shutter case. Tests were conducted in smooth flow at the respective reference wind speed for each vehicle. A prototype smooth underbody was installed on pick-up truck 1, while all other vehicles are referenced to baseline.

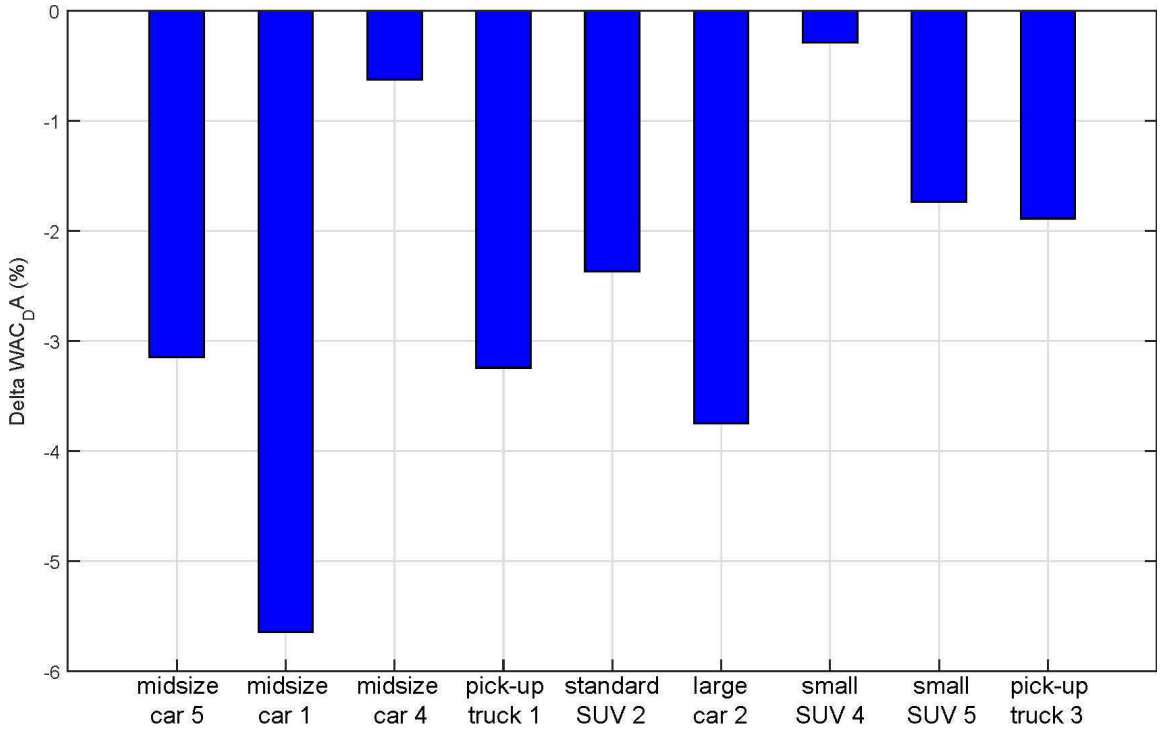

Figure 3.8: Change in wind-averaged drag area due to sealing the external grille with tape with respect to the closed shutter case. Tests were conducted in smooth flow at the respective reference wind speed for each vehicle. A prototype smooth underbody was installed on pick-up truck 1, standard SUV 2 and small SUV 4, while all other vehicles are referenced to baseline.

3.3.3 Influence of turbulence on closing/sealing AGS or external grille

The influence of flow turbulence on AGS performance is shown in Figure 3.9. It can be seen that the AGS remained effective when tested in turbulent flow, but that the turbulence influenced their performance to varying degrees depending on the vehicle. The influence of flow turbulence was strongest for the small car, lowering the drag reduction performance of the AGS by 50%. Turbulent flow had a small to negligible effect on the AGS of the large car and pick-up truck.

Turbulent flow had no statistically significant effect in two other tests of the pick-up truck's cooling system: closing only the lower shutter section of the AGS and sealing the external grille. The results of the latter test are illustrated in Figure 3.10, which also shows that flow turbulence reduced the effectiveness of sealing the external grille of the standard SUV by about 1% in terms of wind-averaged drag area reduction.

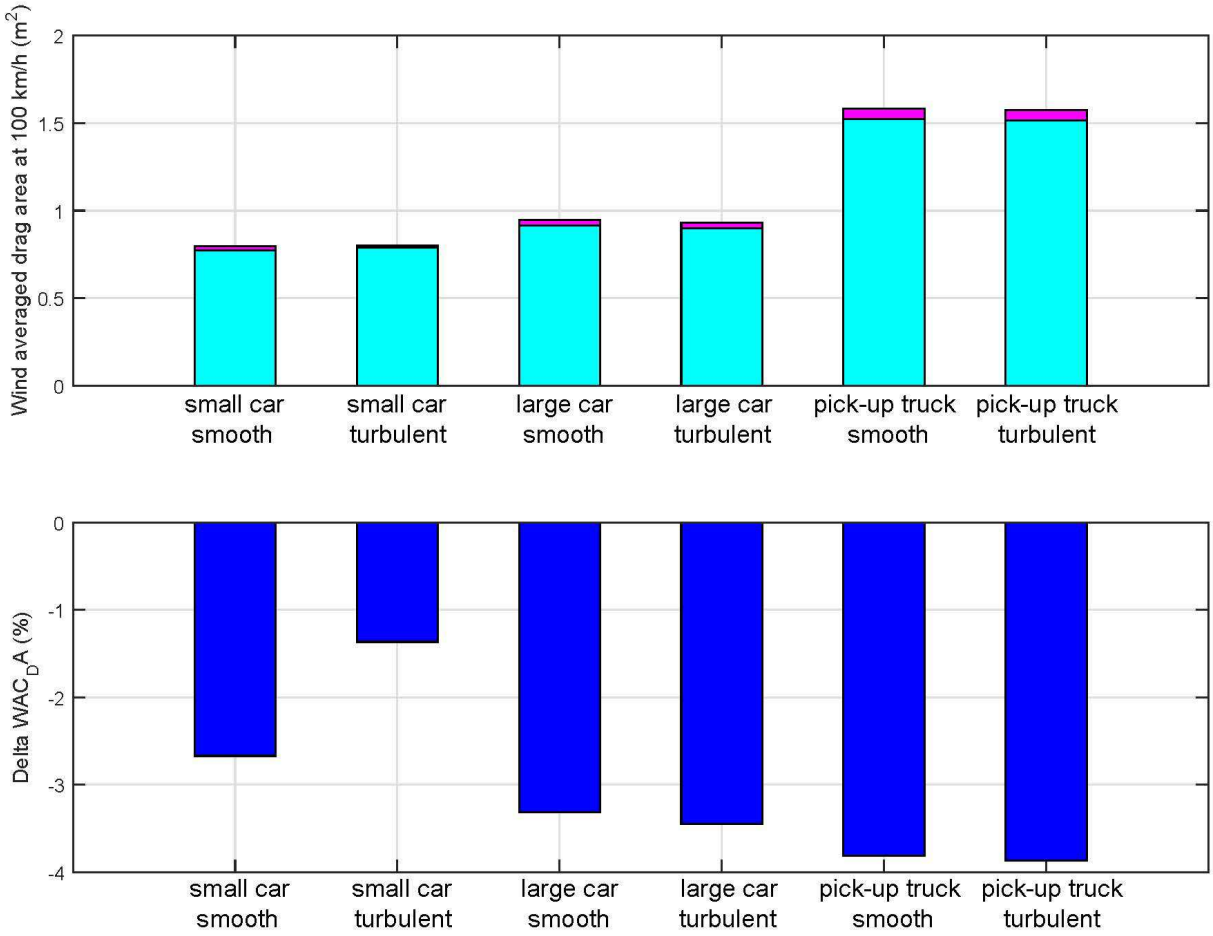

Figure 3.9: Wind-averaged drag area in m^2 (top) and percentage of wind-averaged drag area reduction due to closing grille shutters (bottom) for vehicles tested in smooth and turbulent flow. Shutters closed (light blue); additional wind-averaged drag area associated with fully opening the shutters (magenta).

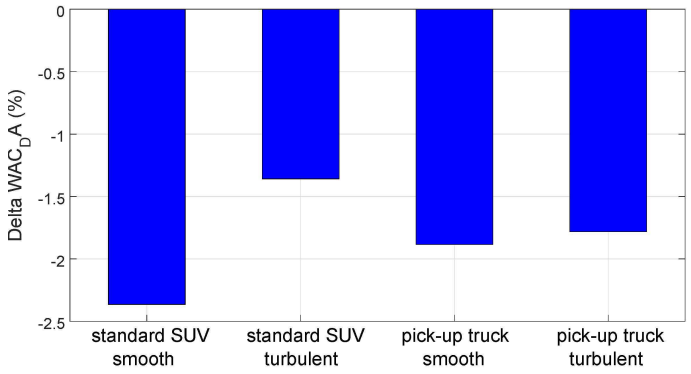

Figure 3.10: Change in wind-averaged drag area due to sealing the external grille with tape with respect to the closed shutter case. Tests were conducted in smooth and turbulent flow at the respective reference wind speed for each vehicle. A prototype smooth underbody was installed on the standard SUV, while the pick-up truck is referenced to baseline.

3.3.4 Grille shutter closing sweeps

For all vehicles equipped with an AGS, a shutter closing sweep was carried out in smooth flow at zero degree yaw and two wind speeds to determine the relationship between shutter fractional closing and drag reduction. For these tests, a representative of Röchling Automotive or Magna International sat on the front passenger seat in the vehicle to adjust the opening of the grille shutters, and remained in the vehicle during the tests. Typical results for a number of cars and larger vehicles are shown in Figure 3.11.

It can be seen that the percentage of total drag area reduction for a given percentage of shutter closure varies significantly between the different vehicles. For roughly 50% shutter closure (45% for small SUV 5), the results vary from an increase in the drag area of 9% of the amount of total drag area reduction for small SUV 5 to a reduction of 57% of the total amount for large car 1. For 75% shutter closure (flaps at 60 degrees), the drag area reduction varies between 43% and 85% of the amount corresponding to 100% closure, the latter amount corresponding to large car 1 at 100 km/h. Pick-up truck 3 is the only vehicle among the examples shown for which 75% closure produced less than 50% of the total drag area reduction at both speeds, and is the only vehicle for which the grille shutters completely cover the radiator.

For less than 50% shutter closure, small increases in drag area were measured for small SUV 5. Although these increases are within the uncertainty of the drag measurements, the process appears to be influenced by the speed of the flow. The flaps have relatively low torsional stiffness. For the smaller closing percentages, the flaps can act as guide vanes and re-direct the flow in a favourable or unfavourable direction. Although 45% shutter closure increases the drag area compared to the open shutter case for small SUV 5 at 100 km/hr, this shutter configuration becomes favourable for drag reduction at 120 km/hr, as shown in Figure 3.11. In general, only about 10% of the maximum drag reduction can be achieved with 25% shutter closure.

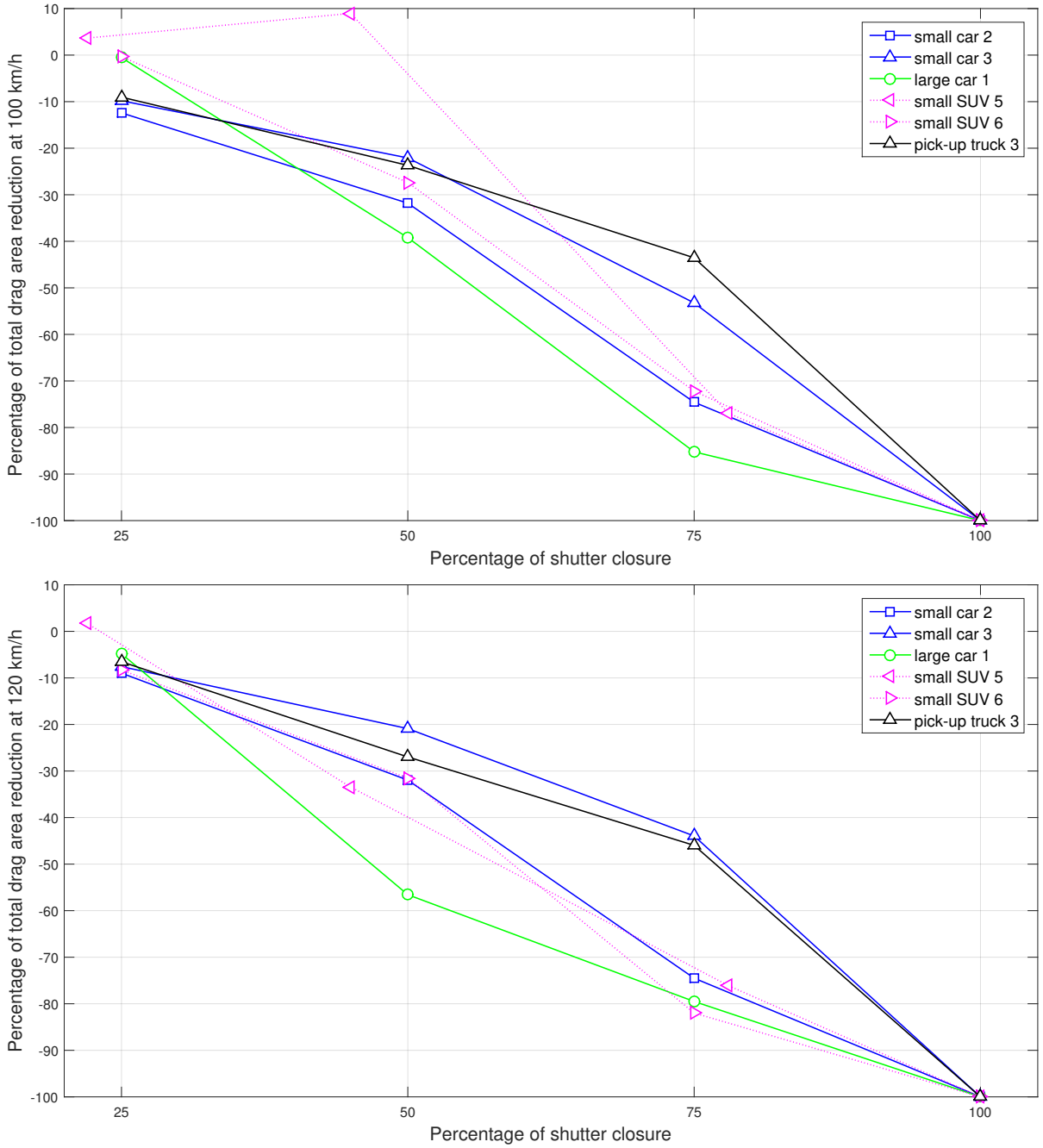

Figure 3.11: Percentage of total drag area reduction as a function of percentage of closure of the AGS at zero degree yaw. Tests were conducted in smooth flow at 100 km/h (top) and at 120 km/h (bottom). The AGS covered the entire radiator for pick-up truck 3 and only the lower part of the radiator for all other vehicles.

3.4 Influence of wheel dams (test category D2)

Wheel dams were observed to be an effective technology to reduce drag with a few exceptions. For cases where front and rear wheel dams were removed independently, front wheel dams were often found to be more effective at reducing wind-averaged drag area than rear wheel dams. In fact, removing only the rear wheel dams almost always reduced the wind-averaged drag area of the vehicle.

Some examples of the effect of wheel dams on drag area as a function of vehicle yaw angle are shown in Figures 3.12 to 3.15. The figures depict variations in drag caused by systematically removing the wheel dams (front or rear or both) relative to a reference condition where the wheel dams were installed. Positive deltas indicate that the wheel dams were effective at reducing the drag area.

The positioning and the dimensioning of the wheel dams to achieve drag reduction not only at 0 degree yaw but also for larger yaw angles is a difficult task. Wheel dam drag reduction performance was almost always better at 0 degree yaw than at the highest yaw angle and

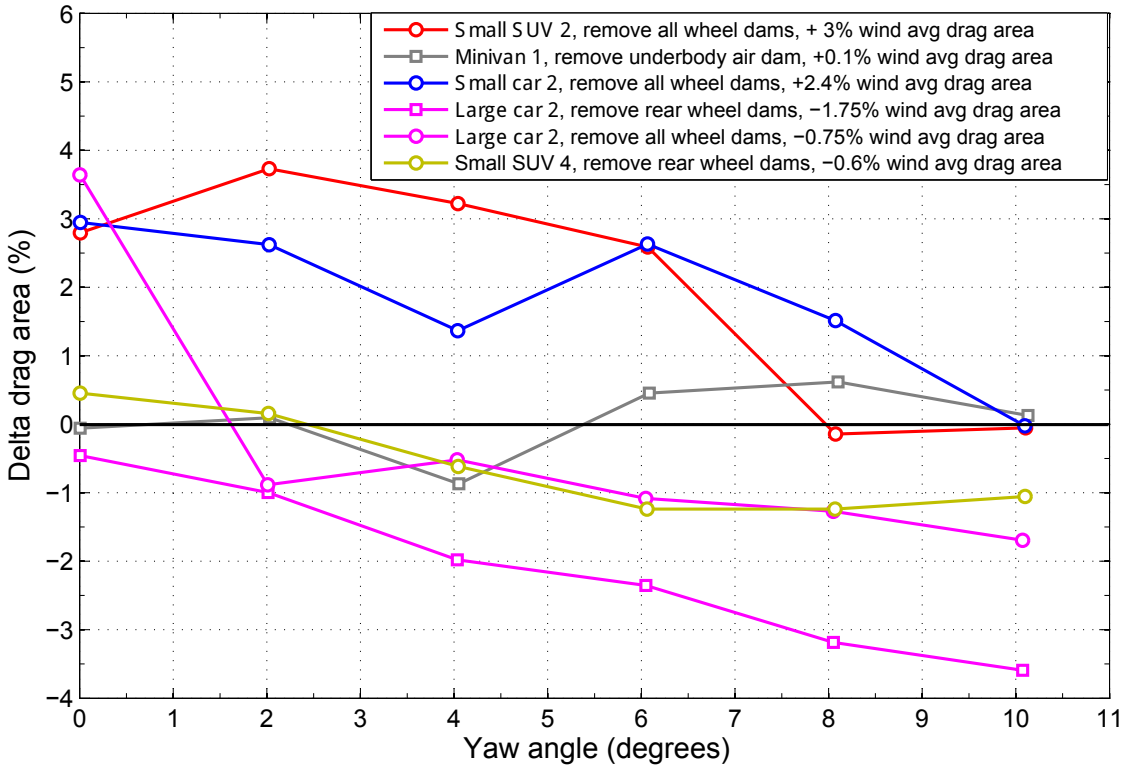

Figure 3.12: Variations of drag area (%) as a function of yaw angle for four vehicles. In all cases, the wheel dams (front and/or rear) were removed. Negative delta drag area indicates that the drag area was actually reduced when the wheel dams were removed when compared to the reference conditions.

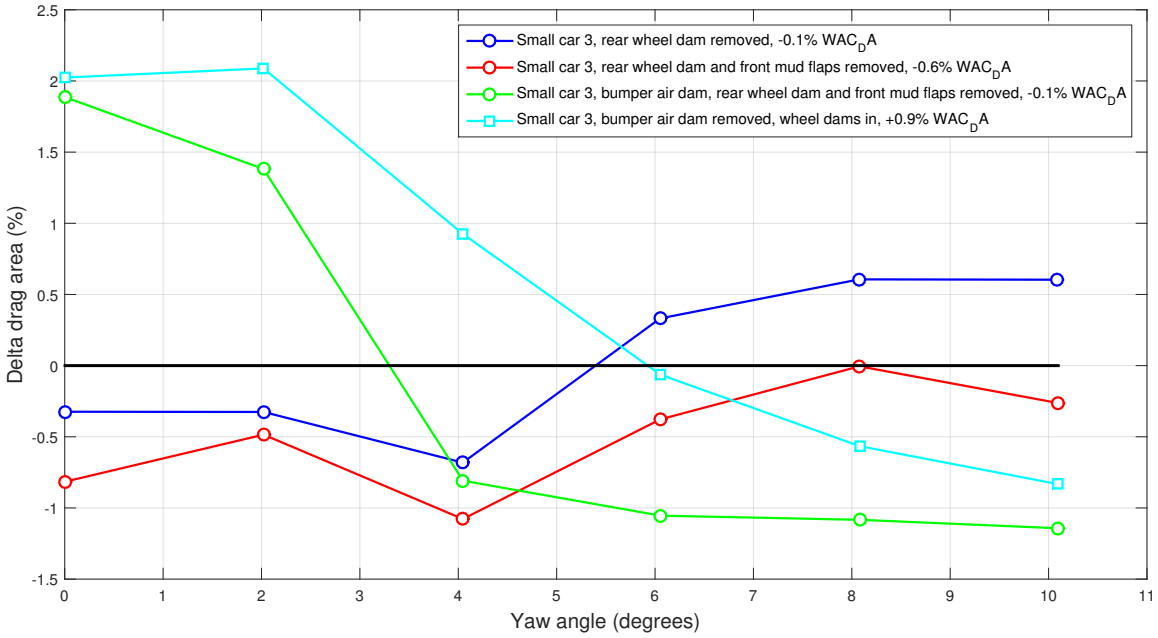

Figure 3.13: Variations of drag area (%) due to wheel dam removal with respect to baseline conditions (shutters 100% closed, baseline ride height) as a function of yaw angle for small car 3.

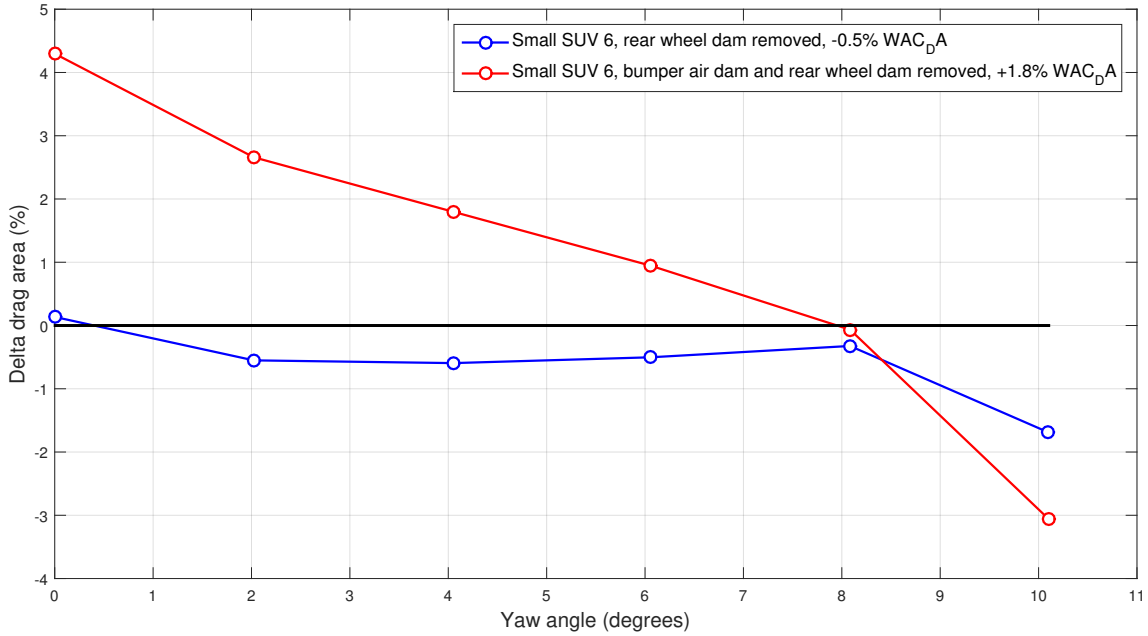

Figure 3.14: Variations of drag area (%) due to wheel dam removal with respect to baseline conditions (shutters 100% closed, baseline ride height) as a function of yaw angle for small SUV 6.

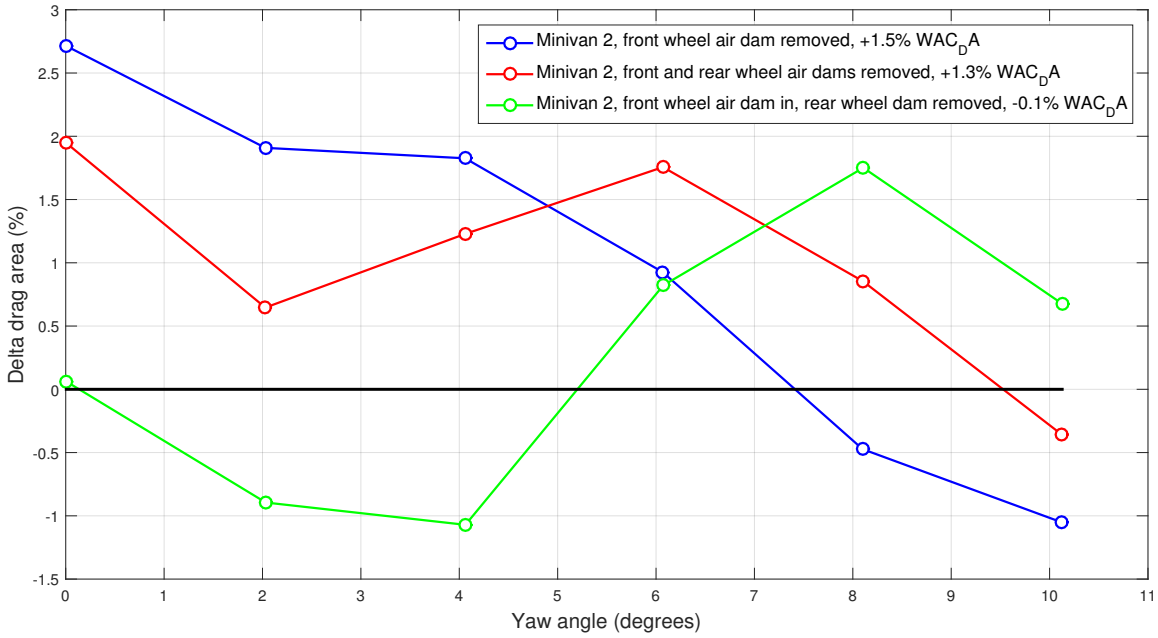

Figure 3.15: Variations of drag area (%) due to wheel dam removal with respect to baseline conditions (shutters 100% closed, baseline ride height) as a function of yaw angle for minivan 2.

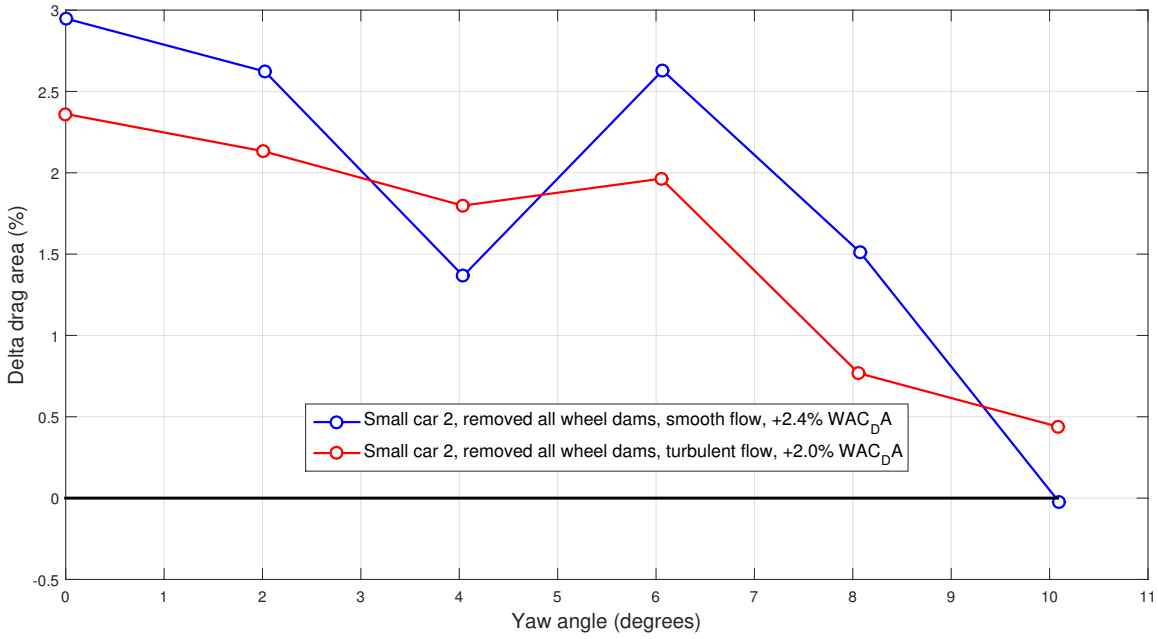

Figure 3.16: Variations of drag area (%) due to wheel dam removal with respect to the reference condition (shutters 100% closed, baseline ride height and all OEM underbody panels removed) as a function of yaw angle for small car 2 in smooth and turbulent flow.

generally degraded with increasing yaw angle. Exceptions to this are the rear wheel dams of minivan 2 and small car 3, which increased drag at low yaw angles but reduced drag at high yaw angles. Optimal positioning requires a good understanding and simulation of the flow field underneath the vehicle. The NRC GESS aims to reproduce on-road underflow vehicle conditions with wheel rollers and a moving ground plane between the wheels. While the simulation provided by such a 5-belt system is not as high-fidelity as that of single or 3-belt systems, for which the ground ahead of the wheels is moving with respect to the vehicle, Wittmeier *et al.* (2016) have demonstrated that the advantages of 5-belt systems, including lower measurement uncertainty, greater repeatability, more accurate ride height adjustment and quicker and easier underfloor access, outweigh those of single- or 3-belt systems for testing vehicles with reasonably high ground clearance, which includes most passenger cars.

Figure 3.12 shows that the wheel dams of small car 2 and of small SUV 2 were particularly effective, reducing drag area by 3% or more at specific yaw angles, and providing a wind-averaged drag area reduction 2.4% and 3%, respectively. These values are significant. The front wheel dams of large car 2 and the rear wheel dams of small SUV 4 (which are quite large) reduced drag only at 0 degree yaw (by over 3.5% for large car 2). The underbody air dam of minivan 1 produced a marginal drag reduction at yaw angles larger than 4 degrees.

The set of front and rear wheel dams of minivan 2 were effective at reducing drag at all but the highest yaw angle, whereas the rear wheel dams reduced drag only for yaw angles larger than 5 degrees. However, the combination of rear wheel dams and front mud flaps of small car 3 increased drag at all yaw angles with and without the bumper air dam installed, and the rear wheel dams of small SUV 6 increased the drag at all yaw angles except 0. For these and other vehicles where the changes in drag area are shown as negative in the figures, it appeared that the technology did not reduce the drag area and might have been optimized for a different function such as splash and spray management or soiling reduction.

The influence of turbulence on wheel dam performance was investigated for a small car. Figure 3.16 presents the results of removing both front and rear wheel dams of small car 2 in smooth and turbulent flow. The variations are given relative to the reference condition with the shutters 100% closed, baseline ride height and all OEM underbody panels removed.

Removing the small car's wheel dams in turbulent flow had a similar but slightly smaller positive effect on drag reduction than in smooth flow, producing a wind-averaged drag area reduction of 2.0%. Although small, this difference of 0.4% between smooth and turbulent flow can be considered statistically significant. In turbulent flow as in smooth flow, drag area reduction due to removal of the wheel dams generally decreased with increasing yaw angle except for a peak at 6 degrees. Wheel dam drag area reduction was lowest at the largest yaw angle of 10 degrees, where it was negligible in smooth flow but just over 0.4% in turbulent flow.

3.5 Influence of bumper air dams (test category D2)

Early tests showed that bumper air dams can have a significant impact on drag, producing changes in drag coefficient ranging from +1% to almost -6% at 0 degree yaw, depending on the vehicle. However, subsequent tests have revealed that the effectiveness of bumper air dams is highly dependent on yaw angle, so that their overall performance should be evaluated in terms of wind-averaged drag area reduction. The shape of the air dam appears to be an important factor governing its effectiveness over a range of yaw angles.

Figure 3.17 illustrates the influence of removing the OEM bumper air dam for a number of vehicles tested in smooth flow. Drag area reductions in excess of 4% can be observed for certain yaw angles. The OEM air dams of large car 1 and pick-up truck 3 have profiles with approximately constant depth across the vehicle, while those of large car 2, small SUV 6 and small car 3 have profiles that vary significantly across the vehicle width. The profiled OEM air dams of small SUV 6 and small car 3 have larger depths ahead of the front wheels and extend across the entire width of the front bumper to cover most of the wheel width. In contrast, the air dam of pick-up truck 3 is narrower than the front bumper and covers only half of the width of the front wheels. The bumper air dam of large car 1, although of approximately constant depth like that of pick-up truck 3, extends the entire width of the front bumper like those of small SUV 6 and small car 3.

It is theorized here that differences in bumper air dam shape explain the differences in the drag area reduction versus yaw angle curves for these vehicles. The air dams of large car 1 and pick-up truck 3 have a maximum effectiveness at or near 0 degree yaw, corresponding to a

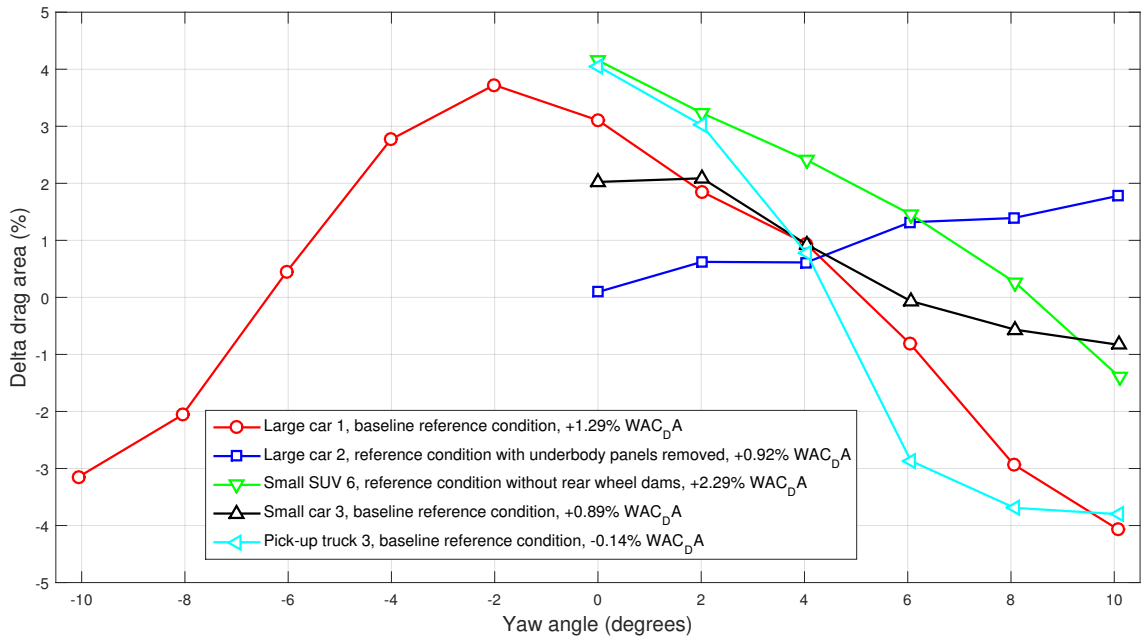

Figure 3.17: Change in drag area as a function of yaw angle due to removing the OEM bumper air dam compared to a reference condition with the air dam installed.

3 to 4% decrease in drag area, which steadily decreases to a roughly equivalent maximum drag penalty at 10 degrees yaw. The effectiveness of the air dam of large car 2 steadily increases from close to drag-neutral at 0 degrees to a maximum at 10 degrees. However, in terms of wind-averaged drag reduction at 100 km/h, the large car air dam designs produced reductions of the order of 1%, while the pick-up truck air dam had a negligible effect. It is interesting to note that at 0 degree yaw, the OEM bumper air dam of pick-up truck 3 was more effective than that of pick-up truck 2, which provided only a 1% reduction. The deeper air dam of pick-up truck 3 is likely the reason for this.

The similarly-shaped profiled air dams of small SUV 6 and small car 3 produced a maximum drag area reduction of 2 to 4% at near-head-wind conditions, and their effectiveness decreased more gradually with increasing yaw angle than that of the near-constant depth air dams of pick-up truck 3 and large car 1. The profiled air dams became only slightly detrimental at the highest yaw angle, for a net reduction in wind-averaged drag area of the order of 1% and 2%, respectively.

The shorter width of the pick-up truck air dam is likely the cause of its reduced effectiveness in reducing wind-averaged drag compared to those of large car 1, small SUV 6 and small car 3. Indeed, the design of the pick-up truck air dam, which stops short of the outer edges of the front bumper ahead of the wheels, opposes that of the profiled air dams which become deeper ahead of the wheels. The profiled air dams' greater overall width and increased depth ahead of the front wheels, particularly for small SUV 6 whose air dam wraps around the front wheels, was likely responsible for their effectiveness at reducing drag area at up to greater yaw angles (up to 6 degrees for small car 3 and up to 8 degrees for small SUV 6) than the near-constant depth air dams. It can be concluded that proper shielding of the front wheels is important in assuring that the drag reduction efficiency of the bumper air dams extends to greater yaw angles, resulting in a net increase in efficiency, characterized by a net decrease in wind-averaged drag area, for all driving conditions.

Figure 3.18 illustrates the influence of removing the OEM bumper air dams of two vehicles in both smooth and turbulent flow. Turbulence caused a small and barely statistically significant net increase in the efficiency of the bumper air dams across the range of yaw angles, producing reductions of 0.31% and 0.36% in wind-averaged drag area compared to the smooth flow case for the large car and pick-up truck respectively. For the pick-up truck, this was entirely due to a greater than 1% increase in effectiveness at a yaw angle of 6 degrees, as the air dam was slightly less effective in turbulent flow at all other yaw angles tested. The air dam of the large car was more effective in turbulent flow than in smooth flow at all yaw angles tested.

The influence of extending the OEM air dam was also studied; the results will be presented subsequently in this report in conjunction with changes in ride height for some of the vehicles.

3.6 OEM underbody panels (test category D1)

OEMs use underbody panels to shield the rough underbody and improve the fuel efficiency of their vehicles. The drag reduction associated with OEM underbody panels was evaluated at 0

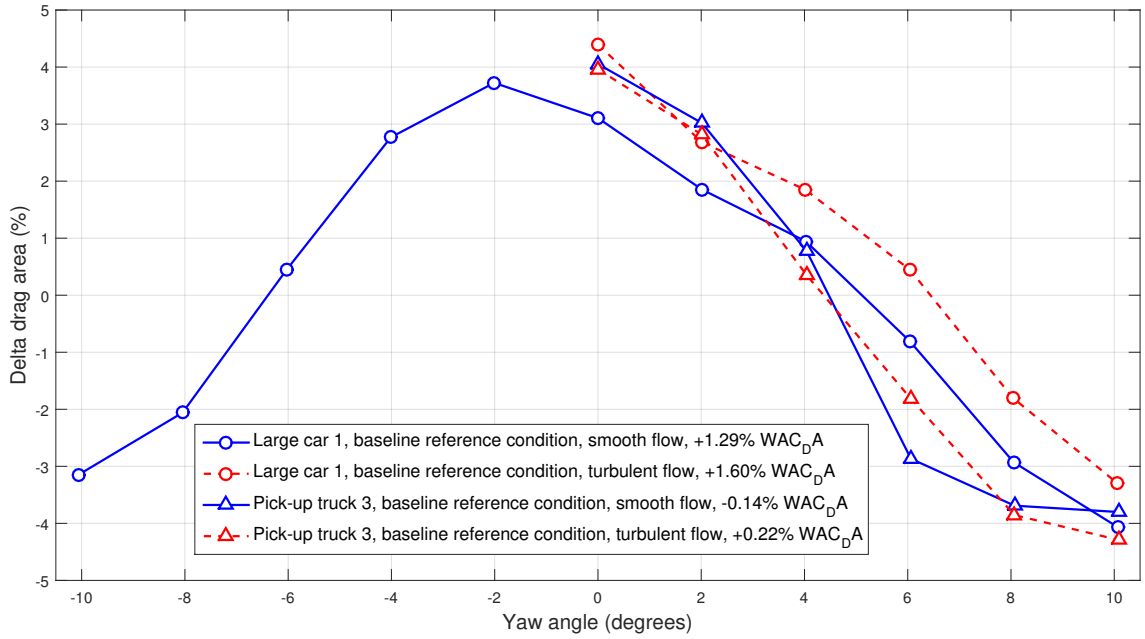

Figure 3.18: Change in drag area as a function of yaw angle due to removing the OEM bumper air dam compared to the baseline configuration (shutters 100% closed, air dam installed) in both smooth and turbulent flow.

degree yaw for the 10 vehicles equipped with this technology early in this study. A systematic study over the full yaw angle range, required to evaluate the wind-averaged drag reduction, was performed in smooth flow for four vehicles and repeated in turbulent flow for one of these vehicles.

For the tests at 0 degree yaw, Figure 3.19 shows the change in drag area due to removing the OEM underbody panels. Removing the production underbody increased the drag of all vehicles by 0.8% to 5.3%, indicating that all underbody panel systems were effective at reducing drag at 0 degrees. Removing the underbody panels of midsize cars 4, 5 and 6 increased the drag by over 4.6%, while removing those of midsize cars 1 and 3 and small car 1 increased drag by between 3% and 3.6%. The panels of midsize car 7, small SUV 1 and pick-up truck 2 had the smallest effect, as removing them increased drag by less than 1.6%. The effectiveness of vehicle underbody panels at reducing drag can be attributed to good panel design or poor underbody design.

The wind-averaged drag area results are summarized in the bar graph of Figure 3.20. The experiments were carried out by removing underbody panels section by section, typically in three stages: rear only; rear and middle sections; rear, middle and front sections. In Figure 3.20, a positive sign of the deltas indicates that the wind-average drag area increased when the underbody panels were removed compared to the wind-averaged drag area for the baseline conditions. A negative sign indicates the opposite; removing the underbody panel actually reduced the drag area of the vehicle, which is not desirable. The latter was observed for small car 2 and standard SUV 1. Removing the panels at the rear of the vehicles (leaving 2/3 of

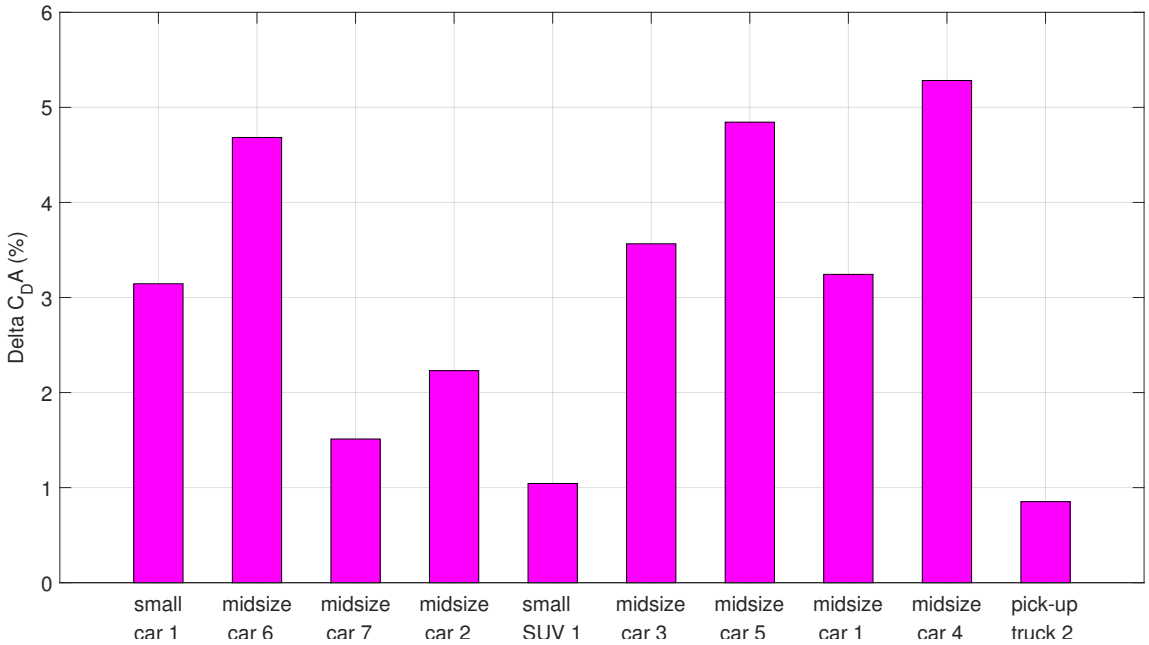

Figure 3.19: Change in drag area at 0 degree yaw associated with the removal of OEM underbody panels, compared to the reference condition with the panels installed.

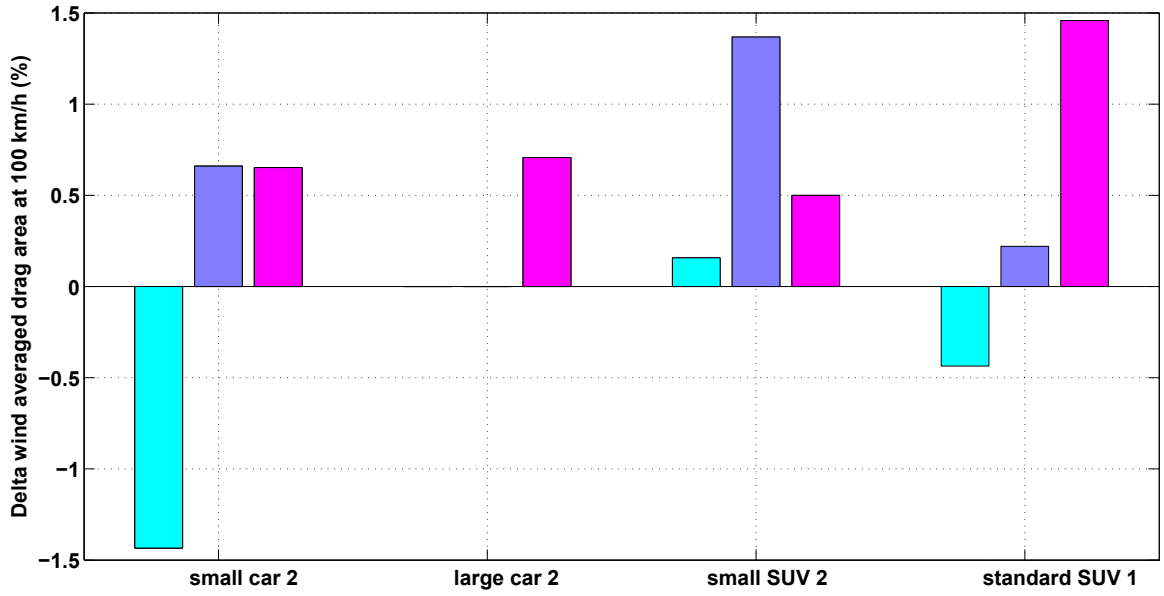

Figure 3.20: Variations of wind-averaged drag area associated with the removal of OEM underbody panels. The test sequence was: 1) removal of rear panels only (pale blue); 2) rear and middle sections (blue); and 3) rear, middle and front sections (magenta).

the underbody paneling in place) reduced the wind-averaged drag area by 0.4% and 1.4%, respectively. It is thought that removing these panels increased the clearance between the underbody of the vehicle and the ground at the rear of the vehicle, creating a stronger underbody diffuser and reducing drag. Subsequently removing the middle underbody panel (leaving 1/3 of the underbody paneling in place) increased the wind-averaged drag area by approximately 0.7% above the baseline case for small car 2. This value was unchanged by removing the front panel (leaving no underbody paneling in place). The front underbody panel alone thus had no effect on the wind-averaged drag area, but produced the lowest wind-averaged drag area when paired with the middle panel only. Installing the front panel as part of the full OEM underbody panel configuration also resulted in lower wind-averaged drag area than for the uncovered underbody in smooth flow. The full underbody paneling systems of all of the vehicles were effective at reducing drag, with reductions in wind-averaged drag area ranging from 0.5 to 1.5%.

The same test procedure was repeated for small car 2 in turbulent flow. The results are summarized and compared with the smooth flow data in the bar graph of Figure 3.21. The underbody panels of the small car had a different effect in turbulent flow. Removing the rear panel had a similar positive effect in turbulent flow but reduced the wind-averaged drag area by roughly half a percent more than in smooth flow, to 1.9% below the baseline value. Removing the middle panel increased the wind-averaged drag area to 0.4% below the baseline value. Removing the front panel further increased the wind-averaged drag area to just 0.1% below baseline, which is not a significant difference. The full OEM underbody panel configuration was thus ineffective as a drag reduction technology for the small car in turbulent flow. The front panel alone produced a small but barely significant reduction in wind-averaged drag area compared to the uncovered underbody. The lowest wind-averaged drag area in turbulent flow was obtained with the front and middle underbody panels, as was the case in smooth flow.

Figure 3.22 shows the change in drag area as a function of yaw angle for the different underbody panel configurations of small car 2 in smooth and turbulent flow compared to the corresponding baseline condition. It can be seen that in both flow regimes, all three underbody panel sections were effective at reducing drag at the two highest yaw angles, and the front and middle panel sections were also effective at reducing drag at 0 degree yaw. However, all panels were more effective in smooth than in turbulent flow at these yaw angles, and in fact less detrimental to drag reduction in smooth flow at all yaw angles except 2 degrees.

3.7 Custom underbody cover study (test category C)

Extending the underbody panels to completely cover the undersurface of a light-duty vehicle is an emerging drag reduction technology. This proved to be an efficient way to reduce drag. Early results, obtained at 0 degree yaw only, showed drag reduction ranging from 0.5% to 8% for full prototype underbody covers with respect to the baseline OEM underbody panels. The highest reduction of 8% was measured for pick-up truck 1. Pick-up trucks are not generally equipped with aerodynamic underbody panels, their underbody being typically designed for durability and off-road clearance rather than aerodynamic efficiency, so any type of paneling would be expected to have a significant effect on drag. In terms of wind-averaged drag area,

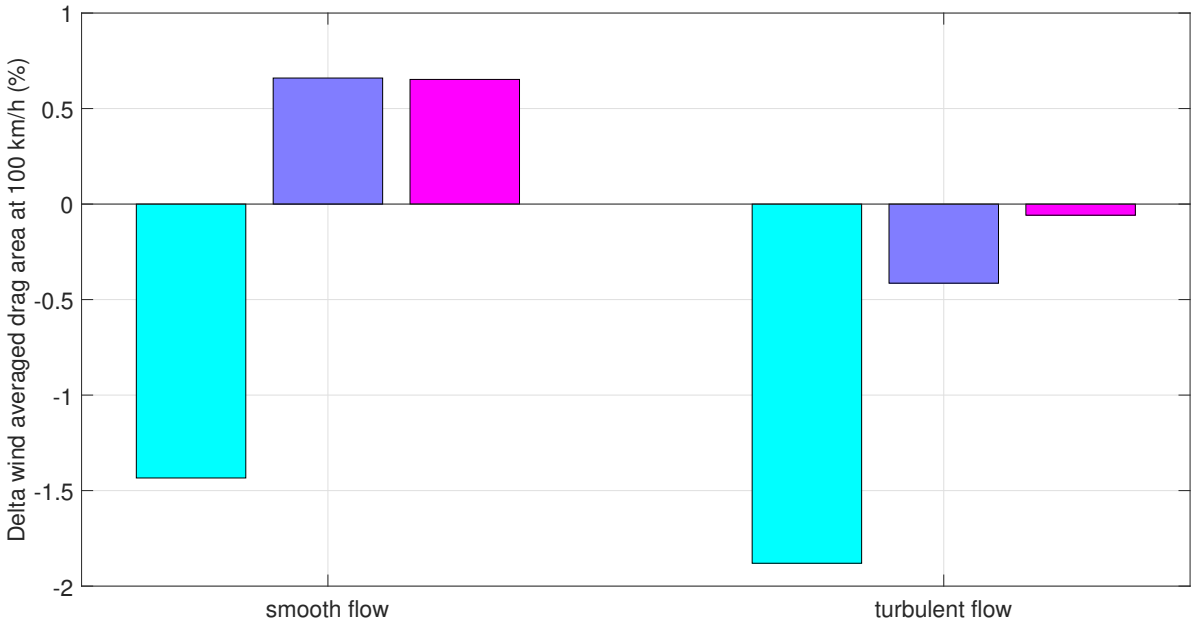

Figure 3.21: Variations of wind-averaged drag area associated with the removal of OEM underbody panels from small car 2 in smooth and turbulent flow. The test sequence was: 1) removal of rear panels only (pale blue); 2) rear and middle sections (blue); and 3) rear, middle and front sections (magenta).

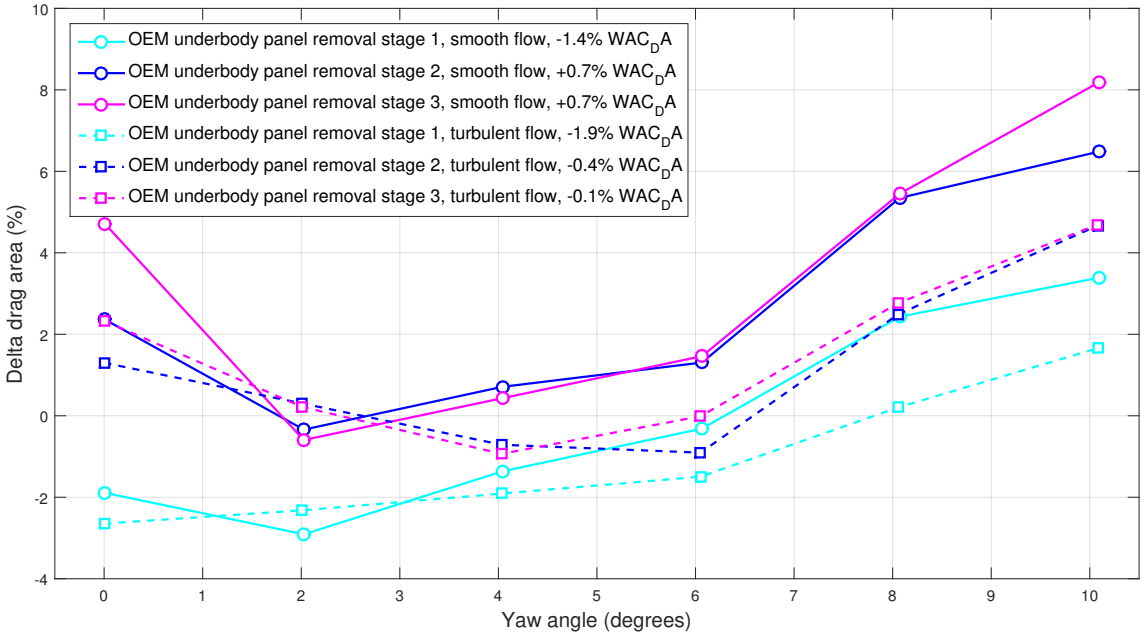

Figure 3.22: Change in drag area with respect to baseline conditions as a function of yaw angle associated with the removal of OEM underbody panels from small car 2, grille shutters 100% closed, in both smooth and turbulent flow.

reductions of 3% to almost 7% were measured for 7 of the 10 vehicles for which this technology was evaluated over a range of yaw angles.

Full underbody covers were custom built and installed at NRC by Röchling Automotive and NRC staff. A typical example of a prototype smooth underbody covering made by Röchling Automotive at NRC can be seen in Figure 3.23.

The efficiency of the custom underbody covers as a drag reduction technology was studied by removing the cover section by section, similar to the procedure used for the OEM underbody panels. The test sequence was 1) underbody fully covered with panels (100% covered); 2) rear section removed (75% covered); 3) rear and middle section removed (25% covered); and 4) all panels removed (including the OEM engine cover if any). The technology was evaluated for 10 vehicles in smooth flow, two of which were also tested in turbulent flow for comparison.

Figure 3.24 presents a bar graph of the reduction of wind-averaged drag area associated with extended underbody coverings for ten vehicles in smooth flow. Significant wind-averaged drag area reductions, of up to 6.8% for minivan 2 with a full underbody cover, were observed. Pick-up truck 3 was close behind, with reductions of close to 5% with the full underbody cover and 6.5% with the front and middle section panels only. These results are not surprising, as pick-up truck underbody design, as previously noted for pick-up truck 1, is generally optimized for off-road underbody clearance and durability rather than for aerodynamic efficiency.

Figure 3.23: Views from below of the underbody of a vehicle completely covered with custom panels, with the exception of the covering of the engine compartment which is a standard OEM part. (Picture taken during the lifting process of the vehicle in the test section of the 9 m Wind Tunnel).

Figure 3.24: Variations of wind-averaged drag area associated with the removal of custom underbody panels for ten vehicles. The test sequence was: 1) underbody completely smooth (pale blue); 2) removal of rear panels only (blue); 3) removal of rear and middle section panels (magenta). Results for each configurations are compared to the baseline where the rear, middle and front section were removed.

Also notable is the 4.5% reduction in wind-averaged drag area for small SUV 4 with a full underbody cover. Wind-averaged drag area reductions of around 3% or more were measured for seven of the ten vehicles in Figure 3.24, the exceptions being small car 3, large car 1 and small SUV 5. A 2% wind-averaged drag area increase was observed for small SUV 5 when the engine compartment was covered with a custom panel compared to the baseline condition which includes an OEM engine cover. This indicates that the aerodynamics of the front end of small SUV 5 has already been optimised with a partial covering around the base of the engine.

For four vehicles, small car 3, small SUV 5, minivan 1 and pick-up truck 3, the wind-averaged drag area was lower for the 75% smooth underbody with the rear custom panel removed than for the fully covered underbody. Similar results were observed for the OEM underbody panels of small car 2 and standard SUV 1. It is believed that the presence of the extra underbody panel at the rear attenuated the potential positive effect of an underbody diffuser by reducing the clearance between the underbody and the ground at the rear of the vehicle.

Half of the vehicles shown in Figure 3.24 experienced an increase of wind-averaged drag, significant in the case of small SUV 5 and standard SUV 2, when only the front section panels were in place compared to the baseline configuration. It is hypothesized that smoothing the front of the underbody increases the propensity of high speed flow to hit the rough underbody of the vehicle, which suggests that underbody coverings work in tandem.

The front panel only configuration of minivan 1 resulted in a 2% decrease in drag with respect to baseline at 0 degree yaw. However, this drop reversed to an increase of 2% at 2 degrees and remained positive at 4 degrees. This led to an overall increase in wind-averaged drag of 0.5%, which would have been missed by considering only the drag at 0 degree yaw.

Turbulent flow results for large car 1, standard SUV 2 and pick-up truck 3 are plotted in Figure 3.25. The custom underbody coverings of the pick-up truck and standard SUV were more effective in turbulent flow than in smooth flow in terms of drag reduction with respect to baseline conditions. The full underbody coverings of standard SUV 2 and pick-up truck 3 reduced the wind-averaged drag area (with respect to baseline conditions) by 1.2% and 1.4% more, respectively, in turbulent flow than in smooth flow, as shown by the pale blue bars in Figure 3.25. The opposite was true for the large car, for which the full cover was 0.3% less effective (in terms of wind-averaged drag area reduction with respect to baseline conditions) in turbulent flow compared to smooth flow, which is a small but statistically significant difference.

Absolute wind-averaged drag area values, as opposed to deltas, are listed in Table 3.2 for the various custom underbody configurations of the three vehicles shown in Figure 3.25. The absolute wind-averaged drag area was lower in turbulent flow than in smooth flow for all three vehicles and for all custom underbody cover configurations with the exception of the 75% smooth configuration for standard SUV 2, for which it was essentially the same in both flow regimes. The biggest difference was noted for the full underbody cover of the pick-up truck, for which the wind-averaged drag area was over 2% lower in turbulent than in smooth flow. This is larger than the 1% difference noted for the large car, and the insignificant difference for the standard SUV, with the full custom underbody.

Figure 3.26 shows the variation of drag area as a function of yaw angle for each of the custom underbody covering cases of pick-up truck 3 in both smooth and turbulent flow. In all cases,

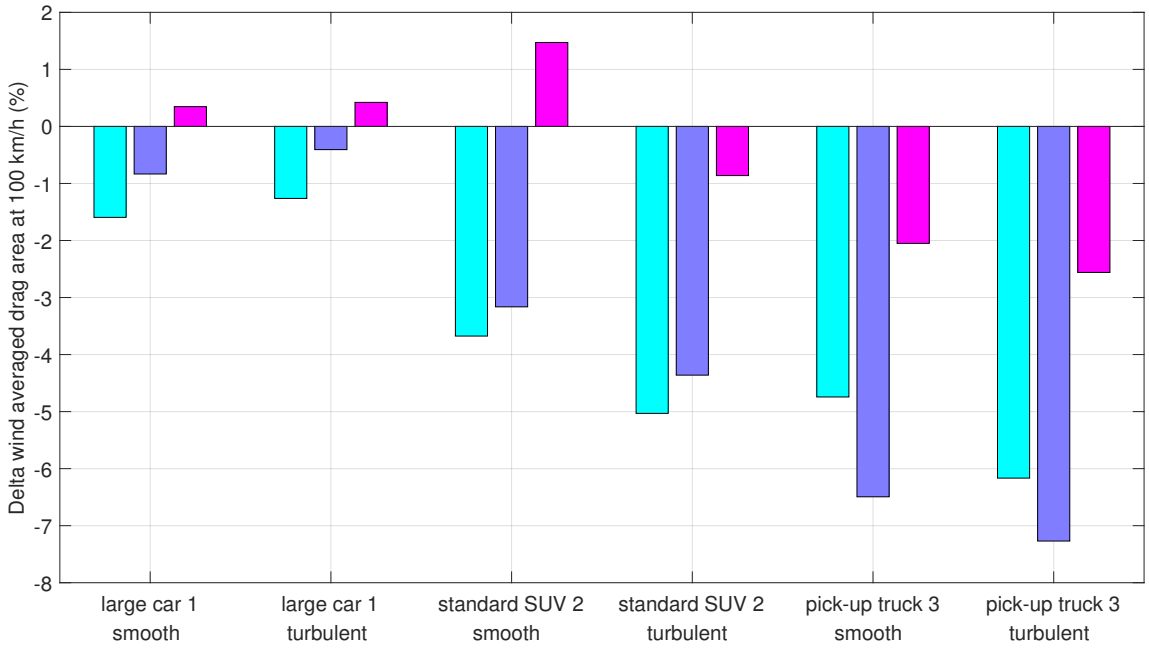

Figure 3.25: Variations of wind-averaged drag area associated with the removal of custom underbody panels from three vehicles tested in smooth and turbulent flow. The test sequence was: 1) underbody 100% covered (pale blue); 2) removal of rear panels only (blue); and 3) removal of rear and middle section panels (magenta). Results for each configurations are compared to the baseline where the rear, middle and front sections were removed.

		Wind-averaged Drag Area (m^2)	
Vehicle	**Configuration**	**Smooth flow**	**Turbulent flow**
Large car 1	100% smooth underbody	0.900	0.889
	75% smooth underbody	0.907	0.897
	25% smooth underbody	0.918	0.904
Standard SUV 2	100% smooth underbody	1.256	1.255
	75% smooth underbody	1.263	1.264
	25% smooth underbody	1.324	1.310
Pick-up truck 3	100% smooth underbody	1.451	1.421
	75% smooth underbody	1.424	1.404
	25% smooth underbody	1.492	1.475

Table 3.2: Wind-averaged drag area associated with the custom underbody cover configurations of three vehicles in smooth and turbulent flow.

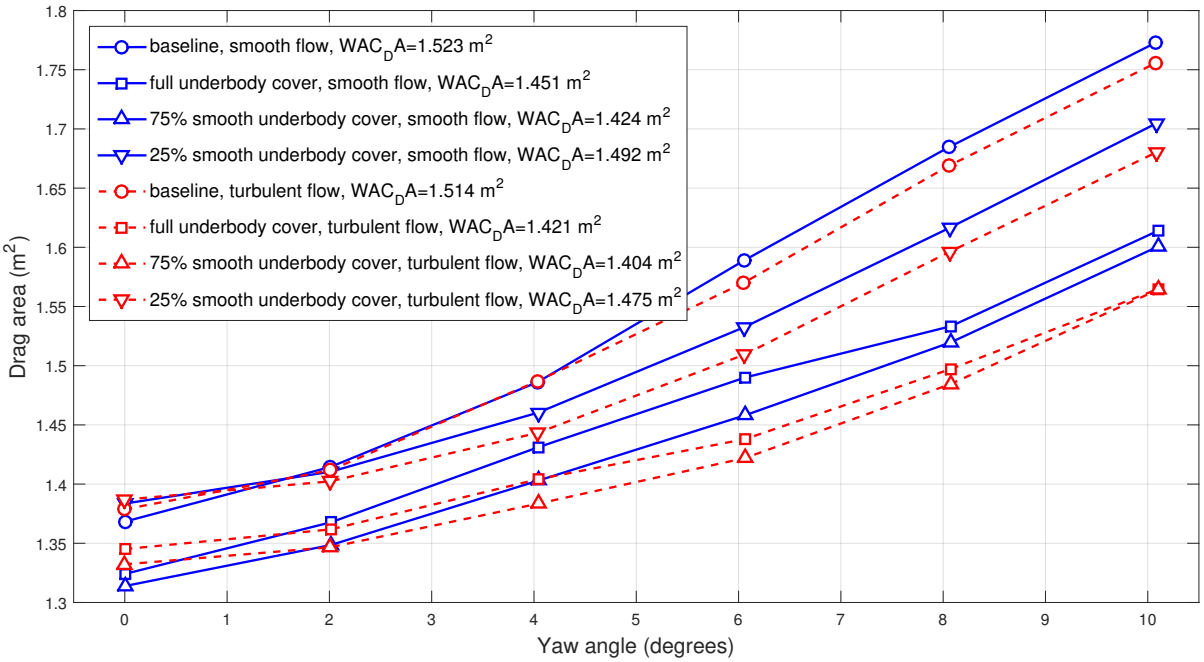

Figure 3.26: Variations of drag area as a function of yaw angle for the different custom underbody cover configurations for pick-up truck 3 in smooth and turbulent flow

the drag area is higher in turbulent flow than in smooth flow at 0 degrees, but the opposite is true at almost all other yaw angles. As well, the drag area for the 25% covered case is higher than the baseline drag area in both smooth and turbulent flow at 0 degrees, but lower at all other yaw angles. These observations underline the importance of considering the wind-averaged drag area when evaluating the performance of, and the effect of turbulence on, any proposed drag reduction technology.

3.8 Ride height study - towards active ride height systems (test category B)

The results of the four phases of this study have highlighted the potential of active ride height technology as an emerging drag reduction technology for the future. Some high-end vehicles are already equipped with a suspension system that reduces the ride height, defined as the clearance between the underbody of a vehicle and the ground, at highway speeds. The results of this study show that such technology shows significant potential for a broad range of vehicles. Significant reductions of wind-averaged drag were observed for all vehicles for which this technology was evaluated.

Using the chassis struts, the ride height was reduced systematically and the influence on vehicle drag of this ride height reduction was monitored. The sequence of the tests was:

1. ride height reduced by 20 mm at the front and by 0 mm at rear (pale blue);

2. ride height reduced by 20 mm at the front and by 20 mm at rear (blue);
3. ride height reduced by 40 mm at the front and by 20 mm at rear(purple); and
4. ride height reduced by 40 mm at the front and by 40 mm at rear (magenta).

Since the exact height reductions listed above could not be attained for all vehicles, values as close as possible to these were used. The actual height reductions are specified in the test logs in Appendix A.

Early tests at 0 degree yaw showed that maximum drag reductions of between 3% and 5% compared to baseline conditions could be obtained by lowering the ride height by up to 40 mm at the front and rear. These tests were conducted on a number of midsize cars, a small SUV and a pick-up truck. When ride height tests were repeated for two midsize cars without OEM underbody panels, even greater drag reduction, of between 5% and 8% with respect to the reference conditions, was obtained. However, the combination of underbody panels and ride height reduction was at least 4% better than either alone.

Wind-averaged drag area results obtained in smooth flow for some vehicles are presented in the bar graph of Figure 3.27. Significant reductions of wind-averaged drag area were observed for all vehicles as the ride height was reduced. More than half of the vehicles experienced maximum reductions of 5% or more. The smallest reductions were observed for the two minivans, indicating that this parameter may be optimized already for this vehicle class. In an effort to maximize cargo/passenger space without increasing overall height and frontal area, it is possible that the OEMs have reduced the ride height of the minivan class in general. The largest reduction, of slightly more than 6%, was observed for large car 2, followed closely by small SUV 6 and small car 3.

For the majority of the wind-averaged tests, the largest drag reductions were associated with a ride height drop at the front of the vehicle of 20 mm more than at the rear, essentially pitching the vehicle nose down, achieved with either a 20 mm frontal drop from the baseline ride height or an additional 20 mm frontal drop from an already 20 mm overall ride height reduction. It was theorized that pitching the vehicle slightly nose down, in addition to a ride height reduction, improves the effectiveness of the air dam or the front bumper features in preventing high speed flow from hitting the rougher surface of the underbody, and may promote an increase in base pressure similar to the effect of an underbody diffuser at the rear of the vehicle. A notable exception to this was the standard SUV 2, for which a 20 mm ride height reduction at the front of the vehicle increased the wind-averaged drag area. The large bumper air dam, which appears to have been optimized for the baseline ride height, may have played a role, as will be reported subsequently.

Figure 3.28 shows the effect of ride height reduction on wind-averaged drag area for three vehicles tested in both smooth and turbulent flow. For all three vehicles, ride height reduction was significantly more effective at reducing drag in turbulent flow than in smooth flow. Reducing the ride height by 40 mm in the front and rear of small car 2 produced a reduction in wind-averaged drag area of over 8% in turbulent flow, which is greater than the 5.6% measured for the same ride height configuration in smooth flow, and is also the highest reduction obtained from ride height reduction alone of all vehicles tested in either smooth or turbulent

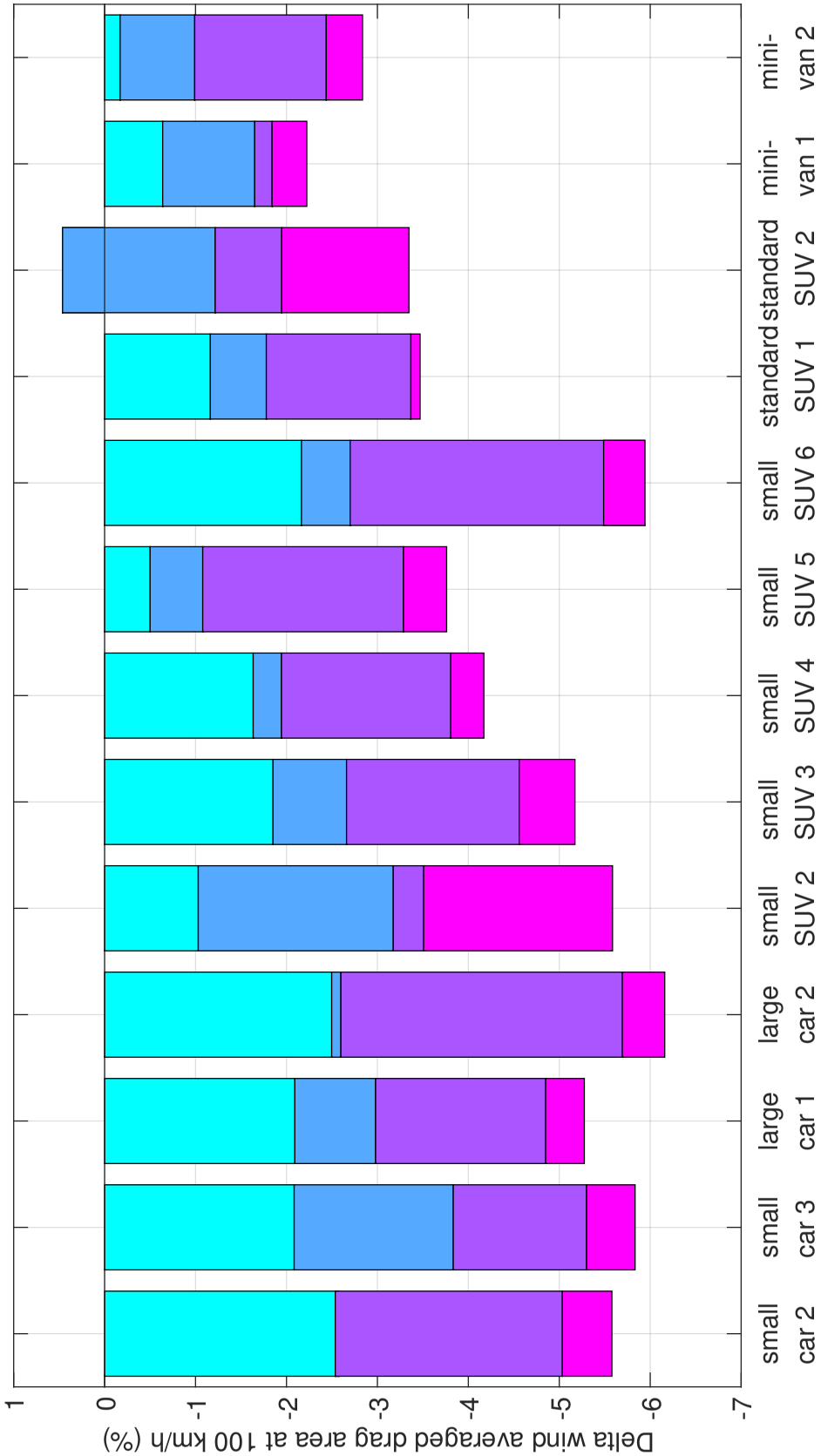

Figure 3.27: Reduction of wind-averaged drag area (%) as a function of ride height for vehicles in smooth flow. All reductions with reference to the baseline ride height, grille shutters 100% closed. Ride height reduction sequence: 20 mm front (pale blue), 20 mm front and rear (blue), 40 mm front 20 mm rear (purple), 40 mm front and 40 mm rear (magenta).

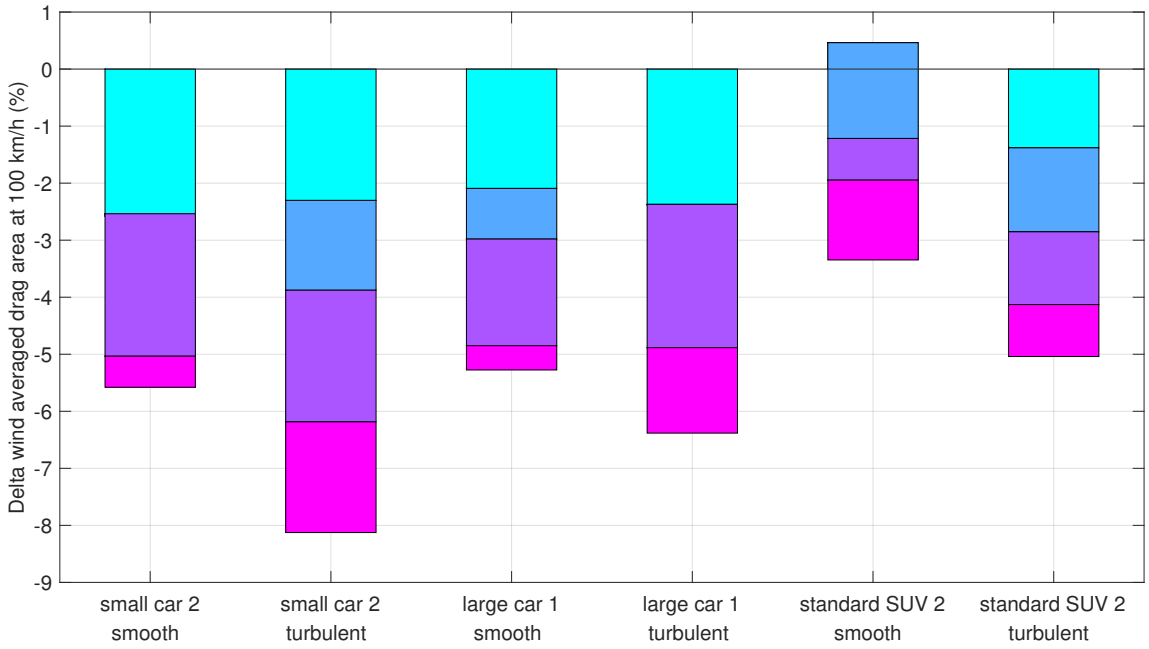

Figure 3.28: Reduction of wind-averaged drag area (%) at 100 km/h as a function of ride height for three vehicles tested in smooth and turbulent flow. All reductions with reference to the baseline ride height, grille shutters 100% closed. Ride height reduction sequence: 20 mm front (pale blue); 20 mm front and rear (blue); 40 mm front, 20 mm rear (purple); and 40 mm front and rear (magenta).

flow. The maximum wind-averaged drag area reduction for large car 1 and standard SUV 2 was between 1 and 2% greater in turbulent flow than in smooth flow.

Figure 3.28 highlights other differences in the drag behaviour of small car 2 in turbulent flow. Contrary to the smooth flow case, for which over 90% of the drag reduction was achieved with the nose pitched down and reducing the rear ride height to level the vehicle produced little or negligible additional drag reduction, significant reductions in wind-averaged drag area were achieved with every stage of the ride height reduction sequence in turbulent flow. Further, each systematic ride height reduction in turbulent flow reduced the drag area consistently across the range of yaw angles, which was not the case in smooth flow (as evidenced by the drag area versus yaw curves of Figures C.2 and C.4 in Appendix C). For the other two vehicles, the distribution of changes in wind-averaged drag reduction among the ride height configurations was also significantly different in smooth and turbulent flow.

The turbulent flow results are important because they indicate that active ride height technology works in road-representative wind conditions, and even more effectively than in smooth flow. Turbulence likely has a strong effect on vehicle underbody flow, which is highly influenced by changes in ride height.

3.9 Combination of extended air dam and ride height - towards active air dam/ride height systems (test categories G & H)

By far, the largest drag reductions of this study were observed when an OEM or custom-built bumper air dam was extended by up to 60% of its initial depth, combined with a reduction of ride height of up to 40 mm. This exercise was carried out to evaluate the scenario where an actively deployed air dam, increasing its depth on the highway for example, is used in combination with an active ride height system that would lower the vehicle at highway speeds. Drag area reductions in excess of 10% were observed for small car 2 and large car 1 in smooth flow at a yaw angle of 0 degrees. Among vehicles tested over a range of yaw angles at ride heights reduced by 35 mm or more, wind-averaged drag area reductions exceeding 6.5% and up to well over 9% were measured for 3 of the 4 cars tested in smooth flow, and for both cars tested in turbulent flow. This is significant given that, based on the rule of thumb for LDVs under average driving conditions, a 10% reduction in drag area for a vehicle can reduce total fuel consumption between 2% to 3% depending on the acceleration pattern of the engine (NAS, 2015).

Figures 3.29 and 3.30 show the results of this investigation for large car 1 and small car 2 obtained in smooth flow at 0 degree yaw. Both figures include some data measured in turbulent flow. It should be noted that the small car's OEM underbody panels were removed during the extended air dam and ride height study. For both cars in smooth flow, any extension of the OEM air dam in place resulted in a reduction of drag area. This reduction was doubled or tripled when the ride height was reduced by 20 mm to 40 mm.

Wind-averaged results are plotted in Figures 3.31 to 3.36. For large car 1, a limited number of ride height/extended air dam combinations were tested over a range of yaw angles in smooth and turbulent flow, as shown in Figure 3.31. In smooth flow, large reductions in wind-averaged drag area were measured at the lowest ride height, from 6.7% for the 13% extension to 9.3% for the 60% extension. The latter is the largest wind-averaged drag area reduction measured for any techonology on any vehicle in this study.

For standard SUV 2, Figure 3.32 shows that none of the custom-built air dams provided a wind-average drag area lower than the OEM-installed air dam, indicating that this feature may have already been optimized by the OEM. However, reducing the ride height with the custom air dam in place resulted in a wind-averaged drag area reduction of 4.5% when the depth of the custom air dam was 30% deeper than the OEM air dam and the ride height was dropped 40 mm. A deeper air dam on its own did not result in such beneficial influences.

Figures 3.33 and 3.34 present the results of the experiments carried out for small car 3 and small SUV 6 in smooth flow. For the small car at baseline ride height, the lowest wind-averaged drag area was obtained when the OEM air dam depth was extended by 30%. This wind-averaged drag area reduction was tripled when the ride height was reduced 20 mm and quadrupled when the ride height was reduced 35 mm. The observation that the lowest drag reduction did not occur for the largest extension of the air dam indicated that the air dam height was likely optimised by the OEM. For the small SUV, Figure 3.34 shows that a reduction of wind-averaged drag area in excess of 6.5% was obtained when the ride height was reduced

by 40 mm, regardless of the amount of extension of the OEM air dam.

Figures 3.30 and 3.29 show that the combination of air dam extension and ride height reduction was 1% to 5% less effective in turbulent flow than in smooth flow at reducing the drag area of small car 2 and large car 1 at 0 degrees. Regardless, drag area reductions of more than 8% were measured at the lowest ride height for 2 of the 3 custom air dam extension lengths (56 mm and 66 mm) tested on small car 2 in turbulent flow, and for the only air dam extension (40%) tested for large car 1 in turbulent flow. For small car 2 in turbulent flow, the 56 mm air dam extension gave reductions that were fairly close to those obtained with ride height reduction only and no air dam, shown in Figure 3.28. However, extending the custom air dam further to 66 mm improved the efficiency over the configuration with no air dam, particularly for the -20 mm ride height configuration.

When considering wind-averaged drag, Figure 3.35 shows that none of the air dam extension lengths tested on small car 2 in turbulent flow were effective at the baseline ride height, even though they produced a small reduction at 0 degree yaw. The corresponding smooth flow results are not available for comparison since this test was only performed at 0 degrees. The effectiveness of this technology generally diminished with increasing yaw angle. At the baseline ride height, custom air dam extension was found to be effective only at 4 degrees yaw or

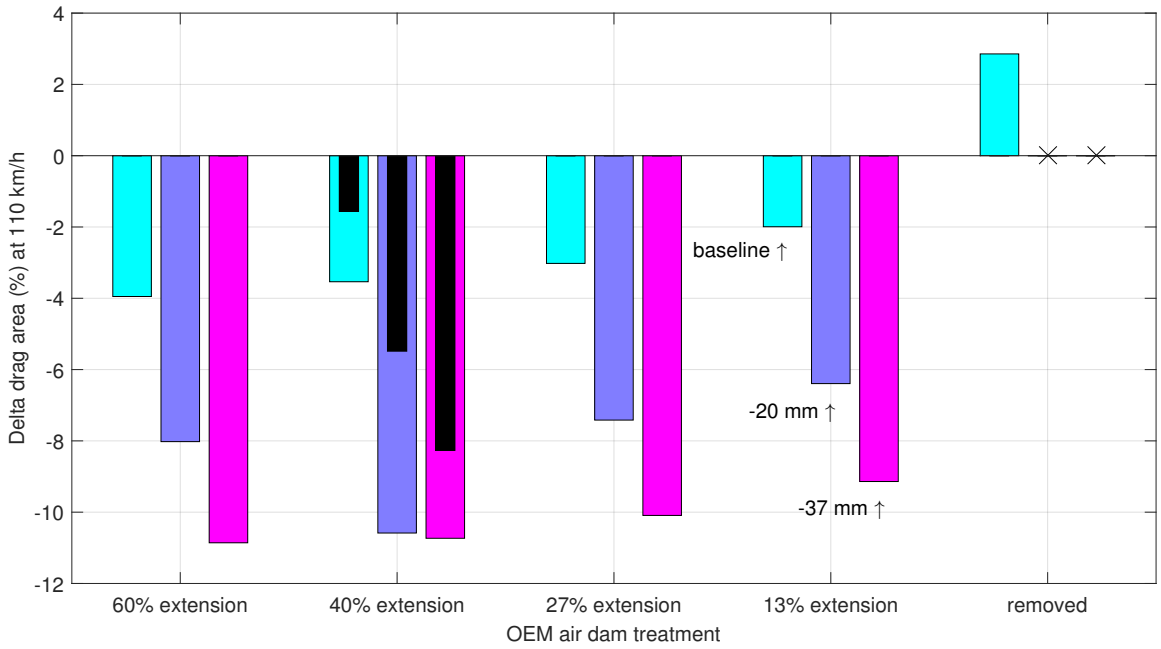

Figure 3.29: Reductions of drag area at 0° yaw associated with the extension of the bumper air dam and ride height variations of large car 1 when compared to the baseline, shutters 100% closed. The OEM air dam was extended by 60% or less and the drag area was evaluated for 1) the baseline ride height (pale blue) ; 2) ride height reduced 20 mm overall (blue); and 3) ride height reduced 37 mm overall (magenta) in smooth flow (wide coloured bars) and turbulent flow (narrow, black bars, for the 40% air dam extension only). The symbol 'x' indicates no data is available.

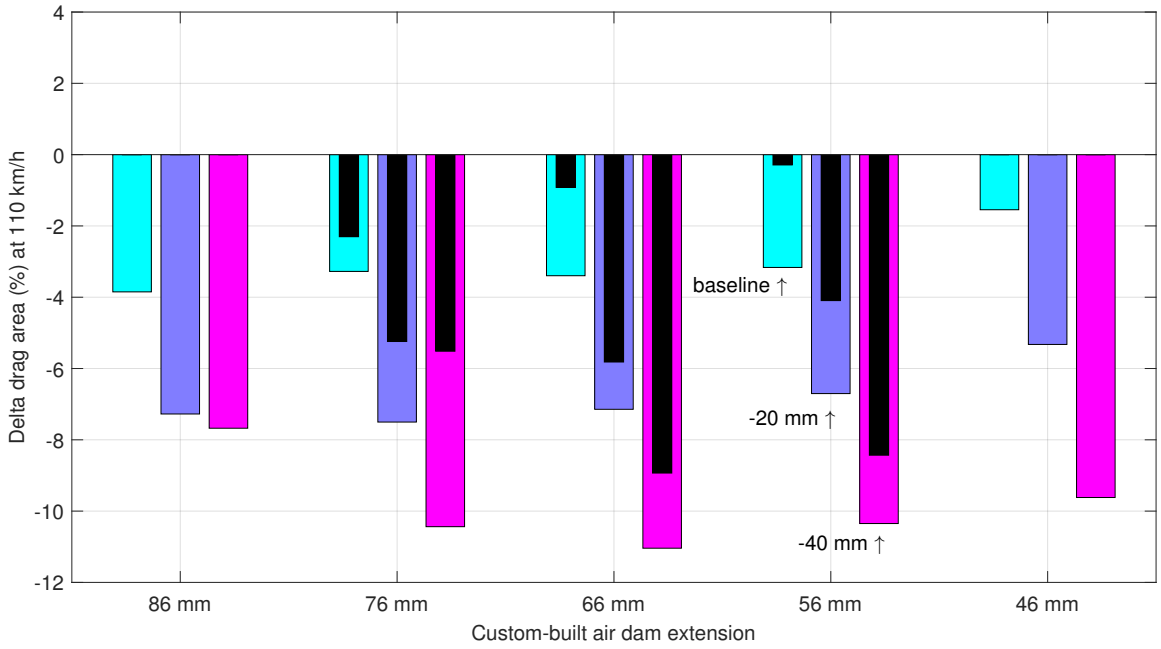

Figure 3.30: Reductions of drag area at 0° yaw associated with the extension of the custom-built bumper air dam and ride height variations of small car 2 with OEM underbody panels removed when compared to the baseline, shutters 100% closed, with OEM underbody panels and without air dam. The custom air dam was extended by 86 mm or less and the drag area was evaluated for 1) the baseline ride height (pale blue); 2) ride height reduced 20 mm overall (blue); and 3) ride height reduced 40 mm overall (magenta) in smooth flow (wide coloured bars) and turbulent flow (narrow, black bars, for the 56-76 mm air dam extensions only).

less for the two largest extensions tested in turbulent flow.

The combined bumper air dam and ride height study was also performed for pick-up truck 3 in smooth and turbulent flow, although ride height adjustment was limited to a 20 mm reduction in the front only. The results are presented in Figure 3.36. In Section 3.5, the OEM air dam was shown to have a minimal effect on wind-averaged drag area: slightly detrimental in smooth flow and marginally beneficial in turbulent flow. Figure 3.36 shows that extending the OEM air dam had very little impact on the wind-averaged drag area at either the baseline ride height or with the front of the vehicle lowered by 20 mm. At the baseline ride height in both smooth and turbulent flow, the extended air dam had a small negative effect which increased with the height of the extension. Turbulent flow appeared to exacerbate this effect at all but the smallest extension of 15%. The only significant gains obtained with this technology was with an air dam extension of 30% or less coupled with a 20 mm front ride height reduction in both smooth and turbulent flow, with no significant difference between the two flow regimes. The best case in both smooth and turbulent flow is the 15% extension with 20 mm front ride height reduction. However, all changes were within 1% of the baseline wind-averaged drag value.

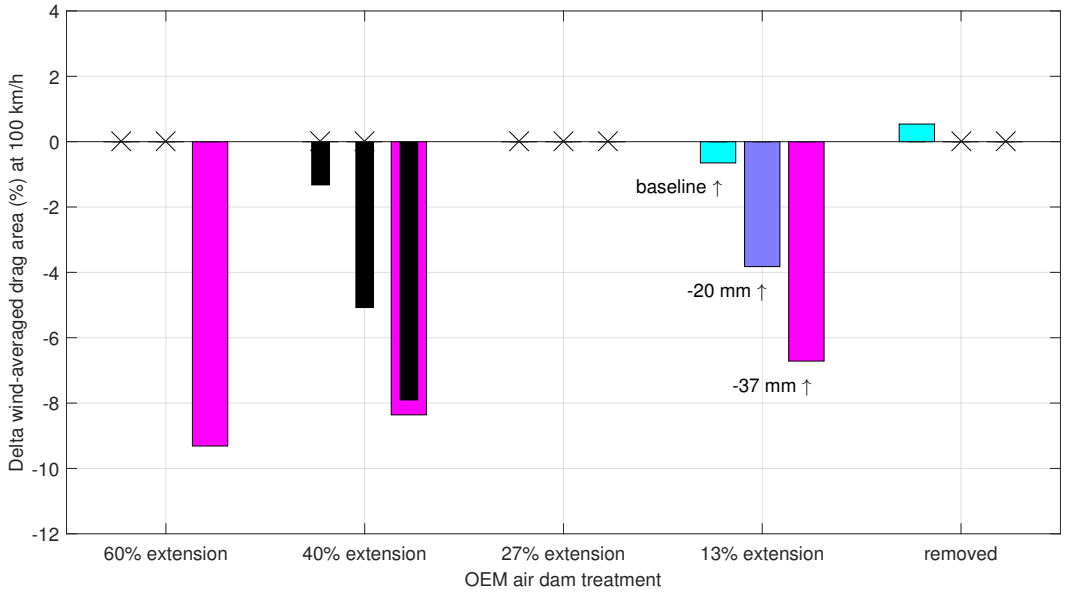

Figure 3.31: Reductions of wind-averaged drag area associated with the extension of the bumper air dam and ride height variations of large car 1 when compared to the baseline, shutters 100% closed. The OEM air dam was extended by 60% or less and the drag area was evaluated for 1) the baseline ride height (pale blue) ; 2) ride height reduced 20 mm overall (blue); and 3) ride height reduced 37 mm overall (magenta) in smooth flow (wide coloured bars) and turbulent flow (narrow, black bars, for the 40% air dam extension only). The symbol 'x' indicates no smooth flow data is available.

It should be noted that reducing the ride height systematically reduces the frontal area of the vehicle, because the front wheels are less exposed to the oncoming flow, while increasing the depth of the OEM air dam increases the vehicle frontal area. The changes in drag area caused by either of these two geometric effects are estimated to be at least of the same order as the changes in wind-averaged drag area shown in Figure 3.36. Clearly, extending the OEM air dam is not an effective drag reduction technology for pick-up truck 3. A custom air dam with an optimized shape that shields more of the front wheels may be more effective in pursuing a combined active air dam and active ride height technology. Also, although a separate ride height investigation was not performed for pick-up truck 3, the limited results of this study suggest that active ride height technology used alone might be effective for this vehicle.

3.10 Influence of drag reduction technologies used in combination (test category J)

The question of the possible compound effects of drag reduction technologies was raised part way through the overall test campaign. If it was observed that drag reduction technologies were effective by themselves, would their benefit be reduced when used in combina-

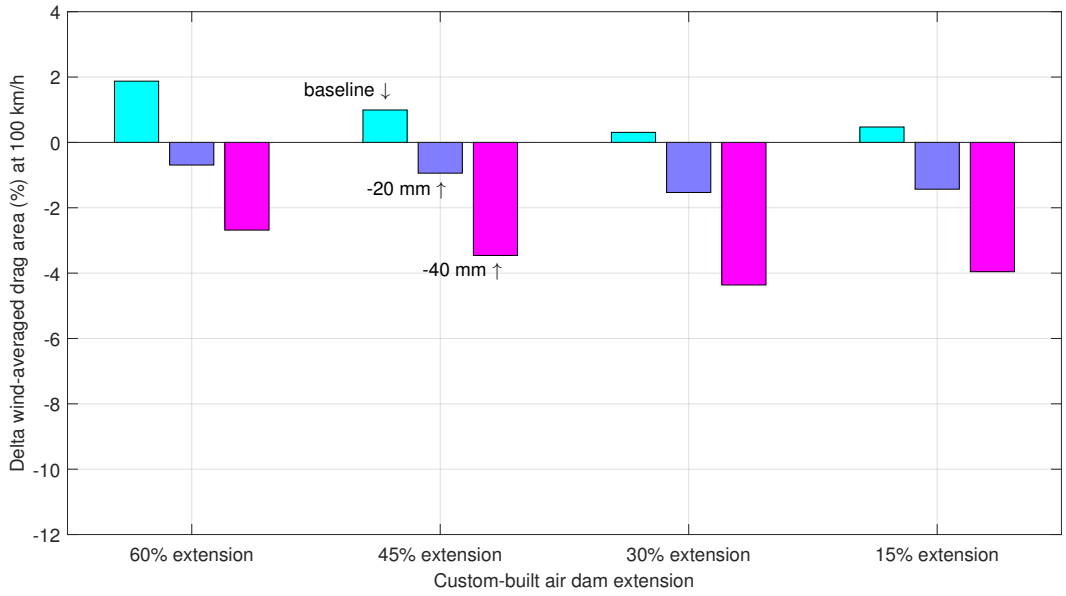

Figure 3.32: Reductions of wind-averaged drag area associated with the depth of a custom-built bumper air dam and ride height variations of standard SUV 2 in smooth flow. The custom air dam was installed and the drag area was evaluated for 1) the baseline ride height (pale blue); 2) ride height reduced 20 mm overall (blue); 3) ride height reduced 40 mm overall (magenta).

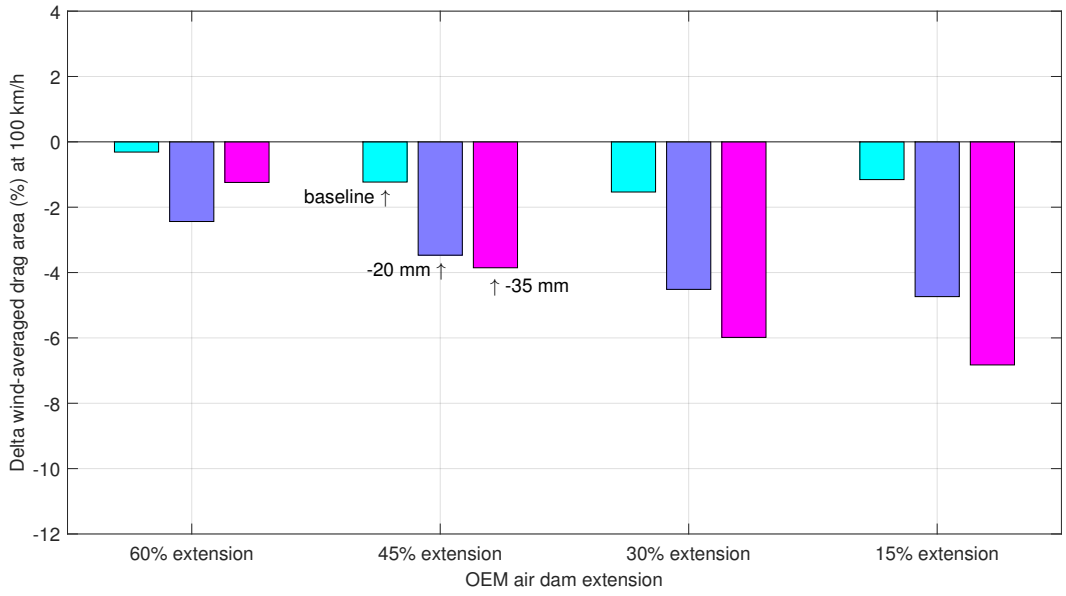

Figure 3.33: Reductions of wind-averaged drag area associated with the depth of a bumper air dam and ride height variations of small car 3 in smooth flow. The OEM air dam was extended and the drag area was evaluated for 1) the baseline ride height (pale blue); 2) ride height reduced 20 mm overall (blue); and 3) ride height reduced 35 mm overall (magenta).

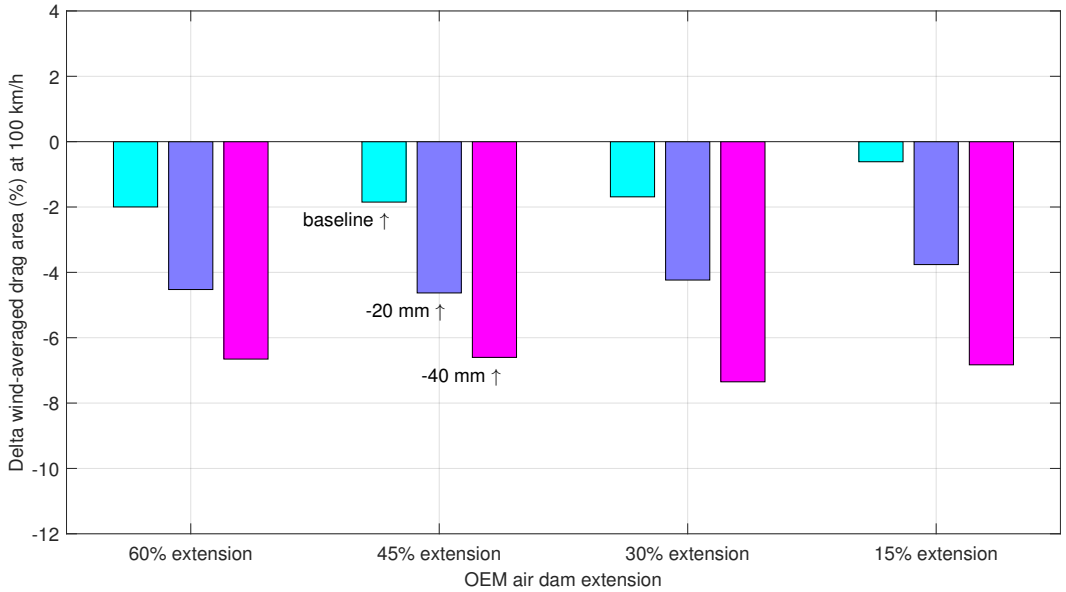

Figure 3.34: Reductions of wind-averaged drag area associated with the depth of a bumper air dam and ride height variations of small SUV 6. The OEM air dam was extended and the drag area was evaluated for 1) the baseline ride height (pale blue); 2) ride height reduced 20 mm overall (blue); and 3) ride height reduced 40 mm overall (magenta).

tion with other technologies? For heavy duty vehicles, it has been demonstrated that some drag reduction technologies work better in combination than in isolation, as a device can alter the flow around the vehicle in a way that increases the effectiveness of another device (McAuliffe, 2015; McAuliffe and Wall, 2016).

The results of the combined bumper air dam/ride height study described in Section 3.9 partially answers this question. It was demonstrated that a reduction of ride height systematically reduced the drag area for all vehicles except one (for which drag area increased only when the front of the vehicle was pitched down 20 mm), up to a maximum reduction of 2% to 6% at the lowest ride height. The same was shown for a bumper air dam, which reduced the wind-averaged drag area by 1% to 2% for the four vehicles for which this technology was evaluated. Would reducing ride height and increasing the depth of the bumper air dam provide even higher drag reduction? The answer was positive: the largest reductions, sometimes reaching 10%, were measured when both technologies were used in combination.

The results obtained in later tests were not so clear. For small car 2 in turbulent flow, the largest wind-averaged drag area reduction caused by bumper air dam extension combined with ride height reduction was slightly less than that measured with ride height reduction alone. For pick-up truck 3, reducing the ride height by 20 mm in the front of the vehicle coupled with extending the OEM air dam by 15% to 30% was more efficient at reducing wind-averaged drag than the original OEM bumper air dam at the baseline ride height in both smooth and turbulent flow. However, the maximum wind-averaged drag area reduction of less than 1% for pick-up truck 3 was small compared to the reductions obtained using these

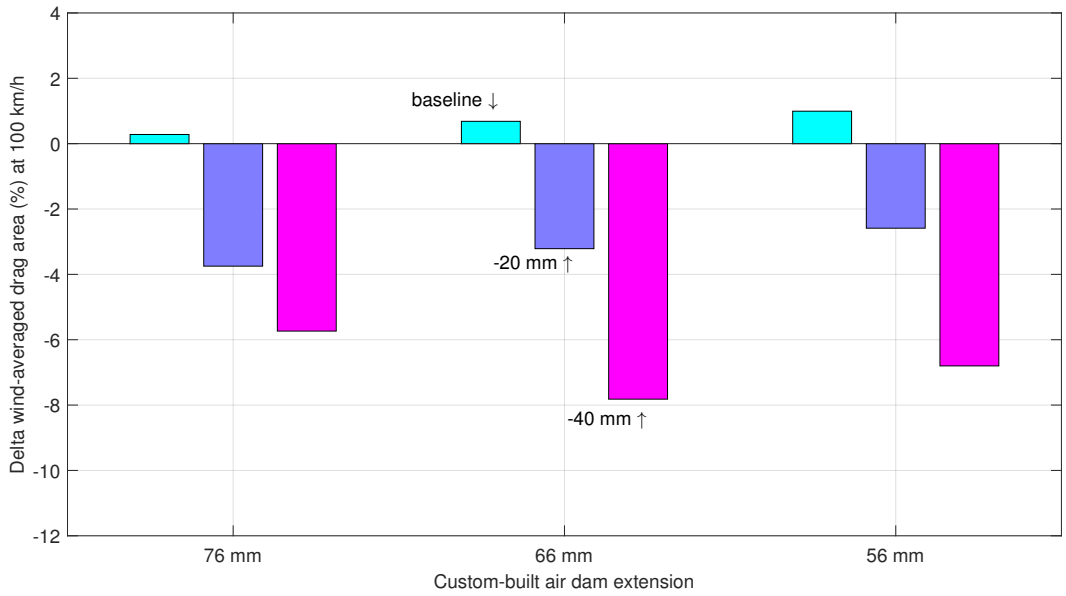

Figure 3.35: Reductions of wind-averaged drag area associated with the depth of a custom-built bumper air dam and ride height variations of small car 2 with OEM underbody panels removed, compared to the baseline condition (shutters 100% closed, with OEM underbody panels and without air dam), in turbulent flow. The custom-built air dam was extended and the drag area was evaluated for 1) the baseline ride height (pale blue); 2) ride height reduced 20 mm overall (blue); and 3) ride height reduced 40 mm overall (magenta).

combined technologies for other vehicles. This indicates that different technologies, used alone or combined, do not have the same effect on all types of vehicles.

In addition to the above, some tests were specifically devised to address the issue of combined technologies. For small car 3 and small SUV 6 the following tests were carried out:

- tests to quantify the influence of fully covering the underbody with and without the OEM bumper air dam in place;
- tests to quantify the influence of closing the active grille shutters with and without the OEM bumper air dam in place; and
- tests to quantify the influence of rear wheel air dams with and without the OEM bumper air dam in place.

The results of some of these experiments are presented in Figures 3.37 to 3.40. The experiments revealed that both the full underbody cover and active grille shutters technologies were more effective at reducing wind-averaged drag area when the OEM bumper air dam was installed. The most beneficial combination was observed for small SUV 6 when the full underbody cover and the OEM air dam were combined to obtain a reduction of 3.6% compared to a reduction of only 1.5% for the underbody cover alone.

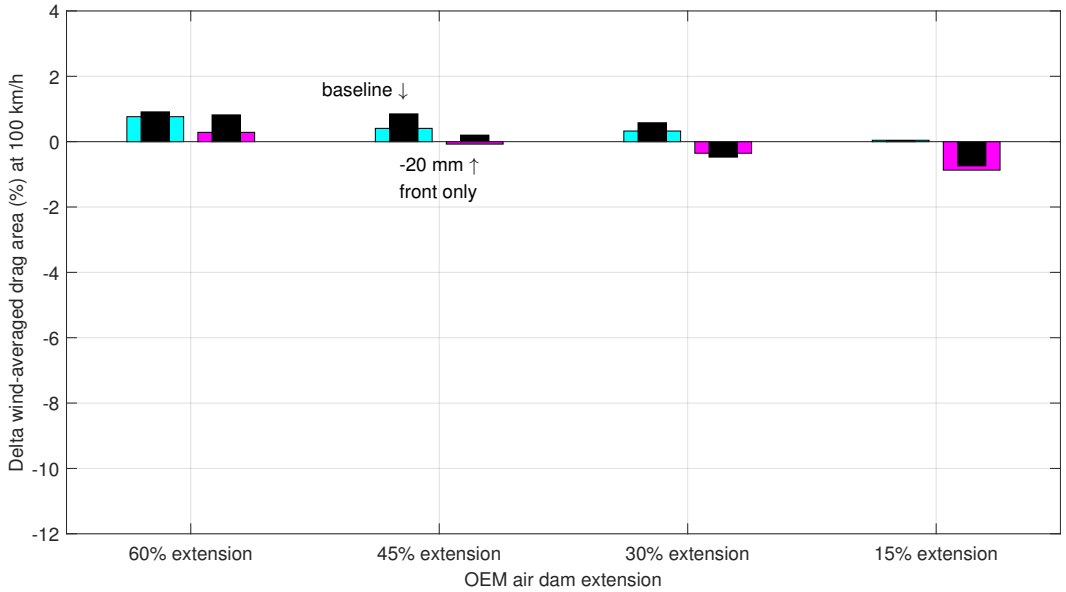

Figure 3.36: Reductions of wind-averaged drag area associated with the depth of a bumper air dam and ride height variations of pick-up truck 3, compared to the baseline condition (shutters 100% closed) in smooth and turbulent flow. The OEM air dam was extended and the drag area was evaluated for 1) the baseline ride height (pale blue); and 2) ride height reduced 20 mm in the front only (magenta) in smooth flow (wide coloured bars) and turbulent flow (narrow black bars).

The test matrix included one other test specifically devised to address the issue of combined technologies. For pick-up truck 3, a test was carried out to quantify the influence of closing the active grille shutters partially (lower shutters closed, upper shutters open) or fully with and without the OEM bumper air dam in place. The results of these experiments are presented in Figure 3.41. The experiments revealed that the active grille shutter technology was more effective, by roughly 1% with grille shutters completely closed, at reducing wind-averaged drag area with the OEM bumper air dam installed in both smooth and turbulent flow. With the air dam installed, the AGS were slightly more effective in turbulent flow, although the difference between smooth and turbulent flow was within the margin of error of the measurements. Interestingly, without the air dam installed, the AGS were more effective in smooth flow, and by a larger margin than could be considered statistically significant. In both flow regimes, closing the shutters completely was significantly more effective at reducing wind-averaged drag area, by 3% with the air dam installed and by slightly more than 2% without the air dam, than closing the lower shutters only.

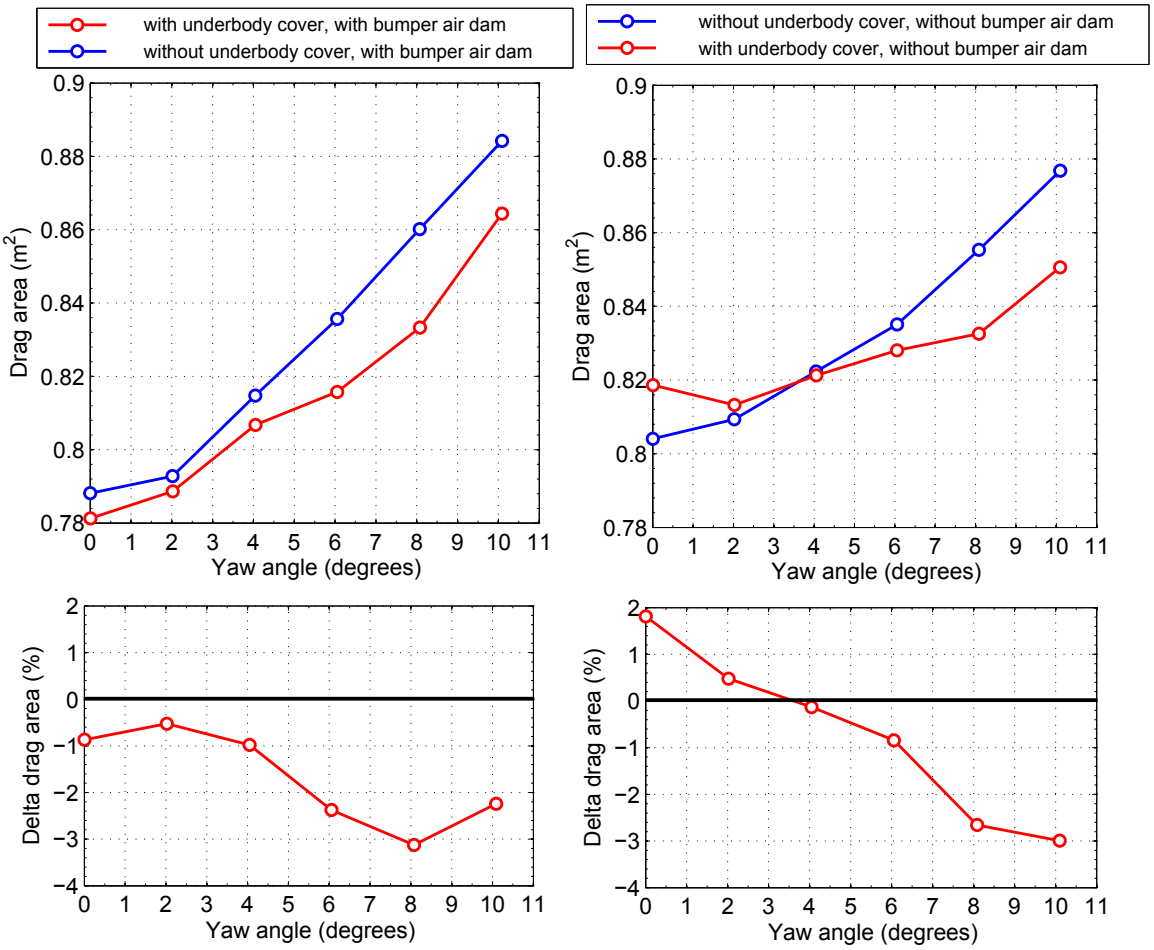

Figure 3.37: Variations of drag area as a function of yaw angles for small car 3, with and without full underbody cover, with and without bumper air dam. The lower graphs show the drag area change in % due to the full underbody cover with the bumper air dam installed (left, -1.4% WAC_DA) or removed (right,-0.2% WAC_DA).

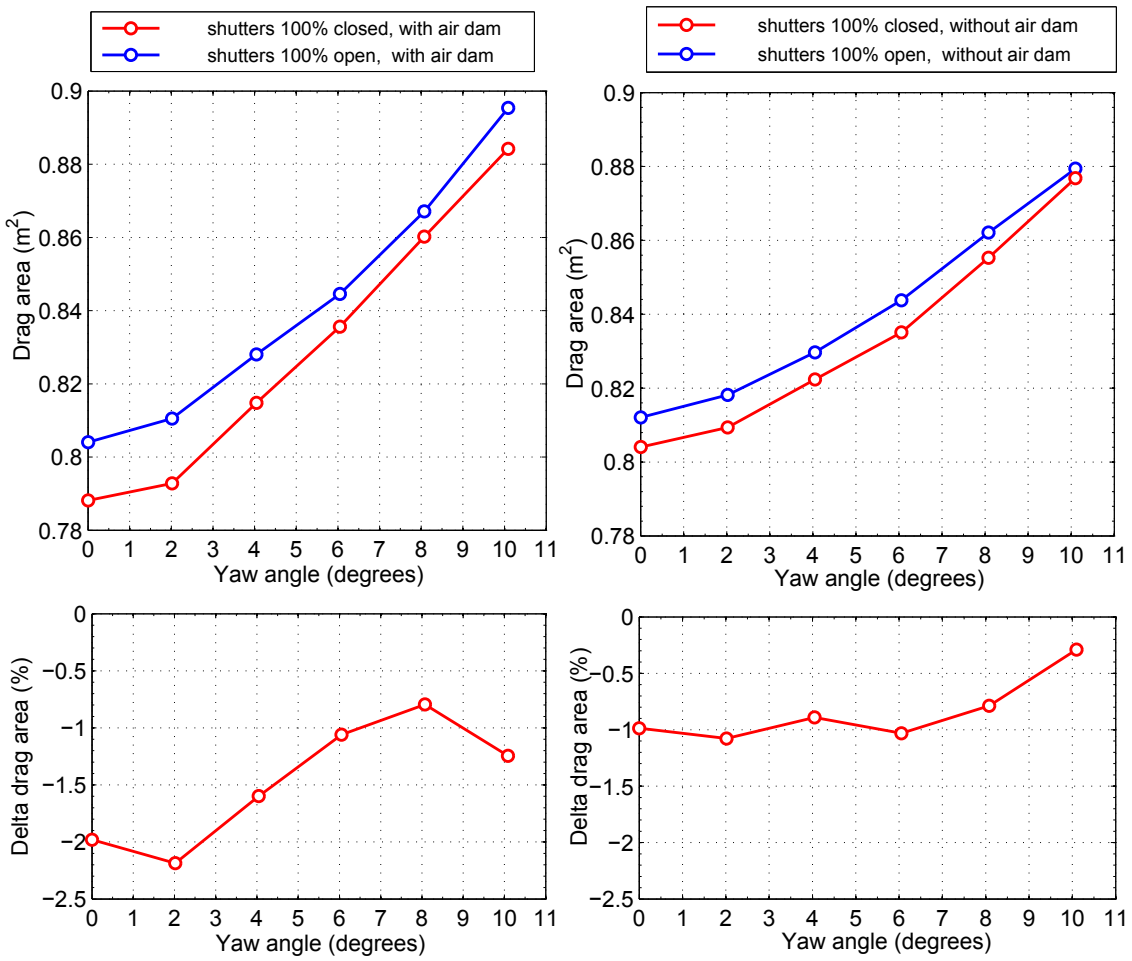

Figure 3.38: Variations of drag area as a function of yaw angles for small car 3, with the grille shutters 100% closed or opened, with and without bumper air dam. The lower graphs show the drag area change in % due to the closing of the shutters with the bumper air dam installed (left, -1.5% WAC_DA) or removed (right,-1.0% WAC_DA).

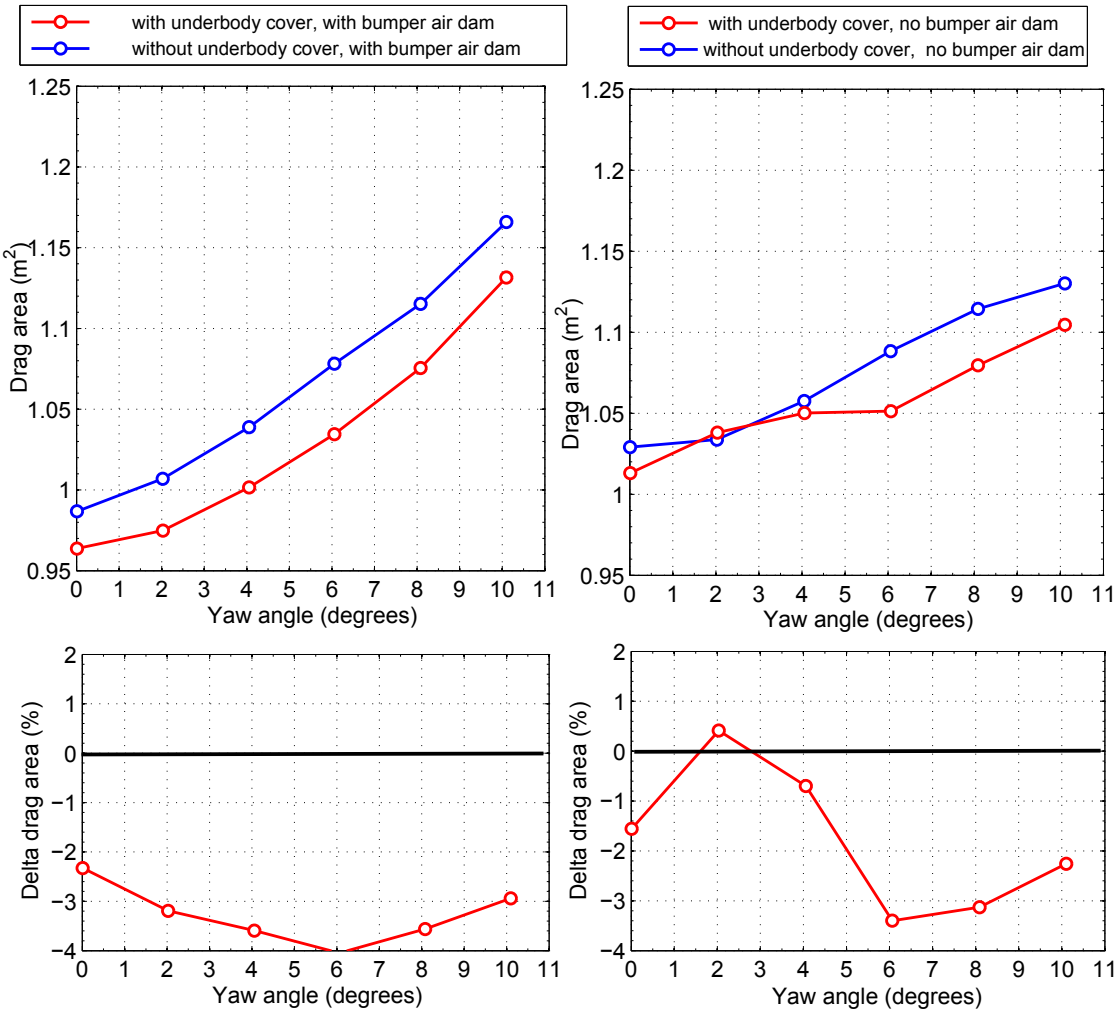

Figure 3.39: Variations of drag area as a function of yaw angles for small SUV 6, with and without full underbody cover, with and without bumper air dam. The lower graphs show the drag area change in % due to the full underbody cover with the bumper air dam installed (left, -3.6% WAC_DA) or removed (right,-1.5% WAC_DA).

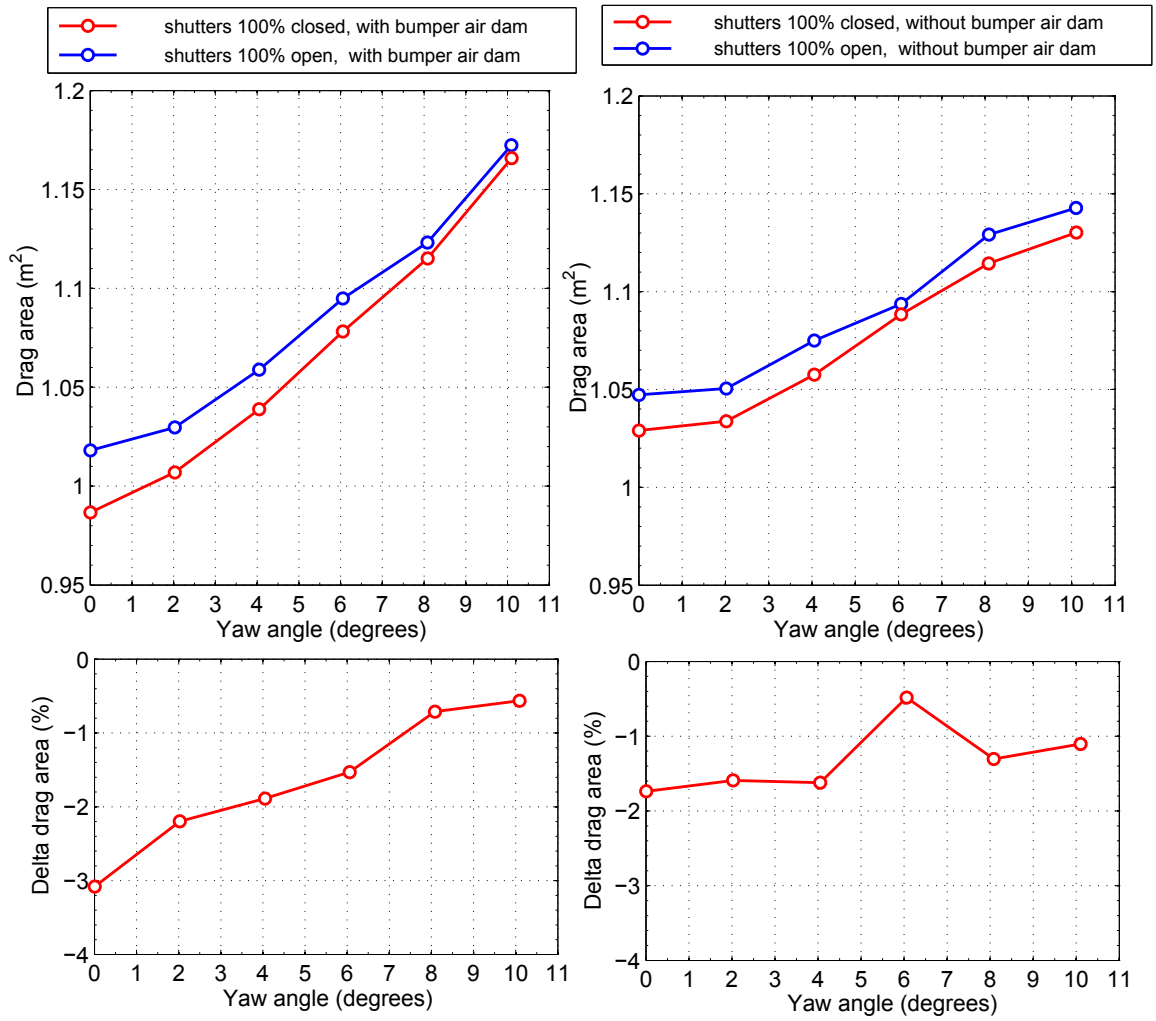

Figure 3.40: Variations of drag area as a function of yaw angles for small SUV 6, with the grille shutters 100% closed or opened, with and without bumper air dam. The lower graphs show the drag area change in % due to the closing of the shutters with the bumper air dam installed (left, -1.8% WAC_DA) or removed (right,-1.1% WAC_DA).

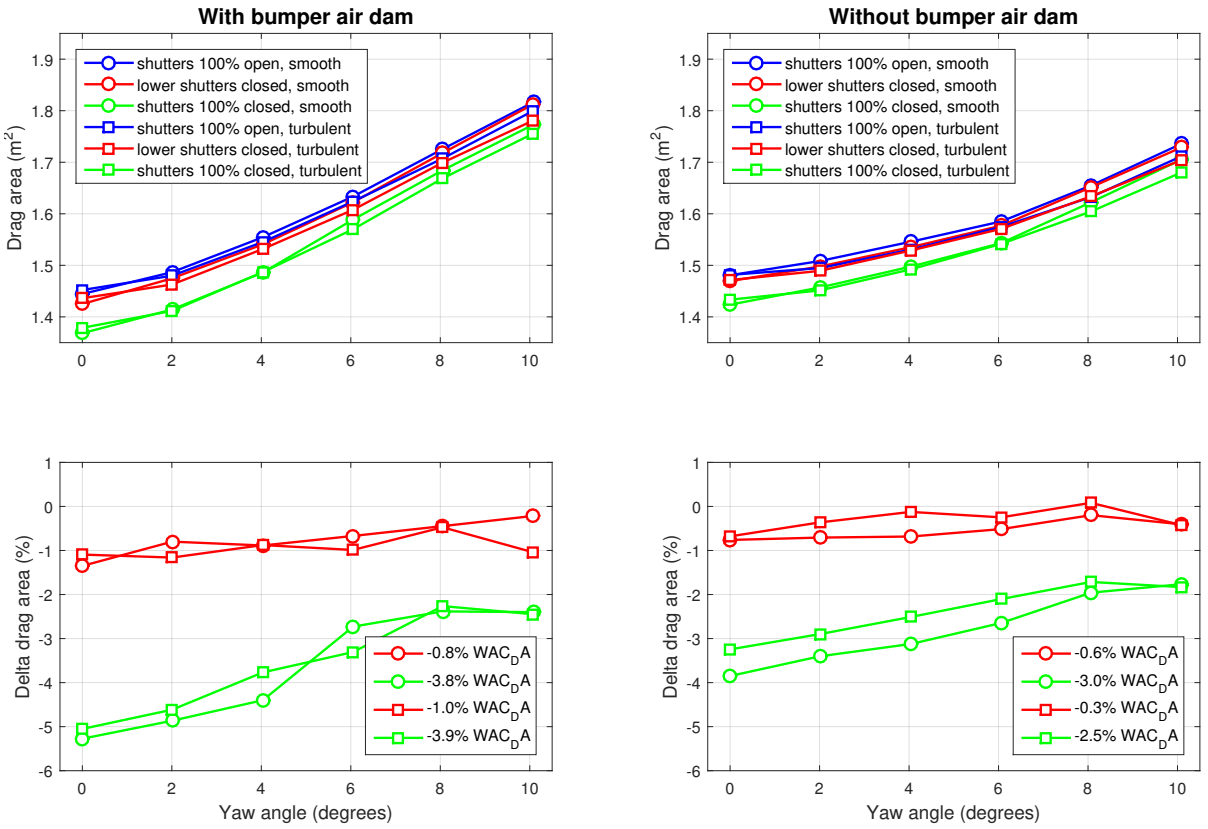

Figure 3.41: Variations of drag area as a function of yaw angles for pick-up truck 3, with the grille shutters 100% closed, lower shutters closed and upper shutters open, or 100% open, with (left) and without (right) the bumper air dam. The lower graphs show the drag area change in % due to the closing of the shutters.

3.11 Miscellaneous tests

The following tests were not conceived to examine operational or aftermarket aerodynamic configurations, as such configurations are not generally governed by federal regulations. However, opportunities arose to examine a few miscellaneous sources of drag on pick-up truck 3.

3.11.1 Front licence plate mount

Most North American LDVs are registered in provinces and states requiring a front licence plate. The front bumper area, where licence plates are typically mounted, may not appear to be an ideal location as this area is exposed to high-speed flow. To quantify the effect of the front licence plate mount, pick-up truck 3 was tested with and without the OEM front licence plate mount. The tests were done in turbulent flow with the bumper air dam removed. Removing the front licence plate mount reduced the drag area at 0 degrees by 0.5%. However, the resulting change in wind-averaged drag was negligible. The reduction in drag area at 0 degrees is small but statistically significant, and slightly more than the maximum change in drag that had been measured in early tests, where three different vehicles were tested with and without the front licence plate mount with an Ontario licence plate installed. In that experiment, the changes in drag observed at 0 degrees were less than 0.35%, approaching the resolution of the experiment, and were considered negligible.

3.11.2 Open tailgate

In the quest to lower fuel consumption of pickup trucks, operators often open or remove the tailgate or replace it with aftermarket louver or net units that promise to lower drag. In reality, the NRC has only ever measured drag increases when operating in any configuration other than the closed OEM tailgate. The most common interpretation of these results is that while a closed tailgate itself may experience high drag, it increases the static pressure in the cargo box which reduces drag on the much larger rear surface of the cab, thus causing lower net drag. This was confirmed in early tests, where opening the tailgate of pick-up truck 2 increased the drag at 0 degrees by 5.2%. It was again confirmed in later tests, as shown in Figure 3.42. Opening the tailgate of pick-up truck 3 increased the drag area at 0 degrees by 5.9% and 5.4%, and the wind-averaged drag area by 3.1% and 2.5%, respectively in smooth and turbulent flow. In both flow regimes, the increase in drag area due to the open tail gate is greatest at 0 degrees and decreases with increasing yaw angle.

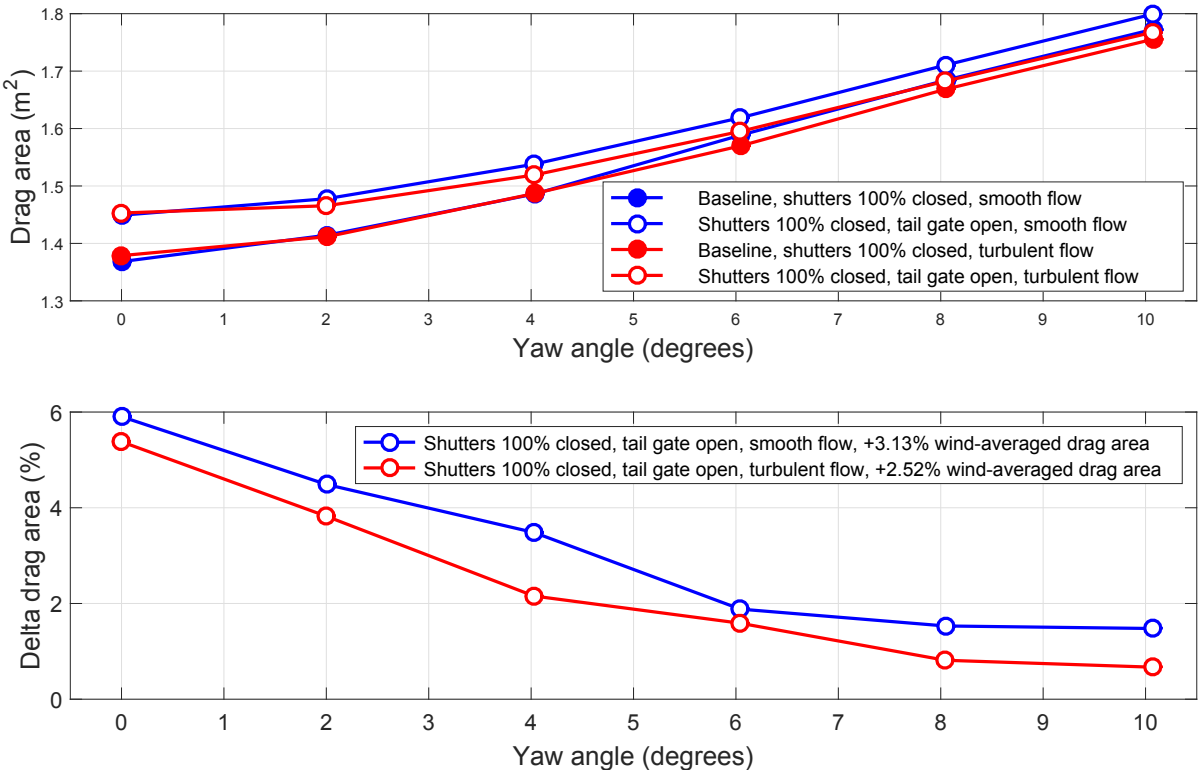

Figure 3.42: Variations of drag area as a function of yaw angle for pick-up truck 3 with the tail gate open and closed in smooth and turbulent flow at 110 km/h, grille shutters 100% closed, baseline ride height. The lower graphs show the drag area change in % due to the open tail gate in smooth and turbulent flow.

3.11.3 Open windows

Opening the windows of a vehicle at highway speed decreases fuel efficiency due to an increase in drag. This drag increase is quantified in Figure 3.43. Fully opening the windows of pick-up truck 3 in smooth flow increased the drag area at 0 degrees by 1.6%, and the wind-averaged drag area by 1.9% with the grille shutters 100% closed at the baseline ride height. The drag increase due to the open windows reached a minimum of 1.2% at 2 degrees, and then increased with yaw angle to reach 4.9% at 10 degrees.

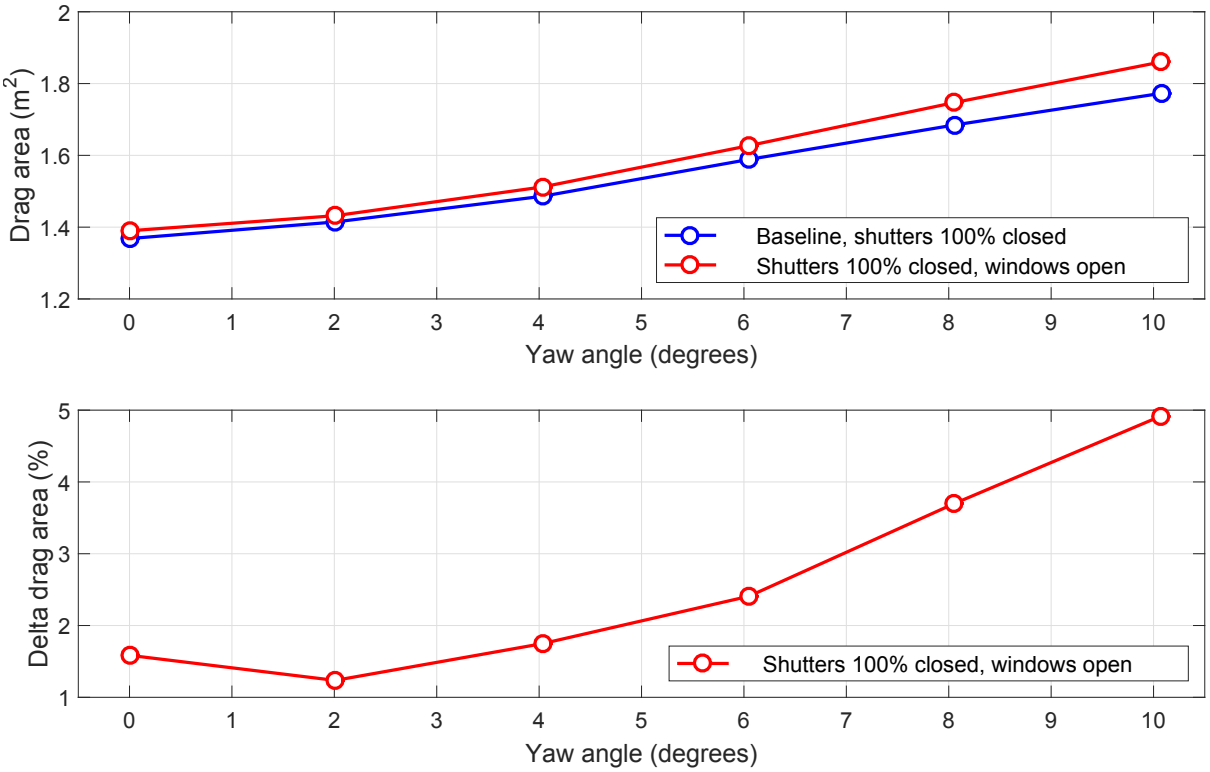

Figure 3.43: Variations of drag area as a function of yaw angle for pick-up truck 3 with the windows fully opened and closed in smooth flow at 110 km/h, grille shutters 100% closed, baseline ride height. The lower graphs show the drag area change in % due to the fully opening the windows in smooth flow.

4. Conclusions

Transport Canada, through its ecoTECHNOLOGY for Vehicles program, and Environment and Climate Change Canada's Transportation Division, commissioned a multi-phase project to investigate the aerodynamics of recently introduced drag reduction technologies for light-duty vehicles. The intent was to evaluate the level of drag reduction associated with each technology as a function of vehicle U.S. EPA class size and to provide guidance to policy makers for the implementation of emerging technologies in Canada and the U.S. This body of work has led to the establishment of a reliable and comprehensive database on the influence of drag reduction technologies for LDVs based on 25 vehicles covering most classes of available production vehicles in North America. The technologies were evaluated through direct measurements of aerodynamic forces on full-scale vehicles equipped with the devices in the 9 m Wind Tunnel of the National Research Council Canada.

In general, the technologies investigated were effective at reducing drag. Of those currently available on the market, active grille shutters, covering most or all of the front surface of the radiator, provided the largest wind-averaged drag area reduction, of up to 5%. Among emerging technologies that are expected to become more commonly available within a few years, active ride height systems, where the clearance between the underbody and the ground is reduced at highway speeds, were shown to be capable of significantly reducing drag for all vehicles tested in this study, with wind-averaged drag area reductions greater than 5% for 7 of 13 vehicles tested. Such systems are currently available only in a few, typically more expensive vehicles. This study demonstrates the potential for a wider implementation of this technology. Full underbody covers were also shown to be a promising emerging technology. The wind-averaged drag area of 7 of 10 cars outfitted with idealized custom underbody panels was reduced by 3% or more. The greatest potential for drag reduction identified in this study was for a scenario in which active ride height is combined with extending the bumper air dam. Reductions exceeding 10% in drag area at 0 degree yaw and 9% in wind-averaged drag area were measured for certain vehicles. On the road, this would be achieved by an automatically extended air dam and lowered ride height at highway speed.

The performance of the investigated technologies in smooth flow is summarized below:

- AGS: 1% to 5% reduction in WAC_DA
- wheel dams: 1.8% increase to 3% reduction in WAC_DA
- bumper air dams: up to 2.3% reduction in WAC_DA
- OEM underbody panels: 0.5% to 1.5% reduction in WAC_DA
- custom underbody panels: 1.5% to close to 7% reduction in WAC_DA
- active ride height: 2% to over 6% reduction in WAC_DA
- active air dam/ride height: 4% to over 9% reduction in WAC_DA

It was observed that drag reduction technologies that worked well for one vehicle, for example AGS, wheel dams and bumper air dams, were not necessarily as effective, or even beneficial,

for another one. In addition, interactions between different technologies might compound or reduce their influence, depending on the vehicle. This highlights the need for vehicle manufacturers to continue to perform validation checks of technologies for each new design and for the regulatory bodies to receive accurate data to apply credits where appropriate.

The concept of wind-averaged drag provides an improved characterization of the aerodynamics of drag reduction technologies for light-duty vehicles. The wind-averaged drag reveals information that would be missed by only taking into account the drag at 0 degree yaw. This can lead to a different optimization, and quantification of the effects, of these technologies. It was observed in several instances that the performance of OEM aerodynamic features such as wheel dams, bumper air dams and underbody panels significantly decreased for yaw angles other than 0 degrees, sometimes to the point that the devices had a negligible or even detrimental effect on wind-averaged drag. Such features were likely optimized for head winds only. Since vehicles experience a range of wind angles on the road, it is important to consider wind-averaged drag values in future studies.

The results of this study have shown that turbulent flow generated by the NRC Road Turbulence System can have a significant effect on the performance of drag reduction technologies, that can vary with the type of vehicle and technology. Some technologies were effective in smooth flow but ineffective in turbulent flow, such as the OEM underbody panels of small car 2, or vice versa, such as the bumper air dam of pick-up truck 3. In both cases the differences between smooth and turbulent flow were small but statistically significant.

Turbulence had a strong but opposite effect on the performance of the active ride height and combined active ride height/extended air dam technologies. Active ride height was more effective in turbulent than in smooth flow for all 3 vehicles for which this was verified, by 1% to 2.5% in terms of wind-averaged drag area reduction. In fact, the largest wind-averaged drag area reduction of all the active ride height tests, of over 8%, was measured in turbulent flow for small car 2. Conversely, the active ride height/extended air dam technology was generally less effective in turbulent than in smooth flow for all 3 vehicles for which this comparison was made, by up to 5% in drag area reduction at 0 degree yaw for small car 2 and large car 1.

Turbulence sometimes had opposite effects on different vehicles. The baseline wind-averaged drag was higher in turbulent flow than in smooth flow for some vehicles, by up to 1.9%, but lower for others, by up to 1.5%. Turbulence appeared to have a stronger effect on the wind-averaged drag area of streamlined vehicles, with fewer sharp edges to "trip" the flow, than boxy vehicles. A wider sample of test vehicles would be required to confirm this trend.

References

EPA (2010), *Model Year 2012-2016 Light-Duty Vehicle Greenhouse Gas Emissions Standards and Corporate Average Fuel Economy Standards*.

Hackett, J. E. and Cooper, K. R. (2001), "Extension to Maskell's Theory for Blockage Effects on Bluff Bodies in Closed Wind Tunnel," Aeronautical Journal 105, pp. 409–418.

Larose, G. L., Tanguay, B., van Every, D. and Bender, T. (2001), "The New Boundary Layer Control System for NRC's 9m x 9m Wind Tunnel," AIAA 39th Aerospace Science Meeting, Reno, Nevada, USA.

McAuliffe, B. (2015), "Improving the Aerodynamic Efficiency of Heavy Duty Vehicles: Wind Tunnel Test Results of Trailer-Based Drag-Reduction Technologies," No. LTR-AL-2015-0272, *National Research Council Canada, Aerodynamics Laboratory*.

McAuliffe, B. and D'Auteuil, A. (2016), "A System for Simulating Road-Representative Atmospheric Turbulence for Ground Vehicles in a Large Wind Tunnel," SAE Int. J. Passeng. Cars - Mech. Syst., **9**, pp. 817–830.

McAuliffe, B. and Wall, A. (2016), "Aerodynamic Performance of Flat-Panel Boat-Tails and Their Interactive Benefits with Side-Skirts," SAE Int. J. Commer. Veh., **9**, pp. 70–82.

McAuliffe, B., Wall, A. and Larose, G. (2016), "Simulation of Atmospheric Turbulence for Wind-Tunnel Tests on Full-Scale Light-Duty Vehicles," SAE Int. J. Passeng. Cars - Mech. Syst., **9**, pp. 583–591.

NAS (2015), "Cost, Effectiveness and Deployment of Fuel Economy Technologies for Light-Duty Vehicles," No. 987-0-309-37388-3, *National Research Council of the National Academies of Science, Washington, USA*.

SAE (2012), "SAE Wind Tunnel Procedure for Trucks and Buses," No. J1252, *Society of Automotive Engineers*.

Wittmeier, F., Michelbach, A., Wiedemann, J. and Senft, V. (2016), "The New Interchangeable Three-belt System in the IVK Full-Scale Wind Tunnel of University of Stuttgart: Design and First Results," SAE Technical Paper 2016-01-1581.

A. Detailed list of runs and experimental conditions

Appendix A presents a copy of the test log for each phase of this study. The test logs contain the list of runs in the order in which they were carried out and the associated main results. In the absence of knowledge of the manufacturer-specified frontal area, the results are presented in terms of $C_D A$ (drag area in m^2) and/or percentage changes of drag area with respect to the $C_D A$ of the baseline configuration.

In this appendix, $C_{D,0^\circ} A$ refers to the drag area of the vehicle at 0 degree yaw. $\Delta C_{D,0^\circ} A$ refers to the change in this drag area with respect to the baseline configuration. The vehicle's wind-averaged drag area is denoted as $C_{D,WA} A$, while $\Delta C_{D,WA} A$ represents the change in the wind-averaged drag area with respect to the baseline configuration. For speed sweeps, the value of the drag area listed in the test log corresponds to highest wind speed.

small car 1

Run #	*Comment*	*Yaw Angle [°]*	*Speed [km/hr]*	$C_{D,0^\circ} \times A\ [m^2]$	$\Delta C_{D,0^\circ} \times A$
9	Upper and lower shutters taped shut	0	103	0.762	-1.0%
13	Upper shutter untaped, lower shutter still taped shut	0	103	0.766	-0.5%
15	Baseline	0	56, 75, 94, 112, 135	0.769	-0.2%
20	Shutters 100% open	0,2,4,6,8,10,0	103	0.812	5.4%
22	Baseline	0,2,4,6,8,10,0	103	0.770	-
25	Shutter sweep (27%, 53%, 73%, 80%, 87%, 93% closed)	0	103	-	-
27	Underbody panel removal - rear suspension shields	0	103	0.771	0.1%
29	Underbody panel removal - engine and bumper panels	0	103	0.794	3.1%
31	Shutters 100% open - repeat	0,1,2,3,4,6,0	103	0.813	5.6%
32	Shutters 100% open	0	56, 75, 94, 112, 135	0.814	5.8%
34	Remove wheel dams	0,1,2,3,4,6,0	103	0.820	0.7%

midsize car 6

Run #	*Comment*	*Yaw Angle [°]*	*Speed [km/hr]*	$C_{D,0^\circ} \times A\ [m^2]$	$\Delta C_{D,0^\circ} \times A$
36	Shutters taped shut	0	103	0.767	0.1%
38	Baseline	0	56, 75, 94, 112, 121	0.768	0.2%
39	Baseline	0,2,4,6,8,10,0	103	0.766	
41	Shutters 100% open	0	56, 75, 94, 112, 131	0.772	0.8%
42	Shutters 100% open	0,2,4,6,8,10,0	103	0.773	0.9%
44	Shutter sweep (27%, 53%, 73%, 80%, 87%, 93% closed)	0	103	-	-
46	Underbody panel removal - rear midbody	0	103	0.778	1.6%
51	Underbody panel removal - fore midbody	0	103	0.783	2.1%
53	Underbody panel removal - engine and bumper panels	0	103	0.802	4.7%
55	Remove rear wheel dams	0	103	0.758	-1.0%
57	Remove all wheel dams	0,2,4,6,8,10,0	103	0.779	1.7%
59	Wheel covers	0	103	0.757	-1.2%
61	Baseline - Repeat	0	103	0.771	0.7%
62	Remove rear wheel dams - Repeat	0	103	0.757	-1.9%
64	Remove front wheel dams	0	103	0.790	2.4%
66	Baseline with separation edges	0	103	0.772	0.0%
68	Lower intake sealed and separation edges	0	110	0.753	-2.3%
70	Upper and lower intakes sealed and separation edges	0	110	0.692	-10.3%
72	Upper and lower intakes sealed	0	110	0.684	-11.3%
74	Lower intake sealed	0	110	0.752	-2.5%

Table A.1: Description of all the runs completed during Phase I of the wind tunnel tests, page 1/8.

76	Ride height: baseline - 20mm front, - 0mm rear	0	110	0.754	-2.2%
78	Ride height: baseline - 20mm front, - 20mm rear	0	110	0.771	0.0%
80	Ride height: baseline - 40mm front, - 20mm rear	0	110	0.754	-2.3%

midsize car 7

Run #	*Comment*	*Yaw Angle(s)*	*Speed [km/hr]*	$C_{D,0} \cdot x\ A\ [m^2]$	$\Delta C_{D,0} \cdot x\ A$
PROTOTYPE UNDERBODY INSTALLED! Remove license plate holder					
84	Shutters taped shut	0	103	0.754	-1.4%
87	"Baseline" (prototype underbody installed)	0	56, 75, 94, 112, 135	0.759	-0.7%
88	"Baseline" (prototype underbody installed)	0,2,4,6,8,10,0	103	0.765	0.0%
89	Shutters 100% open (prototype underbody installed)	0	56, 75, 94, 112, 135	0.779	1.8%
90	Shutters 100% open (prototype underbody installed)	0,2,4,6,8,10,0	103	0.784	2.5%
92	Shutter sweep (27%, 53%, 73%, 80%, 87%, 93% closed)	0	103	-	-
94	Prototype underbody panel removal - rear to midbody	0	103	0.776	1.4%
96	Prototype underbody panel removal - midbody to front - true baseline	0	103	0.783	2.4%
98	Install license plate and holder	0	103	0.781	-0.3%
100	Underbody panel removal - midbody	0	103	0.776	-0.8%
102	Underbody panel removal - engine and bumper panels	0	103	0.795	1.5%
-	Reinstall all underbody panels	0	-	-	-
104	Remove front wheel dams	0	103	0.793	1.3%
106	Wheel covers	0	103	0.729	-6.8%
109	Ride height: baseline - 20mm front, - 0mm rear	0	103	0.754	-3.7%
117	Ride height: baseline - 20mm front, - 20mm rear	0	103	0.760	-2.9%
119	Ride height: baseline - 40mm front, - 20mm rear	0	103	0.749	-4.4%
121	Ride height: baseline - 40mm front, - 40mm rear	0	103	0.746	-4.7%

midside car 2

Run #	*Comment*	*Yaw Angle(s)*	*Speed [km/hr]*	$C_{D,0} \cdot x\ A\ [m^2]$	$\Delta C_{D,0} \cdot x\ A$
PROTOTYPE UNDERBODY INSTALLED! Remove license plate holder					
123	Prototype underbody installed & Shutters taped shut	0	103	0.707	-1.4%
125	Prototype underbody panel removal - diffuser	0	103	0.712	-0.8%
127	Prototype underbody panel removal - midbody	0	103	0.713	-0.6%
130	Prototype underbody panel removal - engine bay	0	103	0.712	-0.8%
133	Baseline	0	56,75,94,103,112,118	0.713	-0.6%
132	Baseline	0,2,4,6,8,10,0	103	0.715	-0.3%
138	Shutter sweep (27%, 53%, 73%, 80%, 87%, 93% closed)	0	110	-	-

Table A.1: Description of all the runs completed during Phase I of the wind tunnel tests, page 2/8.

142	Baseline - Repeat	0	103	0.718	0.3%
144	Shutters 100% open - Repeat	0	103	0.737	2.7%
146	Underbody panel removal - rear axle and midbody	0	103	0.736	2.5%
148	Remove front wheel dams	0	103	0.743	3.5%
150	Underbody panel removal - engine and bumper panels	0,2,4,6,8,10,0	103	0.734	2.2%
152	Air Dam: 100% outer, 100% center	0	103	0.717	-0.1%
154	Air Dam: 100% outer, 66% center	0	103	0.703	-2.1%
156	Air Dam: 100% outer, 33% center	0	103	0.700	-2.5%
158	Air Dam: 100% outer, 0% center	0	103	0.711	-0.9%
160	Air Dam: 66% outer, 66% center	0	103	0.707	-1.4%
162	Air Dam: 66% outer, 33% center	0	103	0.707	-1.5%
164	Air Dam: 66% outer, 0% center	0	103	0.719	0.2%
166	Air Dam: 33% outer, 33% center	0	103	0.712	-0.8%
168	Air Dam: 33% outer, 0% center	0	103	0.717	0.0%
170	Front bumper air dam removed	0	103	0.726	1.2%
172	Ride height: baseline - 20mm front, - 20mm rear	0	103	0.700	-2.5%
173	Ride height: baseline - 40mm front, - 40mm rear	0	103	0.681	-5.1%

small SUV 1

Run #	*Comment*	*Yaw Angle(s)*	*Speed [km/hr]*	$C_{D,0^\circ} \times A\ [m^2]$	$\Delta C_{D,0^\circ} \times A$
PROTOTYPE UNDERBODY INSTALLED!					
178	Prototype underbody installed & Shutters taped shut	0	103	0.942	-3.1%
180	Tape removed from upper grille shutters	0	103	0.947	-2.6%
182	Tape removed from lower grille shutters	0	103	0.947	-2.5%
184	Prototype underbody panel removal - diffuser	0	103	0.950	-2.2%
186	Prototype underbody panel removal - midbody #1	0	103	0.960	-1.2%
188	Prototype underbody panel removal - midbody #2	0	103	0.970	-0.1%
190	Baseline (Front license plate removed)	0	57,76,94,112,128	0.969	-0.2%
191	Baseline	0,2,4,6,8,10,0	104	0.972	
193	Shutters 100% open	0	57,76,94,112,128	1.003	3.3%
194	Shutters 100% open	0,2,4,6,8,10,0	104	1.007	3.7%
196	Shutter sweep (27%, 53%, 73%, 80%, 87%, 93% closed)	0	103	-	-
198	Front passenger door confirmed closed	0	103	0.972	0.1%
200	Externally seal cooling intakes	0	103	0.948	-2.4%
202	Externally seal cooling intakes & Seperation edges	0	103	0.950	-2.2%
204	Grille/Shutters closed & Seperation edges	0	103	0.973	0.1%
206	Grille/Shutters open & Seperation edges	0	103	1.008	3.7%

Table A.1: Description of all the runs completed during Phase I of the wind tunnel tests, page 3/8.

208	Shutters 100% open - Repeat	0	103	1.006	3.5%
210	Underbody panel removal - rear axle and midbody	0	103	0.972	0.1%
212	Underbody panel removal - engine and bumper panels	0,2,4,6,8,10,0	104	0.982	1.0%
214	Wheel covers	0	103	0.950	-2.2%
216	Ride height: baseline - 20mm front, - 20mm rear	0	103	0.947	-2.6%
218	Ride height: baseline - 30mm front, - 30mm rear	0	103	0.935	-3.8%
220	Ride height: baseline - 20mm front, - 0mm rear	0	103	0.952	-2.0%
222	Ride Height: baseline - 30mm front & rear/ yaw sweep	0,2,4,6,8,10,0	103	0.933	-4.0%

midsize car 3

Run #	*Comment*	*Yaw Angle(s)*	*Speed [km/hr]*	$C_{D,0} \cdot x\ A\ [m^2]$	$\Delta C_{D,0} \cdot x\ A$
PROTOTYPE UNDERBODY INSTALLED!					
226	Prototype underbody & Lower shutter taped shut	0	103	0.698	-1.4%
228	Prototype underbody panel removal - diffuser	0	103	0.720	1.7%
230	Prototype underbody panel removal - midbody	0	103	0.726	2.5%
232	Prototype underbody - open service panel in engine cover	0	103	0.721	1.8%
234	Prototype underbody panel removal - engine bay	0	103	0.704	-0.6%
236	Baseline - Tape removed from lower grille shutters	0	103	0.708	-0.1%
238	Baseline	0	56,75,94,112,128	0.707	
239	Baseline	0,2,4,6,8,10,0	103	0.708	
241	Shutters 100% open	0	56,75,94,112,128	0.726	2.5%
242	Shutters 100% open	0,2,4,6,8,10,0	103	0.728	2.7%
244	Shutter sweep (27%, 53%, 73%, 80%, 87%, 93% closed)	0	103	-	-
246	Externally seal lower cooling intake	0	103	0.697	-1.5%
248	Externally seal middle cooling intake	0	103	0.685	-3.3%
250	Smooth upper inlet	0	103	0.675	-4.6%
254	Externally seal lower cooling intake - seperation edges	0	103	0.698	-1.4%
256	Open lower cooling intake - seperation edges	0	103	0.711	0.3%
258	Underbody panel removal - rear midbody	0	103	0.727	2.7%
260	Underbody panel removal - fore midbody	0,2,4,6,8,10,0	103	0.730	3.1%
262	Underbody panel removal - engine bay	0	103	0.734	3.6%
264	Air dam removal (center) - Rough underbody	0	103	0.742	4.7%
266	Air dam removal (outer) - Rough underbody	0	103	0.771	8.9%
268	Air dam removal - Stock (smoother) underbody	0	103	0.748	5.6%
270	Front wheel dam removal - w/o air dam	0,2,4,6,8,10,0	103	0.739	4.3%

Table A.1: Description of all the runs completed during Phase I of the wind tunnel tests, page 4/8.

midsize car 5

Run #	Comment	Yaw Angle(s)	Speed [km/hr]	$C_{D,0^\circ} \times A$ [m^2]	$\Delta C_{D,0^\circ} \times A$
PROTOTYPE UNDERBODY INSTALLED!					
275	Prototype underbody & Shutters/duct gaps taped shut	0	103	0.705	-3.5%
277	Remove upper shutter tape	0	103	0.707	-3.2%
278	Remove lower shutter tape	0	103	0.710	-2.9%
280	Remove duct sealing tape	0	103	0.709	-3.0%
282	Prototype underbody panel removal - diffuser	0	103	0.714	-2.2%
284	Prototype underbody panel removal - rear midbody	0	103	0.729	-0.2%
286	Baseline (prototype underbody panel removal - front midbody)	0	56,75,94,112,128	0.726	
287	Baseline	0,2,4,6,8,10,0	103	0.731	
290	Shutters 100% open	0	56,75,94,112,130	0.742	1.5%
291	Shutters 100% open	0,2,4,6,8,10,0	103	0.744	1.8%
293	Shutter sweep (27%, 53%, 73%, 80%, 87%, 93% closed)	0	103	-	-
295	Remove front license plate and holder	0	103	0.731	0.0%
297	Ride height: baseline - 20mm front, - 0mm rear	0	103	0.728	-0.4%
299	Ride height: baseline - 20mm front, - 20mm rear	0	103	0.719	-1.5%
301	Ride height: baseline - 40mm front, - 20mm rear	0	103	0.703	-3.7%
304	Ride height: baseline - 40mm front, - 40mm rear	0,2,4,6,8,10,0	103	0.695	-4.8%
308	Externally seal cooling intakes & Seperation edges (large)	0	103	0.746	2.2%
310	Open upper cooling intake & Seperation edges (large)	0	103	0.757	3.6%
312	Open lower cooling intake & Seperation edges (large)	0	103	0.759	3.9%
314	Open cooling & Seperation edges	0,2,4,6,8,10,0	103	0.741	1.5%
316	Lower cooling intake sealed & Seperation edges	0,2,4,6,8,10,0	103	0.738	1.1%
318	Both cooling intakes sealed & Seperation edges	0,2,4,6,8,10,0	103	0.723	-1.0%
320	Externally seal both cooling intakes	0,2,4,6,8,10,0	103	0.716	-2.0%
322	Open upper cooling intake	0,2,4,6,8,10,0	103	0.733	0.3%
324	Baseline repeat	0	103	0.735	0.7%
327	Wheel covers	0,2,4,6,8,10,0	103	0.720	-1.5%
330	Remove mid-underbody panels	0,2,4,6,8,10,0	103	0.765	4.7%
332	Remove engine bay/bumper underbody panels	0,2,4,6,8,10,0	103	0.766	4.8%
334	Ride height: baseline - 40mm front, - 40mm rear	0,2,4,6,8,10,0	103	0.724	-0.9%

midsize car 1

Run #	Comment	Yaw Angle(s)	Speed [km/hr]	$C_{D,0^\circ} \times A$ [m^2]	$\Delta C_{D,0^\circ} \times A$
337	Baseline with shutters taped	0,2,4,6,8,10,0	103	0.769	-0.3%

Table A.1: Description of all the runs completed during Phase I of the wind tunnel tests, page 5/8.

341	Rear underbody panels removed	0,1,2,4,6,8,10,0	103	0.776	0.6%
343	Central underbody panels removed	0,1,2,4,6,8,10,0	103	0.777	0.8%
345	Engine bay/bumper underbody panels removed	0,1,2,4,6,8,10,0	103	0.794	2.9%
348	Front wheel dams/jets removed	0,1,2,4,6,8,10,0	103	0.801	3.9%
350	Ride height: baseline - 40mm front, - 40mm rear	0,1,2,4,6,8,10,0	103	0.773	0.3%
352	Baseline with shutters taped	0	103	0.769	-0.3%
354	Baseline	0	57,75,94,112,130	0.771	
356	Baseline	0,1,2,3,4,5,6,7,8, 10,0	103	0.771	
358	Shutters 100% open	0	56,75,94,112,130	0.783	1.6%
359	Shutters 100% open	0,1,2,4,6,8,10,0	103	0.782	1.4%
361	Shutter sweep (27%, 53%, 73%, 80%, 87%, 93% closed)	0	103	-	-
363	Seal outlet of wheel jets	0,1,2,4,6,8,10,0	103	0.768	-0.4%
365	Seal outlet of wheel well louvers	0,1,2,4,6,8,10,0	103	0.764	-0.9%
367	Seal outlet of brake ducts	0,1,2,4,6,8,10,0	103	0.761	-1.3%
369	Seal lower intake	0,1,2,4,6,8,10,0	103	0.732	-5.1%
371	Seal both intakes	0,1,2,4,6,8,10,0	103	0.719	-6.8%
372	Seal upper intake	0,1,2,4,6,8,10,1	103	0.764	-0.9%
374	Baseline repeat	0,1,2,4,6,8,10,0,-1, -2,-4,-6,-8,-10,0	103	0.772	0.1%
376	Ride height: baseline - 40mm front, - 20mm rear	0,1,2,4,6,8,10,0	103	0.738	-4.3%

midsize car 4

Run #	*Comment*	*Yaw Angle(s)*	*Speed [km/hr]*	$C_{D,0} \cdot x\ A\ [m^2]$	$\Delta C_{D,0} \cdot x\ A$
382	Lower grille taped	0,2,4,6,8,10,0	103	0.706	-1.0%
385	Upper and lower grille taped	0,2,4,6,8,10,0	103	0.697	-2.3%
387	Upper grille taped	0,2,4,6,8,10,0	103	0.703	-1.5%
389	Baseline	0	56,75,94,112,130	0.710	
391	Baseline	0,2,4,6,8,10,0,-2, -4,-6,-8,-10,0	103	0.714	
393	Shutters 100% open	0	56,75,94,112,130	0.739	3.6%
394	Shutters 100% open	0,2,4,6,8,10,0	103	0.741	3.9%
396	Shutter sweep (27%, 53%, 73%, 80%, 87%, 93% closed)	0	103	-	-
399	Wheel covers	0,2,4,6,8,10,0	103	0.690	-3.3%
401	Remove rear wheel dams	0,2,4,6,8,10,0	103	0.709	-0.6%
403	Remove front wheel dams	0,2,4,6,8,10,0	103	0.741	3.9%
405	Remove diffuser underbody panels	0,2,4,6,8,10,0	103	0.751	5.2%

Table A.1: Description of all the runs completed during Phase I of the wind tunnel tests, page 6/8.

409	Remove mid-underbody panels	0,2,4,6,8,10,0	103	0.754	5.7%
411	Remove engine bay/bumper underbody panels	0,2,4,6,8,10,0	103	0.781	9.4%
413	Ride height: baseline - 40mm front, - 40mm rear	0,2,4,6,8,10,0	103	0.720	0.8%
415	Ride height: baseline - 40mm front, - 40mm rear	0,2,4,6,8,10,0	103	0.681	-4.5%
417	Ride height: baseline - 40mm front, - 20mm rear	0,2,4,6,8,10,0	103	0.685	-4.0%
419	Ride height: baseline - 20mm front, - 0mm rear	0	103	0.703	-1.5%
421	Ride height: baseline - 20mm front, - 20mm rear	0	103	0.697	-2.3%

pick-up truck 1

Run #	*Comment*	*Yaw Angle(s)*	*Speed [km/hr]*	$C_{D,0^\circ} \times A\ [m^2]$	$\Delta C_{D,0^\circ} \times A$
426	Grille taped, Duct Taped, Prototype underbody installed	0	102	1.207	-4.8%
428	Remove upper grille tape, Prototype underbody installed	0	103	1.209	-4.6%
430	Remove lower grille tape, Prototype underbody installed	0	103	1.216	-4.1%
432	Remove duct sealing, Prototype underbody installed	0	103	1.219	-3.8%
434	Remove emergency grille tape, Prototype underbody installed	0	103	1.243	-1.9%
437	Externally seal the grille	0,2,4,6,8,10,0	102	1.195	-5.7%
440	Prototype underbody baseline	0,2,4,6,8,10,0	102	1.243	-2.0%
442	Air dam removed - smooth underbody	0,2,4,6,8,10,0	102	1.226	-3.3%
444	Underbody - open engine bay vent	0,2,4,6,8,10,0	102	1.236	-2.5%
446	Underbody - rear panels removed	0,2,4,6,8,10,0	102	1.257	-0.8%
448	Underbody - mid panels removed	0,2,4,6,8,10,0	102	1.298	2.4%
450	Underbody - fore panels removed	0,2,4,6,8,10,0	102	1.332	5.1%
452	Baseline	0,2,4,6,8,10,0,-2, -4,-6,-8,-10,0	102	1.267	
454	Shutters 100% open	0	102	1.306	3.1%
456	Shutter sweep (27%, 53%, 73%, 80%, 87%, 93% closed)	0	102	-	-
459	Ride height: baseline + 20mm front, + 20mm rear	0,2,4,6,8,10,0	102	1.296	2.2%
461	Ride height: baseline - 20mm front, - 20mm rear	0	102	1.247	-1.6%
464	Ride height: baseline - 33mm front, - 33mm rear	0,2,4,6,8,10,0	102	1.228	-3.1%
466	Ride height: baseline - 44mm front, - 10mm rear	0,2,4,6,8,10,0	102	1.241	-2.1%
468	Ride height: baseline - 18mm front, - 00mm rear	0	102	1.255	-1.0%
470	Ride height: baseline + 00mm front, + 20mm rear	0,2,4,6,8,10,0	102	1.279	0.9%
472	Baseline repeat	0	102	1.268	0.0%
474	Remove tonneau cover	0,2,4,6,8,10,0	102	1.314	3.7%
477	Air Dam: 133% outer, 100% center	0	102	1.366	7.8%
479	Air Dam: 100% outer, 100% center	0	102	1.354	6.8%
481	Air Dam: 100% outer, 66% center	0	102	1.396	10.2%

Table A.1: Description of all the runs completed during Phase I of the wind tunnel tests, page 7/8.

483	Air Dam: 100% outer, 33% center	0	102	1.341	5.8%
485	Air Dam: 100% outer, 0% center	0	102	1.322	4.3%
487	Air Dam: 66% outer, 66% center	0	102	1.397	10.3%
489	Air Dam: 66% outer, 33% center	0	102	1.335	5.3%
491	Air Dam: 66% outer, 0% center	0	102	1.316	3.8%
493	Air Dam: 33% outer/33% center	0	102	1.341	5.8%
495	Air Dam: 33% outer/0% center	0	102	1.321	4.2%
497	Alternate wheels	0,2,4,6,8,10,0	102	1.356	7.0%

pick-up truck 2

Run #	*Comment*	*Yaw Angle(s)*	*Speed [km/hr]*	$C_{D,0^\circ} \times A\ [m^2]$	$\Delta C_{D,0^\circ} \times A$
500	Externally sealed grille	0	103	1.486	-6.3%
503	Baseline, redo	0,2,4,6,8,10,0	103	1.587	0.0%
505	Underbody - remove engine bay panels	0	103	1.600	0.9%
507	Underbody - remove air dam	0,2,4,6,8,10,0	103	1.617	1.9%
509	Open tailgate	0,2,4,6,8,10,0	102	1.694	6.7%
511	Remove tailgate	0	99	1.730	9.0%
513	Remove running boards	0	99	1.727	8.8%
515	Alternate wheels	0,2,4,6,8,0	94	1.759	10.8%

Table A.1: Description of all the runs completed during Phase I of the wind tunnel tests, page 8/8.

1 standard SUV 1

Run #	*Comment*	*Yaw Angle(s)*	*Speed [km/h]*	$C_{D,0} \cdot x\,A\ [m^2]$	$\Delta C_{D,0} \cdot x\,A$	$C_{D,WA}\ x\,A\ [m^2]$	$\Delta C_{D,WA}\ x\,A$
	Test A1 - AGS						
11	Shutters 100% open, speed sweep	0	60,80,100,120,140	1.098	3.4%		
12	Shutters 100% open, yaw sweep	0, 2, 4, 6 ,8 10, 0	110	1.098	3.4%	1.170	2.6%
14	Baseline, shutters 100% closed, yaw sweep **reference**	0, 2, 4, 6 ,8 10, 0	110	1.062	0.0%	1.140	0.0%
15	Baseline, shutters 100% closed, speed sweep	0	60,80,100,120,140	1.056	-0.5%		
16	Shutters 50% closed, yaw	0, 2, 4, 6 ,8 10, 0	110	1.083	2.0%	1.158	1.6%
18	Shutter closing, 25% open,	0	100	1.077	1.4%		
20	Shutter closing, 25%open, 50%open, 75%open, 100%open	0	100	-			
21	Shutter closing, 25%open, 50%open, 75%open, 100%open	0	120	-			
	Test B - Variable ride height						
23	Shutters 100% closed, ride height reduced by 20 mm front	0, 2, 4, 6 ,8 10, 0	110	1.031	-2.9%	1.126	-1.2%
24	Shutters 100% closed, ride height reduced by 20 mm front and back	0, 2, 4, 6 ,8 10, 0	110	1.032	-2.8%	1.119	-1.8%
26	Shutters 100% closed, ride height reduced by 40 mm front	0, 2, 4, 6 ,8 10, 0	110	1.006	-5.3%	1.101	-3.4%
27	Shutters 100% closed, ride height reduced by 40 mm front and back	0, 2, 4, 6 ,8 10, 0	110	1.010	-4.9%	1.100	-3.5%
	Test D1 OEM Under-body panel study						
29	Shutters 100% closed, baseline ride height, underbody panel removal stage 1	0, 2, 4, 6 ,8 10, 0	110	1.057	-0.5%	1.135	-0.4%
30	Shutters 100% closed, baseline ride height, underbody panel removal stage 2	0, 2, 4, 6 ,8 10, 0	110	1.078	1.5%	1.142	0.2%
32	Shutters 100% closed, baseline ride height, underbody panel removal stage 3	0, 2, 4, 6 ,8 10, 0	110	1.102	3.8%	1.156	1.5%

2 small SUV 2

Run #	*Comment*	*Yaw Angle(s)*	*Speed [km/h]*	$C_{D,0} \cdot x\,A\ [m^2]$	$\Delta C_{D,0} \cdot x\,A$	$C_{D,WA}\ x\,A\ [m^2]$	$\Delta C_{D,WA}\ x\,A$
	Test A1 - AGS						
34	Shakedown	0	140	0.906	-0.6%		
36	Shutters 100% closed, radiator 100% sealed	0	110	0.910	-0.1%		
38	Baseline, shutters 100% closed, speed sweep	0	60,80,100,120,140	0.914	0.2%		
39	Baseline, shutters 100% closed, yaw sweep	0, 2, 4, 6 ,8 10	110	0.912	0.0%	0.989	0.0%
40	Shutters 100% open, yaw sweep	0, 2, 4, 6 ,8 10	110	0.933	2.4%	1.011	2.2%
41	Shutters 100% open, speed sweep	0	60,80,100,120,140	0.932	2.2%		
42	Shutters 50% closed, yaw	0, 2, 4, 6 ,8 10	110	0.923	1.3%	0.999	1.1%
44	Shutter closing, 25%, 50%, 75%, 100%	0	100	-			
45	Shutter closing, 25%, 50%, 75%, 100%	0	120	-			
	Test B - Variable ride height						
47	Shutters 100% closed, ride height adjusted to 2 passenger weight (Front 30 3/16,,)	0, 2, 4, 6 ,8 10	110	0.904	-0.8%	0.978	-1.0%
48	Shutters 100% closed, ride height reduced by 20 mm front and back	0, 2, 4, 6 ,8 10	110	0.890	-2.3%	0.957	-3.2%
49	Shutters 100% closed, ride height reduced by 40 mm front	0, 2, 4, 6 ,8 10	110	0.885	-2.9%	0.954	-3.5%
50	Shutters 100% closed, ride height reduced by approx 40 mm (front 28 5/16, 28.5, back 29 5/16 29 9/16)	0, 2, 4, 6 ,8 10	110	0.870	-4.5%	0.933	-5.6%
	Test D1 - OEM Under-body panel study						
51	Shutters 100% closed, normal ride height, underbody panel removal stage 1	0, 2, 4, 6 ,8 10	110	0.916	0.5%	0.990	0.2%
52	Shutters 100% closed, normal ride height, underbody panel removal stage 2	0, 2, 4, 6 ,8 10	110	0.930	2.0%	1.002	1.4%
53	Shutters 100% closed, normal ride height, underbody panel removal stage 3	0, 2, 4, 6 ,8 10	110	0.933	2.4%	0.993	0.5%
	Test D2 - OEM Air dam						

Table A.2: Description of all the runs completed during Phase II of the wind tunnel tests, page 1/8.

54	Shutters 100% closed, normal ride height, underbody panel removal stage 3, remove all wheel dams	0, 2, 4, 6 ,8 10	110	0.960	5.3%	1.024	3.6%

3 small SUV 3

Run #	*Comment*	*Yaw Angle(s)*	*Speed [km/h]*	$C_{D,0} \cdot x\,A\ [m^2]$	$\Delta C_{D,0} \cdot x\,A$	$C_{D,WA}\ x\,A\ [m^2]$	$\Delta C_{D,WA}\ x\,A$
	Test C- Custom underbody panel study						
62	Shakedown			1.027			
64	Shutters 100% closed, radiator 100% sealed	0	110	1.030	-0.3%		
66	Shutters 100% closed, completely smooth underbody (reference for test C)	0, 2, 4, 6 ,8 10	110	1.033	0.0%	1.074	0.0%
67	Shutters 100% closed, 75% smooth underbody	0, 2, 4, 6 ,8 10	110	1.042	0.9%	1.089	1.4%
68	Shutters 100% closed, 25% smooth underbody	0, 2, 4, 6 ,8 10	110	1.067	3.3%	1.109	3.2%
	Test A1 - AGS						
71	Baseline, shutters 100% closed, speed sweep	0	60,80,100,120,140	1.051	-0.3%		
72	Baseline, shutters 100% closed, yaw sweep	0, 2, 4, 6 ,8 10	110	1.055	0.0%	1.107	0.0%
73	Shutters 100% open, yaw sweep	0, 2, 4, 6 ,8 10	110	1.079	2.3%	1.125	1.7%
74	Shutters 100% open, speed sweep	0	60,80,100,120,140	1.075			
75	Shutters 50% open, yaw	0, 2, 4, 6 ,8 10	110	1.063	0.8%	1.114	0.6%
77	Shutter closing, 25%, 50%, 75%, 100%	0	100	-			
78	Shutter closing, 25%, 50%, 75%, 100%	0	120	-			
	Test B - Variable ride height						
80	Shutters 100% closed, ride height reduced by 20 mm front and back	0, 2, 4, 6 ,8 10	110	1.026	-2.7%	1.077	-2.7%
81	Shutters 100% closed, ride height reduced by 40 mm front and back	0, 2, 4, 6 ,8 10	110	0.997	-5.4%	1.050	-5.2%
82	Shutters 100% closed, ride height reduced by 40 mm front 20 mm back	0, 2, 4, 6 ,8 10	110	1.003	-4.9%	1.056	-4.6%
83	Shutters 100% closed, ride height reduced by 20 mm front 0 mm back	0, 2, 4, 6 ,8 10	110	1.036	-1.8%	1.086	-1.8%

4 minivan 1

Run #	*Comment*	*Yaw Angle(s)*	*Speed [km/h]*	$C_{D,0} \cdot x\,A\ [m^2]$	$\Delta C_{D,0} \cdot x\,A$	$C_{D,WA}\ x\,A\ [m^2]$	$\Delta C_{D,WA}\ x\,A$
	Test C- Custom underbody panel study						
85	Shakedown			0.976			
87	Shutters 100% closed, completely smooth underbody (reference for test C)	0, 2, 4, 6 ,8 10	110	0.980	0.0%	1.042	0.0%
88	Shutters 100% closed, 75% smooth underbody	0, 2, 4, 6 ,8 10	110	0.953	-2.8%	1.039	-0.2%
90	Shutters 100% closed, 25% smooth underbody	0, 2, 4, 6 ,8 10	110	0.998	1.8%	1.082	3.9%
	Test B - Variable ride height						
91	Shakedown			0.994	-2.0%		
93	Shutters 100% closed, ride height reduced by 20 mm front	0, 2, 4, 6 ,8 10	110	1.002	-1.2%	1.069	-0.6%
94	Shutters 100% closed, ride height reduced by 37 mm front, 20 mm back	0, 2, 4, 6 ,8 10	110	0.982	-3.2%	1.056	-1.9%
95	Shutters 100% closed, ride height reduced by 37 mm front and back	0, 2, 4, 6 ,8 10	110	0.983	-3.1%	1.052	-2.2%
97	Shutters 100% closed, ride height reduced by 20 mm front and back	0, 2, 4, 6 ,8 10	110	0.994	-2.0%	1.058	-1.7%
	Test A1 - AGS						
98	Baseline, shutters 100% closed, speed sweep	0	60,80,100,120,140	1.010			
99	Baseline, shutters 100% closed, yaw sweep	0, 2, 4, 6 ,8 10	110	1.014	0.0%	1.076	0.0%
100	Shutters with mesh mock up, yaw	0, 2, 4, 6 ,8 10	110	1.033	1.9%	1.086	0.9%
101	Shutters 100% open, yaw sweep	0, 2, 4, 6 ,8 10	110	1.036	2.2%	1.088	1.1%
102	Shutters 100% open, speed sweep	0	60,80,100,120,140	1.032	1.8%	0.000	
103	Shutters 100% open, underbody air dams removed, yaw sweep	0, 2, 4, 6 ,8 10	110	1.035	2.1%	1.088	1.2%

Table A.2: Description of all the runs completed during Phase II of the wind tunnel tests, page 2/8.

5	**small car 2**						
Run #	*Comment*	*Yaw Angle(s)*	*Speed [km/h]*	$C_{D,0} \cdot x\ A\ [m^2]$	$\Delta C_{D,0} \cdot x\ A$	$C_{D,WA}\ x\ A\ [m^2]$	$\Delta C_{D,WA}\ x\ A$
105	Shakedown			0.672			
	Test B - Variable ride height						
107	Shutters 100% closed, ride height reduced by 40 mm front and back	0, 2, 4, 6 ,8 10	110	0.675	-5.6%	0.731	-5.6%
108	Shutters 100% closed, ride height reduced by 20 mm front and back	0, 2, 4, 6 ,8 10	110	0.688	-3.7%	0.755	-2.6%
110	Shutters 100% closed, ride height reduced by 40 mm front, 20 back	0, 2, 4, 6 ,8 10	110	0.677	-5.1%	0.735	-5.1%
111	Shutters 100% closed, ride height reduced by 20 mm front, neutral back	0, 2, 4, 6 ,8 10	110	0.698	-2.2%	0.754	-2.6%
	Test F- HVAC study						
113	Shutters 100% closed, normal ride height, HVAC: recirculation mode (reference for test F)	0	110	0.721	0.0%		
113	Shutters 100% closed, normal ride height, HVAC: fan low, no air conditioning	0	110	0.718	-0.3%		
113	Shutters 100% closed, normal ride height, HVAC: fan high, no air conditioning	0	110	0.717	-0.5%		
113	Shutters 100% closed, normal ride height, HVAC: fan low, with air conditioning	0	110	0.719	-0.2%		
113	Shutters 100% closed, normal ride height, HVAC: fan high, with air conditioning	0	110	0.717	-0.5%		
113	Shutters 100% closed, normal ride height, HVAC: recirculation, windows open 1/4 of the way	0	110	0.751	4.2%		
	Test A1 - AGS						
115	Baseline, shutters 100% closed, speed sweep	0	60,80,100,120,140	0.713	-0.2%		
116	Baseline, shutters 100% closed, yaw sweep	0, 2, 4, 6 ,8 10	110	0.714	0.0%	0.774	0.0%
117	Shutters 100% open, speed sweep	0	60,80,100,120,140	0.739	3.4%		
118	Shutters 100% open, yaw sweep	0, 2, 4, 6 ,8 10	110	0.744	4.2%	0.796	2.7%
119	Shutters 50% closed, yaw	0, 2, 4, 6 ,8 10	110	0.737	3.2%	0.789	1.9%
121	Shutter closing, 25%, 50%, 75%, 100%	0	100	-			
122	Shutter closing, 25%, 50%, 75%, 100%	0	120	-			
	Test D1 - OEM Under-body panel study						
124	Shutters 100% closed, normal ride height, underbody panel removal stage 1	0, 2, 4, 6 ,8 10	110	0.701	-1.9%	0.763	-1.4%
125	Shutters 100% closed, normal ride height, underbody panel removal stage 2	0, 2, 4, 6 ,8 10	110	0.731	2.4%	0.780	0.7%
126	Shutters 100% closed, normal ride height, underbody panel removal stage 3 (reference for test H)	0, 2, 4, 6 ,8 10	110	0.748	4.7%	0.779	0.7%
5	**small car 2 - day 2**						
128	Shakedown	0	140	0.716			
	Test H - OEM Air dam height study, *ride height sweep: baseline, 20 mm, 40 mm*				wrt Run 126		
130	Shutters 100% closed, underbody panels removed, air dam height increased by 60%, baseline height	0	110	0.719	-3.9%		
131	Shutters 100% closed, underbody panels removed, air dam height increased by 60%, down 20 mm	0	110	0.693	-7.3%		
132	Shutters 100% closed, underbody panels removed, air dam height increased by 60%, down 40 mm	0	110	0.690	-7.7%		
134	Shutters 100% closed, underbody panels removed, air dam height increased by 45%, down 40 mm	0	110	0.670	-10.4%		
135	Shutters 100% closed, underbody panels removed, air dam height increased by 45%, down 20 mm	0	110	0.692	-7.5%		
136	Shutters 100% closed, underbody panels removed, air dam height increased by 45%, baseline height	0	110	0.723	-3.3%		
137	Shutters 100% closed, underbody panels removed, air dam height increased by 30%, baseline height	0	110	0.722	-3.4%		
138	Shutters 100% closed, underbody panels removed, air dam height increased by 30%, down 20 mm	0	110	0.694	-7.1%		
139	Shutters 100% closed, underbody panels removed, air dam height increased by 30%, down 40 mm	0	110	0.665	-11.0%		
141	Shutters 100% closed, underbody panels removed, air dam height increased by 15%, down 40 mm	0	110	0.670	-10.3%		
143	Shutters 100% closed, underbody panels removed, air dam height increased by 15%, down 20 mm	0	110	0.698	-6.7%		
144	Shutters 100% closed, underbody panels removed, air dam height increased by 15%, baseline height	0	110	0.724	-3.2%		
147	Shutters 100% closed, underbody panels removed, air dam height increased by 0%, baseline height	0	110	0.736	-1.5%		

Table A.2: Description of all the runs completed during Phase II of the wind tunnel tests, page 3/8.

149	Shutters 100% closed, underbody panels removed, air dam height increased by 0%, down 20 mm	0	110	0.708	-5.3%		
151	Shutters 100% closed, underbody panels removed, air dam height increased by 0%, down 40 mm	0	110	0.676	-9.6%		
	Test D2 - OEM Air dam				wrt Run 116		
153	Shutters 100% closed, normal ride height, last underbody panel removal stage 4, remove Leo's air dam	0, 2, 4, 6 ,8 10	110	0.751	5.2%	0.784	1.3%
154	Shutters closed, normal ride height, underbody panel rem. stage 4, no air dam, remove all wheel dams	0, 2, 4, 6 ,8 10	110	0.774	8.3%	0.803	3.7%

6 large car 1

Run #	*Comment*	*Yaw Angle(s)*	*Speed [km/h]*	$C_{D,0} \cdot x\,A\ [m^2]$	$\Delta C_{D,0} \cdot x\,A$	$C_{D,WA}\ x\,A\ [m^2]$	$\Delta C_{D,WA}\ x\,A$
159	Shutters 100% closed, radiator 100% sealed	0	110	0.843	-3.6%		
	Test C- Custom underbody panel study						
161	Shutters 100% closed, completely smooth underbody	0, 2, 4, 6 ,8 10	110	0.843	-3.6%	0.900	-1.6%
163	Shutters 100% closed, 75% smooth underbody	0, 2, 4, 6 ,8 10	110	0.861	-1.5%	0.907	-0.8%
165	Shutters 100% closed, 25% smooth underbody	0, 2, 4, 6 ,8 10	110	0.871	-0.4%	0.918	0.3%
	Test A1 - AGS						
167	Baseline, shutters 100% closed, speed sweep	0	60,80,100,120,140	0.874			
168	Baseline, shutters 100% closed, full yaw sweep	-10 to +10 incr 2	110	0.874	0.0%	0.914	0.0%
196	Shutters 100% open, yaw sweep	0, 2, 4, 6 ,8 10	110	0.908	3.9%	0.946	3.4%
197	Shutters 100% open, speed sweep	0	60,80,100,120,140	0.911	4.2%		
199	Shutters 50% closed, yaw	0, 2, 4, 6 ,8 10	110	0.882	0.9%	0.931	1.8%
201	Shutter closing, 25%, 50%, 75%, 100%	0	100	-			
202	Shutter closing, 25%, 50%, 75%, 100%	0	120	-			
170	Baseline, shutters 100% closed, speed sweep, spoiler installed	0	60,80,100,120,140	0.873	-0.2%		
171	Baseline, shutters 100% closed, yaw sweep, spoiler installed	0, 2, 4, 6 ,8 10	110	0.874	-0.1%	0.917	0.3%
	Test B - Variable ride height						
191	Shutters 100% closed, ride height reduced by 20 mm front	0, 2, 4, 6 ,8 10	110	0.836	-4.4%	0.895	-2.1%
193	Shutters 100% closed, ride height reduced by 20 mm front and back	0, 2, 4, 6 ,8 10	110	0.834	-4.6%	0.887	-3.0%
194	Shutters 100% closed, ride height reduced by 37 mm front	0, 2, 4, 6 ,8 10	110	0.804	-8.0%	0.870	-4.8%
195	Shutters 100% closed, ride height reduced by 37 mm front and back	0, 2, 4, 6 ,8 10	110	0.808	-7.6%	0.866	-5.3%
	Test H - OEM Air dam height study, *ride height sweep: baseline, 20 mm, 40 mm*						
172	Shutters 100% closed, underbody panels removed, air dam height increased by 60%, baseline height	0	110	0.841	-3.9%		
174	Shutters 100% closed, underbody panels removed, air dam height increased by 60%, down 20 mm	0	110	0.805	-7.9%		
175	Shutters 100% closed, underbody panels removed, air dam height increased by 60%, down 37 mm	0	110	0.772	-11.7%		
178	Shutters 100% closed, underbody panels removed, air dam height increased by 60%, down 37 mm	0, 2, 4, 6 ,8 10	110	0.780	-10.8%	0.829	-9.3%
179	Shutters 100% closed, underbody panels removed, air dam height increased by 40%, down 37 mm	0, 2, 4, 6 ,8 10	110	0.781	-10.7%	0.838	-8.4%
180	Shutters 100% closed, underbody panels removed, air dam height increased by 40%, down 20 mm	0	110	0.783	-10.5%		
181	Shutters 100% closed, underbody panels removed, air dam height increased by 40%, baseline height	0	110	0.844	-3.5%		
183	Shutters 100% closed, underbody panels removed, air dam height increased by 27%, baseline height	0	110	0.849	-2.9%		
184	Shutters 100% closed, underbody panels removed, air dam height increased by 27%, down 20 mm	0	110	0.810	-7.3%		
185	Shutters 100% closed, underbody panels removed, air dam height increased by 27%, down 37 mm	0	110	0.787	-10.0%		
187	Shutters 100% closed, underbody panels removed, air dam height increased by 13%, down 37 mm	0, 2, 4, 6 ,8 10	110	0.795	-9.1%	0.853	-6.7%
188	Shutters 100% closed, underbody panels removed, air dam height increased by 13%, down 20 mm	0, 2, 4, 6 ,8 10	110	0.819	-6.3%	0.879	-3.8%
189	Shutters 100% closed, underbody panels removed, air dam height increased by 13%, baseline height	0, 2, 4, 6 ,8 10	110	0.858	-1.9%	0.908	-0.6%
	Test D2 - OEM Air dam						
205	Shutters 100% closed, baseline ride height remove air dam	-10 to +10 incr 2	110	0.902	3.1%	0.919	0.5%

Table A.2: Description of all the runs completed during Phase II of the wind tunnel tests, page 4/8.

206	Shutters 100% closed, baseline ride height remove air dam	0	60,80,100,120,140	0.903	3.2%		

7 standard SUV 2

Run #	*Comment*	*Yaw Angle(s)*	*Speed [km/h]*	$C_{D,0} \cdot x\ A\ [m^2]$	$\Delta C_{D,0} \cdot x\ A$	$C_{D,WA}\ x\ A\ [m^2]$	$\Delta C_{D,WA}\ x\ A$
	Test A2 - Cooling study						
208	Shakedown			1.145			
210	Front external grille sealed with tape, Shutters 100% closed, 100% smooth underbody	-10 to +10 incr 2	110	1.145	-5.3%	1.239	-5.2%
	Test C- Custom underbody panel study						
211	Shutters 100% closed, completely smooth underbody	0, 2, 4, 6 ,8 10	110	1.163	-3.8%	1.256	-3.8%
213	Shutters 100% closed, 75% smooth underbody	0, 2, 4, 6 ,8 10	110	1.178	-2.6%	1.263	-3.3%
215	Shutters 100% closed, 25% smooth underbody	0, 2, 4, 6 ,8 10	110	1.203	-0.5%	1.324	1.3%
	Test B - Variable ride height						
219	Shutters 100% closed, ride height reduced by 20 mm front and back	0, 2, 4, 6 ,8 10	110	1.184	-2.1%	1.289	-1.4%
220	Shutters 100% closed, ride height reduced by 40 mm front and back	0, 2, 4, 6 ,8 10	110	1.158	-4.2%	1.261	-3.5%
221	Shutters 100% closed, ride height reduced by 40 mm front 20 mm back	0, 2, 4, 6 ,8 10	110	1.169	-3.4%	1.279	-2.1%
222	Shutters 100% closed, ride height reduced by 20 mm front	0, 2, 4, 6 ,8 10	110	1.199	-0.9%	1.311	0.3%
	Test G - Custom Air dam height study, ***ride height sweep: baseline, 20 mm, 40 mm***						
223	Shutters 100% closed, underbody panels removed, air dam height increased by 60%, baseline height	0, 2, 4, 6 ,8 10	110	1.191	-1.5%	1.329	1.7%
224	Shutters 100% closed, underbody panels removed, air dam height increased by 60%, down 20 mm	0, 2, 4, 6 ,8 10	110	1.168	-3.4%	1.296	-0.8%
225	Shutters 100% closed, underbody panels removed, air dam height increased by 60%, down 40 mm	0, 2, 4, 6 ,8 10	110	1.150	-4.9%	1.270	-2.8%
227	Shutters 100% closed, underbody panels removed, air dam height increased by 45%, down 40 mm	0, 2, 4, 6 ,8 10	110	1.140	-5.8%	1.259	-3.6%
229	Shutters 100% closed, underbody panels removed, air dam height increased by 45%, down 20 mm	0, 2, 4, 6 ,8 10	110	1.162	-3.9%	1.292	-1.1%
231	Shutters 100% closed, underbody panels removed, air dam height increased by 45%, baseline height	0, 2, 4, 6 ,8 10	110	1.191	-1.5%	1.318	0.8%
233	Shutters 100% closed, underbody panels removed, air dam height increased by 30%, baseline height	0, 2, 4, 6 ,8 10	110	1.188	-1.8%	1.309	0.2%
234	Shutters 100% closed, underbody panels removed, air dam height increased by 30%, down 20 mm	0, 2, 4, 6 ,8 10	110	1.163	-3.9%	1.285	-1.7%
236	Shutters 100% closed, underbody panels removed, air dam height increased by 30%, down 40 mm	0, 2, 4, 6 ,8 10	110	1.141	-5.7%	1.248	-4.5%
237	Shutters 100% closed, underbody panels removed, air dam height increased by 15%, down 40 mm	0, 2, 4, 6 ,8 10	110	1.140	-5.7%	1.253	-4.1%
238	Shutters 100% closed, underbody panels removed, air dam height increased by 15%, down 20 mm	0, 2, 4, 6 ,8 10	110	1.169	-3.3%	1.286	-1.6%
240	Shutters 100% closed, underbody panels removed, air dam height increased by 15%, baseline height	0, 2, 4, 6 ,8 10	110	1.188	-1.7%	1.311	0.3%
241	Shutters 100% closed, underbody panels removed, air dam height increased by 10%, baseline height	0, 2, 4, 6 ,8 10	110	1.195	-1.2%	1.312	0.4%
	Test A1 - AGS						
244	Baseline, shutters 100% closed, speed sweep	0	60,80,100,120,140	1.211	0.2%		
245	Baseline, shutters 100% closed, yaw sweep	-10 to +10 incr 2	110	1.209	0.0%	1.307	0.0%
247	Shutters with mesh, yaw	0, 2, 4, 6 ,8 10	110	1.273	5.3%	1.354	3.6%
249	Shutters 100% open, speed sweep	0	60,80,100,120,140	1.280	5.8%		
250	Shutters 100% open, yaw sweep	-10 to +10 incr 2	110	1.279	5.8%	1.358	4.0%
	Install turbulent flow exposure						
	Reinstall custom underbody panels						
252	Shakedown			1.163			
254	Front external grille sealed with tape, Shutters 100% closed, 100% smooth underbody	0,-10 to +10 incr 2	110	1.173	-5.6%	1.230	-6.6%
	Test C- Custom underbody panel						
258	Shutters 100% closed, completely smooth underbody	0, 2, 4, 6 ,8 10	110	1.199	-3.5%	1.255	-4.7%
260	Shutters 100% closed, 75% smooth underbody	0, 2, 4, 6 ,8 10	110	1.219	-1.9%	1.264	-4.0%

Table A.2: Description of all the runs completed during Phase II of the wind tunnel tests, page 5/8.

261	Shutters 100% closed, 25% smooth underbody	0, 2, 4, 6 ,8 10	110	1.235	-0.6%	1.310	-0.5%
	Test A - AGS turbulent flow (remove all 3 custom underbody panels)						
265	Baseline, shutters 100% closed, speed sweep	0	60,80,100,120,140	1.231			
264	Baseline, shutters 100% closed, yaw sweep	0,-10 to +10 incr 2	110	1.242	0.0%	1.317	0.0%
	Test G - Custom Air dam height study						
268	Shutters 100% closed, air dam as run 241 in smooth flow, baseline ride height	0, 2, 4, 6 ,8 10	110	1.232	-0.9%	1.312	-0.4%
	Test B - Variable ride height						
270	Shutters 100% closed, ride height reduced by 20 mm front	0, 2, 4, 6 ,8 10	110	1.229	-1.1%	1.304	-1.1%
271	Shutters 100% closed, ride height reduced by 20 mm front and back	0, 2, 4, 6 ,8 10	110	1.213	-2.4%	1.284	-2.5%
273	Shutters 100% closed, ride height reduced by 40 mm front 20 mm back	0, 2, 4, 6 ,8 10	110	1.201	-3.4%	1.267	-3.8%
275	Shutters 100% closed, ride height reduced by 40 mm front and back	0, 2, 4, 6 ,8 10	110	1.190	-4.2%	1.255	-4.7%

6 large car 1

reference area is WxH=1.935*1.542=2.984 square metres

Run #	*Comment*	*Yaw Angle(s)*	*Speed [km/h]*	$C_{D,0} \cdot x\ A\ [m^2]$	$\Delta C_{D,0} \cdot x\ A$	$C_{D,WA}\ x\ A\ [m^2]$	$\Delta C_{D,WA}\ x\ A$
	Reinstall custom underbody panels and air dams						
279	Shakedown			0.834			
	Test C- Custom underbody panel study						
282	Shutters 100% closed, completely smooth underbody	0, 2, 4, 6 ,8, 10	110	0.835	-3.0%	0.889	-1.3%
283	Shutters 100% closed, 75% smooth underbody	0, 2, 4, 6 ,8, 10	110	0.848	-1.4%	0.897	-0.4%
285	Shutters 100% closed, 25% smooth underbody	0, 2, 4, 6 ,8, 10	110	0.870	1.1%	0.904	0.4%
	Test A - AGS turbulent flow						
287	Baseline, shutters 100% closed, speed sweep	0	60,80,100,120,140	0.861	0.1%		
288	Baseline, shutters 100% closed, yaw sweep	0,-10 to +10 incr 2	110	0.861	0.0%	0.900	0.0%
289	Baseline, shutters 100% open, yaw sweep	0, 2, 4, 6 ,8, 10	110	0.902	4.8%	0.932	3.6%
290	Shutters 50% closed, yaw	0, 2, 4, 6 ,8, 10	110	0.875	1.7%	0.916	1.7%
292	Baseline, shutters 100% closed, speed sweep, spoiler installed	0	60,80,100,120,140	0.875	1.7%		
293	Baseline, shutters 100% closed, yaw sweep, spoiler installed	0, 2, 4, 6 ,8 10	110	0.872	1.3%	0.908	0.9%
	Test B - Variable ride height						
294	Shutters 100% closed, ride height reduced by 20 mm front	0, 2, 4, 6 ,8, 10	110	0.837	-2.8%	0.879	-2.4%
295	Shutters 100% closed, ride height reduced by 20 mm front and back	0, 2, 4, 6 ,8, 10	110	0.841	-2.3%	0.879	-2.4%
296	Shutters 100% closed, ride height reduced by 40 mm front, 20 mm back	0, 2, 4, 6 ,8, 10	110	0.811	-5.8%	0.856	-4.9%
297	Shutters 100% closed, ride height reduced by 40 mm front and back	0, 2, 4, 6 ,8, 10	110	0.802	-6.8%	0.843	-6.4%
	Test H - OEM Air dam height study, *ride height sweep: baseline, 20 mm, 40 mm*						
298	Shutters 100% closed, underbody panels removed, air dam height increased by 40%, down 37 mm	0, 2, 4, 6 ,8, 10	110	0.790	-8.2%	0.829	-7.9%
299	Shutters 100% closed, underbody panels removed, air dam height increased by 40%, down 20 mm	0, 2, 4, 6 ,8, 10	110	0.814	-5.4%	0.854	-5.1%
300	Shutters 100% closed, underbody panels removed, air dam height increased by 40%, baseline height	0, 2, 4, 6 ,8, 10	110	0.848	-1.5%	0.888	-1.3%
	Test D2 - OEM Air dam						
302	Shutters 100% closed, baseline ride height remove air dam	0	60,80,100,120,140	0.897	4.2%		
303	Shutters 100% closed, baseline ride height remove air dam	0, 2, 4, 6 ,8, 10	110	0.898	4.4%	0.915	1.6%

Table A.2: Description of all the runs completed during Phase II of the wind tunnel tests, page 6/8.

8 large car 2

Run #	*Comment*	*Yaw Angle(s)*	*Speed [km/h]*	$C_{D,0} \cdot x\ A\ [m^2]$	$\Delta C_{D,0} \cdot x\ A$	$C_{D,WA}\ x\ A\ [m^2]$	$\Delta C_{D,WA}\ x\ A$
	Test A1 - AGS						
306	Shakedown (external grille sealed)	0	140	0.737	-3.9%		
308	Shakedown (external grille sealed)	0	110	0.731	-4.7%		
311	External front grille 100% closed (sealed)	0, 2, 4, 6 ,8 10	110	0.733	-4.4%	0.807	-3.8%
314	Shutters 100% closed, lower radiator sealed	0	110	0.763	-0.4%		
316	Baseline, shutters 100% closed, speed sweep	0	60,80,100,120,140	0.767			
317	Baseline, shutters 100% closed, yaw sweep	0, 2, 4, 6 ,8 10	110	0.767		0.839	
319	Shutters 100% open, yaw sweep	0, 2, 4, 6 ,8 10	110	0.782	1.9%	0.852	1.5%
320	Shutters 100% open, speed sweep	0	60,80,100,120,140	0.781			
322	Shutter closing, 25% closed, 50% closed, 75% closed, 100% closed,	0	110				
	Test B - Variable ride height						
324	Shutters 100% closed, ride height reduced by 20 mm front and back	0, 2, 4, 6 ,8 10	110	0.753	-1.8%	0.817	-2.6%
325	Shutters 100% closed, ride height reduced by 40 mm front and back	0, 2, 4, 6 ,8 10	110	0.734	-4.3%	0.788	-6.2%
327	Shutters 100% closed, ride height reduced by 40 mm front	0, 2, 4, 6 ,8 10	110	0.728	-5.0%	0.791	-5.7%
328	Shutters 100% closed, ride height reduced by 20 mm front	0, 2, 4, 6 ,8 10	110	0.747	-2.6%	0.818	-2.5%
330	Shutters 100% closed,optimum ride height ,40 mm down front, 20 mm down back oem air dam removed	0, 2, 4, 6 ,8 10	110	0.753	-1.8%	0.807	-3.8%
332	Shutters 100% closed,baseline ride height , oem air dam removed	0, 2, 4, 6 ,8 10	110	0.772	0.7%	0.847	1.0%
	Test D1 OEM Under-body panel study						
334	Shutters 100% closed, baseline ride height, all panels removed at once	0, 2, 4, 6 ,8 10	110	0.771	0.5%	0.845	0.7%
	Test D2 - OEM Air dam						
336	Shutters 100% closed, baseline ride height, custom air dam extended by 50 mm	0, 2, 4, 6 ,8 10	110	0.747	-2.6%	0.823	-1.9%
338	Shutters 100% closed, baseline ride height, custom air dam extended to Taurus height (70 mm)	0, 2, 4, 6 ,8 10	110	0.738	-3.7%	0.812	-3.2%
340	Shutters 100% closed, baseline ride height, custom air dam center closed	0, 2, 4, 6 ,8 10	110	0.757	-1.3%	0.819	-2.4%
342	Shutters 100% closed, baseline ride height, oem air dam removed	0, 2, 4, 6 ,8 10	110	0.772	0.6%	0.853	1.6%
344	Shutters 100% closed, baseline ride height, oem rear wheel dam removed	0, 2, 4, 6 ,8 10	110	0.768	0.2%	0.838	-0.2%
346	Shutters 100% closed, baseline ride height, oem front wheel dam removed	0, 2, 4, 6 ,8 10	110	0.800	4.3%	0.846	0.8%

9 small SUV 4

Run #	*Comment*	*Yaw Angle(s)*	*Speed [km/h]*	$C_{D,0} \cdot x\ A\ [m^2]$	$\Delta C_{D,0} \cdot x\ A$	$C_{D,WA}\ x\ A\ [m^2]$	$\Delta C_{D,WA}\ x\ A$
348	Shakedown (external grille sealed)	0	140	0.985			
350	External front grille 100% closed (sealed)	0, 2, 4, 6 ,8 10	110	0.991	-6.7%	1.088	-4.8%
	Test C- Custom underbody panel study						
353	Shutters 100% closed, completely smooth underbody	0, 2, 4, 6 ,8 10	110	0.996	-6.3%	1.091	-4.6%
355	Shutters 100% closed, 75% smooth underbody	0, 2, 4, 6 ,8 10	110	1.018	-4.2%	1.105	-3.3%
357	Shutters 100% closed, 25% smooth underbody	0, 2, 4, 6 ,8 10	110	1.044	-1.8%	1.141	-0.2%
	Test B - Variable ride height						
359	Shutters 100% closed, ride height reduced by 20 mm front and back	0, 2, 4, 6 ,8 10	110	1.039	-2.2%	1.121	-1.9%
361	Shutters 100% closed, ride height reduced by 40 mm front and back	0, 2, 4, 6 ,8 10	110	1.010	-4.9%	1.096	-4.2%
363	Shutters 100% closed, ride height reduced by 40 mm front, 20 mm back	0, 2, 4, 6 ,8 10	110	1.015	-4.5%	1.100	-3.8%
365	Shutters 100% closed, ride height reduced by 20 mm front	0, 2, 4, 6 ,8 10	110	1.044	-1.8%	1.125	-1.6%
	Test D2 - OEM Air dam						

Table A.2: Description of all the runs completed during Phase II of the wind tunnel tests, page 7/8.

367	Shutters 100% closed, baseline ride height, oem air dam extended 15 mm	0, 2, 4, 6 ,8 10	110	1.050	-1.2%	1.137	-0.5%
369	Shutters 100% closed, baseline ride height, oem air dam extended 30 mm	0, 2, 4, 6 ,8 10	110	1.035	-2.6%	1.135	-0.7%
373	Shutters 100% closed, baseline ride height, oem air dam extended 60 mm	0, 2, 4, 6 ,8 10	110	1.015	-4.5%	1.121	-2.0%
375	Shutters 100% closed, baseline ride height, OEM air dam, rear wheel air dam removed	0, 2, 4, 6 ,8 10	110	1.068	0.5%	1.136	-0.6%
	Test A1 - AGS						
377	Baseline, shutters 100% closed, speed sweep	0	60,80,100,120,140	1.057	-0.6%		
378	Baseline, shutters 100% closed, yaw sweep	0, 2, 4, 6 ,8 10	110	1.063	0.0%	1.143	0.0%
380	Shutters with mock up frame, yaw sweep	0, 2, 4, 6 ,8 10	110	1.132	6.5%	1.186	3.8%
382	Shutters 100% open, yaw sweep	0, 2, 4, 6 ,8 10	110	1.154	8.5%	1.204	5.3%

Table A.2: Description of all the runs completed during Phase II of the wind tunnel tests, page 8/8.

1 **small car 3**

Run #	Comment	Yaw Angle(s)	Speed [km/h]	$C_{D,0} \cdot x\ A\ [m^2]$	$\Delta C_{D,0} \cdot x\ A$	$C_{D,WA}\ x\ A\ [m^2]$	$\Delta C_{D,WA}\ x\ A$
4	Shakedown, with air dam removed	0	110	0.819	3.9%		
	Test C- Custom underbody panel study						
8	Shutters 100% closed, full under body cover, removed bumber air dam, test J	0, 2, 4, 6 ,8 10	110	0.819	3.9%	0.832	0.7%
	reinstall bumper air dam		0				
10	Shutters 100% closed, completely smooth underbody	0, 2, 4, 6 ,8 10	110	0.781	-0.9%	0.814	-1.5%
12	Shutters 100% closed, 75% smooth underbody	0, 2, 4, 6 ,8 10	110	0.776	-1.5%	0.808	-2.2%
15	Shutters 100% closed, 25% smooth underbody	0, 2, 4, 6 ,8 10	110	0.782	-0.8%	0.818	-1.0%
17	Baseline, shutters 100% closed, yaw sweep	0, 2, 4, 6 ,8 10	110	0.788	0.0%	0.826	0.0%
18	Baseline, shutters 100% closed, speed sweep	0	60,80,100,120,140	0.787	-0.1%		
	Test H- OEM air dam and ride height study						
19	Shutters 100% closed, OEM air dam extended 60%, baseline ride height	0, 2, 4, 6 ,8 10	110	0.779	-1.2%	0.824	-0.3%
20	Shutters 100% closed, OEM air dam extended 60%, ride height 20 mm down front and back	0, 2, 4, 6 ,8 10	110	0.789	0.2%	0.806	-2.4%
21	Shutters 100% closed, OEM air dam extended 60%, ride height 35 mm down front and back	0, 2, 4, 6 ,8 10	110	0.812	3.0%	0.816	-1.2%
22	Shutters 100% closed, OEM air dam extended 45%, ride height 35 mm down front and back	0, 2, 4, 6 ,8 10	110	0.780	-1.0%	0.794	-3.9%
23	Shutters 100% closed, OEM air dam extended 45%, ride height 20 mm down front and back	0, 2, 4, 6 ,8 10	110	0.764	-3.1%	0.797	-3.5%
25	Shutters 100% closed, OEM air dam extended 45%, baseline ride height	0, 2, 4, 6 ,8 10	110	0.762	-3.3%	0.816	-1.2%
26	Shutters 100% closed, OEM air dam extended 30%, baseline ride height	0, 2, 4, 6 ,8 10	110	0.766	-2.7%	0.813	-1.5%
27	Shutters 100% closed, OEM air dam extended 30%, ride height 20 mm down front and back	0, 2, 4, 6 ,8 10	110	0.743	-5.8%	0.789	-4.5%
28	Shutters 100% closed, OEM air dam extended 30%, ride height 35 mm down front and back	0, 2, 4, 6 ,8 10	110	0.748	-5.1%	0.777	-6.0%
29	Shutters 100% closed, OEM air dam extended 15%, ride height 35 mm down front and back	0, 2, 4, 6 ,8 10	110	0.725	-8.0%	0.770	-6.8%
31	Shutters 100% closed, OEM air dam extended 15%, ride height 20 mm down front and back	0, 2, 4, 6 ,8 10	110	0.744	-5.5%	0.787	-4.7%
32	Shutters 100% closed, OEM air dam extended 15%, baseline ride height	0, 2, 4, 6 ,8 10	110	0.772	-2.1%	0.817	-1.2%
	Test B - Variable ride height						
36	Shutters 100% closed, ride height reduced by 20 mm front and back	0, 2, 4, 6 ,8 10	110	0.762	-3.4%	0.794	-3.8%
38	Shutters 100% closed, ride height reduced by 35 mm front and back	0, 2, 4, 6 ,8 10	110	0.745	-5.5%	0.778	-5.8%
39	Shutters 100% closed, ride height reduced by 35 mm front and 20 mm back	0, 2, 4, 6 ,8 10	110	0.750	-4.8%	0.782	-5.3%
41	Shutters 100% closed, ride height reduced by 20 mm front and 0 mm back	0, 2, 4, 6 ,8 10	110	0.773	-1.9%	0.809	-2.1%
	Test D2 - OEM Air dam						
43	Shutters 100% closed, baseline ride height, rear wheel air dam removed	0, 2, 4, 6 ,8 10	110	0.786	-0.3%	0.825	-0.1%
44	Shutters 100% closed, baseline ride height, front aero mud flaps removed	0, 2, 4, 6 ,8 10	110	0.782	-0.8%	0.821	-0.6%
47	Shutters 100% closed, baseline ride height, oem bumper air dam, rear wheel dam and front aero mud flap removed	0, 2, 4, 6 ,8 10	110	0.803	1.9%	0.825	-0.1%
48	Shutters 100% closed, resinstall wheel dam and mud flaps, bumper air dam removed	0, 2, 4, 6 ,8 10	110	0.804	2.0%	0.833	0.9%
50	Removed bumper air dam and open AGS shutters	0, 2, 4, 6 ,8 10	110	0.812	3.0%	0.842	1.9%
	reinstall bumper air dam						
	Test A1 - AGS						
52	Shutters 100% open, yaw sweep	0, 2, 4, 6 ,8 10	110	0.804	2.0%	0.839	1.6%
54	Shutters opening sweep, 25% closed, 50% closed, 75% closed, 100% closed	0	100				
55	Shutters opening sweep, 25% closed, 50% closed, 75% closed, 100% closed	0	120				

Table A.3: Description of all the runs completed during Phase III of the wind tunnel tests, page 1/4.

2 minivan 2

Run #	Comment	Yaw Angle(s)	Speed [km/h]	$C_{D,0} \cdot x\,A\ [m^2]$	$\Delta C_{D,0} \cdot x\,A$	$C_{D,WA}\ x\,A\ [m^2]$	$\Delta C_{D,WA}\ x\,A$
57	Shakedown	0	140	0.989	-8.2%		
	Test C- Custom underbody panel study						
59	Shutters 100% closed, completely smooth underbody	0, 2, 4, 6 ,8 10	110	0.992	-8.0%	1.047	-6.5%
61	Shutters 100% closed, 75% smooth underbody, remove OEM underbody diffuser	0, 2, 4, 6 ,8 10	110	0.999	-7.3%	1.070	-4.4%
63	Shakedown ,Shutters 100% closed, 25% smooth underbody			1.048	-2.8%		
64	Shutters 100% closed, 25% smooth underbody	0, 2, 4, 6 ,8 10	110	1.022	-5.1%	1.096	-2.1%
67	Shutters 100% closed, underbody removed	0, 2, 4, 6 ,8 10	110	1.077	-0.1%	1.120	0.1%
69	Baseline, shutters 100% closed, yaw sweep, reinstall OEM underbody diffuser	0, 2, 4, 6 ,8 10	110	1.078	0.0%	1.119	0.0%
70	Baseline, shutters 100% closed, speed sweep	0	60,80,100,120,140	1.078	0.1%		
	Test B - Variable ride height					`	
72	Shutters 100% closed, ride height reduced by 20 mm front and back	0	110	1.061	-1.5%		
74	Shutters 100% closed, ride height reduced by 20 mm front and back	0, 2, 4, 6 ,8 10	110	1.060	-1.7%	1.108	-1.0%
75	Shutters 100% closed, ride height reduced by 40 mm front and back	0, 2, 4, 6 ,8 10	110	1.042	-3.4%	1.088	-2.8%
77	Shutters 100% closed, ride height reduced by 40 mm front and 20 mm back	0, 2, 4, 6 ,8 10	110	1.054	-2.2%	1.092	-2.4%
78	Shutters 100% closed, ride height reduced by 20 mm front and 0 mm back	0, 2, 4, 6 ,8 10	110	1.076	-0.1%	1.117	-0.2%
	Test D2 - OEM Air dam						
80	Shutters 100% closed, baseline ride height, front wheel air dam removed	0, 2, 4, 6 ,8 10	110	1.107	2.7%	1.136	1.5%
81	Shutters 100% closed, baseline ride height, rear wheel air dam removed	0, 2, 4, 6 ,8 10	110	1.099	1.9%	1.134	1.3%
83	Shutters 100% closed, baseline ride height, front wheel dam installed, rear wheel dam rem.	0, 2, 4, 6 ,8 10	110	1.078	0.1%	1.118	-0.1%
	reinstall all wheel air dams						
	Test A1 - AGS						
84	Remove top mock up AGS, yaw sweep	0, 2, 4, 6 ,8 10	110	1.118	3.7%	1.137	1.6%
86	Shutters 100% open, yaw sweep	0, 2, 4, 6 ,8 10	110	1.136	5.4%	1.163	3.9%

3 small SUV 5

Run #	Comment	Yaw Angle(s)	Speed [km/h]	$C_{D,0} \cdot x\,A\ [m^2]$	$\Delta C_{D,0} \cdot x\,A$	$C_{D,WA}\ x\,A\ [m^2]$	$\Delta C_{D,WA}\ x\,A$
88	Shakedown						
		0	140	0.898	2.67%		
	Test C- Custom underbody panel study						
90	Shutters 100% closed, completely smooth underbody	0, 2, 4, 6 ,8 10	110	0.882	0.82%	0.947	-1.48%
92	Shutters 100% closed, 75% smooth underbody	0, 2, 4, 6 ,8 10	110	0.868	-0.73%	0.940	-2.23%
94	Shutters 100% closed, 25% smooth underbody	0, 2, 4, 6 ,8 10	110	0.908	3.84%	0.981	2.10%
96	Shutters 100% closed, remove all cover including OEM engine cover	0, 2, 4, 6 ,8 10	110	0.901	3.04%	0.973	1.21%
98	Shakedown			0.876	0.13%		
100	Baseline, shutters 100% closed, yaw sweep, OEM engine cover reinstalled	0, 2, 4, 6 ,8 10	110	0.874	0.00%	0.961	0.00%
101	Baseline, shutters 100% closed, speed sweep	0	60,80,100,120,140	0.875	0.08%		

Table A.3: Description of all the runs completed during Phase III of the wind tunnel tests, page 2/4.

	Test A1 - AGS						
102	Shutters 100% open, yaw sweep	0, 2, 4, 6 ,8 10	110	0.897	2.56%	0.978	1.74%
103	Shutters 100% open, speed sweep	0	60,80,100,120,140	0.899	2.77%		
105	Shutters opening sweep, 22% closed,45% closed, 78% closed, 100% closed	0	100				
106	Shutters opening sweep, 22% closed, 45% closed, 78% closed, 100% closed	0	120				
108	Shutters 100% closed, front grille sealed with tape	0, 2, 4, 6 ,8 10	110	0.852	-2.51%	0.944	-1.74%
	Test B - Variable ride height						
109	Shutters 100% closed, ride height reduced by 20 mm front and back	0, 2, 4, 6 ,8 10	110	0.874	-0.09%	0.951	-1.08%
110	Shutters 100% closed, ride height reduced by 40 mm front and back	0, 2, 4, 6 ,8 10	110	0.857	-1.97%	0.925	-3.76%
112	Shutters 100% closed, ride height reduced by 40 mm front and 20 mm back	0, 2, 4, 6 ,8 10	110	0.868	-0.77%	0.930	-3.29%
114	Shutters 100% closed, ride height reduced by 20 mm front and 0 mm back	0, 2, 4, 6 ,8 10	110	0.885	1.23%	0.956	-0.50%

4 small SUV 6

Run #	*Comment*	*Yaw Angle(s)*	*Speed [km/h]*	$C_{D,0} \cdot x\,A\ [m^2]$	$\Delta C_{D,0} \cdot x\,A$	$C_{D,WA}\ x\,A\ [m^2]$	$\Delta C_{D,WA}\ x\,A$
116	Shakedown	0	140	1.019	3.3%		
	Test C- Custom underbody panel study						
118	Shutters 100% closed, full under body cover, remove bumper air dam, Test J	0, 2, 4, 6 ,8 10	110	1.013	2.7%	1.059	0.2%
	reinstall bumper air dam		0				
120	Shutters 100% closed, completely smooth underbody	0, 2, 4, 6 ,8 10	110	0.964	-2.3%	1.019	-3.6%
122	Shutters 100% closed, 75% smooth underbody	0, 2, 4, 6 ,8 10	110	0.984	-0.3%	1.043	-1.4%
124	Shutters 100% closed, 25%smooth undercover	0, 2, 4, 6 ,8 10	110	0.987	0.0%	1.057	0.0%
126	Shutters 100% closed, removed OEM engine cover	0, 2, 4, 6 ,8 10	110	0.976	-1.1%	1.049	-0.8%
128	Baseline, shutters 100% closed, yaw sweep, reinstall engine cover	0, 2, 4, 6 ,8 10	110	0.987	0.0%	1.057	0.0%
129	Baseline, shutters 100% closed, speed sweep	0	60,80,100,120,140	0.990	0.4%		
131	Shakedown,start of July 24, Shutters 100% open	0	140	1.018	3.1%		
	Test A1 - AGS						
133	Shutters 100% open, yaw sweep	0, 2, 4, 6 ,8 10	110	1.018	3.2%	1.077	1.9%
135	Shutters opening sweep, 25% closed, 50% closed, 75% closed, 100% closed	0	100				
136	Shutters opening sweep, 25% closed, 50% closed, 75% closed, 100% closed	0	120				
	Test B - Variable ride height						
138	Shutters 100% closed, ride height reduced by 20 mm front and back	0, 2, 4, 6 ,8 10	110	0.960	-2.7%	1.028	-2.7%
139	Shutters 100% closed, ride height reduced by 40 mm front and back	0, 2, 4, 6 ,8 10	110	0.927	-6.1%	0.999	-5.5%
141	Shutters 100% closed, ride height reduced by 40 mm front and 20 mm back	0, 2, 4, 6 ,8 10	110	0.915	-7.2%	0.994	-5.9%
142	Shutters 100% closed, ride height reduced by 20 mm front and 0 mm back	0, 2, 4, 6 ,8 10	110	0.963	-2.4%	1.034	-2.2%
	Test H- OEM air dam and ride height study						
144	Shutters 100% closed, OEM air dam extended 60%, baseline ride height	0, 2, 4, 6 ,8 10	110	0.948	-3.9%	1.036	-2.0%
145	Shutters 100% closed, OEM air dam extended 60%, ride height 20 mm down front and back	0, 2, 4, 6 ,8 10	110	0.928	-5.9%	1.009	-4.5%
147	Shutters 100% closed, OEM air dam extended 60%, ride height 40 mm down front and back	0, 2, 4, 6 ,8 10	110	0.927	-6.0%	0.987	-6.7%
149	Shutters 100% closed, OEM air dam extended 45%, ride height 40 mm down front and back	0, 2, 4, 6 ,8 10	110	0.915	-7.3%	0.987	-6.6%

Table A.3: Description of all the runs completed during Phase III of the wind tunnel tests, page 3/4.

150	Shutters 100% closed, OEM air dam extended 45%, ride height 20 mm down front and back	0, 2, 4, 6 ,8 10	110	0.927	-6.1%	1.008	-4.6%
152	Shutters 100% closed, OEM air dam extended 45%, baseline ride height	0, 2, 4, 6 ,8 10	110	0.956	-3.1%	1.037	-1.9%
154	Shutters 100% closed, OEM air dam extended 30%, baseline ride height	0, 2, 4, 6 ,8 10	110	0.963	-2.4%	1.039	-1.7%
156	Shutters 100% closed, OEM air dam extended 30%, ride height 20 mm down front and back	0, 2, 4, 6 ,8 10	110	0.934	-5.3%	1.012	-4.2%
158	Shutters 100% closed, OEM air dam extended 30%, ride height 40 mm down front and back	0, 2, 4, 6 ,8 10	110	0.908	-8.0%	0.979	-7.4%
160	Shutters 100% closed, OEM air dam extended 15%, ride height 40 mm down front and back	0, 2, 4, 6 ,8 10	110	0.915	-7.3%	0.985	-6.8%
162	Shutters 100% closed, OEM air dam extended 15%, ride height 20 mm down front and back	0, 2, 4, 6 ,8 10	110	0.945	-4.2%	1.017	-3.8%
166	Shutters 100% closed, OEM air dam extended 15%, baseline ride height	0, 2, 4, 6 ,8 10	110	0.982	-0.5%	1.051	-0.6%
	Test D2 - OEM Air dam						
167	Shutters 100% closed, baseline ride height, rear wheel air dam removed	0, 2, 4, 6 ,8 10	110	0.988	0.1%	1.052	-0.5%
169	Shutters 100% closed, baseline ride height, oem bumper air dam and rear wheel dam rem.	0, 2, 4, 6 ,8 10	110	1.029	4.3%	1.076	1.8%
	reinstall rear wheel air dams						
	Test J - Combination						
171	Shutters 100% open, oem bumper air dam removed	0, 2, 4, 6 ,8 10	110	1.047	6.1%	1.088	2.9%

Table A.3: Description of all the runs completed during Phase III of the wind tunnel tests, page 4/4.

1 small car 2 - turbulent flow

Run #	Comment	Yaw Angle(s)	Speed [km/h]	$C_{D,0} \cdot x\,A\ [m^2]$	$\Delta C_{D,0} \cdot x\,A$	$C_{D,WA}\ x\,A\ [m^2]$	$\Delta C_{D,WA}\ x\,A$
4	Shakedown	0	140	0.729	-1.2%		
	Test A1 - AGS						
6	Baseline, shutters 100% closed, speed sweep	0	60,80,100,120,140	0.731			
7	Baseline, shutters 100% closed, yaw sweep	0, 2, 4, 6 ,8 10 ,0	110	0.738		0.789	
9	Shutters 100% open, speed sweep	0	60,80,100,120,140	0.745	0.9%		
10	Shutters 100% open, yaw sweep	0, 2, 4, 6 ,8 10, 0	110	0.750	1.6%	0.800	1.4%
	Test B - Variable ride height						
12	Shutters 100% closed, ride height reduced by 20 mm front and rear	0, 2, 4, 6 ,8 10	110	0.706	-4.4%	0.758	-3.9%
14	Shutters 100% closed, ride height reduced by 40 mm front and rear	0, 2, 4, 6 ,8 10	110	0.678	-8.2%	0.725	-8.1%
16	Shutters 100% closed, ride height reduced by 40 mm front, 20 rear	0, 2, 4, 6 ,8 10	110	0.691	-6.4%	0.740	-6.2%
18	Shutters 100% closed, ride height reduced by 20 mm front, 0 mm rear	0, 2, 4, 6 ,8 10	110	0.722	-2.2%	0.771	-2.3%
	Test D1 - OEM Under-body panel study						
20	Shutters 100% closed, normal ride height, underbody panel removal stage 1	0, 2, 4, 6 ,8 10	110	0.718	-2.6%	0.774	-1.9%
22	Shutters 100% closed, normal ride height, underbody panel removal stage 2	0, 2, 4, 6 ,8 10	110	0.747	1.3%	0.786	-0.4%
24	Shutters 100% closed, normal ride height, underbody panel removal stage 3	0, 2, 4, 6 ,8 10	110	0.755	2.3%	0.788	-0.1%
	Test H - OEM Air dam height study, *ride height sweep: baseline, 20 mm, 40 mm*						
26	Shutters 100% closed, underbody panels removed, air dam height 76 mm, baseline height	0, 2, 4, 6 ,8 10	110	0.738	0.0%	0.791	0.2%
27	Shutters 100% closed, underbody panels removed, air dam height 76 mm, down 20 mm	0, 2, 4, 6 ,8 10	110	0.715	-3.0%	0.759	-3.8%
29	Shutters 100% closed, underbody panels removed, air dam height 76 mm, down 40 mm	0	110	0.713	-3.3%		
31	Shutters 100% closed, underbody panels removed, air dam height 76 mm, down 40 mm	0, 2, 4, 6 ,8 10	110	0.713	-3.3%	0.743	-5.8%
33	Shutters 100% closed, underbody panels removed, air dam height 66 mm, down 40 mm	0, 2, 4, 6 ,8 10	110	0.688	-6.8%	0.727	-7.9%
34	Shutters 100% closed, underbody panels removed, air dam height 66 mm, down 20 mm	0, 2, 4, 6 ,8 10	110	0.711	-3.6%	0.763	-3.3%
36	Shutters 100% closed, underbody panels removed, air dam height 66 mm, baseline height	0, 2, 4, 6 ,8 10	110	0.748	1.4%	0.794	0.6%
37	Shutters 100% closed, underbody panels removed, air dam height 56 mm, baseline height	0, 2, 4, 6 ,8 10	110	0.753	2.0%	0.796	0.9%
38	Shutters 100% closed, underbody panels removed, air dam height 56 mm, baseline height, repeat	8, 10	110				
39	Shutters 100% closed, underbody panels removed, air dam height 56 mm, down 20 mm	0, 2, 4, 6 ,8 10	110	0.724	-1.9%	0.768	-2.6%
41	Shutters 100% closed, underbody panels removed, air dam height 56 mm, down 40 mm	0, 2, 4, 6 ,8 10	110	0.691	-6.3%	0.735	-6.9%
	Test D2 - OEM Air dam						
43	Shutters 100% closed, baseline ride height, last underbody panel removal stage 4, remove Leo's air dam	0, 2, 4, 6 ,8 10	110	0.761	3.2%	0.795	0.8%
44	Shutters 100% closed, baseline ride height, underbody panel removal stage 4, no air dam, remove all wheel dams	0, 2, 4, 6 ,8 10	110	0.779	5.6%	0.811	2.8%

2 pick up truck 3 - turbulent flow

Run #	Comment	Yaw Angle(s)	Speed [km/h]	$C_{D,0} \cdot x\,A\ [m^2]$	$\Delta C_{D,0} \cdot x\,A$	$C_{D,WA}\ x\,A\ [m^2]$	$\Delta C_{D,WA}\ x\,A$
47	Shakedown	0	140	1.371			

Table A.4: Description of all the runs completed during Phase IV of the wind tunnel tests, page 1/3.

	Test C- Custom underbody panel study						
50	Shutters 100% closed, completely smooth underbody	0, 2, 4, 6 ,8 10	110	1.345	-2.4%	1.421	-6.2%
52	Shutters 100% closed, 75% smooth underbody	0, 2, 4, 6 ,8 10	110	1.332	-3.4%	1.404	-7.3%
54	Shutters 100% closed, 25% smooth underbody	0, 2, 4, 6 ,8 10	110	1.387	0.6%	1.475	-2.6%
56	Baseline, shutters 100% closed, yaw sweep	0, 2, 4, 6 ,8 10	110	1.379	0.0%	1.514	0.0%
57	Baseline, shutters 100% closed, speed sweep	0	60,80,100,120,140	1.378	-0.1%		
	Test H- OEM air dam and ride height study						
59	Shutters 100% closed, OEM air dam extended 60%, baseline ride height	0, 2, 4, 6 ,8 10	110	1.425	3.4%	1.528	0.9%
70	Shutters 100% closed, OEM air dam extended 60%, ride height 20 mm down front only	0, 2, 4, 6 ,8 10	110	1.467	6.4%	1.527	0.8%
69	Shutters 100% closed, OEM air dam extended 45%, ride height 20 mm down front only	0, 2, 4, 6 ,8 10	110	1.422	3.1%	1.517	0.2%
61	Shutters 100% closed, OEM air dam extended 45%, baseline ride height	0, 2, 4, 6 ,8 10	110	1.392	1.0%	1.527	0.9%
63	Shutters 100% closed, OEM air dam extended 30%, baseline ride height	0, 2, 4, 6 ,8 10	110	1.384	0.3%	1.523	0.6%
67	Shutters 100% closed, OEM air dam extended 30%, ride height 20 mm down front only	0, 2, 4, 6 ,8 10	110	1.387	0.6%	1.507	-0.5%
66	Shutters 100% closed, OEM air dam extended 15%, ride height 20 mm down front only	0, 2, 4, 6 ,8 10	110	1.363	-1.1%	1.503	-0.7%
64	Shutters 100% closed, OEM air dam extended 15%, baseline ride height	0, 2, 4, 6 ,8 10	110	1.376	-0.2%	1.515	0.0%
72	Day 2 shakedown	0		1.341	-2.7%		
	Test A1 - AGS						
75	Shutters 100% closed, external grilled sealed	0, 2, 4, 6 ,8 10	110	1.346	-2.4%	1.487	-1.8%
77	Lower shutter closed, upper shutters open, yaw sweep	0, 2, 4, 6 ,8 10	110	1.436	4.2%	1.559	3.0%
78	Shutters 100% open, yaw sweep	0, 2, 4, 6 ,8 10	110	1.452	5.3%	1.575	4.0%
80	Shutters 100% closed, tail gate open	0, 2, 4, 6 ,8 10	110	1.453	5.4%	1.552	2.5%
	Test D2 - OEM Air dam						
82	Shutters 100% closed, removed bumper air dam	0, 2, 4, 6 ,8 10	110	1.433	4.0%	1.517	0.2%
84	Lower shutter closed, upper shutters open, bumper air dam removed	0, 2, 4, 6 ,8 10	110	1.471	6.7%	1.552	2.5%
86	Shutters 100% open, bumper air dam removed	0, 2, 4, 6 ,8 10	110	1.481	7.4%	1.556	2.8%
87	Shutters 100% closed, bumper air dam removed, front license plate cover removed	0, 2, 4, 6 ,8 10	110	1.426	3.5%	1.517	0.2%

3 pick-up truck 3 - smooth flow

Run #	*Comment*	*Yaw Angle(s)*	*Speed [km/h]*	$C_{D,0} \cdot x\,A\ [m^2]$	$\Delta C_{D,0} \cdot x\,A$	$C_{D,WA}\ x\,A\ [m^2]$	$\Delta C_{D,WA}\ x\,A$
93	shakedown	0	140	1.321	-3.5%		
	Test C- Custom underbody panel study						
95	Shutters 100% closed, completely smooth underbody	0, 2, 4, 6 ,8 10	110	1.324	-3.2%	1.451	-4.7%
97	Shutters 100% closed, 75% smooth underbody	0, 2, 4, 6 ,8 10	110	1.314	-4.0%	1.424	-6.5%
99	Shutters 100% closed, 25% smooth underbody	0, 2, 4, 6 ,8 10	110	1.384	1.1%	1.492	-2.1%
101	Baseline, shutters 100% closed, yaw sweep	0, 2, 4, 6 ,8 10	110	1.368	0.0%	1.523	0.0%
102	Baseline, shutters 100% closed, speed sweep	0	60,80,100,120,140	1.365	-0.2%		
	Test A1 - AGS						
112	shakedown, grill taped, tail gate open	0		1.402	2.5%		
114	Shutters 100% closed, external grilled sealed	0, 2, 4, 6 ,8 10	110	1.318	-3.7%	1.494	-1.9%
104	Lower shutter closed, upper shutters open, yaw sweep	0, 2, 4, 6 ,8 10	110	1.425	4.1%	1.571	3.2%

Table A.4: Description of all the runs completed during Phase IV of the wind tunnel tests, page 2/3.

105	Shutters 100% open, yaw sweep	0, 2, 4, 6 ,8 10	110	1.445	5.6%	1.583	4.0%
107	Shutters opening sweep, 25% closed, 50% closed, 75% closed, 100% closed	0	100				
108	Shutters opening sweep, 25% closed, 50% closed, 75% closed, 100% closed	0	120				
110	Shutters 100% closed, tail gate open	0, 2, 4, 6 ,8 10	110	1.449	5.9%	1.571	3.1%
	Test D2 - OEM Air dam						
116	Shutters 100% closed, removed bumper air dam	0, 2, 4, 6 ,8 10	110	1.424	4.1%	1.521	-0.1%
118	Lower shutter closed, upper shutters open, bumper air dam removed	0, 2, 4, 6 ,8 10	110	1.470	7.4%	1.558	2.3%
119	Shutters 100% open, bumper air dam removed	0, 2, 4, 6 ,8 10	110	1.481	8.2%	1.568	3.0%
	Test H- OEM air dam and ride height study						
121	Shutters 100% closed, OEM air dam extended 60%, baseline ride height	0, 2, 4, 6 ,8 10	110	1.391	1.7%	1.535	0.8%
122	Shutters 100% closed, OEM air dam extended 45%, baseline ride height	0, 2, 4, 6 ,8 10	110	1.371	0.2%	1.529	0.4%
124	Shutters 100% closed, OEM air dam extended 30%, baseline ride height	0, 2, 4, 6 ,8 10	110	1.358	-0.8%	1.528	0.3%
125	Shutters 100% closed, OEM air dam extended 15%, baseline ride height	0, 2, 4, 6 ,8 10	110	1.359	-0.7%	1.524	0.0%
127	Shutters 100% closed, OEM air dam extended 15%, ride height 20 mm down front only	0, 2, 4, 6 ,8 10	110	1.339	-2.2%	1.510	-0.9%
128	Shutters 100% closed, OEM air dam extended 30%, ride height 20 mm down front only	0, 2, 4, 6 ,8 10	110	1.368	0.0%	1.518	-0.4%
129	Shutters 100% closed, OEM air dam extended 45%, ride height 20 mm down front only	0, 2, 4, 6 ,8 10	110	1.401	2.4%	1.522	-0.1%
131	Shutters 100% closed, OEM air dam extended 60%, ride height 20 mm down front only	0, 2, 4, 6 ,8 10	110	1.442	5.4%	1.527	0.3%
133	Shutters 100% closed, OEM air dam re-installed, windows fully open	0, 2, 4, 6 ,8 10	110	1.390	1.6%	1.552	1.9%

Table A.4: Description of all the runs completed during Phase IV of the wind tunnel tests, page 3/3.

B. Photographs of the vehicles

Appendix B presents photographic documentation of the experiments.

B.1 Overall views

Figure B.1: View from upstream of the 2013 BMW 528i on the GESS in the 9 m Wind Tunnel.

Figure B.2: View from upstream of the 2014 Chevrolet Cruze on the GESS in the 9 m Wind Tunnel.

Figure B.3: View from upstream of the 2014 Ford Escape on the GESS in the 9 m Wind Tunnel.

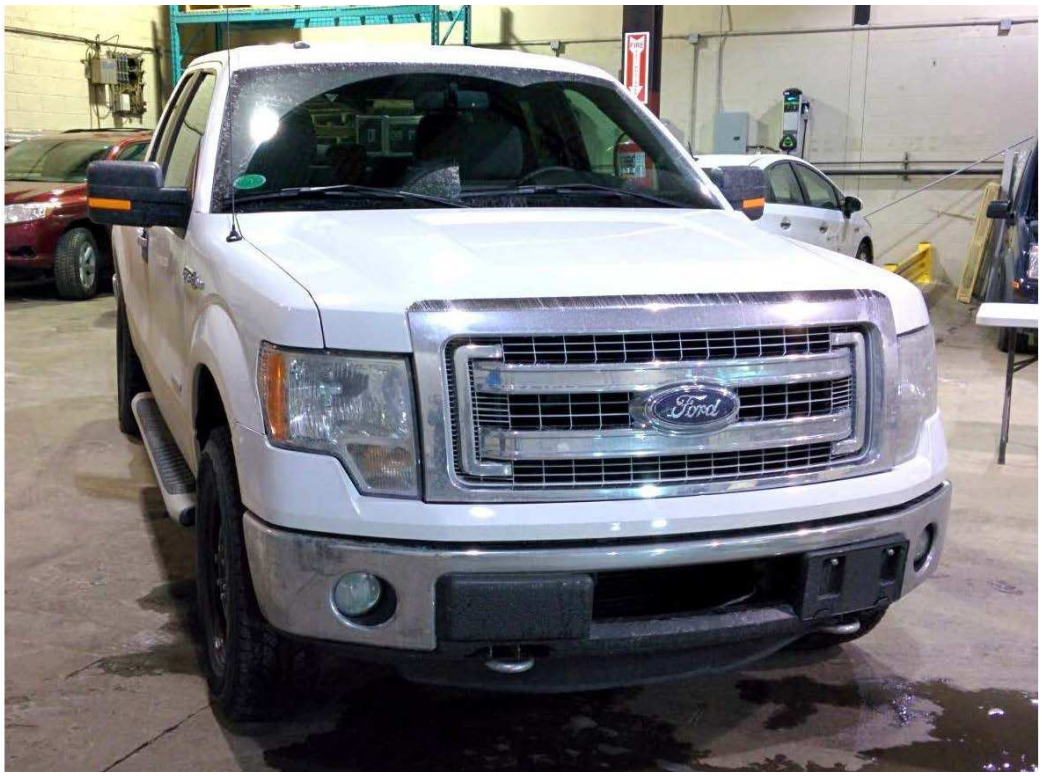

Figure B.4: View from upstream of the 2013 Ford F-150.

Figure B.5: View from upstream of the 2013 Ford Focus on the GESS in the 9 m Wind Tunnel.

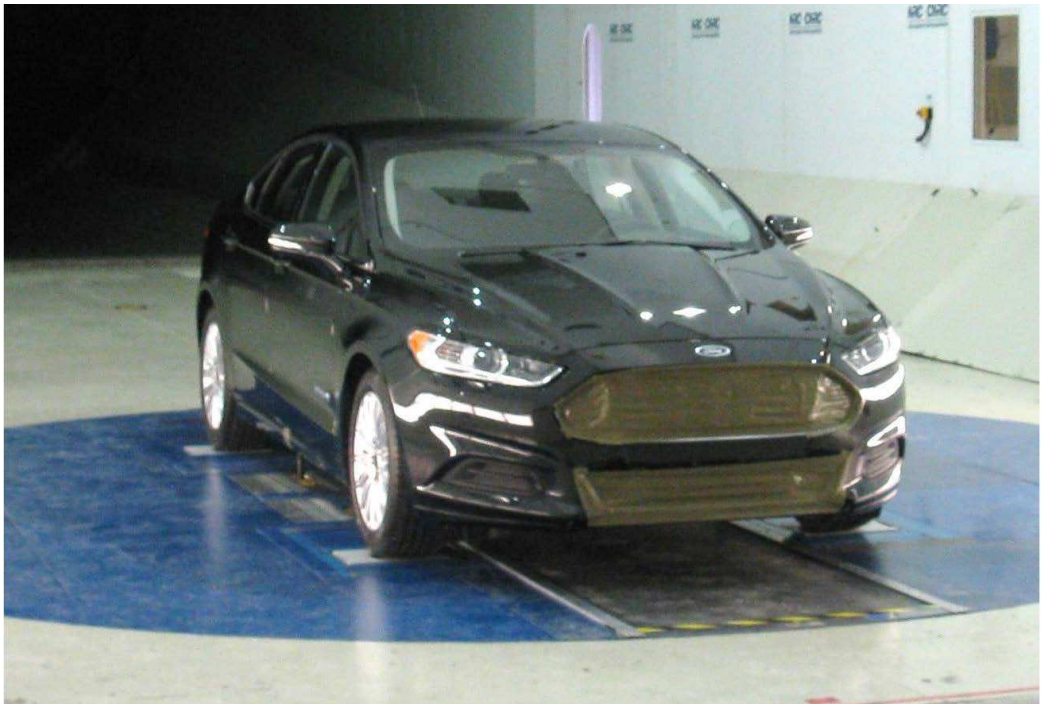

Figure B.6: View from upstream of the 2013 Ford Fusion on the GESS in the 9 m Wind Tunnel.

Figure B.7: View from upstream of the 2014 Mazda 3.

Figure B.8: View from upstream of the 2014 Mazda 6 on the GESS in the 9 m Wind Tunnel.

Figure B.9: View from upstream of the 2013 Dodge Ram.

Figure B.10: View from upstream of the 2014 BMW X5 on the GESS in the 9 m Wind Tunnel.

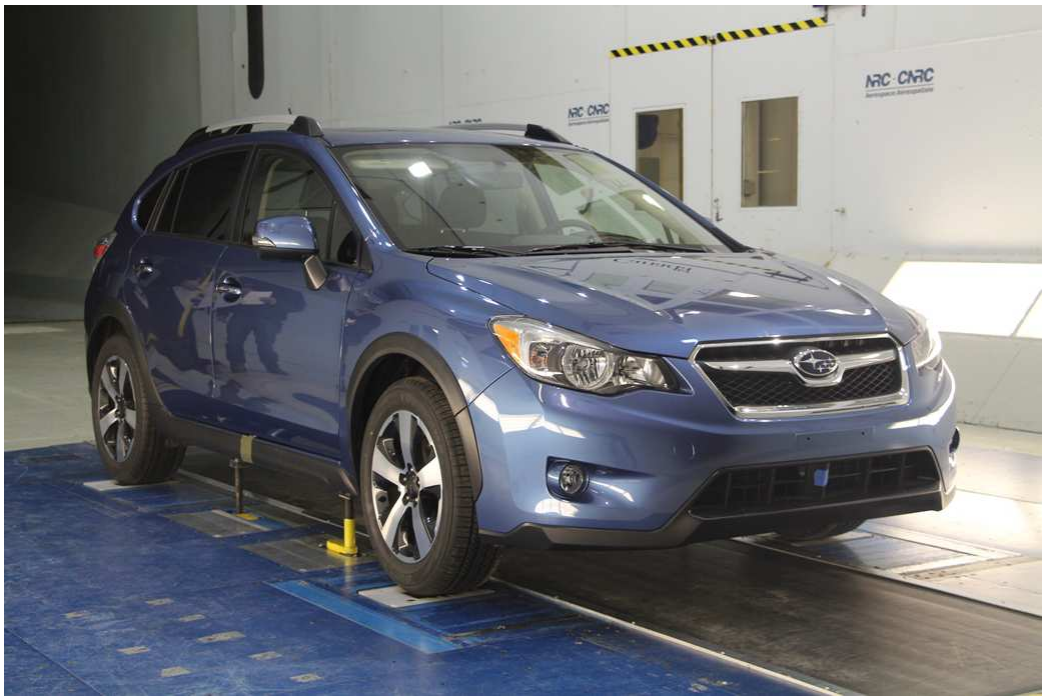

Figure B.11: View from upstream of the 2014 Subaru Crosstrek on the GESS in the 9 m Wind Tunnel.

Figure B.12: View from upstream of the 2014 Ford Edge on the GESS in the 9 m Wind Tunnel.

Figure B.13: View from upstream of the 2014 Honda Odyssey on the GESS in the 9 m Wind Tunnel.

Figure B.14: View from upstream of the 2014 Chevy Spark EV on the GESS in the 9 m Wind Tunnel.

Figure B.15: View from upstream of the 2014 Ford Taurus on the GESS in the 9 m Wind Tunnel.

Figure B.16: View from upstream of the 2015 Chevy Tahoe on the GESS in the 9 m Wind Tunnel.

Figure B.17: View from upstream of the 2014 Chevy Impala on the GESS in the 9 m Wind Tunnel.

Figure B.18: View from upstream of the 2015 Nissan Pathfinder on the GESS in the 9 m Wind Tunnel.

Figure B.19: View from upstream of the 2014 Nissan Versa Note Plus on the GESS in the 9 m Wind Tunnel.

Figure B.20: View from upstream of the 2014 Jeep Cherokee on the GESS in the 9 m Wind Tunnel.

Figure B.21: View from upstream of the 2015 Nissan Murano on the GESS in the 9 m Wind Tunnel.

Figure B.22: View from upstream of the 2015 Toyota Sienna on the GESS in the 9 m Wind Tunnel.

Figure B.23: View from upstream of the 2016 Ford F-150 on the GESS in the 9 m Wind Tunnel.

B.2 Detailed views

(a) Rocker panel clamps installed on a vehicle.

(b) Mounts on a pick-up truck with the struts in the raised position.

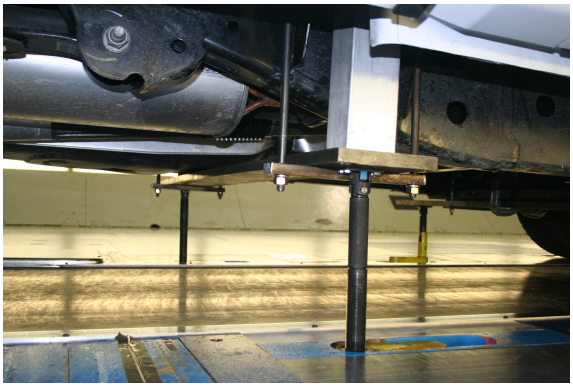

(c) Rear strut mounts on a pick-up truck.

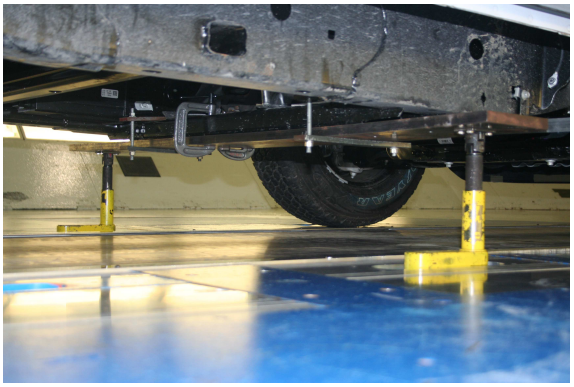

(d) Front strut mounts on a pick-up truck.

Figure B.24: Vehicle mounts.

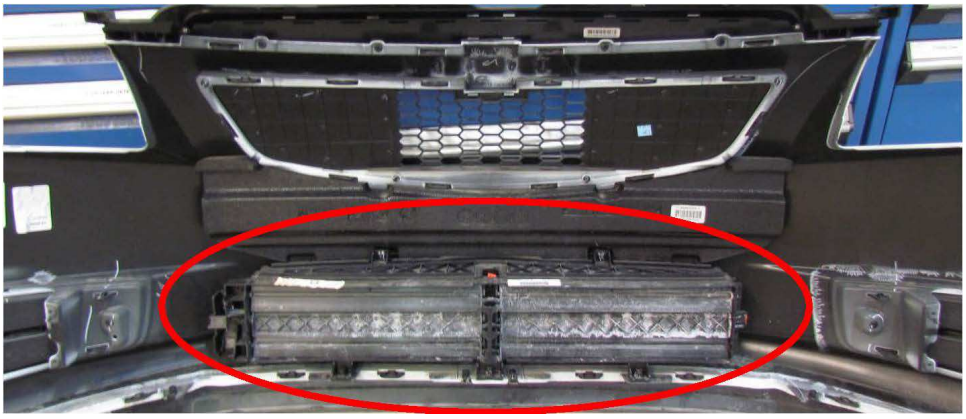

(a) AGS viewed from inside vehicle nose

(b) Upper and lower grille shutters (open) with front fascia removed

(c) Upper and lower grille shutters (closed), front fascia removed.

Figure B.25: Views of AGS systems.

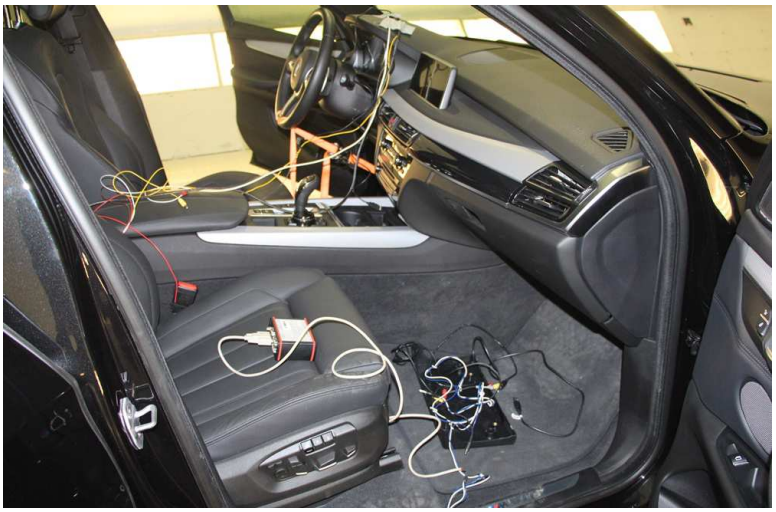

(a) Controlling the AGS

(b) Vehicle with AGS open

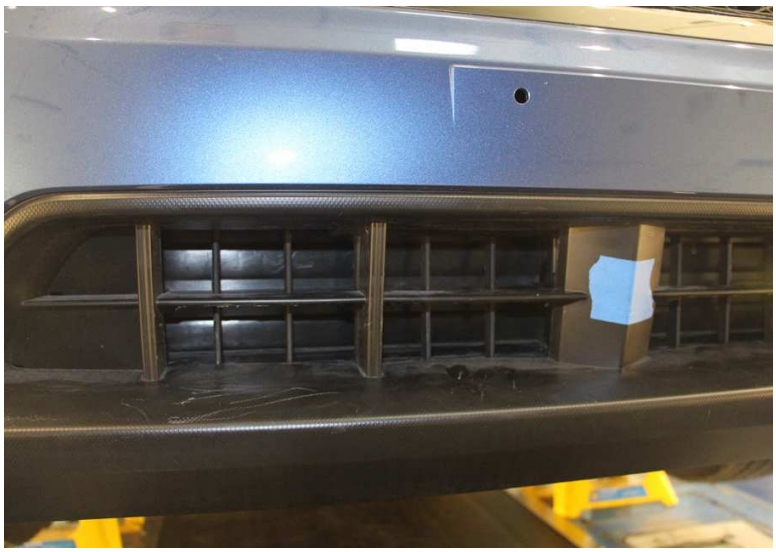

(c) Vehicle with AGS 100% closed

Figure B.26: Views of AGS and AGS control systems.

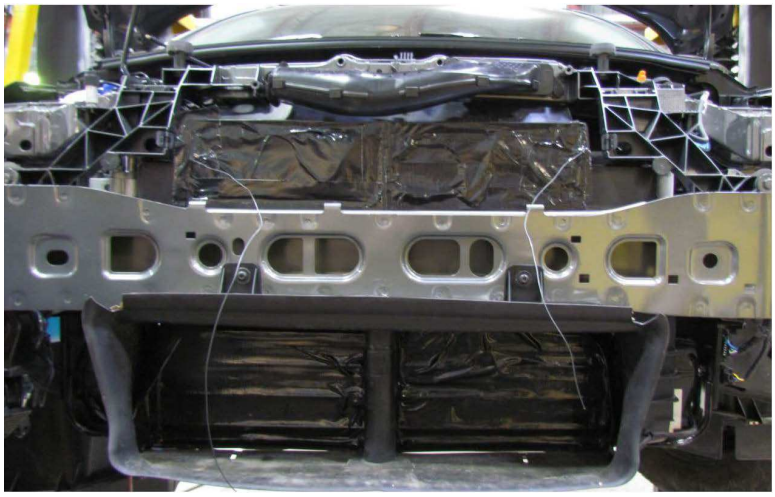

(a) Vehicle with grille shutters taped, front fascia removed.

(b) Vehicle with AGS on lower radiator sealed

(c) Vehicle with AGS on lower radiator sealed

Figure B.27: Examples of vehicles with sealed AGS.

Figure B.28: Examples of vehicles with external grille sealed.

(a) Bumper air dam (foreground) and wheel dams (circled in red)

(b) Custom air dam

(c) OEM air dam

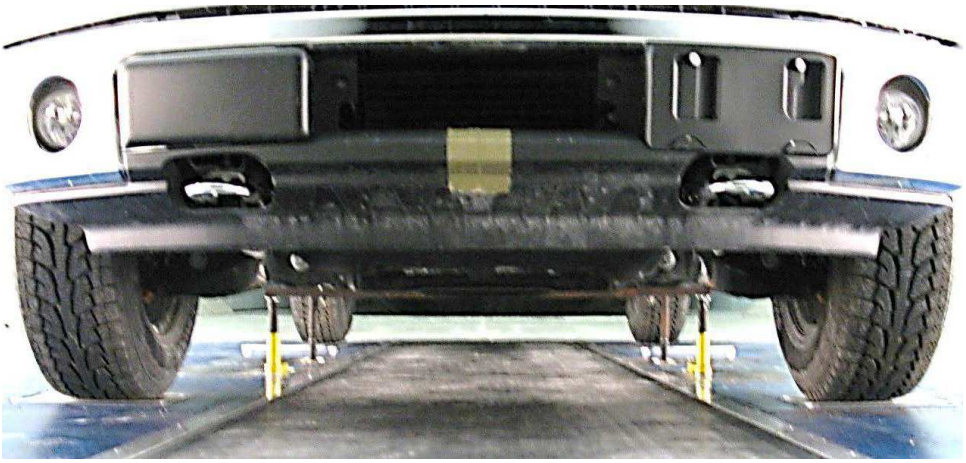

(d) Front view of vehicle with OEM bumper air dam

Figure B.29: Views of bumper air and wheel dams.

(a) Front wheel with wheel air dam

(b) Rear wheel air dam

(c) Rear wheel air dam

(d) Front wheel air dam

(e) Front wheel air dam

(f) Rear wheel air dam

(g) Front wheel air dam

(h) Rear wheel air dam

Figure B.30: Close-up views of wheel air dams.

(a) Full set

(b) Full set

(c) OEM front underbody panel

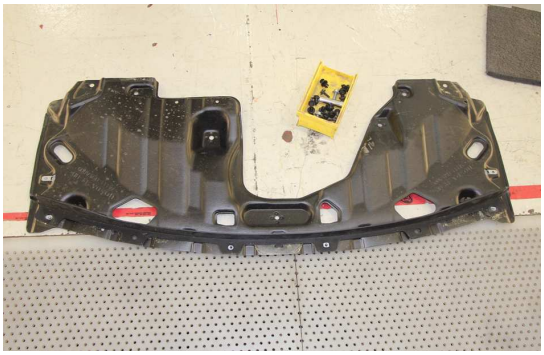

(d) OEM front panel with air dam

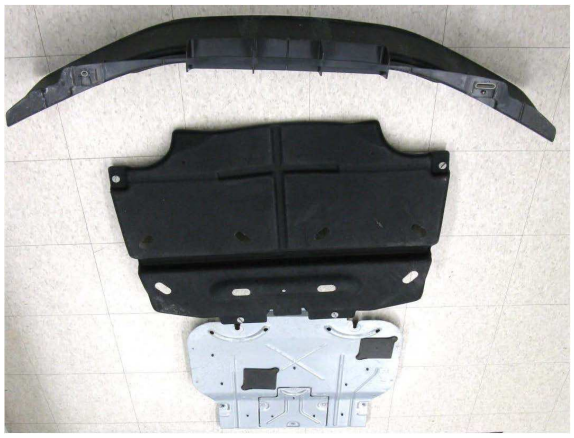

(e) Full set

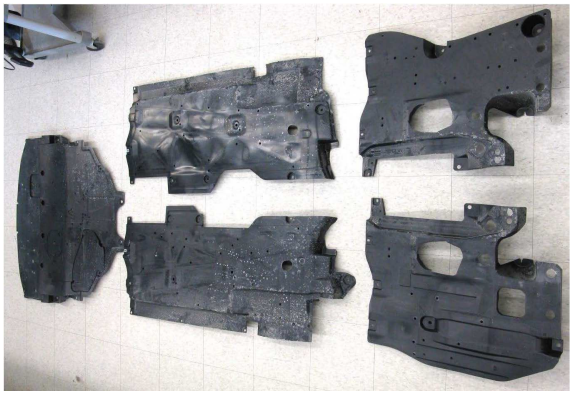

(f) Full set

Figure B.31: Examples of OEM underbody panels, removed.

(a) Vehicle underbody with OEM panels removed

(b) Vehicle underbody with OEM panels removed

Figure B.32: Views of vehicle underbodies with OEM panels removed.

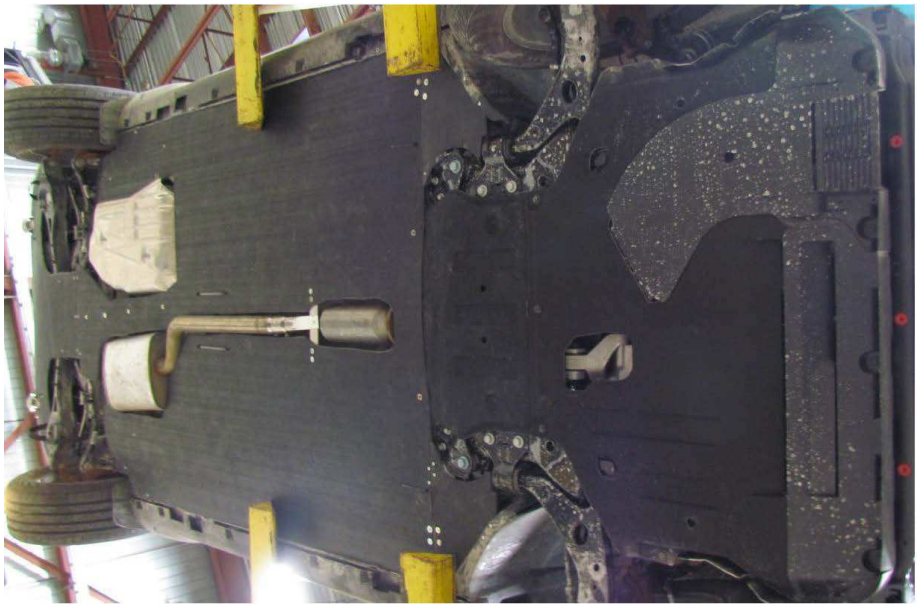

(a) Vehicle with OEM underbody panels at front and custom underbody panels at rear

(b) Vehicle with OEM underbody panels (left) and custom underbody panels (right)

(c) Vehicle with OEM underbody panels (left) and custom underbody panels (right)

Figure B.33: Examples of OEM and custom underbody covers.

(a) Vehicle with smooth OEM underbody

(b) Vehicle with smooth OEM rear underbody panel

(c) Rear (left), middle (center) and front (right) custom underbody panel sections on a vehicle

(d) Rear (left), middle (center) and front (right) custom underbody panel sections removed from a vehicle

Figure B.34: Examples of smooth OEM and custom underbody covers.

(a) Adjusting the front ride height of a vehicle

(b) Adjusting the front ride height of a vehicle

(c) Adjusting the rear ride height of a vehicle

Figure B.35: Adjusting the vehicle ride height.

(a) Extended OEM air dam

(b) Adjusting the extended OEM air dam

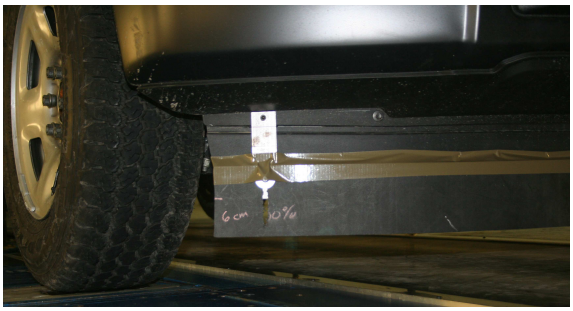

(c) Extended OEM air dam

(d) Adjusting the extended air dam

(e) Vehicle with extended OEM air dam

(f) Vehicle with extended OEM air dam

(g) Vehicle with extended OEM air dam

Figure B.36: Examples of extended OEM bumper air dams.

Figure B.37: Examples of vehicles fitted with custom-built bumper air dams.

C. Results in graphical form for all vehicles

Appendix C presents graphs of the variations of drag area with yaw angle for all the vehicles of this study.

C.1 Graphical results for small cars

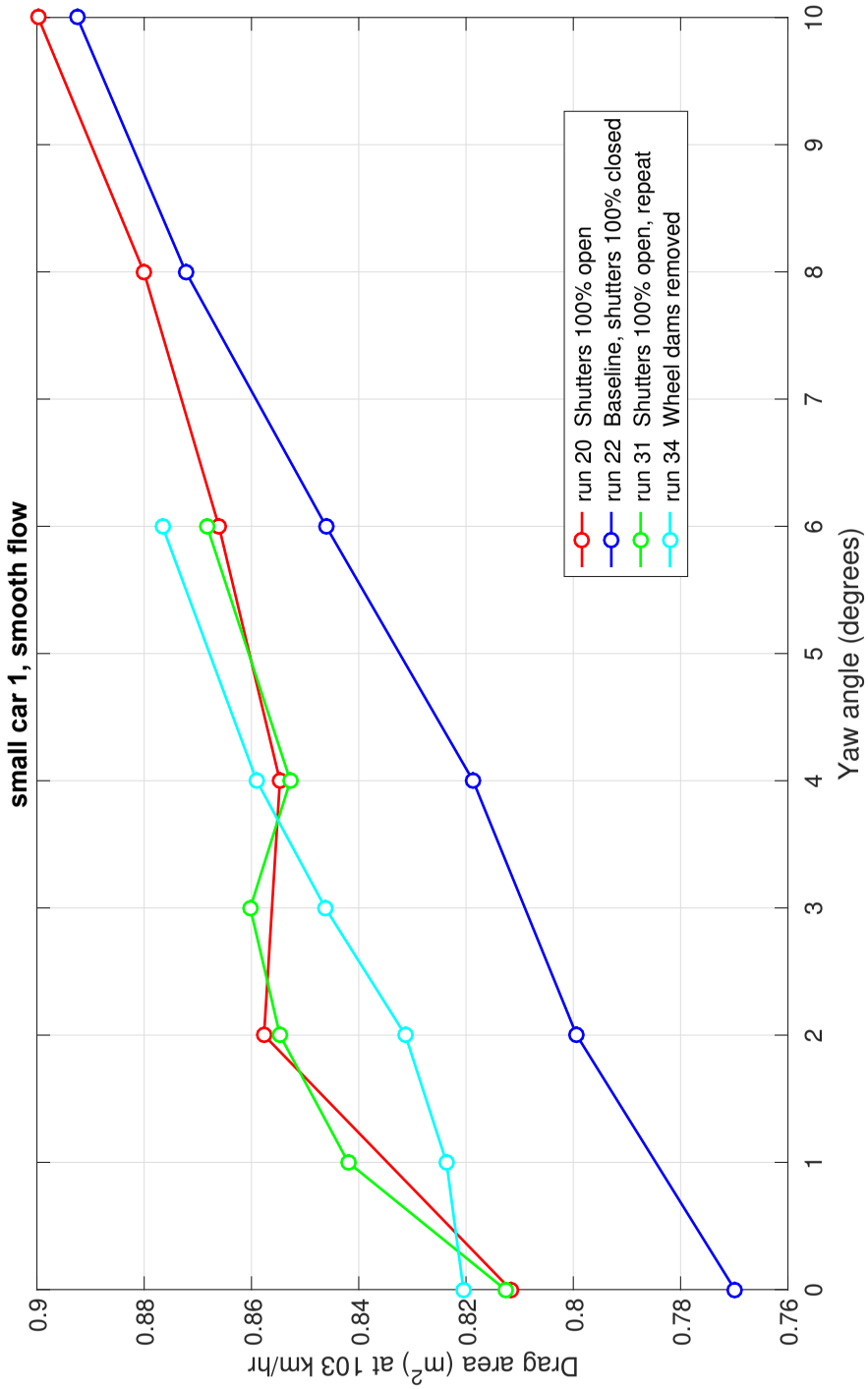

Figure C.1: Variations of drag area for small car 1 in smooth flow as a function of yaw angle for all yaw sweeps of this study.

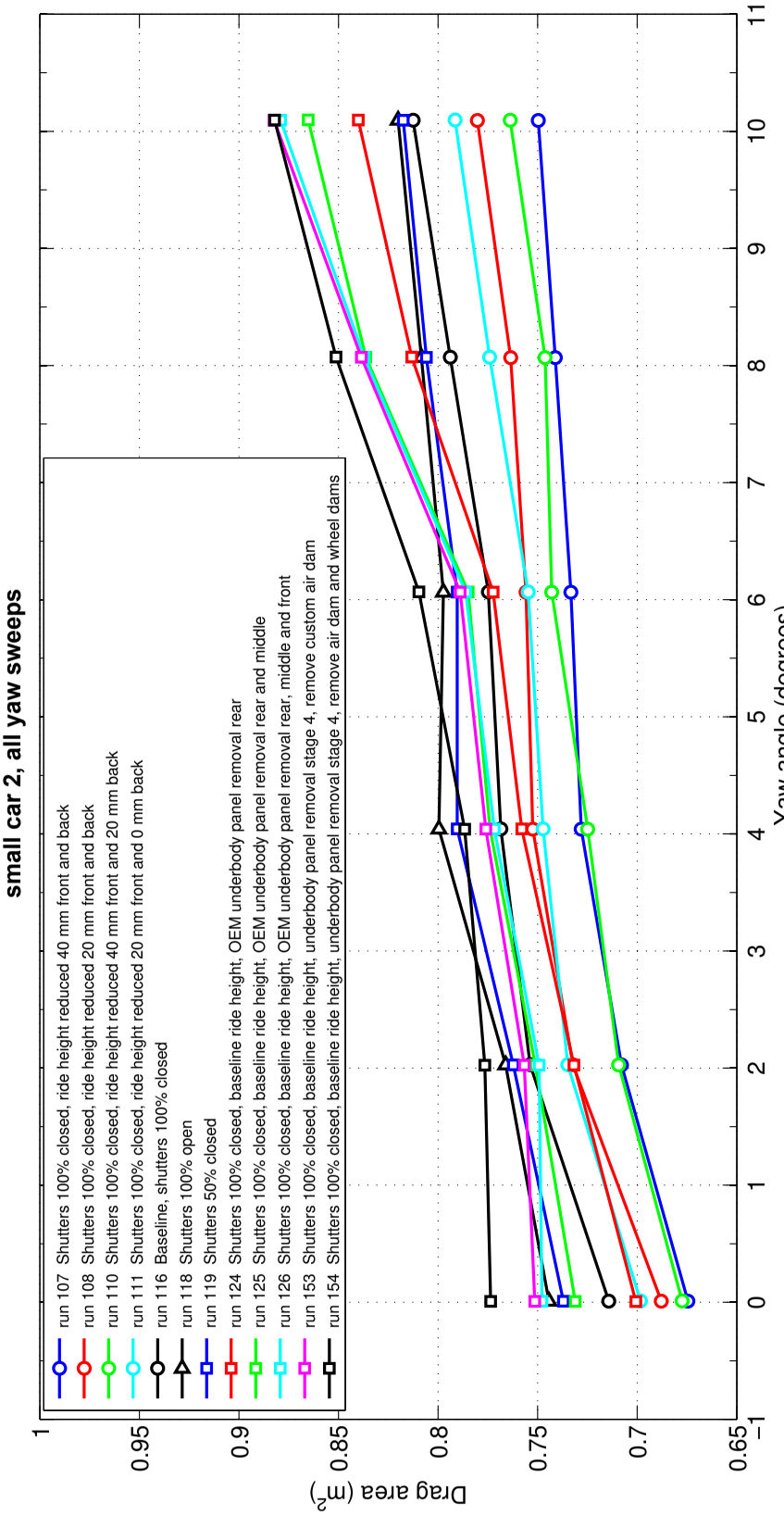

Figure C.2: Variations of drag area for small car 2 in smooth flow as a function of yaw angle for all yaw sweeps.

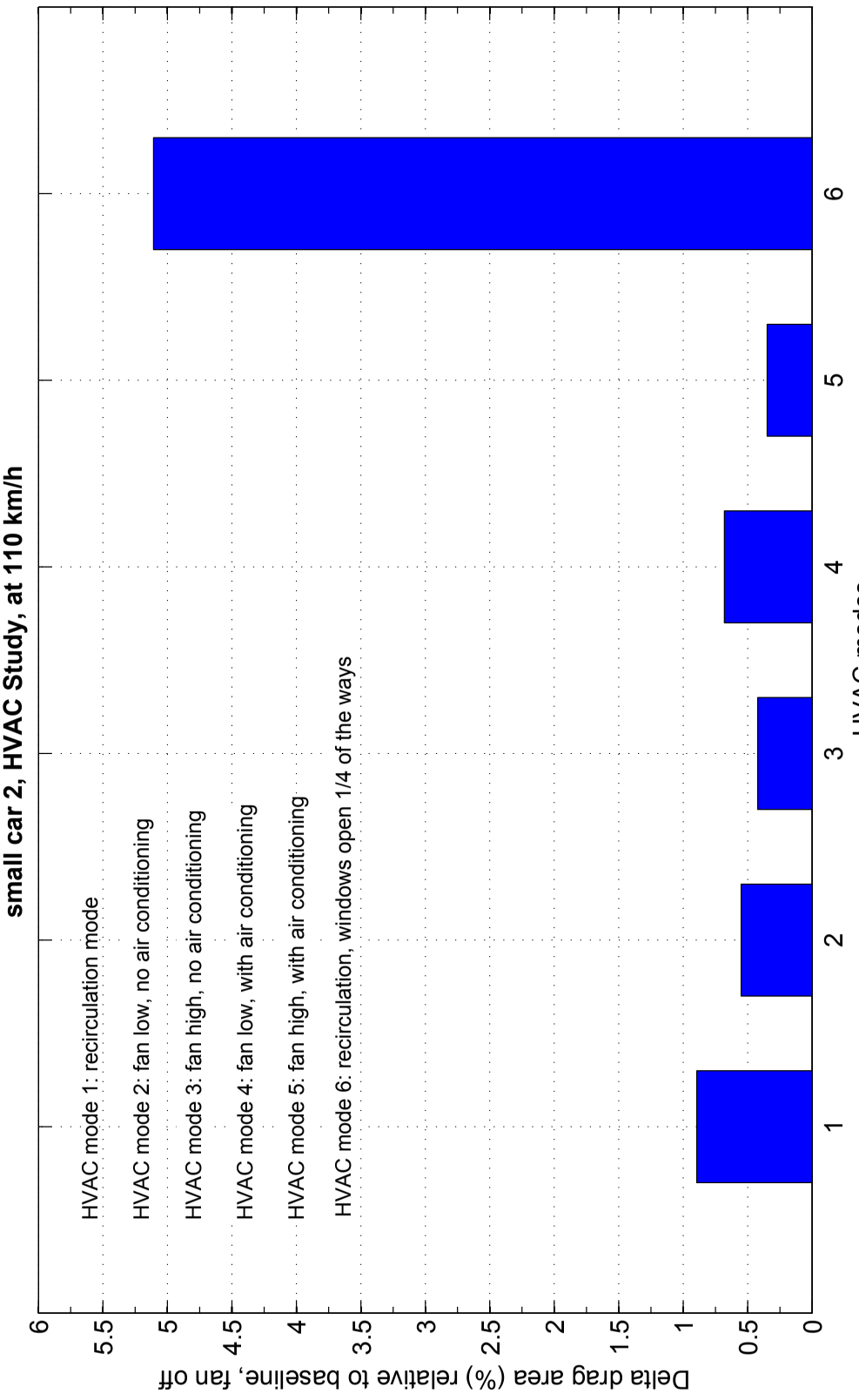

Figure C.3: Variations of drag area with reference to the baseline conditions for small car 2 in smooth flow as a function of HVAC mode.

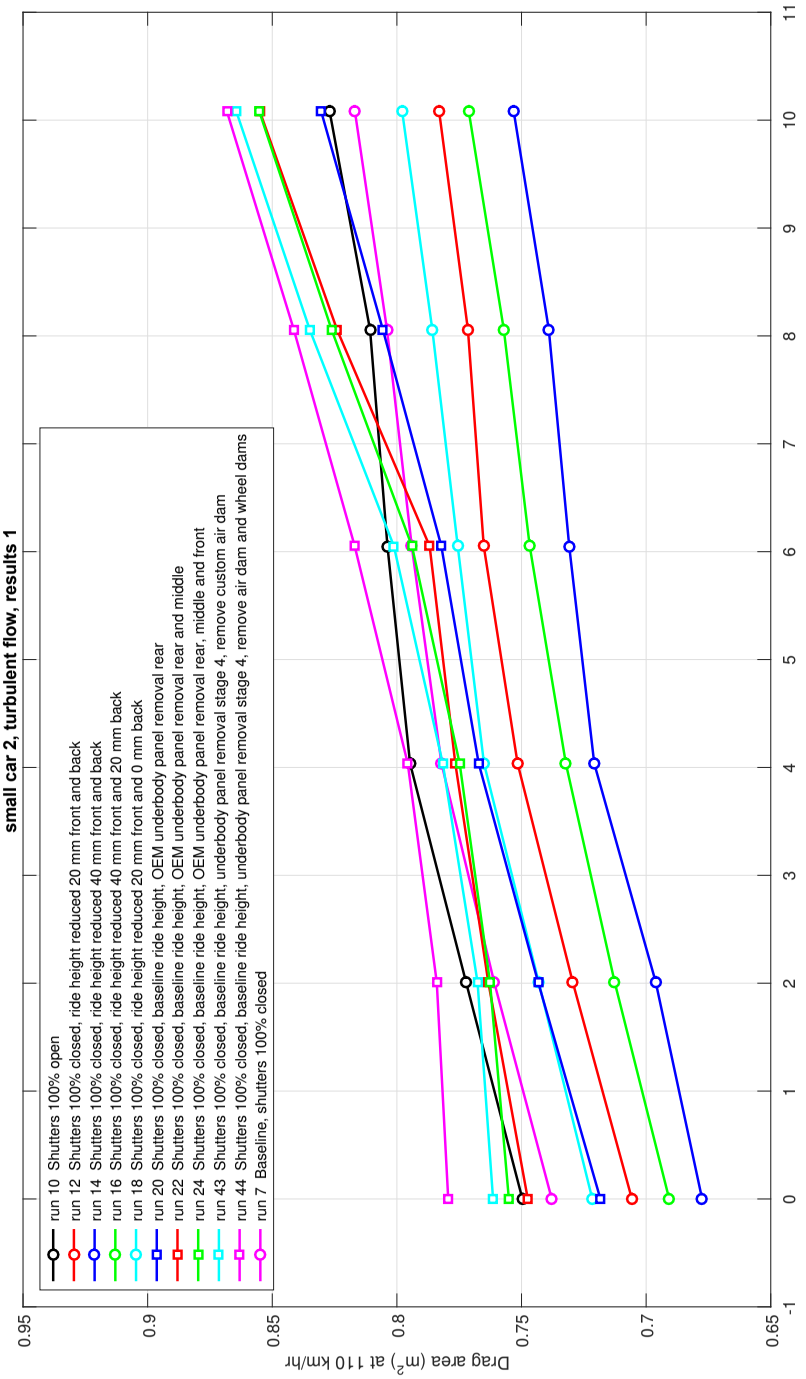

Figure C.4: Variations of drag area for small car 2 in turbulent flow as a function of yaw angle for several yaw sweeps.

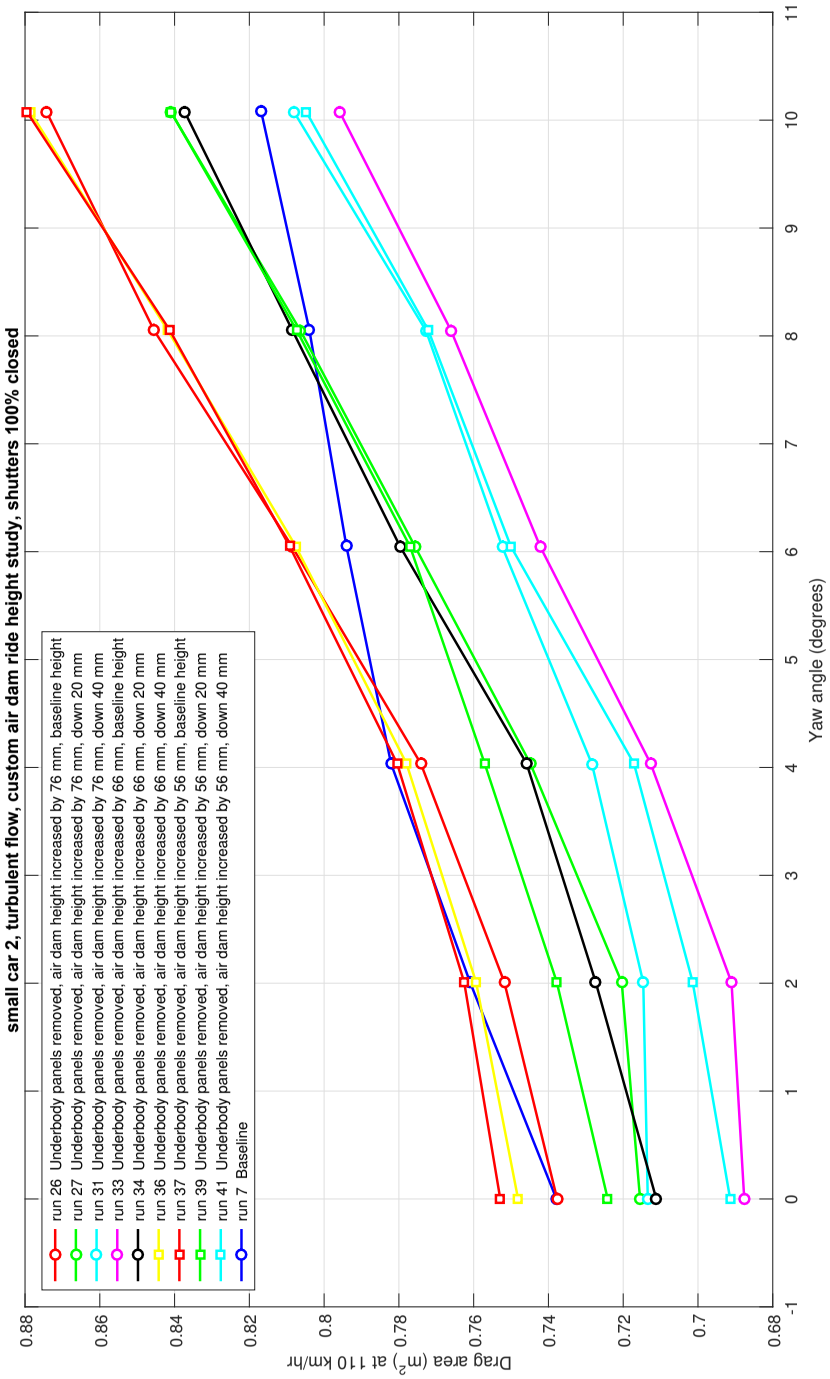

Figure C.5: Variations of drag area for small car 2 in turbulent flow as a function of yaw angle for several yaw sweeps.

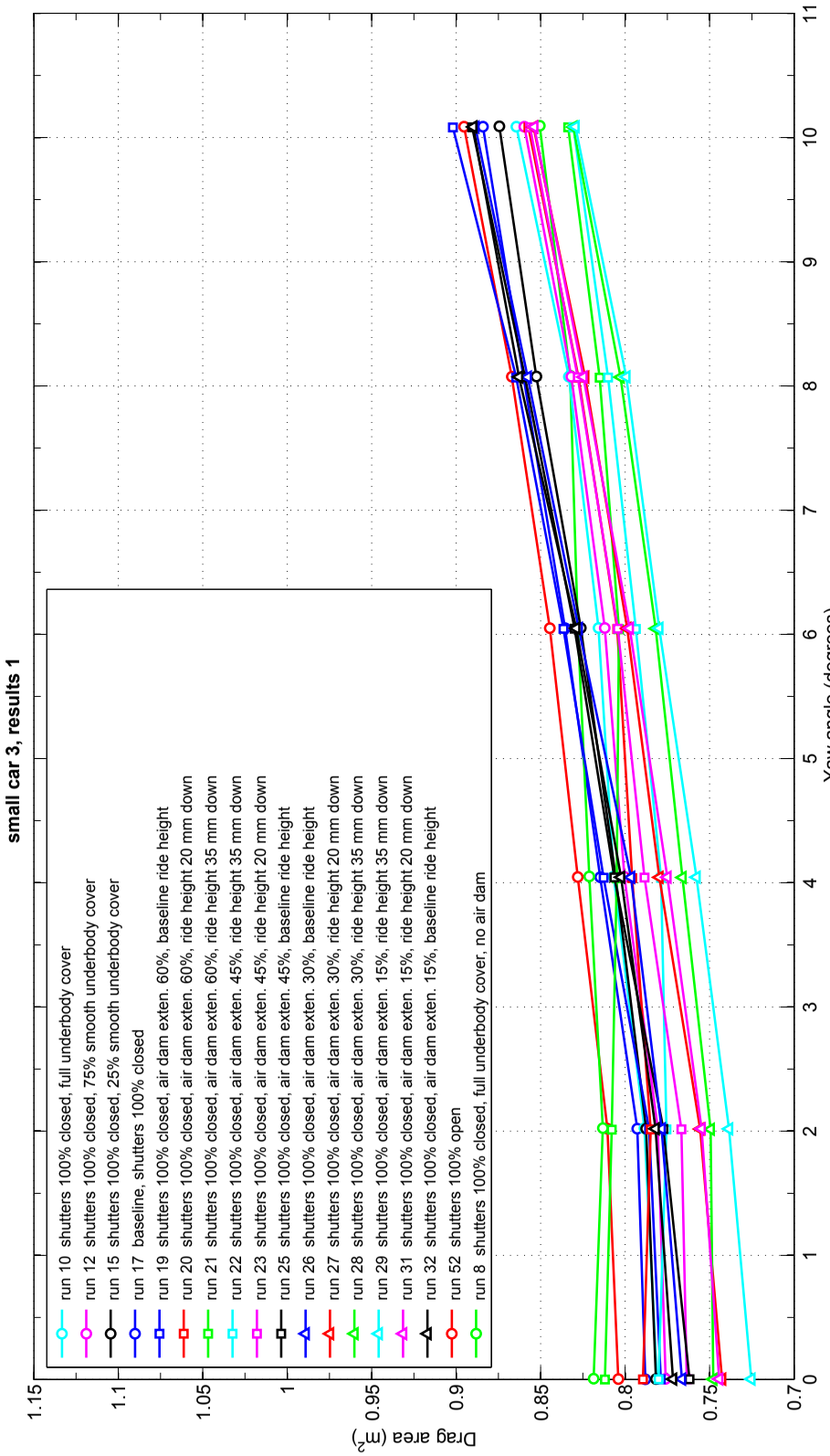

Figure C.6: Variations of drag area for small car 3 in smooth flow as a function of yaw angle for several yaw sweeps.

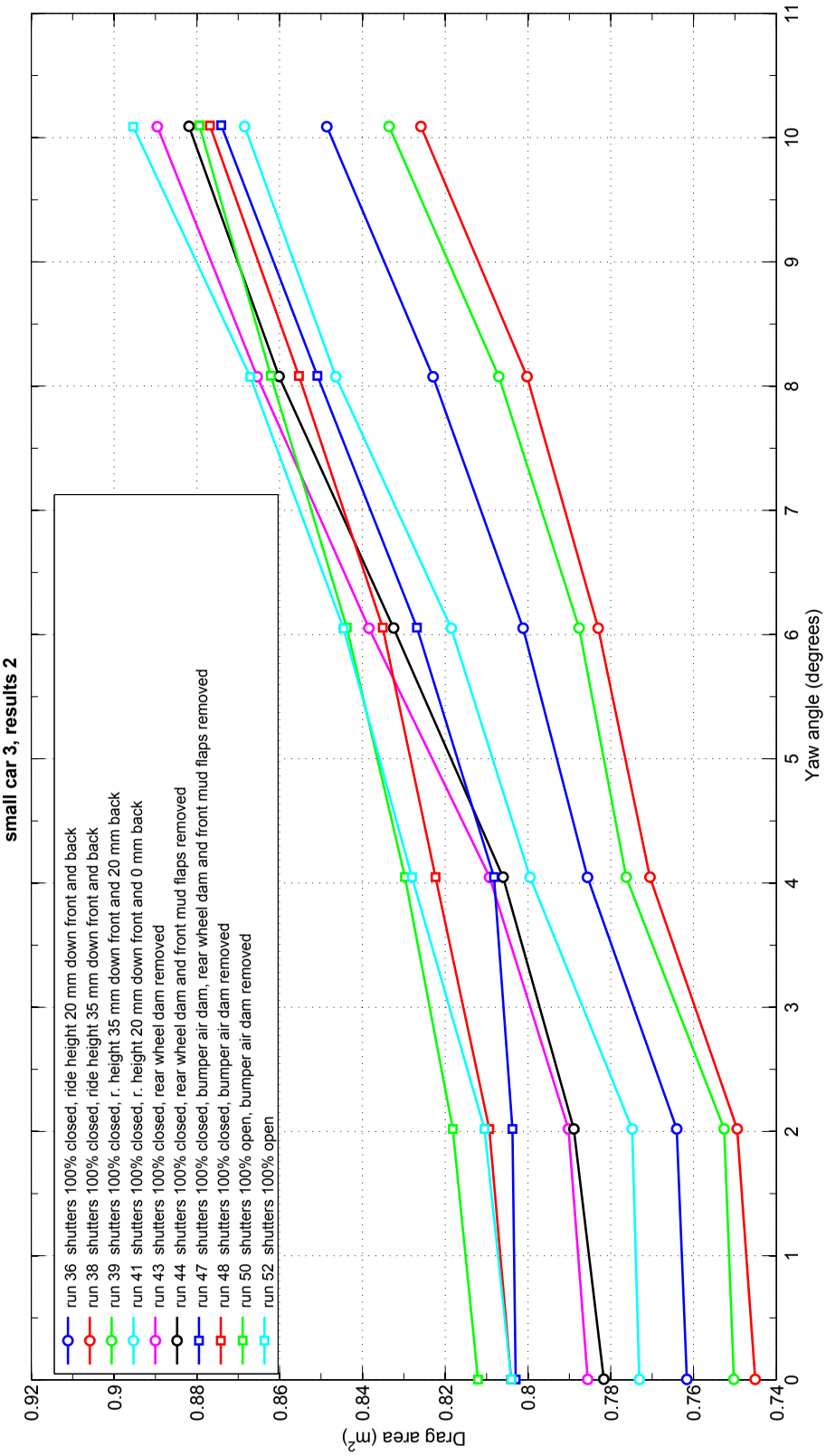

Figure C.7: Variations of drag area for small car 3 in smooth flow as a function of yaw angle for several yaw sweeps.

C.2 Graphical results for midsize cars

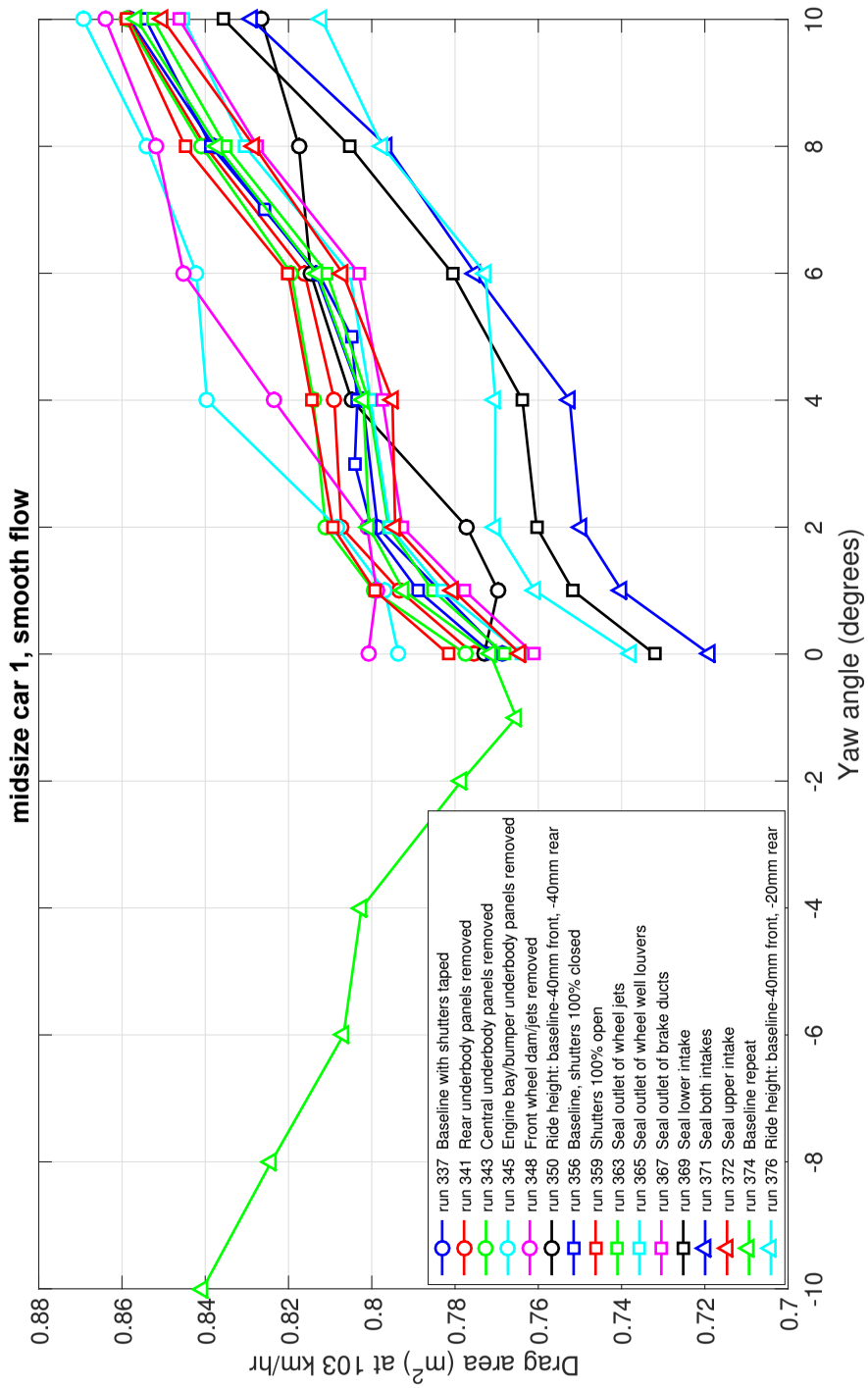

Figure C.8: Variations of drag area for midsize car 1 in smooth flow as a function of yaw angle for all yaw sweeps.

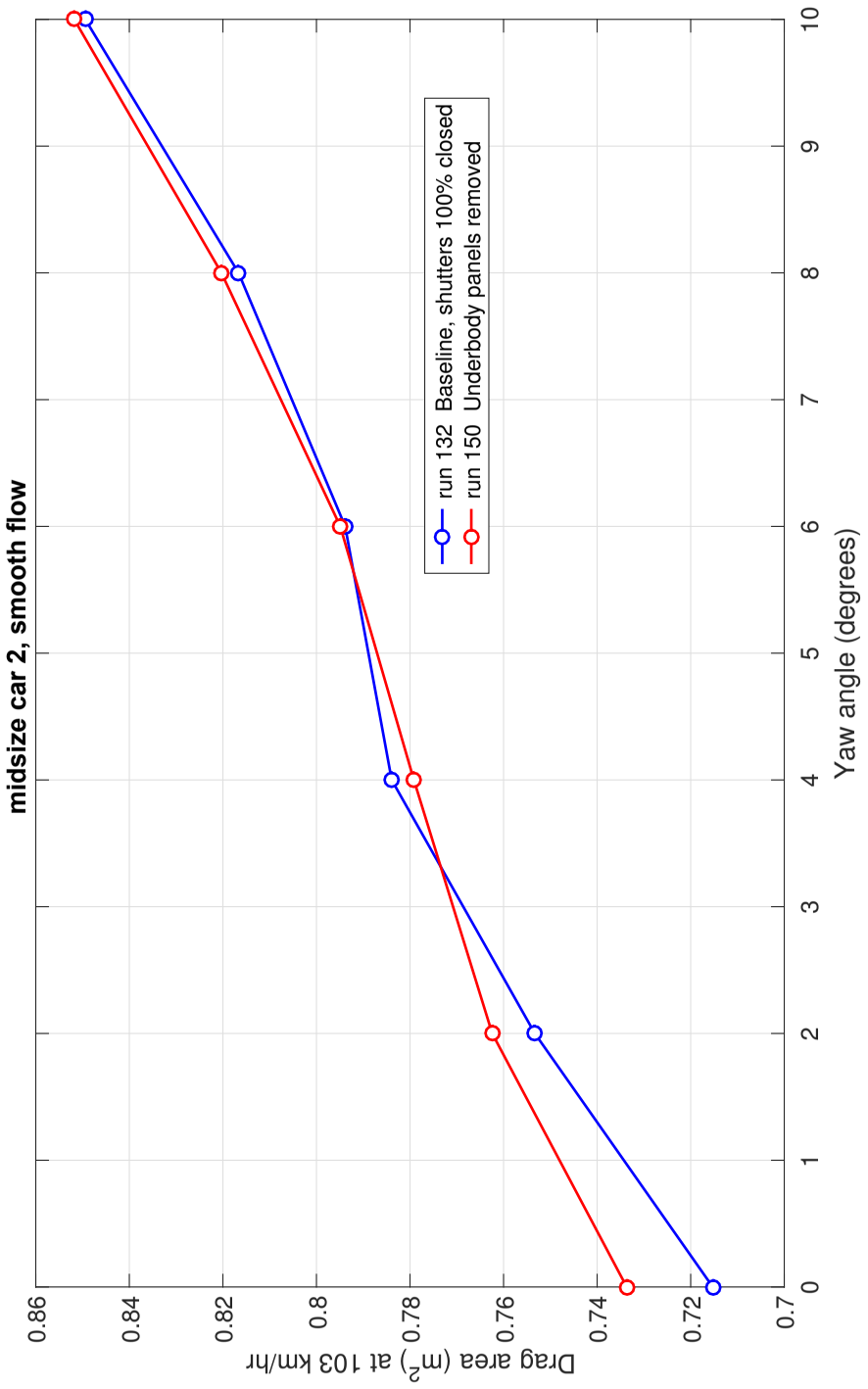

Figure C.9: Variations of drag area for midsize car 2 in smooth flow as a function of yaw angle for all yaw sweeps.

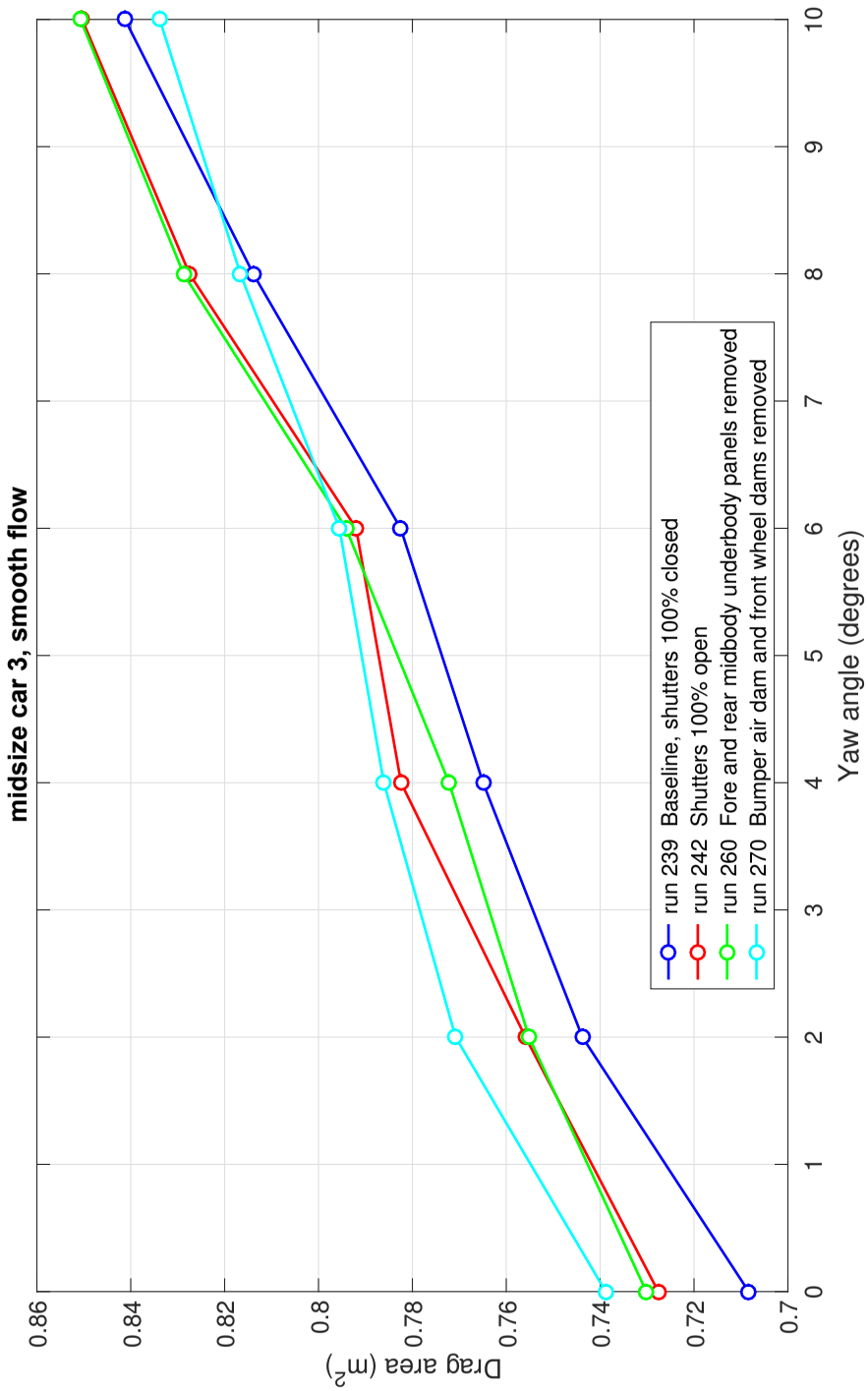

Figure C.10: Variations of drag area for midsize car 3 in smooth flow as a function of yaw angle for all yaw sweeps.

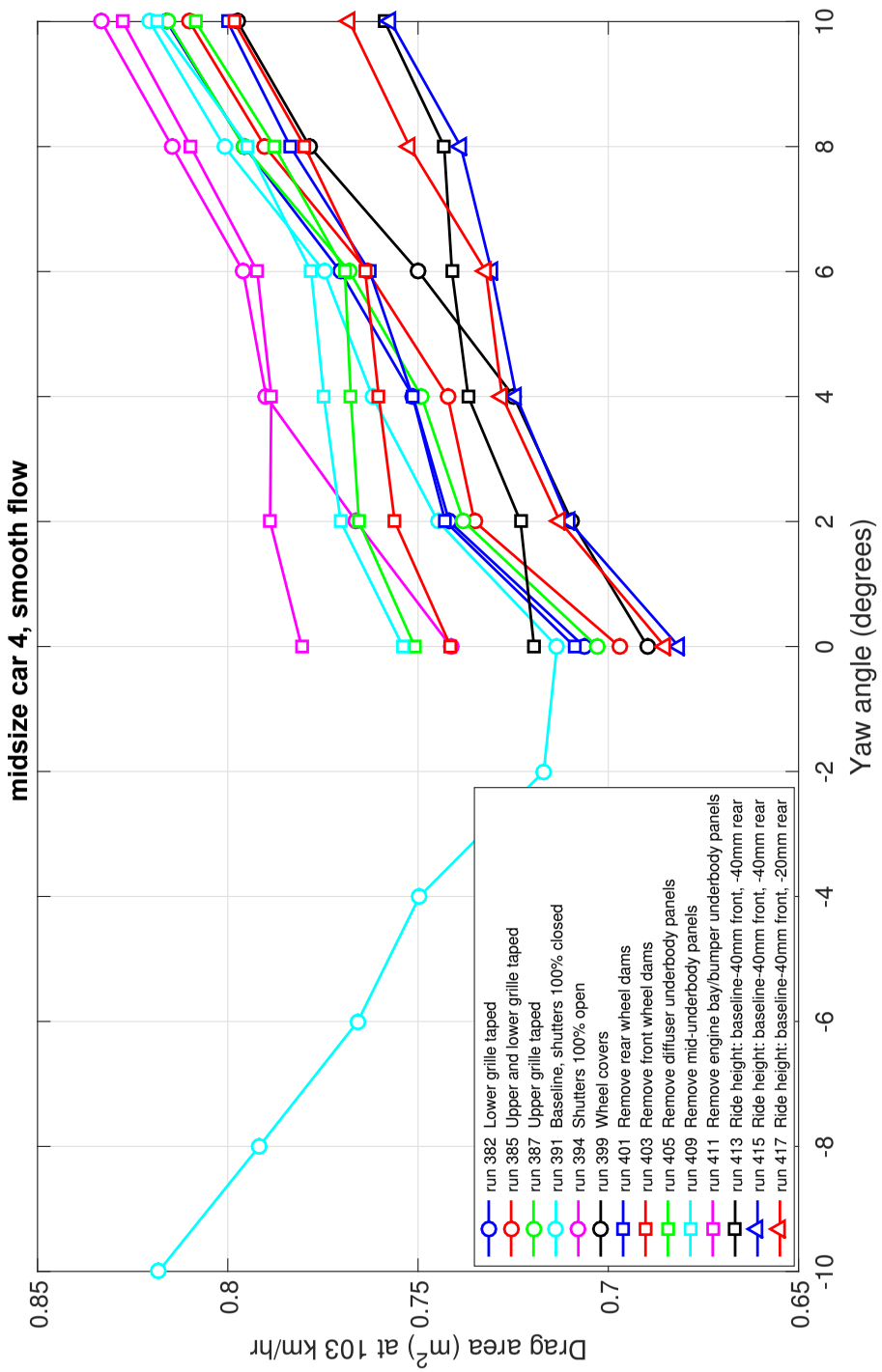

Figure C.11: Variations of drag area for midsize car 4 in smooth flow as a function of yaw angle for all yaw sweeps.

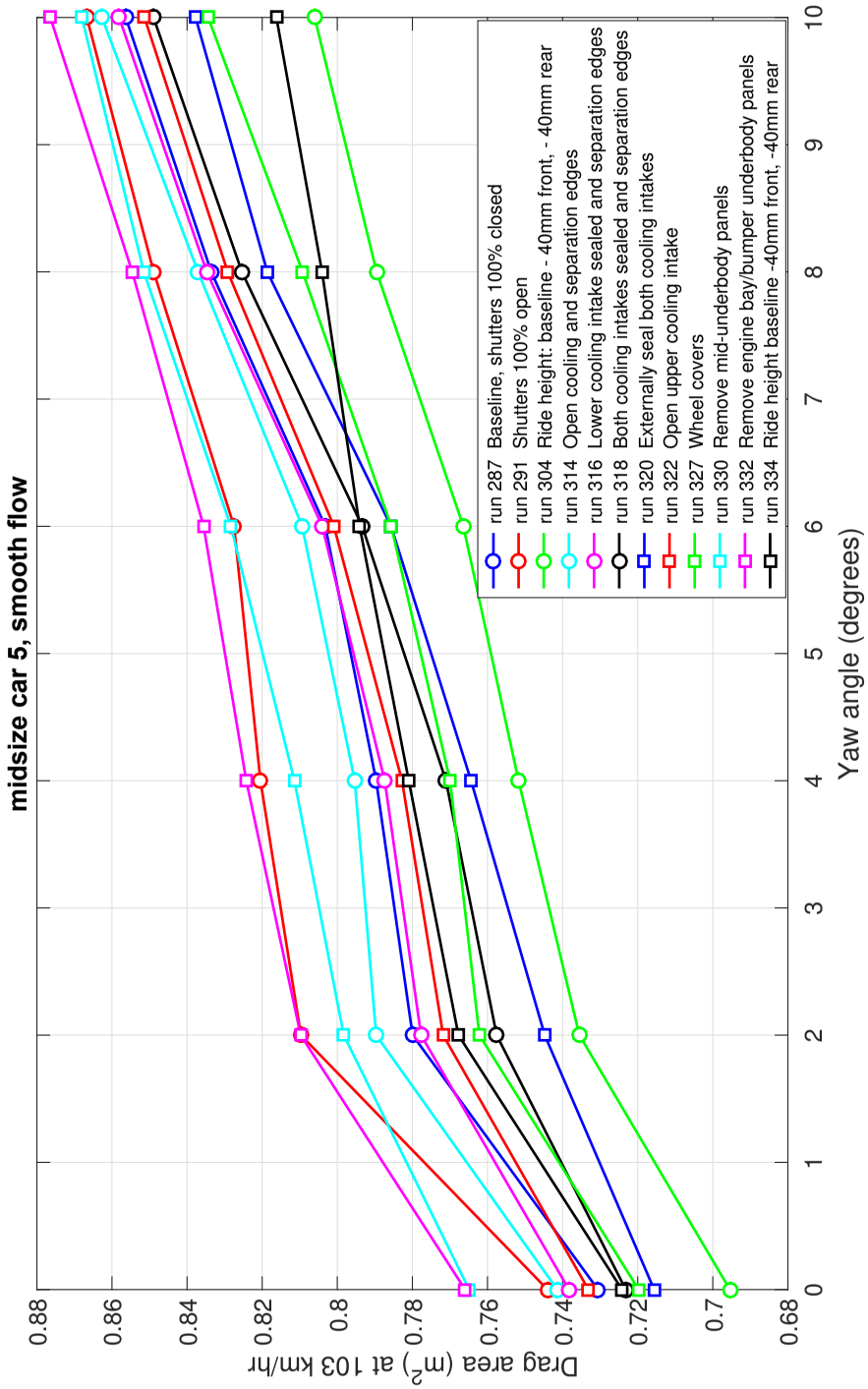

Figure C.12: Variations of drag area for midsize car 5 in smooth flow as a function of yaw angle for all yaw sweeps.

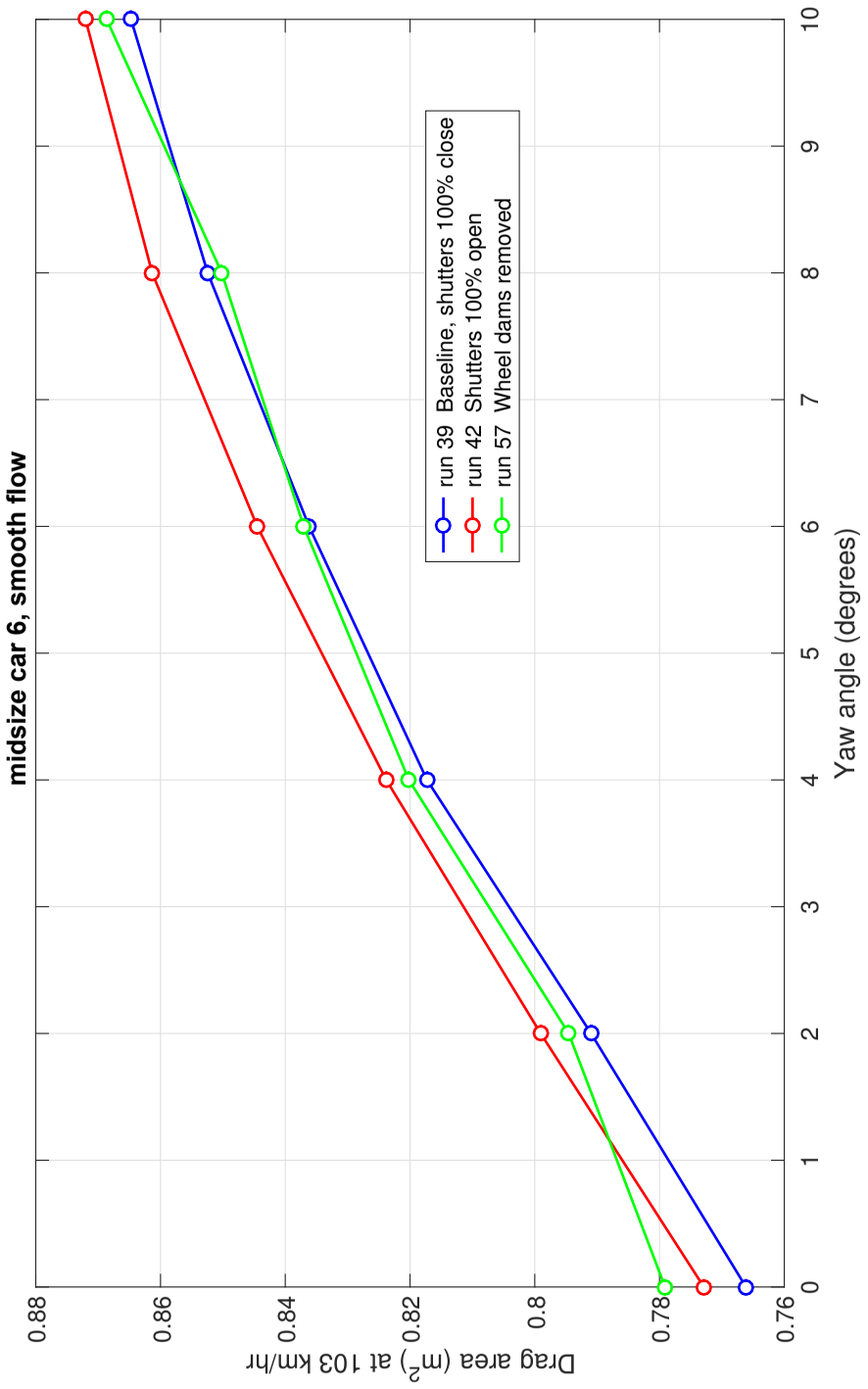

Figure C.13: Variations of drag area for midsize car 6 in smooth flow as a function of yaw angle for all yaw sweeps.

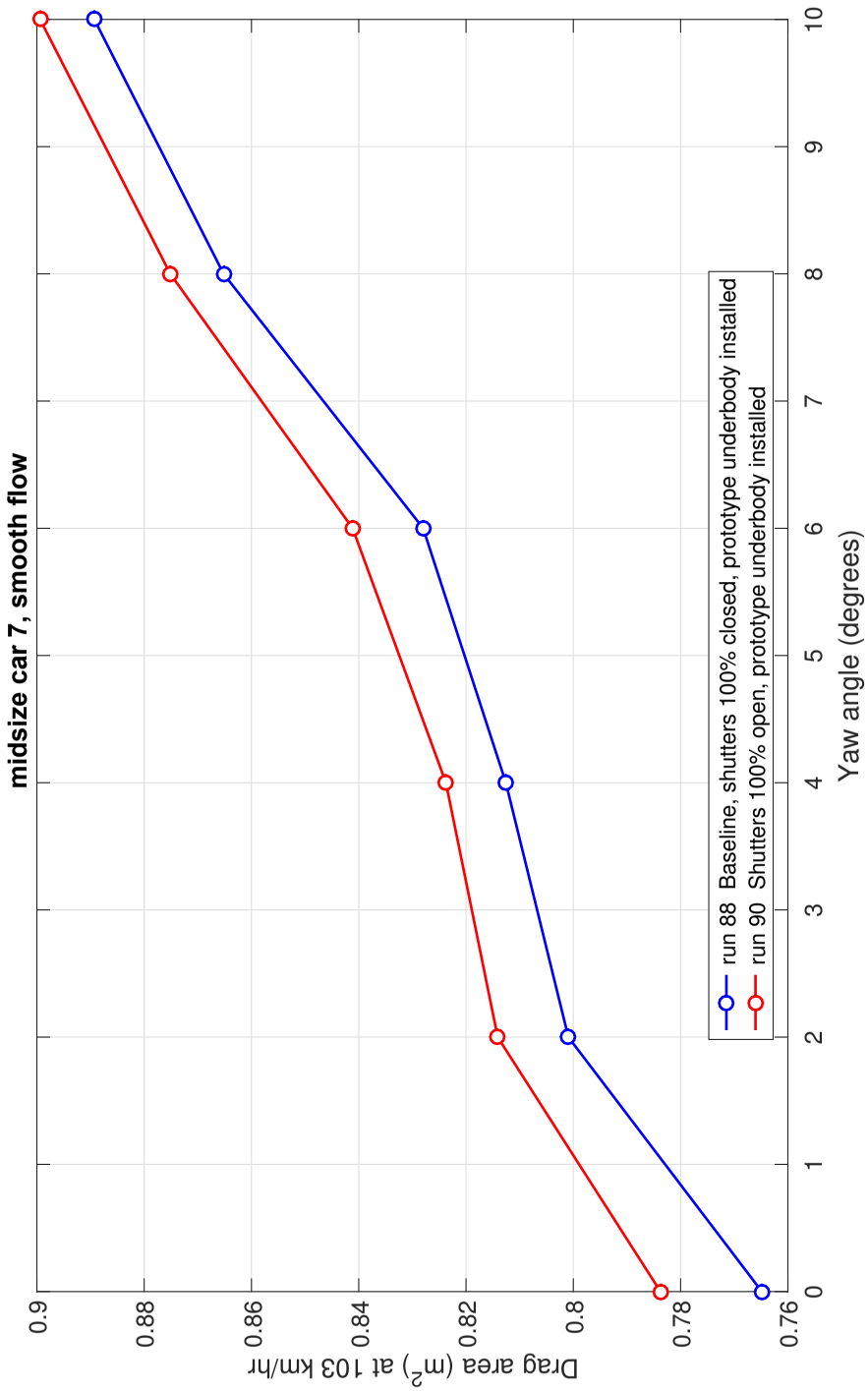

Figure C.14: Variations of drag area for midsize car 7 in smooth flow as a function of yaw angle for all yaw sweeps.

C.3 Graphical results for large cars

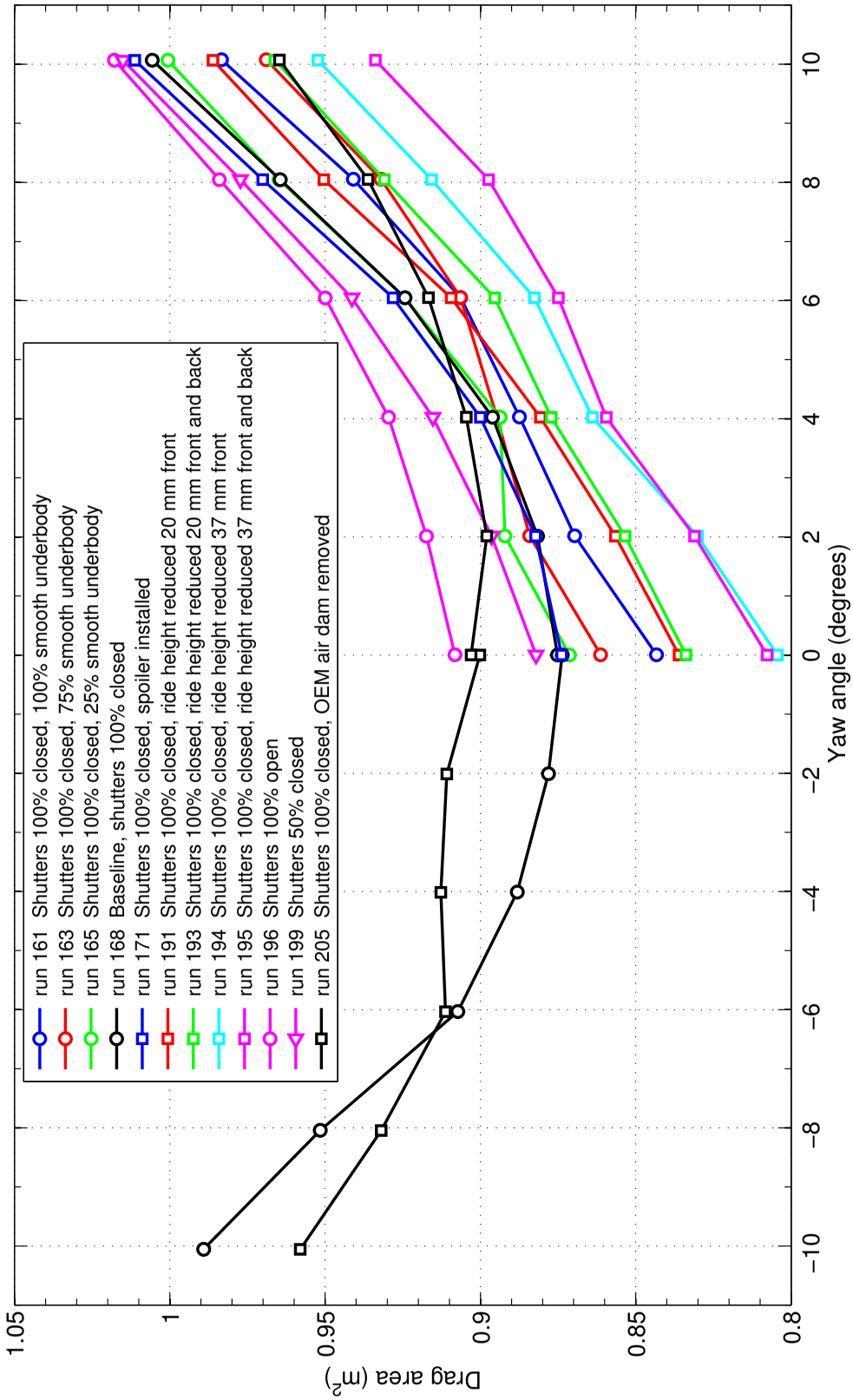

Figure C.15: Variations of drag area for large car 1 in smooth flow as a function of yaw angle for all yaw sweeps.

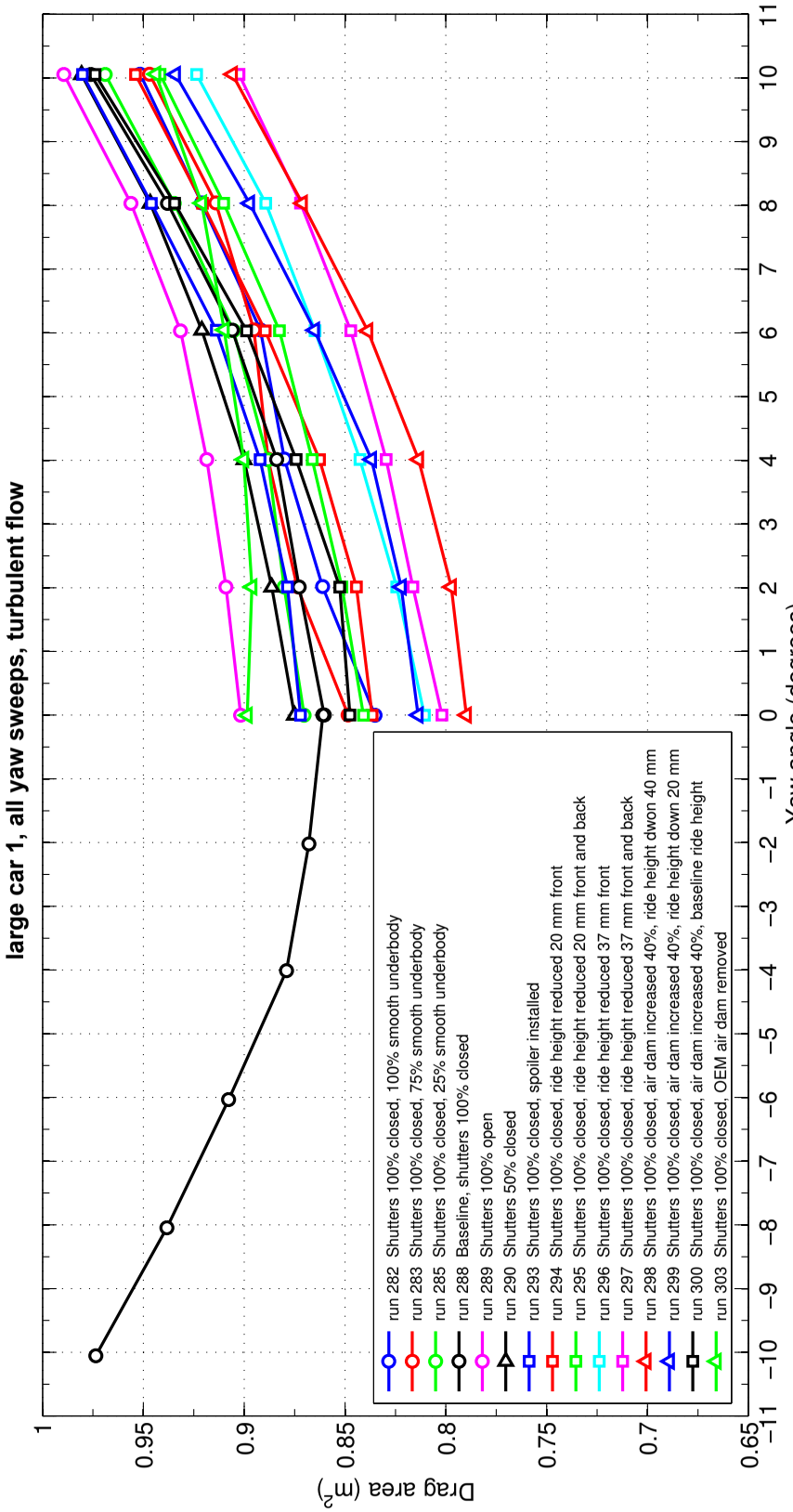

Figure C.16: Variations of drag area for large car 1 in turbulent flow as a function of yaw angle for all yaw sweeps.

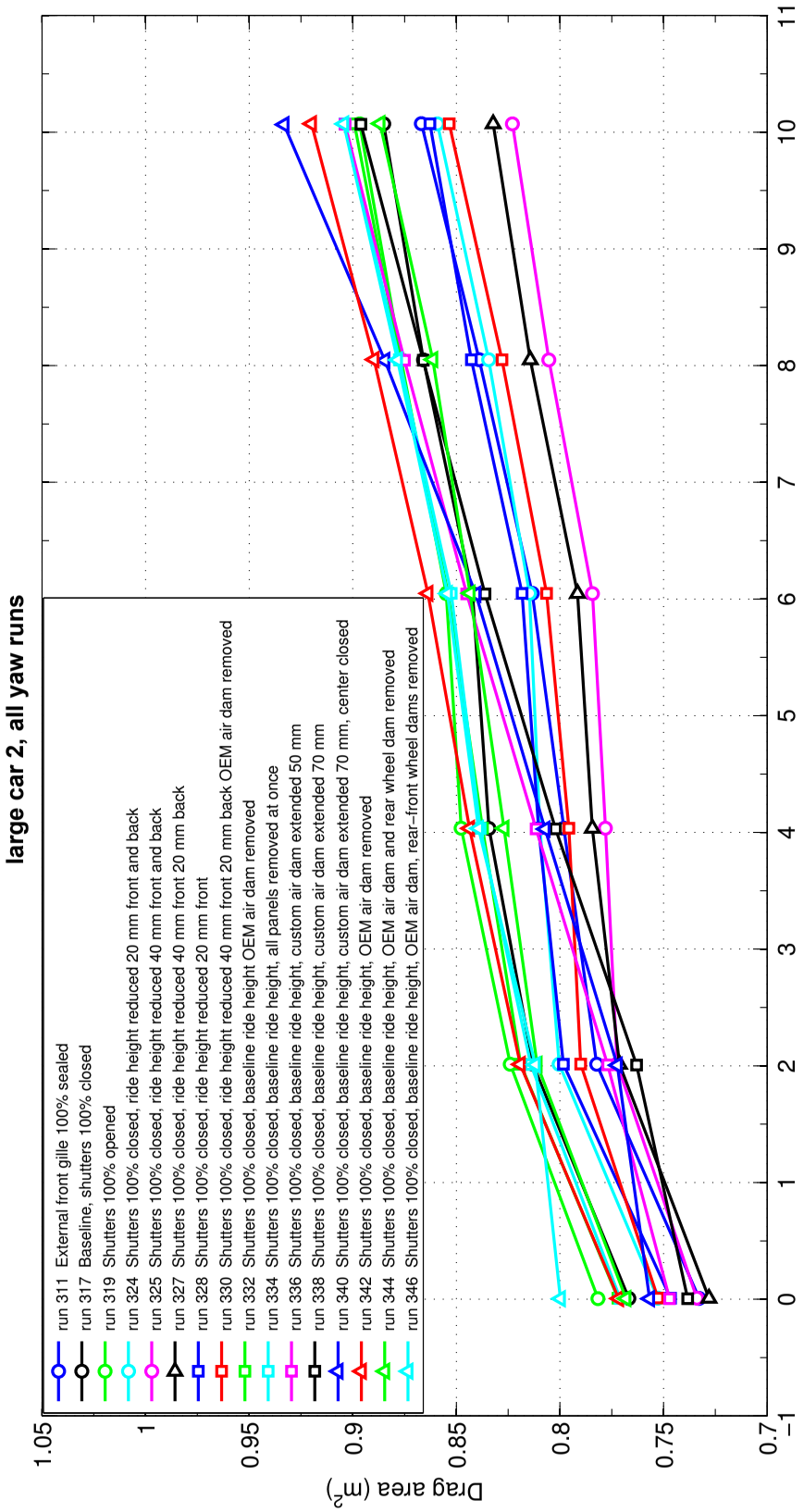

Figure C.17: Variations of drag area for large car 2 in smooth flow as a function of yaw angles for all yaw sweeps.

C.4 Graphical results for small SUVs

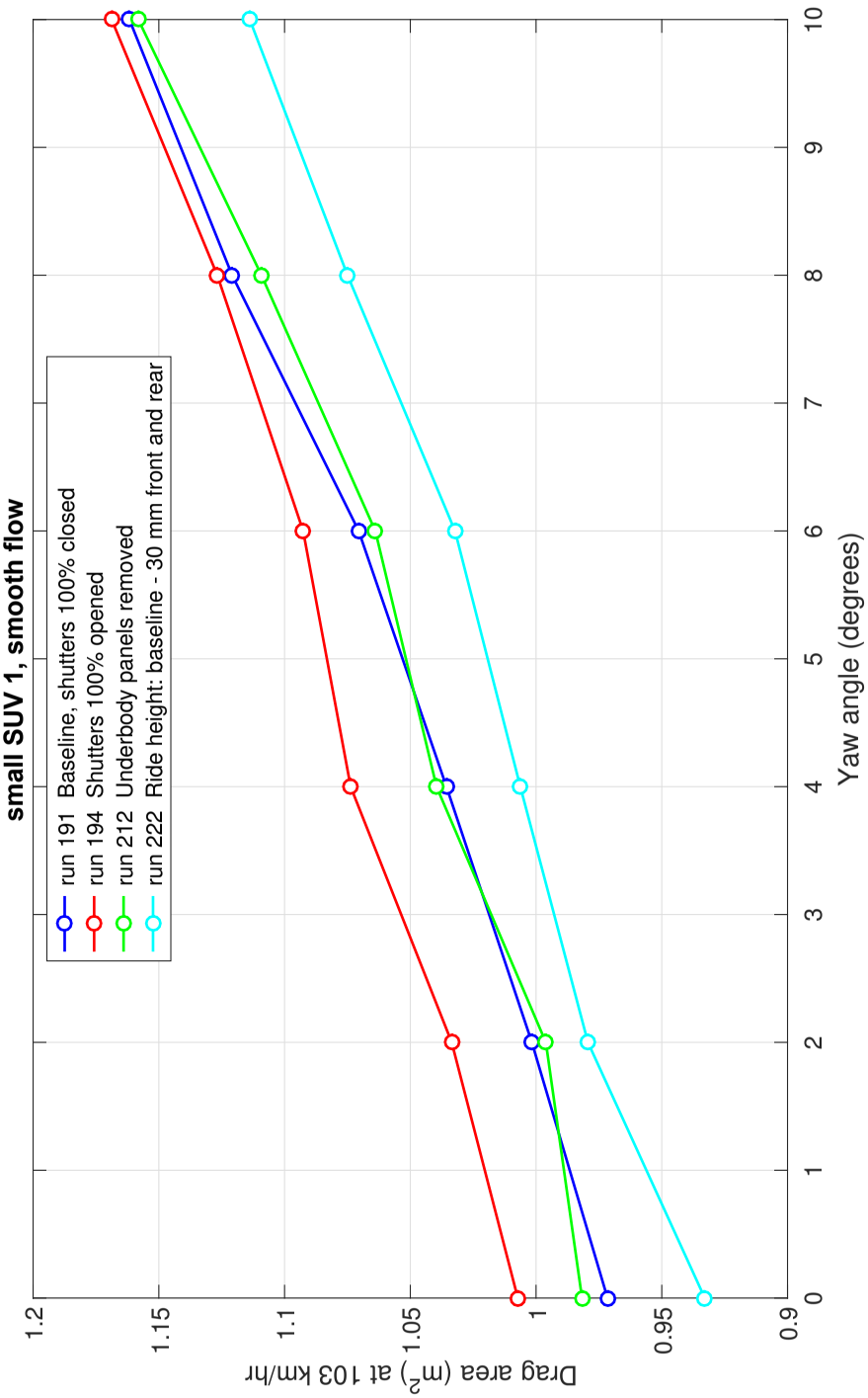

Figure C.18: Variations of drag area for small SUV 1 in smooth flow as a function of yaw angle for all yaw sweeps.

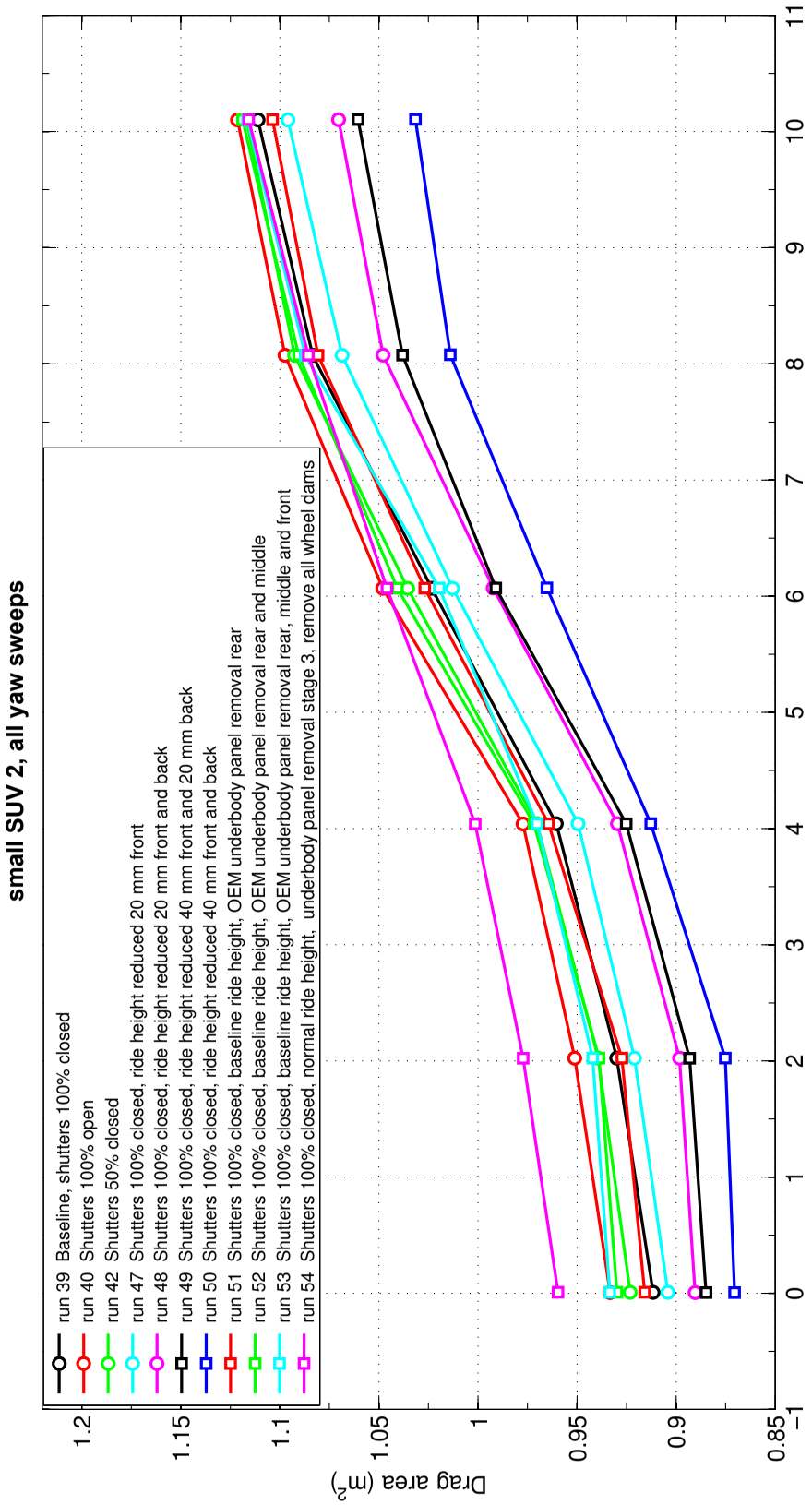

Figure C.19: Variations of drag area for small SUV 2 in smooth flow as a function of yaw angle for all yaw sweeps.

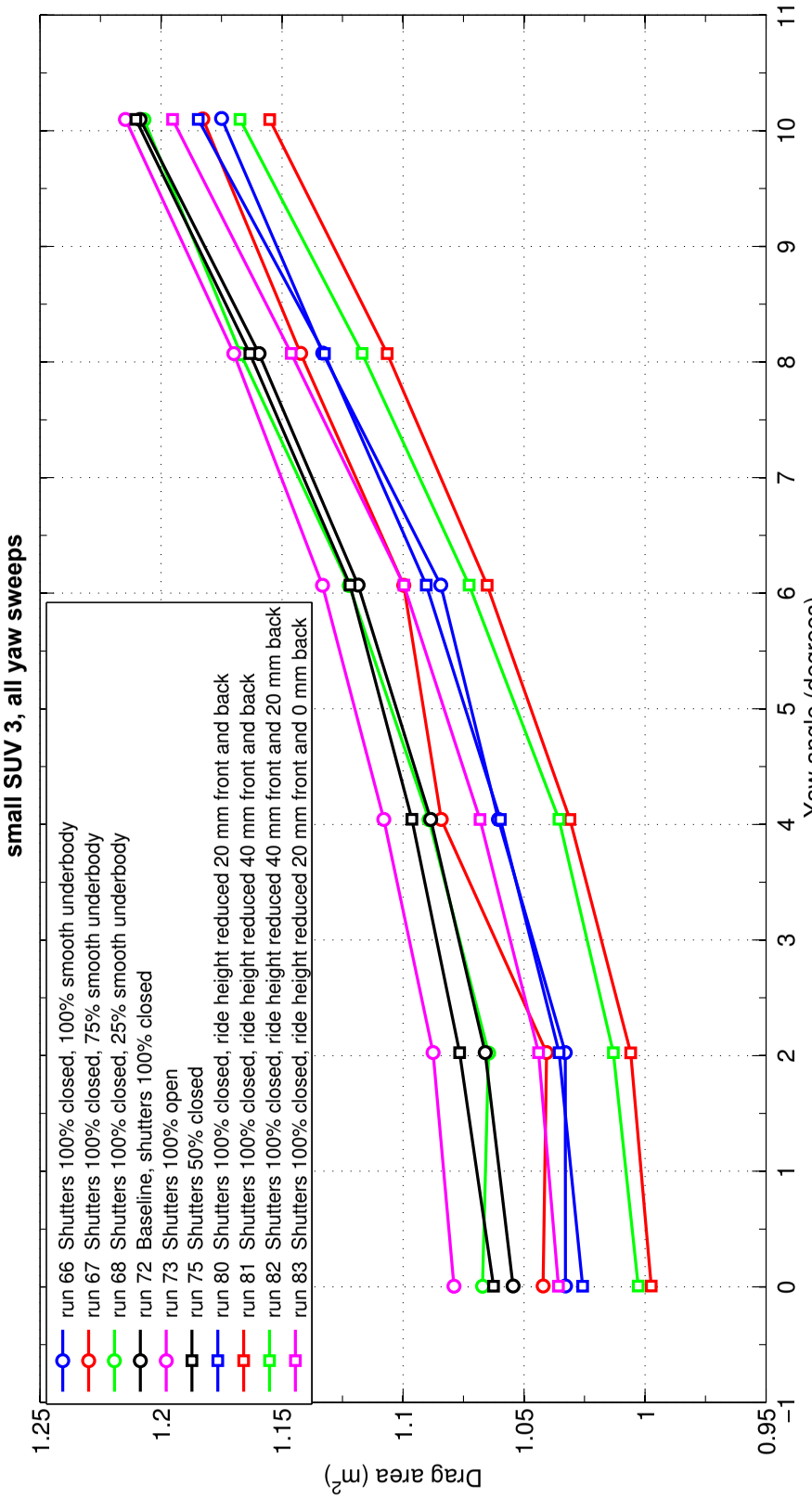

Figure C.20: Variations of drag area for small SUV 3 in smooth flow as a function of yaw angle for all yaw sweeps.

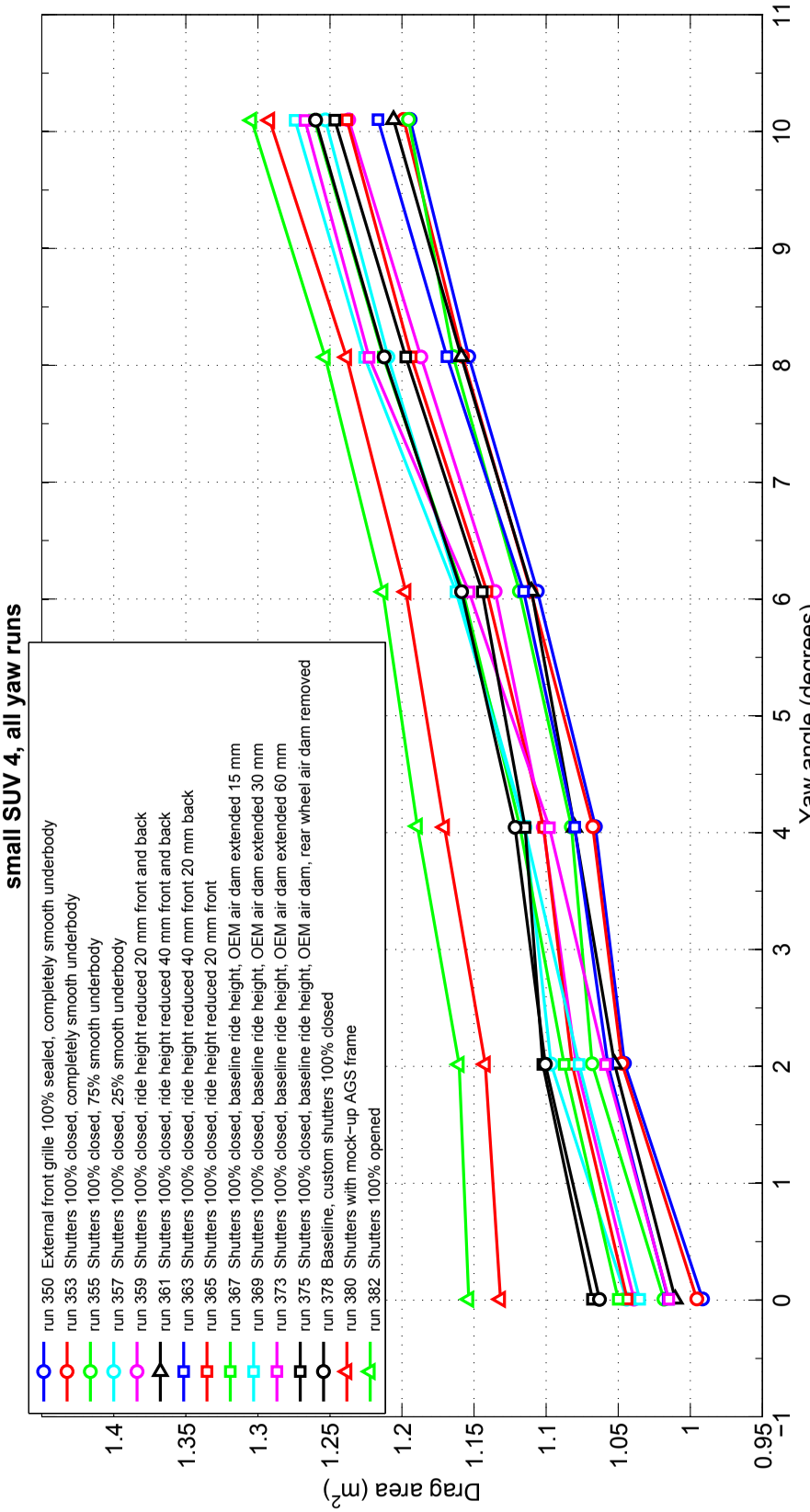

Figure C.21: Variations of drag area for small SUV 4 in smooth flow as a function of yaw angle for all yaw sweeps.

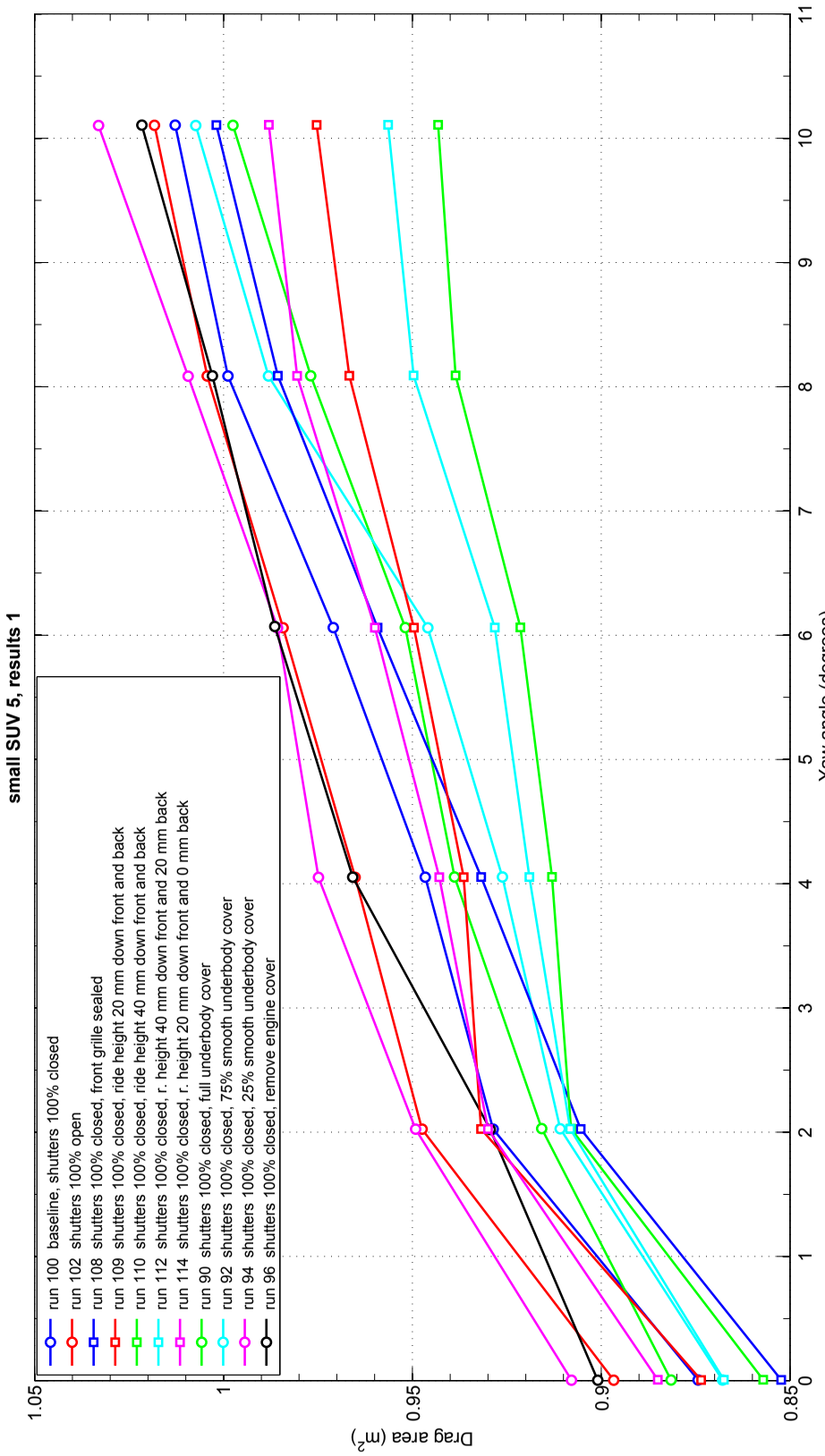

Figure C.22: Variations of drag area for small SUV 5 in smooth flow as a function of yaw angle for all yaw sweeps.

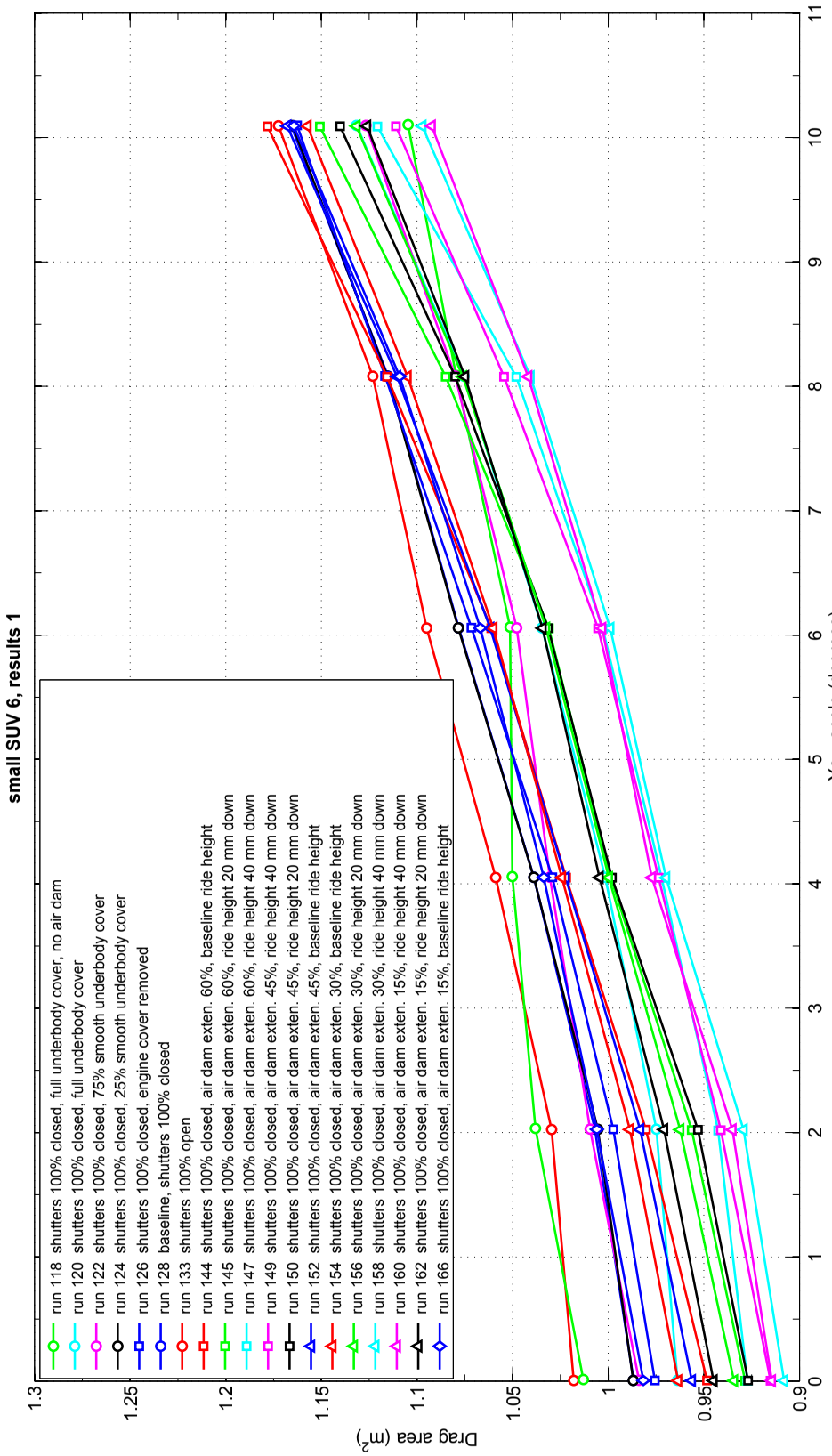

Figure C.23: Variations of drag area for small SUV 6 in smooth flow as a function of yaw angle for several yaw sweeps.

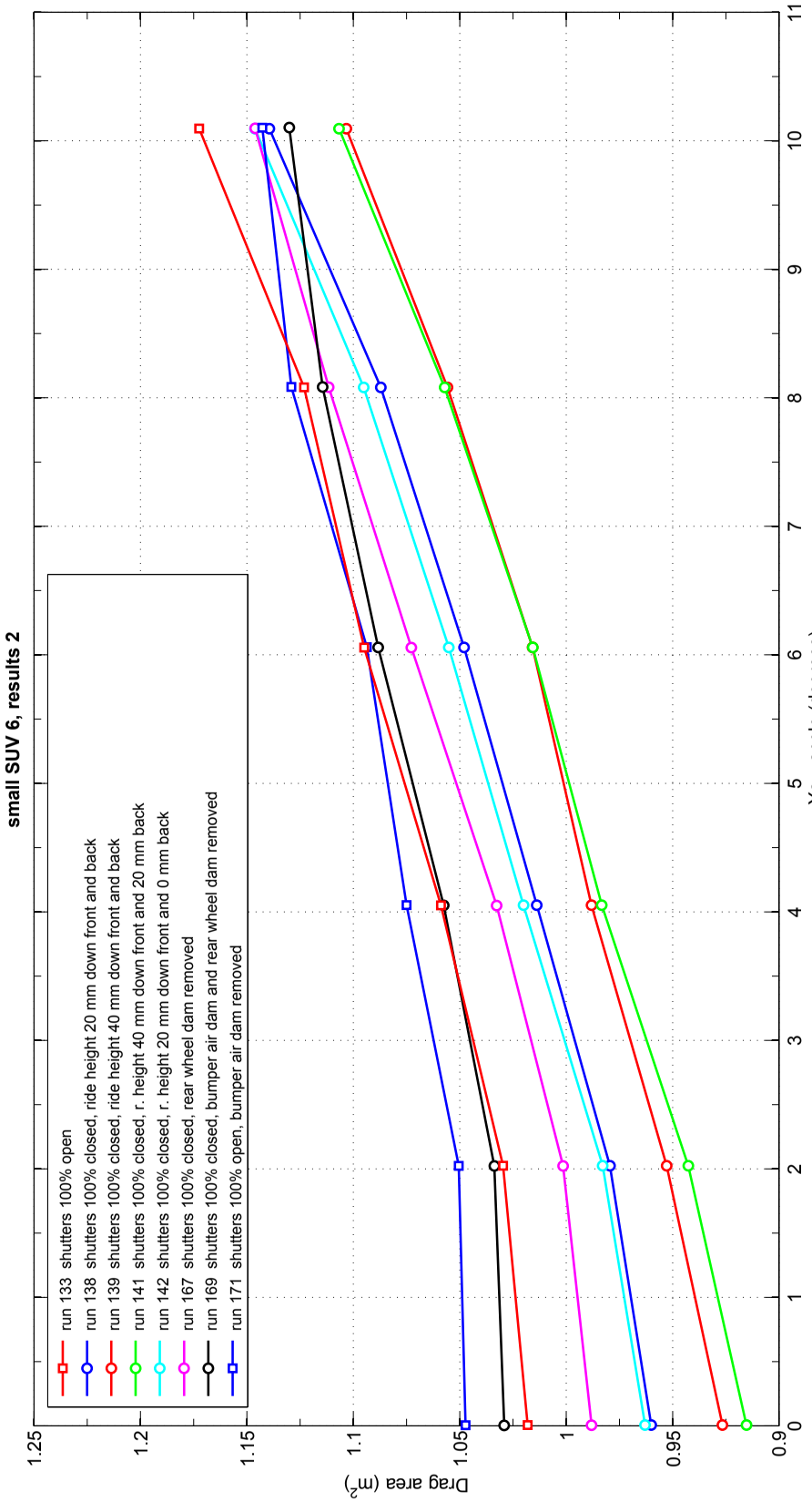

Figure C.24: Variations of drag area for small SUV 6 in smooth flow as a function of yaw angle for several yaw sweeps.

C.5 Graphical results for standard SUVs

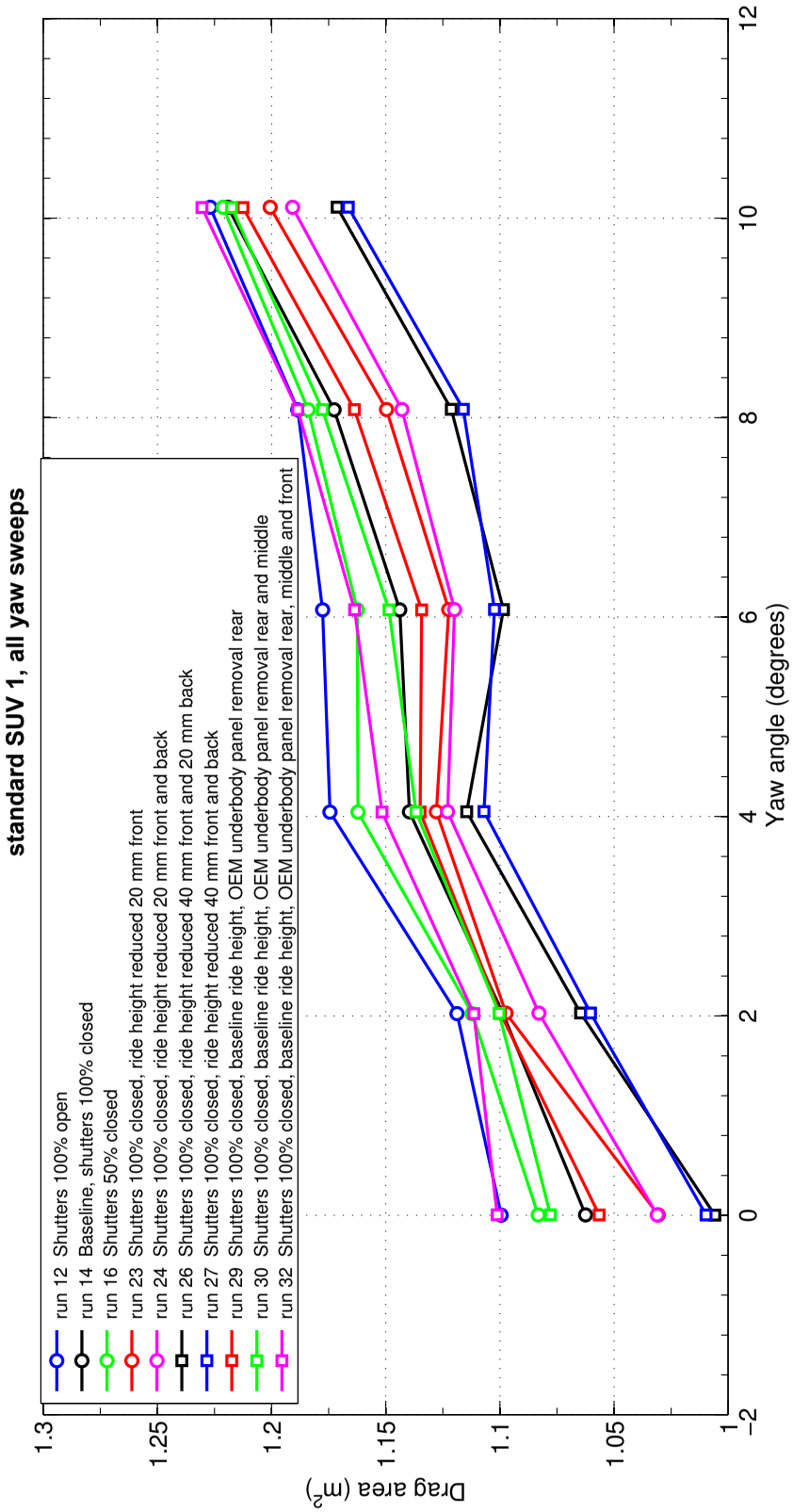

Figure C.25: Variations of drag area for standard SUV 1 in smooth flow as a function of yaw angle for all yaw sweeps.

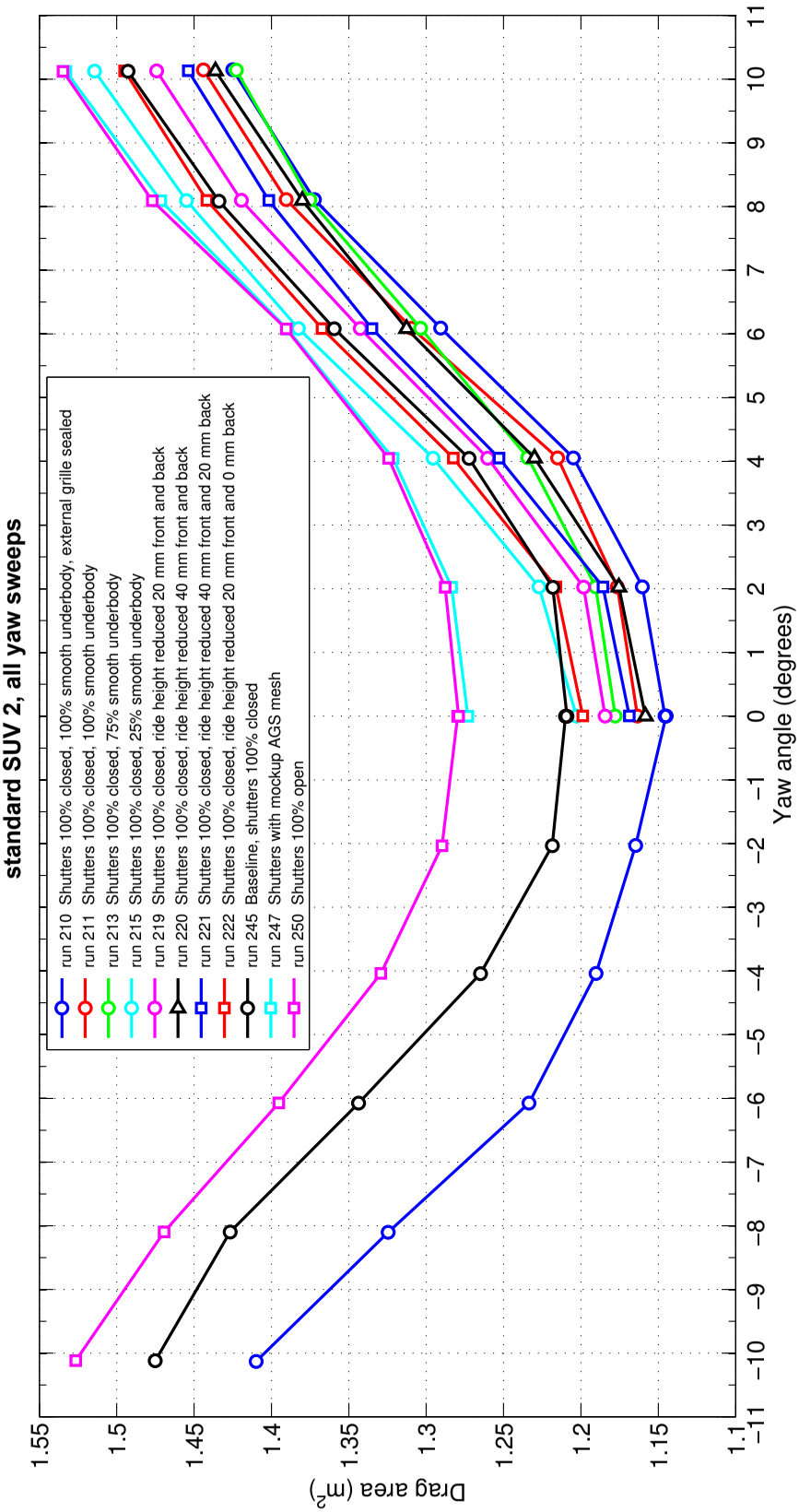

Figure C.26: Variations of drag area for standard SUV 2 in smooth flow as a function of yaw angle for all yaw sweeps.

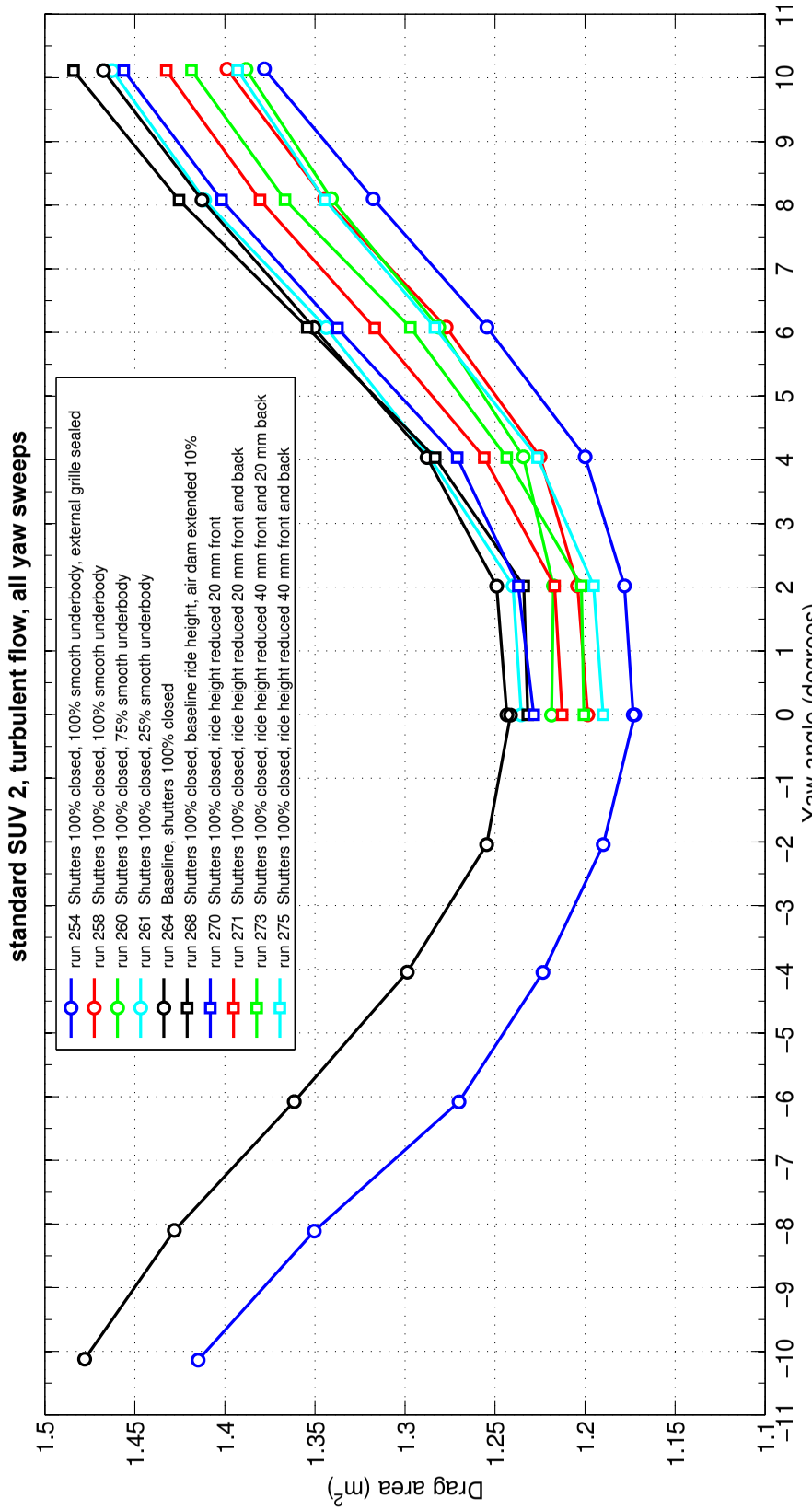

Figure C.27: Variations of drag area for standard SUV 2 in turbulent flow as a function of yaw angle for all yaw sweeps.

C.6 Graphical results for minivans

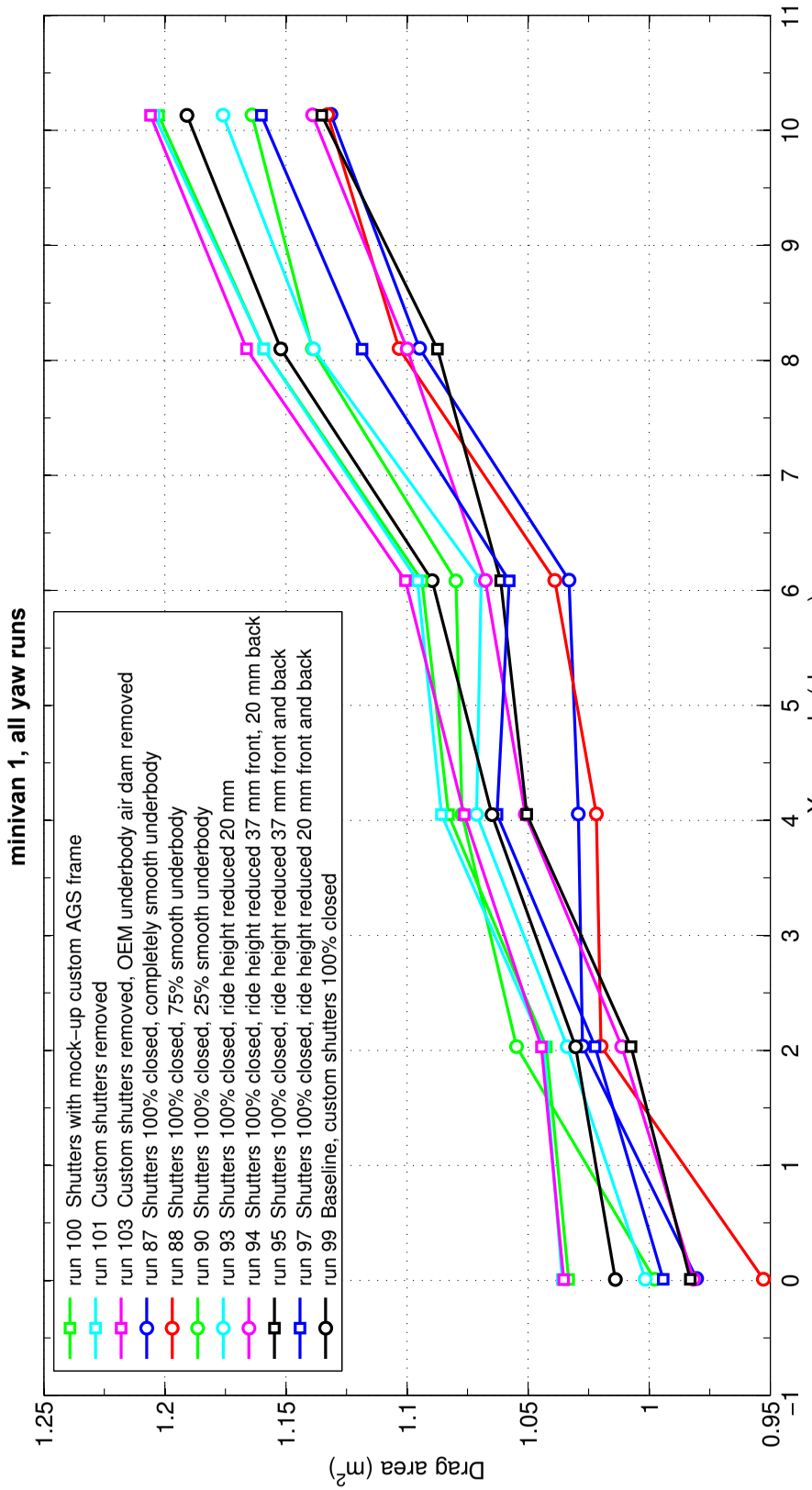

Figure C.28: Variations of drag area for minivan 1 in smooth flow as a function of yaw angle for all yaw sweeps.

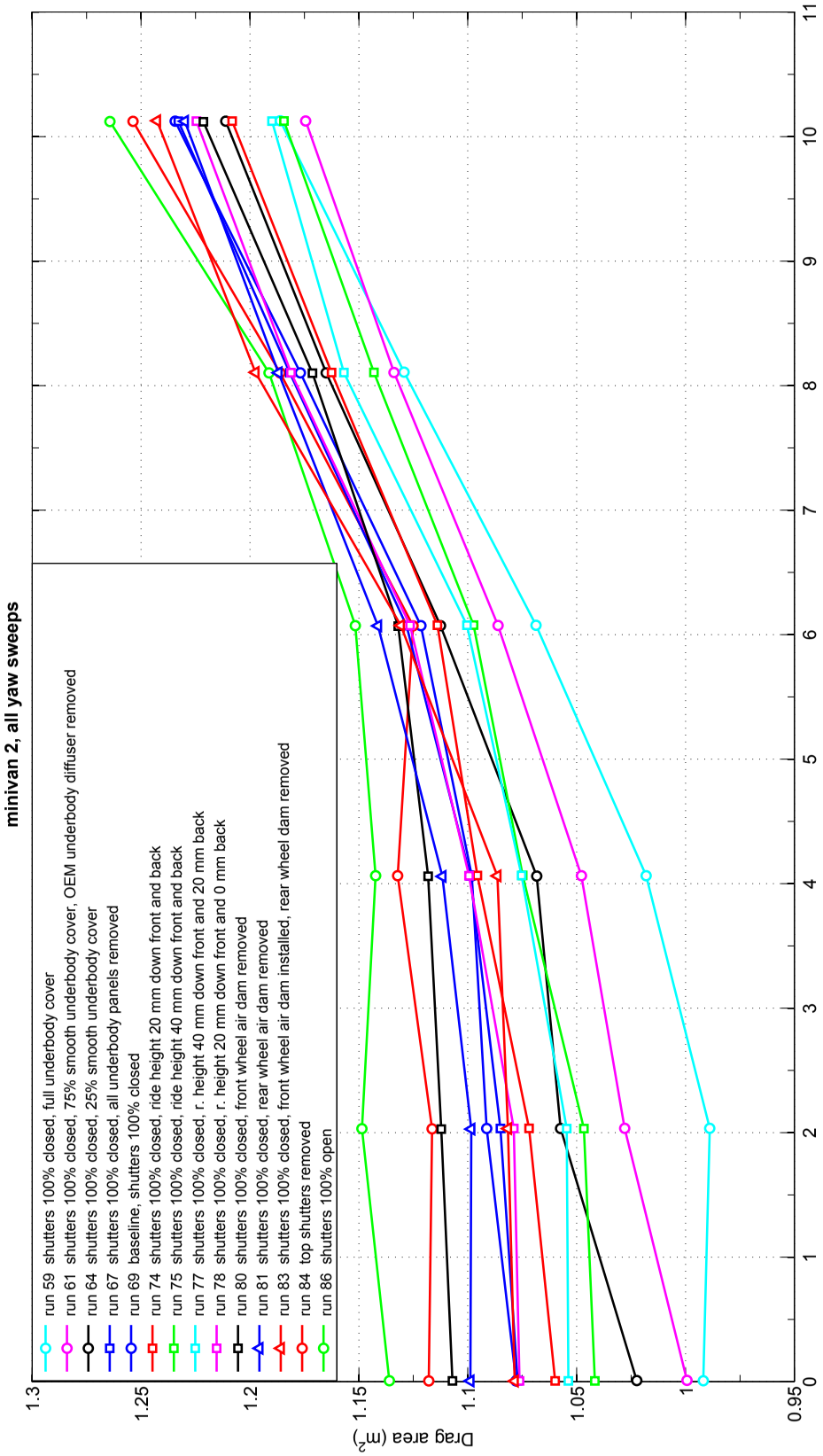

Figure C.29: Variations of drag area for minivan 2 in smooth flow as a function of yaw angle for all yaw sweeps.

C.7 Graphical results for pick-up trucks

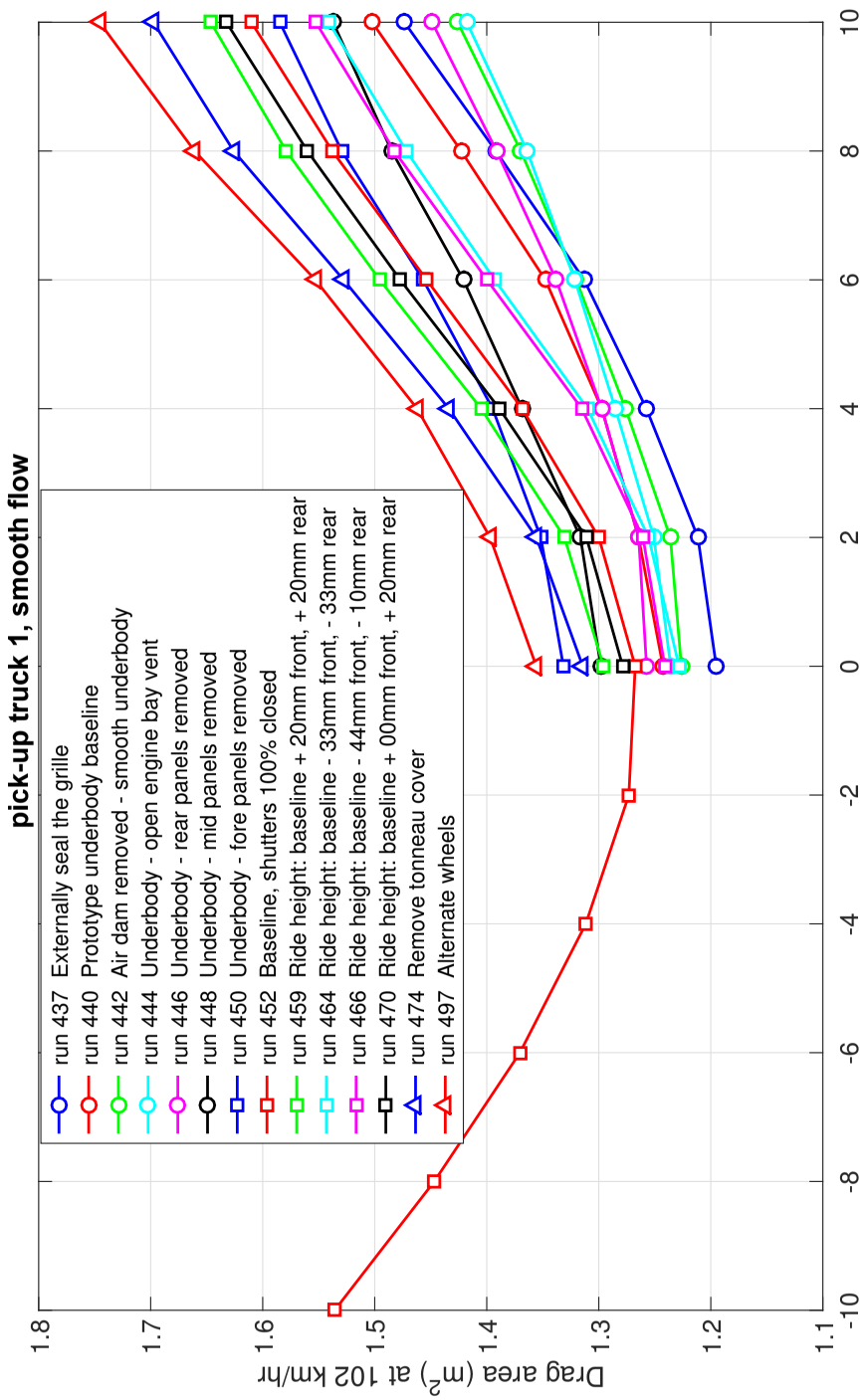

Figure C.30: Variations of drag area for pick-up truck 1 in smooth flow as a function of yaw angle for all yaw sweeps.

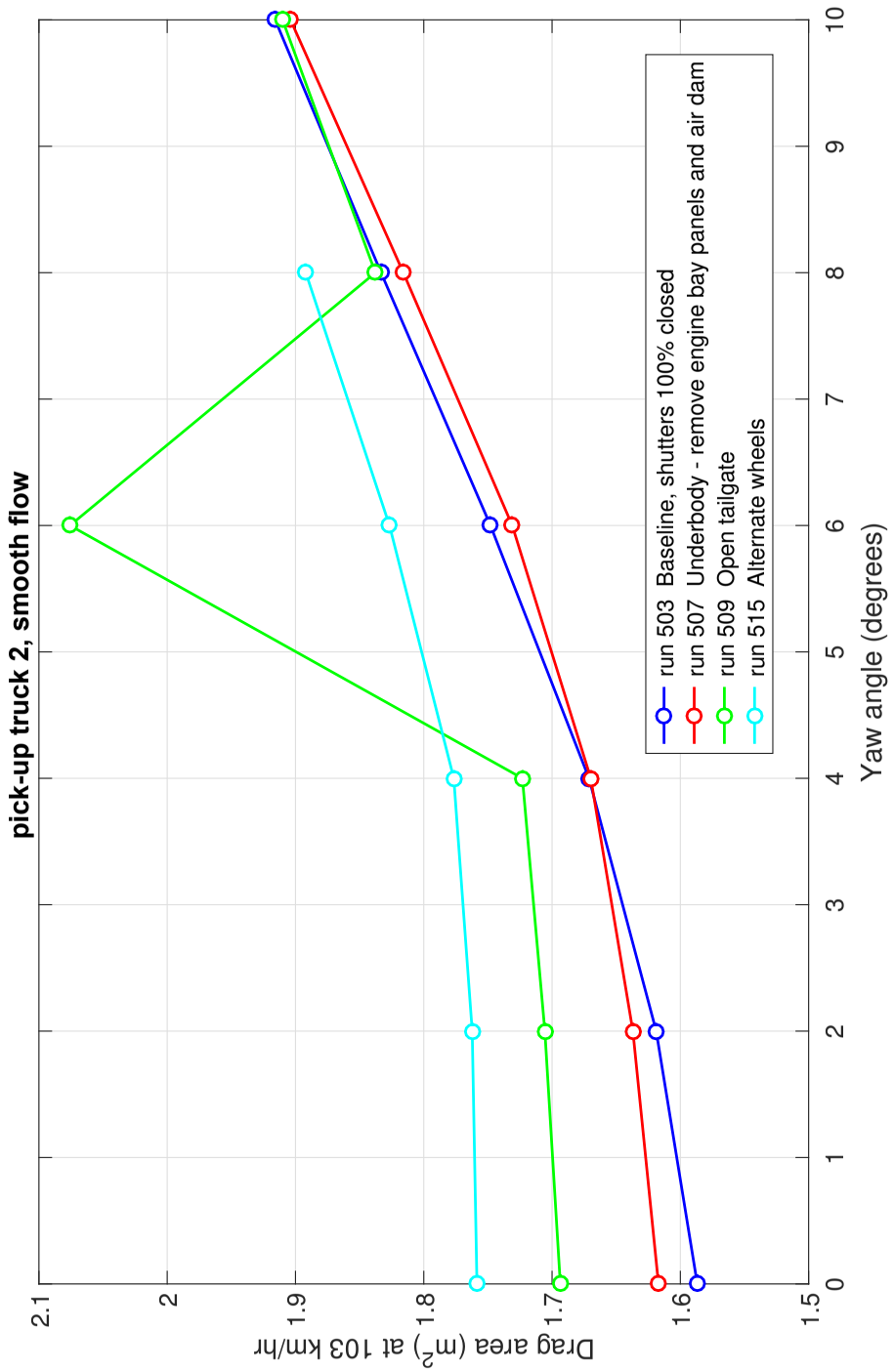

Figure C.31: Variations of drag area for pick-up truck 2 in smooth flow as a function of yaw angle for all yaw sweeps.

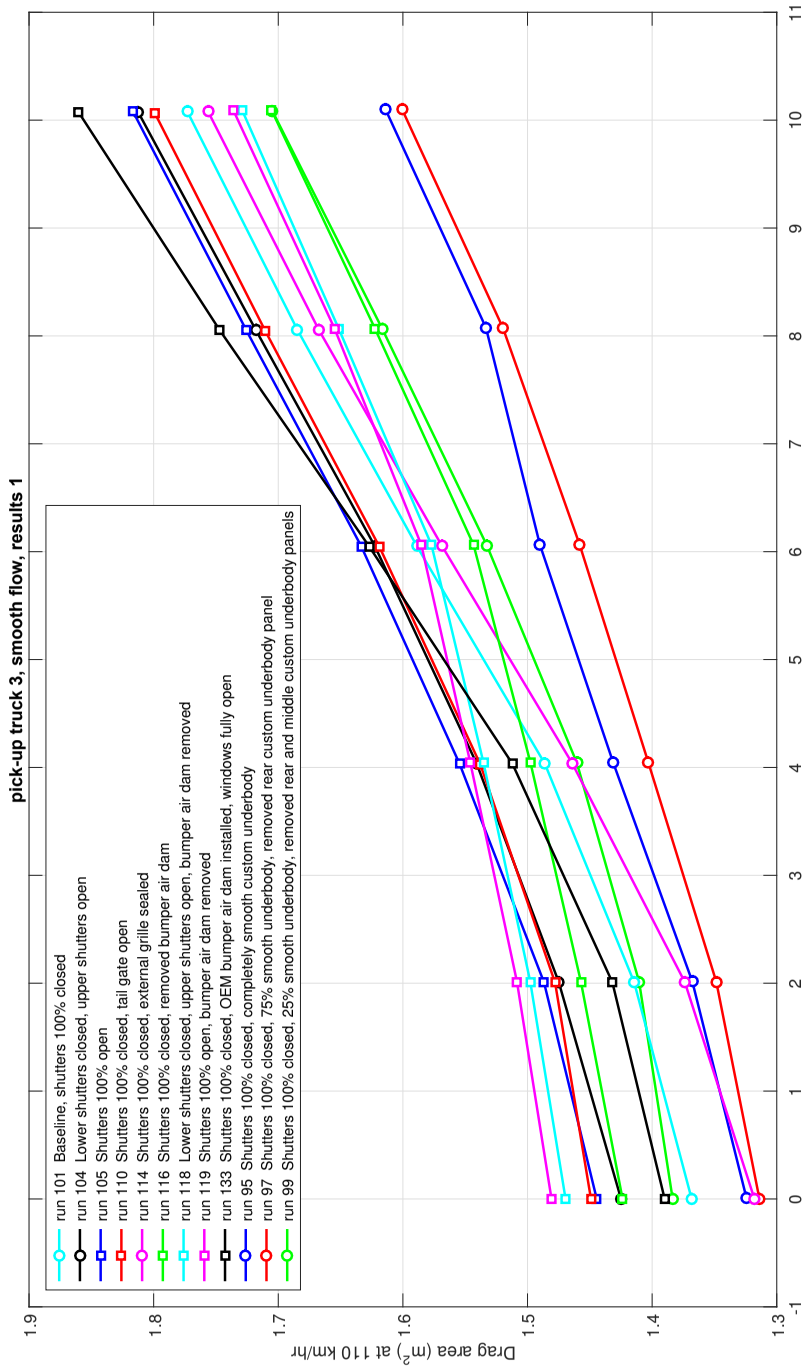

Figure C.32: Variations of drag area for pick-up truck 3 in smooth flow as a function of yaw angle for several yaw sweeps.

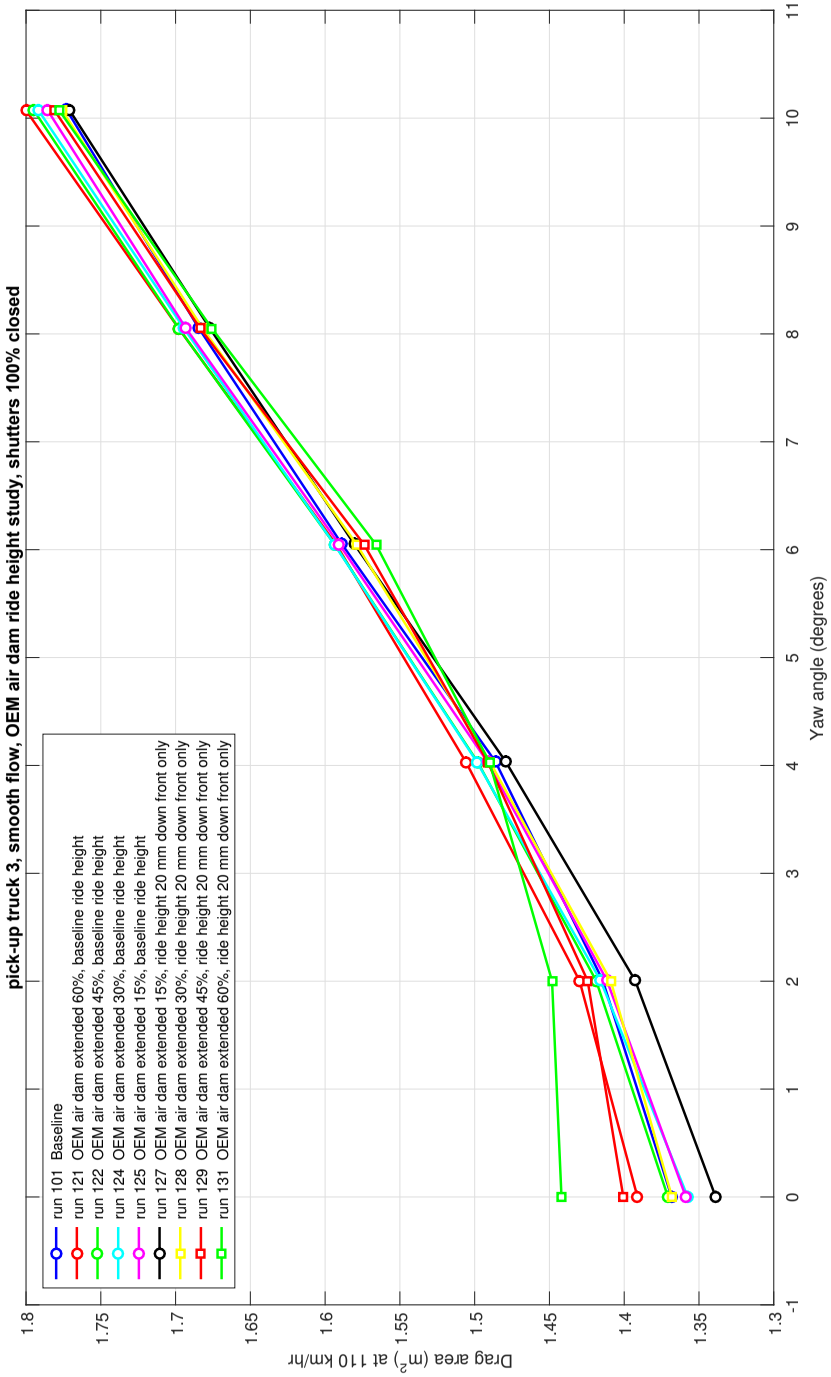

Figure C.33: Variations of drag area for pick-up truck 3 in smooth flow as a function of yaw angle for several yaw sweeps.

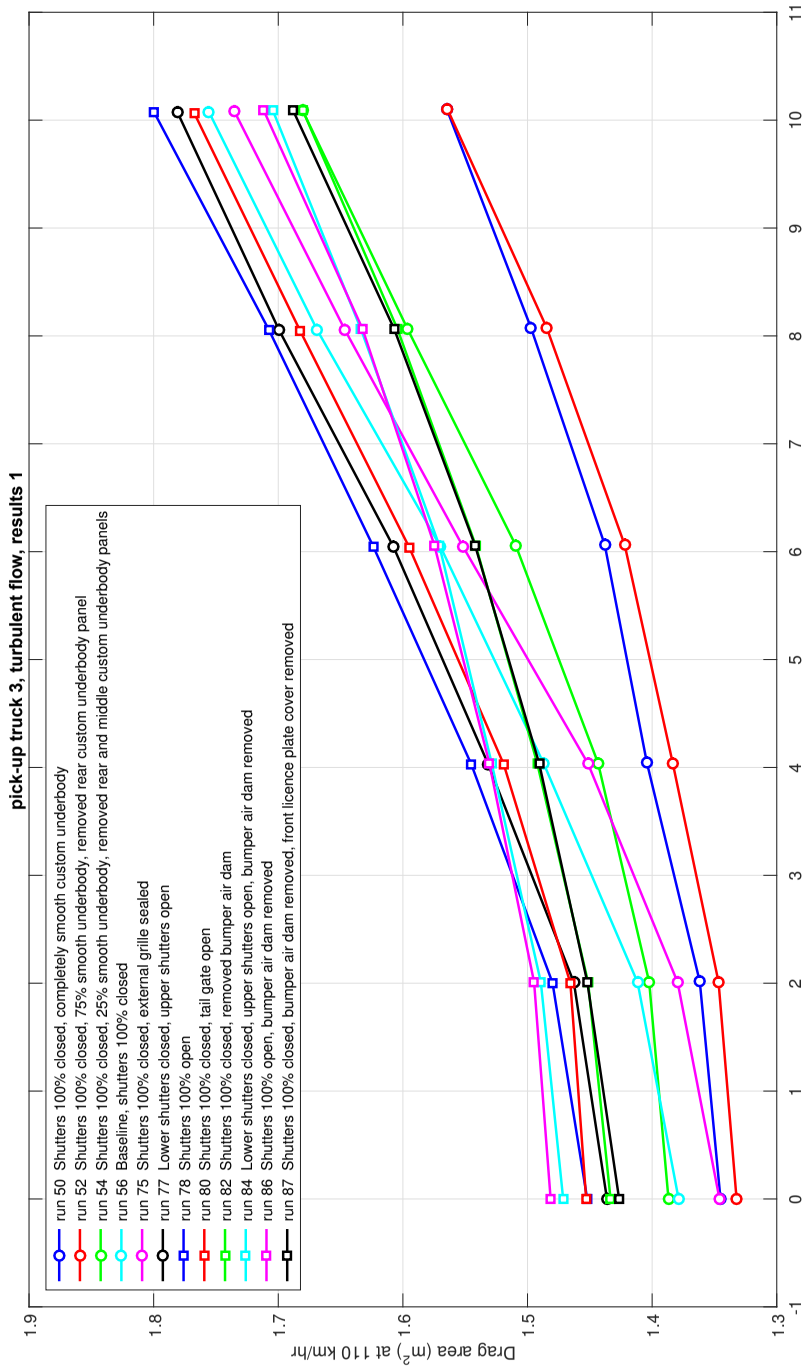

Figure C.34: Variations of drag area for pick-up truck 3 in turbulent flow as a function of yaw angle for several yaw sweeps.

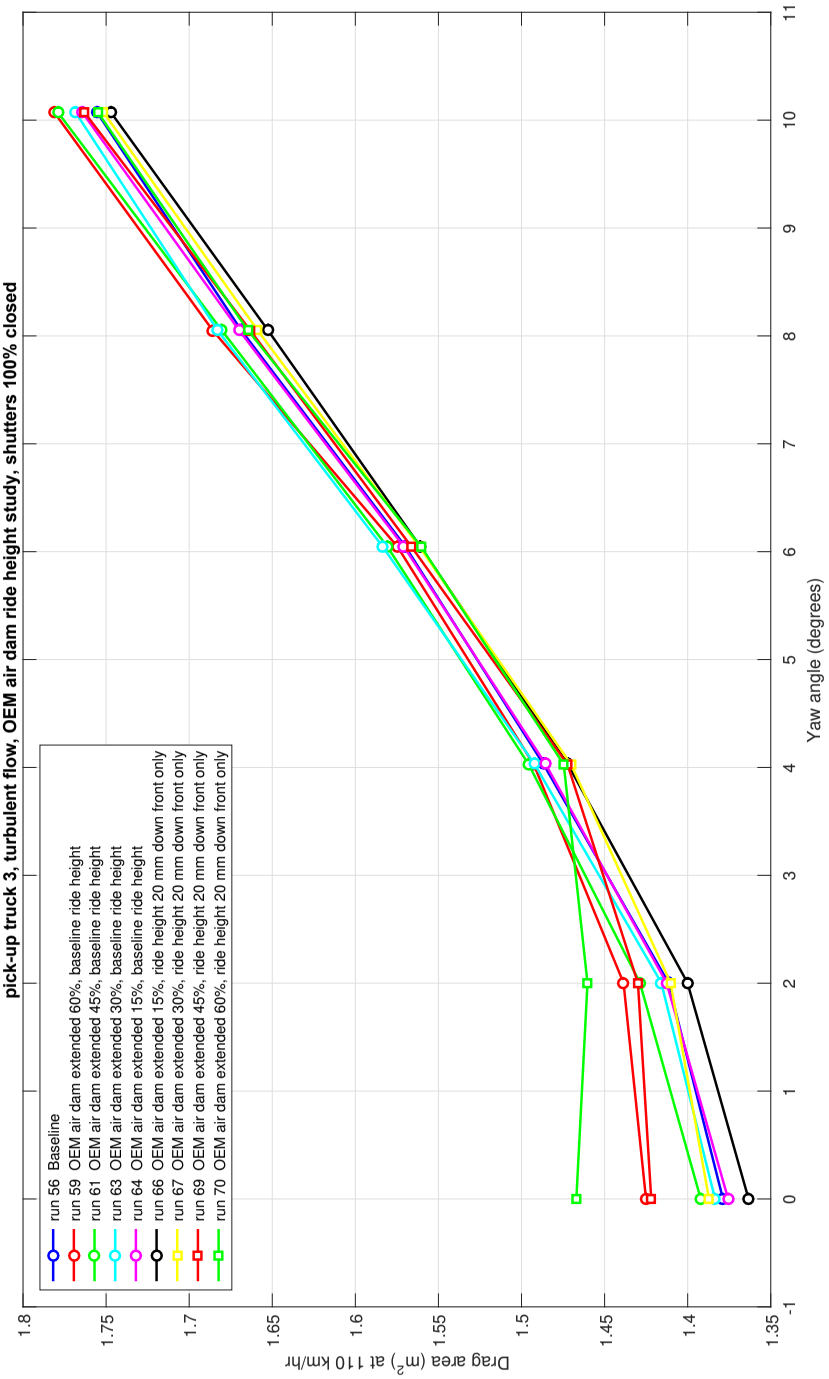

Figure C.35: Variations of drag area for pick-up truck 3 in turbulent flow as a function of yaw angle for several yaw sweeps.